



1-1-2015

# On Abelian and Discrete Symmetries in F-Theory

Hernan Augusto Piragua

University of Pennsylvania, [hpiragua@sas.upenn.edu](mailto:hpiragua@sas.upenn.edu)

Follow this and additional works at: <http://repository.upenn.edu/edissertations>



Part of the [Physics Commons](#)

---

## Recommended Citation

Piragua, Hernan Augusto, "On Abelian and Discrete Symmetries in F-Theory" (2015). *Publicly Accessible Penn Dissertations*. 1949.  
<http://repository.upenn.edu/edissertations/1949>

This paper is posted at ScholarlyCommons. <http://repository.upenn.edu/edissertations/1949>  
For more information, please contact [libraryrepository@pobox.upenn.edu](mailto:libraryrepository@pobox.upenn.edu).

---

# On Abelian and Discrete Symmetries in F-Theory

## Abstract

In this dissertation, we systematically construct and study global F-theory compactifications with abelian and discrete gauge groups. These constructions are of fundamental relevance for both conceptual and phenomenological reasons.

In the case of abelian symmetries, we systematically engineer compactifications that support  $U(1) \times U(1)$  and  $U(1) \times U(1) \times U(1)$  gauge groups. The engineered geometries are elliptic fibrations with Mordell-Weil group rank two and three respectively. The bases of the fibrations are arbitrary, but as proofs of concept, we explicitly create examples with bases  $\mathbb{P}^2$  and  $\mathbb{P}^3$ . We study the low energy physics of these compactifications, we calculate the matter spectrum and confirm that it is anomaly free. In 4D compactifications, the  $G_4$  flux is designed and the existence of Yukawa couplings is verified.

We consider F-theory compactifications on genus-one fibered Calabi-Yau manifolds with their fibers realized as hypersurfaces in the toric varieties associated to the 16 reflexive 2D polyhedra. We present a base-independent analysis of the codimension one, two and three singularities of these fibrations. We

explore the network of Higgsings relating these theories. Such Higgsings geometrically correspond

to extremal transitions induced by blow-ups in the 2D toric varieties. The discrete gauge groups  $\mathbb{Z}_3$  and  $\text{U}(1) \times \mathbb{Z}_2$  are naturally found when  $\mathbb{P}^2$  and  $\mathbb{P}^1 \times \mathbb{P}^1$  are used as fiber ambient spaces. We also find the first realization of matter with  $U(1)$  charge three.

Finally, we study the discrete gauge group  $\mathbb{Z}_3$  in detail. We find the three elements of the Tate-Shafarevich (TS) group. We make use of the Higgs mechanism with the charge three hypermultiplets and the Kaluza-Klein reduction from 6D to 5D. The results are interpreted from the F-M-theory duality perspective. In F-theory, compactifications over any of the three elements of the TS groups yield the same low energy physics, however, M-theory compactifications over the same elements give rise to different gauge groups.

## Degree Type

Dissertation

## Degree Name

Doctor of Philosophy (PhD)

## Graduate Group

Physics & Astronomy

## First Advisor

Mirjam Cvetič

---

**Second Advisor**

Justin Khoury

**Keywords**

F-theory, Phenomenology, String Theory

**Subject Categories**

Physics

ON ABELIAN AND DISCRETE SYMMETRIES  
IN F-THEORY

Hernan Augusto Piragua

A DISSERTATION

in

Physics and Astronomy

Presented to the Faculties of the University of Pennsylvania

in

Partial Fulfillment of the Requirements for the

Degree of Doctor of Philosophy

2015

---

Mirjam Cvetič, Professor of Physics and Astronomy  
Supervisor of Dissertation

---

Justin Khoury, Professor of Physics and Astronomy  
Graduate Group Chairperson

Dissertation Committee

Mirjam Cvetič, Professor of Physics and Astronomy

Justin Khoury, Professor of Physics and Astronomy

Elliot Lipeles, Professor of Physics and Astronomy

Antonella Grassi, Professor of Mathematics

Charles Kane, Professor of Physics and Astronomy

ON ABELIAN AND DISCRETE SYMMETRIES

IN F-THEORY

COPYRIGHT

2015

Hernan Augusto Piragua

## ACKNOWLEDGMENTS

This dissertation would not have been possible without the support of my family, my advisor, my research group and my good friends.

First and foremost, I want to thank my parents, Narcizo and Mariela, for all the love and support they have been given me all my life. I also want to thank my brother, Andres, for always being there. I wish him the best with his new family.

I would like to thank my advisor, Mirjam Cvetič, for her guidance, wisdom, moral and academic support. In my academic upbringing, Denis Klevers and James Halverson are the other two great mentors I had. I thank them for being so patient and at the same time, for making the learning and research process so fun. I particularly want to thank Denis, because he had to deal with me for over two and a half years. I not only consider him a colleague but also a very close friend.

I want to thank my collaborators, Antonella Grassi who was also my AG professor, Wati Taylor, Ron Donagi, Maximilian Poretschkin, Damian Kaloni Mayorga Pena, Paul-Konstantin Oehlmann, Jonas Reuter and Peng Song.

I appreciate all the help and nurturing environment that the High Energy Theory group gave me. I am specially thankful to the professors Justin Khoury, Mark Trodden and Burt Ovrut and the postdocs Yi-Zen Chu, Lasha Berezhiani.

I am grateful I had such wonderful friends and colleagues, just to name a few in alphabetical order: Stephanie Cheng, Karel Gamboa, Andres Plazas, Dio Saldana-Greco, Zain Saleem, James Stokes, Prashant Subbarao, and Saad Zaheer. Thank you all for being there in the difficult and cheerful times.

I would also like to thank Millicent Minnick for being so patient and caring. Thanks for solving all our problems at 2E4 so diligently.

ABSTRACT  
ON ABELIAN AND DISCRETE SYMMETRIES  
IN F-THEORY

Hernan Augusto Piragua

Mirjam Cvetič

In this dissertation, we systematically construct and study global F-theory compactifications with abelian and discrete gauge groups. These constructions are of fundamental relevance for both conceptual and phenomenological reasons.

In the case of abelian symmetries, we systematically engineer compactifications that support  $U(1) \times U(1)$  and  $U(1) \times U(1) \times U(1)$  gauge groups. The engineered geometries are elliptic fibrations with Mordell-Weil group rank two and three respectively. The bases of the fibrations are arbitrary, but as proofs of concept, we explicitly create examples with bases  $\mathbb{P}^2$  and  $\mathbb{P}^3$ . We study the low energy physics of these compactifications, we calculate the matter spectrum and confirm that it is anomaly free. In 4D compactifications, the  $G_4$  flux is designed and the existence of Yukawa couplings is verified.

We consider F-theory compactifications on genus-one fibered Calabi-Yau manifolds with their fibers realized as hypersurfaces in the toric varieties associated to the 16 reflexive 2D polyhedra. We present a base-independent analysis of the codimension one, two and three singularities of these fibrations. We explore the network of Higgsings relating these theories. Such Higgsings geometrically correspond to extremal transitions induced by blow-ups in the 2D toric varieties. The discrete gauge groups  $\mathbb{Z}_3$  and  $U(1) \times \mathbb{Z}_2$  are naturally found when  $\mathbb{P}^2$  and  $\mathbb{P}^1 \times \mathbb{P}^1$  are used as fiber ambient spaces. We also find the first realization of matter with  $U(1)$  charge three.

Finally, we study the discrete gauge group  $\mathbb{Z}_3$  in detail. We find the three elements of the

Tate-Shafarevich (TS) group. We make use of the Higgs mechanism with the charge three hypermultiplets and the Kaluza-Klein reduction from 6D to 5D. The results are interpreted from the F- M- theory duality perspective. In F-theory, compactifications over any of the three elements of the TS groups yield the same low energy physics, however, M-theory compactifications over the same elements give rise to different gauge groups.



# Table of Contents

<b>1</b>	<b>Introduction and Overview</b>	<b>1</b>
<b>2</b>	<b>String Compactifications, F-theory and a little bit of Geometry</b>	<b>5</b>
2.1	String Compactifications . . . . .	6
2.1.1	Phenomenology . . . . .	6
2.1.2	Conceptual Motivations . . . . .	9
2.2	F-theory . . . . .	10
2.2.1	F-theory Compactifications . . . . .	11
2.2.2	Non-Abelian Gauge Groups, Matter and Yukawas . . . . .	12
2.2.3	Abelian Symmetries . . . . .	14
2.2.4	Discrete Symmetries . . . . .	15
2.3	Geometry . . . . .	15
2.3.1	Elliptic Fibration . . . . .	15
2.3.2	Geometry of the Elliptic Fibration . . . . .	16
2.3.3	Toric Varieties . . . . .	18
<b>3</b>	<b>Engineering <math>U(1) \times U(1)</math> in 6D</b>	<b>19</b>
3.1	Basics of Abelian Gauge Sectors in F-theory . . . . .	20

3.1.1	Elliptic Curves with Multiple Rational Points . . . . .	20
3.1.2	Elliptic Calabi-Yau Manifolds with Rational Sections . . . . .	22
3.1.3	Abelian Gauge Sectors in F-Theory . . . . .	26
3.2	Elliptic Fibrations with Two Rational Sections . . . . .	28
3.2.1	Constructing an Elliptic Curve with two Rational Points . . . . .	29
3.2.2	Resolved Elliptic Curve in $dP_2$ and its Elliptic Fibrations . . . . .	39
3.3	Matter Spectrum: Codimension Two Singularities . . . . .	43
3.3.1	Factorized Weierstrass Form: charges $(1,0)$ and $(0,1)$ . . . . .	46
3.3.2	Doubly-Factorized Weierstrass Form: charge $(1,1)$ . . . . .	50
3.3.3	Singular Rational Sections: charges $(-1,1)$ , $(-1,-2)$ , $(0,2)$ . . . . .	53
3.3.4	Calculating Matter Multiplicities . . . . .	58
3.4	Anomaly Cancellation: a Consistency Check . . . . .	63
3.5	Compactifications for a General Base: $U(1)\times U(1)$ . . . . .	67
3.5.1	Construction of the Fibration . . . . .	67
3.5.2	Hypermultiplet Matter Representations and Multiplicities . . . . .	70
3.5.3	Anomaly Cancellation . . . . .	73
<b>4</b>	<b>Engineering <math>U(1)\times U(1)</math> in 4D - Adding <math>G_4</math> Flux</b>	<b>75</b>
4.1	The Elliptic Curve in $dP_2$ And Its Fibrations . . . . .	77
4.1.1	General Calabi-Yau Fibrations with $dP_2$ -Elliptic Fiber . . . . .	77
4.2	Calabi-Yau Fourfolds with Rank Two Mordell-Weil . . . . .	85
4.2.1	Singularities of the Fibration: Matter Surfaces & Yukawa Points . . . . .	86
4.2.2	The Cohomology Ring and the Chern Classes of $\hat{X}$ . . . . .	96
4.3	$G_4$ -Flux Conditions in F-Theory from CS-Terms: Kaluza-Klein States on the 3D Coulomb Branch . . . . .	106
4.3.1	A Brief Portrait of $G_4$ -Flux in M-Theory . . . . .	107

4.3.2	Deriving Conditions on $G_4$ -Flux in F-theory . . . . .	108
4.4	$G_4$ -Flux & Chiralities on Fourfolds with Two U(1)s . . . . .	117
4.4.1	$G_4$ -Flux on Fourfolds with Two Rational Sections . . . . .	118
4.4.2	4D Chiralities from Matter Surfaces & 3D CS-Terms . . . . .	123
4.4.3	4D Anomaly Cancellation: F-Theory with Multiple U(1)s . . . . .	129
<b>5</b>	<b>Engineering U(1)<sup>3</sup> in 6D</b>	<b>133</b>
5.1	Three Ways to the Elliptic Curve with Three Rational Points . . . . .	134
5.1.1	The Elliptic Curve as Intersection of Two Quadrics in $\mathbb{P}^3$ . . . . .	135
5.1.2	Resolved Elliptic Curve as Complete Intersection in $\text{Bl}_3\mathbb{P}^3$ . . . . .	138
5.1.3	Connection to the cubic in $dP_2$ . . . . .	143
5.1.4	Weierstrass Form with Three Rational Points . . . . .	151
5.2	Elliptic Fibrations with Three Rational Sections . . . . .	152
5.2.1	Constructing Calabi-Yau Elliptic Fibrations . . . . .	153
5.2.2	Basic Geometry of Calabi-Yau Manifolds with $\text{Bl}_3\mathbb{P}^3$ -elliptic Fiber .	157
5.2.3	All Calabi-Yau manifolds $\hat{X}$ with $\text{Bl}_3\mathbb{P}^3$ -elliptic fiber over $B$ . . . . .	160
5.3	Matter in F-Theory Compactifications with a Rank Three Mordell-Weil Group	163
5.3.1	Matter at the Singularity Loci of Rational Sections . . . . .	167
5.3.2	Matter from Singularities in the Weierstrass Model . . . . .	175
5.3.3	6D Matter Multiplicities and Anomaly Cancellation . . . . .	179
<b>6</b>	<b>Compactifications on all Toric Hypersurface Fibrations</b>	<b>186</b>
6.1	Introduction & Summary of Results . . . . .	188
6.2	Geometry & Physics of F-theory Backgrounds . . . . .	193
6.2.1	Genus-one, Jacobian and elliptic fibrations with Mordell-Weil groups	193
6.2.2	Divisors on genus-one fibrations and their intersections . . . . .	196
6.2.3	The spectrum of F-theory on genus-one fibrations . . . . .	198

6.2.4	Explicit examples: Calabi-Yau hypersurfaces in 2D toric varieties . . . . .	205
6.3	Analysis of F-theory on Toric Hypersurface Fibrations . . . . .	207
6.3.1	Three basic ingredients: the cubic, biquadric and quartic . . . . .	210
6.4	Fibration of the polyhedrons $F_1$ , $F_2$ and $F_3$ . . . . .	217
6.4.1	Polyhedron $F_1$ : $G_{F_1} = \mathbb{Z}_3$ . . . . .	218
6.4.2	Polyhedron $F_2$ : $G_{F_2} = \text{U}(1) \times \mathbb{Z}_2$ . . . . .	222
6.4.3	Polyhedron $F_3$ : $G_{F_3} = \text{U}(1)$ . . . . .	232
<b>7</b>	<b>Vacua with <math>\mathbb{Z}_3</math> Gauge Symmetry</b>	<b>243</b>
7.1	Introduction . . . . .	243
7.2	The Tate-Shafarevich group in M- and F-theory . . . . .	247
7.3	Identifying 5D Higgs Fields for the $\mathbb{Z}_3$ Tate-Shafarevich group . . . . .	252
7.3.1	Resolving by the toric blow-up . . . . .	254
7.3.2	Resolving by a complete intersection resolution . . . . .	258
<b>8</b>	<b>Concluding Remarks</b>	<b>263</b>
	<b>Bibliography</b>	<b>265</b>

# List of Tables

3.1	Matter spectrum with $U(1) \times U(1)$ -charges $(q_1, q_2)$ in the first and multiplicities in the second column. The integers $n_2, n_{12}$ are defined in (3.53). . .	45
3.2	Codimension two loci with singular behavior of the sections. The identifications of the isolated curves are explained in (3.80), (3.83) and (3.87). . . .	54
3.3	Matter multiplicities. . . . .	61
6.1	Charged matter representation under $\mathbb{Z}_3$ and corresponding codimension two fiber of $X_{F_1}$ . . . . .	221
6.2	Charged matter representations under $U(1) \times \mathbb{Z}_2$ and corresponding codimension two fibers of $X_{F_2}$ . . . . .	228
6.3	Codimension three locus and corresponding Yukawa coupling for $X_{F_2}$ . . . .	242
6.4	Charged matter representation under $U(1)$ and codimension two fibers of $X_{F_3}$ . . . .	242
6.5	Codimension three loci and corresponding Yukawa couplings for $X_{F_3}$ . . . .	242
7.1	Intersection numbers of the sections $\tilde{S}_0, \tilde{S}_1$ with the curves in the $I_2$ -fiber at $s_8 = s_9 = 0$ and corresponding $U(1)_{6d}$ charges in the toric resolution of the $dP_1$ -model. . . . .	257

7.2 Intersection numbers of the sections  $S'_0, S'_1$  with the curves in the  $I_2$ -fiber at  $s_8 = s_9 = 0$  and corresponding  $U(1)_{6d}$  charges in the complete intersection resolution of the  $dP_1$ -model. . . . . 262

# List of Figures

2.1	Web of dualities in Sting Theory. . . . .	7
2.2	Web of dualities in Sting Theory with F-theory at its center. . . . .	10
2.3	Schematics of the geometry of F-theory compactifications. . . . .	12
2.4	Schematics of the compact geometry and the low energy physics in F-theory compactifications. . . . .	13
2.5	Generic elliptic fiber with rank two Mordell-Weil group. . . . .	14
2.6	Construction of the elliptically fibered Calabi-Yau. . . . .	16
3.1	Fan of $\mathbb{P}^2$ on the left and its dual polytope on the right. . . . .	31
3.2	Fan of $dP_2$ on the left and its dual polytope on the right. . . . .	32
3.3	On the left it is shown a regular fiber with rational sections at generic points. In the center, a singular fiber is displayed with a section crossing the singularity where charged matter sits. On the right, the curve is shown after resolution. The isolated curve gives rise to an hypermultiplet charged under the corresponding Abelian gauge field. . . . .	47
3.4	Fibers where two out of the three sections collide. The intersections occur when $s_7$ or/and $s_9$ vanish on the base $B$ . . . . .	54
3.5	How the fiber degenerates at the three loci $(-1,1)$ , $(0,2)$ and $(-1,-2)$ respectively.	56

4.1	Each dot corresponds to a $dP_2$ -fibration over $\mathbb{P}^3$ with generic Calabi-Yau $\hat{X}$ .	85
4.2	$I_2$ -fiber from resolving a codimension two singularity of the fibration of $\hat{X}$ .	90
4.3	The region of allowed values for $(n_7, n_9)$ from figure 4.1. On the entire region, there are two conditions on the flux. In the interior of this region, (4.82) holds. On the red and the blue boundary, there are only four independent $(2, 2)$ -forms in the expansion (4.81). On the blue boundary, $\hat{s}_P$ is holomorphic.	120
5.1	Toric fan of $\text{Bl}_3\mathbb{P}^3$ and the 2D projections to the three coordinate planes, each of which yielding the polytope of $dP_2$ .	143
6.1	The network of Higgsings between all F-theory compactifications on toric hypersurface fibrations $X_{F_i}$ . The axes show the rank of the MW-group and the total rank of the gauge group of $X_{F_i}$ . Each Calabi-Yau $X_{F_i}$ is abbreviated by $F_i$ and its corresponding gauge group is shown. The arrows indicate the existence of a Higgsing between two Calabi-Yau manifolds.	191
6.2	The 16 two dimensional reflexive polyhedra [49]. The polyhedron $F_i$ and $F_{17-i}$ are dual for $i = 1 \dots 6$ and self-dual for $i = 7 \dots 10$ .	207
6.3	Polyhedron $F_1$ with choice of projective coordinates and its dual with corresponding monomials.	212
6.4	Polyhedron $F_2$ with choice of projective coordinates and its dual with corresponding monomials.	215
6.5	Polyhedron $F_3$ with a choice of projective coordinates and its dual $F_{14}$ with the corresponding monomials. We have set $e_1 = 1$ for brevity of our notation. The zero section is indicated by the dot.	232



## Introduction and Overview

Compactifications of F-theory [114, 101, 102] are a very interesting and broad class of string vacua. On the one hand, they are non-perturbative, controllable, and sitting at the heart of the web of string dualities, and on the other hand, they realize promising particle physics, allowing for the construction of phenomenologically appealing models.

Interest in F-theory compactifications, and string compactifications in general, can be broadly grouped in two categories: theoretical, where conceptual questions are studied, and phenomenological, where models are constructed. In particular, for phenomenological purposes, F-theory GUTs have drawn a lot of attention in the recent years, first in context of local models [42, 8, 43] following and later also in compact Calabi-Yau manifolds [11, 90, 24]. Both of these approaches rely on the well-understood realization of non-Abelian gauge symmetries that are engineered by constructing codimension one singularities of elliptic fibrations, for which the full classification is known in terms of the Weierstrass or Tate model [81, 112]. On more theoretical grounds, there are important open conceptual questions, for example the finiteness of the F-theory landscape and which consistent 6D and 4D supergravity (SUGRA) theories can be realized in F-theory [97, 100]. There are also important topics that are relevant for both theory and phenomenology. In par-

ticular, the geometric origins of abelian, discrete symmetries and analogous field theoretic mechanisms, are both interesting for conceptual reasons and crucial for the phenomenology of F-theory models.

Abelian gauge symmetries are crucial ingredients for extensions both of the standard model as well as of GUTs. However, the concrete construction of Abelian gauge symmetries as well as their matter content has only recently been addressed systematically in global F-theory compactifications [58, 97, 17]. This is due to the fact that U(1) gauge symmetries in F-theory are not related to local codimension one singularities, but instead, to the global properties of the elliptic fibration of the Calabi-Yau manifold. Concretely, the number of U(1)-factors in an F-theory compactification is given by the rank of the Mordell-Weil group of the elliptic fibration.

Discrete symmetries play a key part for constructing extensions of the standard model of particle physics. In particular, discrete symmetries are used to forbid terms in the MSSM superpotential that would allow for fast proton decay or other processes which are highly suppressed in the standard model. Some well known examples are provided by R-parity, baryon triality and proton hexality. Thus, the understanding of the geometrical origin of discrete gauge symmetries in F-theory compactifications is of crucial interest. The origin of discrete gauge symmetries in F-theory arise from Calabi-Yau geometries which are only genus-one fibrations without section, in contrast to elliptic fibrations with sections. Recently, there has been progress in understanding the physics of such compactifications,[18, 3, 99, 48, 93, 94]. A natural object which is attached to this kind of compactifications is given by the Tate-Shafarevich (TS) group of the genus-one fibration which is a discrete group that organizes inequivalent genus one geometries which share the same associated Jacobian fibration.

Another line of research, on more theoretical grounds and keeping in mind finiteness and 4D/6D SUGRA matching [83, 84], is the systematical extension of the set of Calabi-

Yau manifolds that can be used for F-theory compactifications. The different approaches can be roughly sorted into two groups. The first group of approaches focuses on the classification and construction of all bases that are admissible for F-theory [98, 99]. The second group, which we advance in this dissertation, focuses on generalizing the type of fiber and the ways in which it can be fibered in a Calabi-Yau manifold. Questions about the number, nature or even a parametrization of all possible CY spaces are still open and important.

The need of further research in these important topics is the main motivation for this dissertation. Then, here we extend the boundaries of F-theory compactifications focusing in abelian and discrete symmetries, in both 4D/6D compactifications.

This dissertation is organized as follows.

We start in chapter 2 introducing the foundations for the rest of this work. We briefly talk about string compactifications, introduce F-theory, touching on non-abelian, abelian and discrete symmetries and finish with the geometry of the elliptic compactifications.

The novel results start in chapter 3, where we explicitly construct geometries that support  $U(1) \times U(1)$  in 6 dimensions. In the elliptic fibrations, for concreteness first we use the specific base  $\mathbb{P}^2$ , then we generalize to arbitrary bases. We calculate the full spectrum of the theory and check that it is anomaly free. The results of this chapter were published in [34, 33, 37].

In chapter 4 we construct 4D compactifications with  $U(1) \times U(1)$  gauge groups. In order to obtain chiral matter we add flux to the compactifications. We obtain base independent results. We calculate the spectrum and the Yukawa couplings of the theory. The results were published in [30].

Continuing our abelian symmetry journey, in chapter 5, geometries supporting  $U(1) \times U(1) \times U(1)$  were explicitly engineered. As an interesting result, the ambient space of the fiber in these compactifications are two dimensions higher than the fiber curve. The analysis of these geometries required the use of different geometric tools, however, the

spectrum is rich and slightly un-expected, pointing to exceptional groups. We finalize the chapter checking anomaly cancellation. The results of this chapter were published in [35].

In a slightly different research direction, in chapter 6, we focus on constructing genus one fibrations of curves living in all two dimensional toric varieties. This chapter is full of surprises. Gauge discrete symmetries appear naturally, an underlying  $E_6$  seems to be looming, extremal transitions connect the different geometries and are naturally interpreted as the Higgs mechanism and a charge 3 hypermultiplet is found. The results were published in [80].

In chapter 7 we go deeper into the discrete gauge symmetry  $\mathbb{Z}_3$ . We study the F- M-theory duality using the higgs mechanism and construct the Tate-Shafarovich group explicitly. This short note was published in [37].

We conclude in chapter 8 summarizing the most important results of this dissertation.

# **String Compactifications, F-theory and a little bit of Geometry**

The title of this dissertation, ‘On Abelian and Discrete symmetries in F-theory’, might sound extremely technical and arid. Thus, the purpose of this chapter is to alleviate this problem, trying to get the reader acquainted with some of the topics of this dissertation. All the subjects introduced here are mentioned only at the intuitive level, leaving most of the technical details for the later chapters.

In this chapter we start discussing the motivations for string compactifications, the phenomenology program and the conceptual questions. We also mention how this dissertation fits into this quest. We follow with a very brief introduction to F-theory, highlighting some very interesting properties of the theory. We also mention abelian and discrete symmetries in F-theory and try to motivate the need for this dissertation. We conclude with some selected topics of geometry that will help the reader get a better ‘picture’ of the string compactification setups.

## 2.1 String Compactifications

In this section we will briefly mention some of the important motivations that fuel the research in string theory compactifications. We divide them into two categories, phenomenological and conceptual motivations.

### 2.1.1 Phenomenology

String theory, discovered over 40 years ago, has proved to be a fertile framework to unify all forces of nature, including the elusive gravity. This property makes the theory a promising candidate for the ‘theory of everything’ of our universe. Unification however is just a little part of the puzzle. Among the many other required properties of the theory, and probably the most important, is the realization of the Standard Model of particle physics. This defines one of the main objective of String Phenomenology: the use of the string theory framework to reproduce either the Standard Model or a generalization of it, and then, use this model to make predictions at other scales and regimes.

This is not an easy task. Attempts have been made since the very early years of the String discovery and although we have expanded our understanding of the theory to great extend, to this date, a complete and precise Standard Model has not been obtained in String Theory.

We could group the reasons of this ‘failure’ into two big categories: the lack of understanding of String theory and the particularity of the Standard model. In the rest of this section we elaborate on these two points and then comment on the topics of this dissertation in this context.

String Theory theory was developed over a simple idea: the quantization of a string. However, it is known that consistency of this simple idea quickly develops into a theory of many dynamic fields and objects interacting among each other. Furthermore, the fields

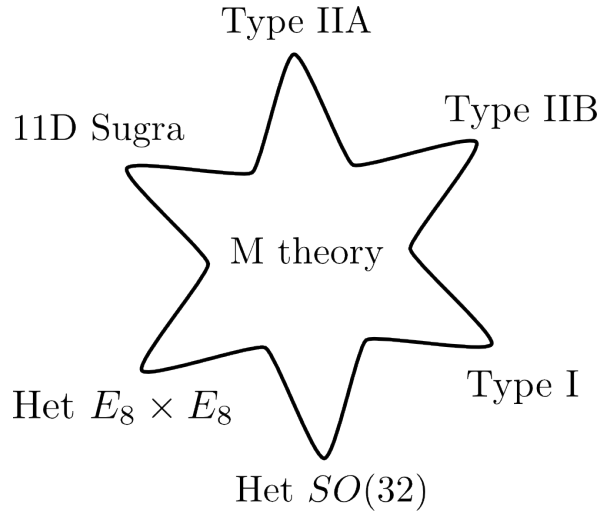


Figure 2.1: Web of dualities in Sting Theory.

and objects are not uniquely defined, in fact they depend on the particular location of the ‘string landscape’. See figure 2.1. Much progress has been made in different corners of this landscape, however a full description of the theory is lacking.

The Standard Model of particle physics is very particular. There is no doubt about the success of the model. It has been evaluated for 50 years, passing all tests with flying colors. It explains phenomena in a big range of scales with astonishing precision. However, the model is far from being trivial or generic. The Standard Model has 19 unspecified parameters and a seemingly arbitrary selection of Lie groups and representations among other ‘particularities’.

A comprehensive list of the desired features of any string model was compiled in [69]. Known as ‘The Ibañez Wish List’, it reads explicitly:

- |   |   |
|---|---|
| 1. Chirality  | compulsory).                                |
| 2. Gauge group contains and can be broken to $SU(3) \times SU(2) \times U(1)$ . | 4. Contains standard quark-lepton families. |
| 3. $N = 1$ SUSY in $d = 4$ (convenient, not                                     | 5. Contains Weinberg-Salam doublets.        |

- |   |  |
|---|--|
| 6. Three quark-lepton generations.  | 10. No flavor-changing neutral currents.                     |
| 7. Proton is sufficiently stable (lifetime $> 10^{34}$ years).                        | 11. Light or so left handed neutrinos.                       |
| 8. Correct prediction: $\sin^2 \theta_W \approx 0.23$ ,<br>$M_p \approx 10^{18}$ GeV. | 12. Weak CP violation exists.                                |
| 9. No exotic gauge boson with mass $\leq 1$ TeV.                                      | 13. Potentially realistic Yukawa couplings (fermion masses). |
|   | 14. $SU(2) \times U(1)$ breaking feasible.                   |
|   | 15. Small supersymmetry breaking.                            |

Just to reemphasize, this is a long non-trivial list. There are String models that can reproduce some of these features, however, to this date not a single model has all characteristics previously mentioned.

Coming back to this dissertation, the purpose of this work is to expand our understanding of string theory, more specifically of F-theory. We hope that the results obtained in this work will help our ultimate endeavor of finding the complete string model of our universe. However, and although some phenomenological models were constructed as proofs of concepts, we have to be honest and admit that the main results of this dissertation are theoretical. But the motivation of this research was phenomenologically inspired. In fact, the areas we chose to explore, the abelian sector and discrete symmetries, are fundamental ingredients in the construction of any realistic string theory model. Just to remind the reader, some examples where these symmetries appear in particle physics phenomenology are: the texture of Yukawa couplings, the avoidance of proton decay operators, R-parity, Baryon triality, the  $\mu$  problem and  $Z'$  bosons.



## 2.1.2 Conceptual Motivations

Besides the phenomenological reasons mentioned in the previous section, there is a plethora of ideas and lines of research that uses string theory as an inspiring muse. Let us comment on some of them.

It is striking that the string landscape, i.e. the possible low energy vacua, is finite. Yes, it is a big number, however it is finite, unlike the possible set of all field theories. The parametrization and understanding of the properties of the full landscape is still in its infancy. Some progress through systematic studies have been achieved in some corners of the star, however, there is not a full approach to this problem. A slightly related line of research to this topic, is the well defined question: are all SUGRA theories in different dimensions realized in string theory? With the use of F-theory substantial progress has been made in 6D in the last couple of years and some glimpses of hope have started to appear in 4D.

Taking a break from the standard model, string theory may also help us understand general relativity. Even after 100 years since its discovery, GR has many deep and perturbing puzzles. The most natural questions are: the dynamics around curvature singularities, the origin of macroscopic entropy and the non-renormalizability. String theory has provided some hope and in some cases has solved these puzzles, unless in the supersymmetric cases. We hope that the elegant solutions that the nature of extended objects brings, can point to similar mechanisms for the general questions i.e. non-supersymmetric cases.

From a completely different energy scale point of view, string theory compactifications have shed light to the geometrization of some strongly coupled phases. Randall Sundrum and ADS/CFT are probably the most obvious examples. Finite density QFT is another region where string compactifications have helped us make some progress, the poster child in this case is ADS/CMT.

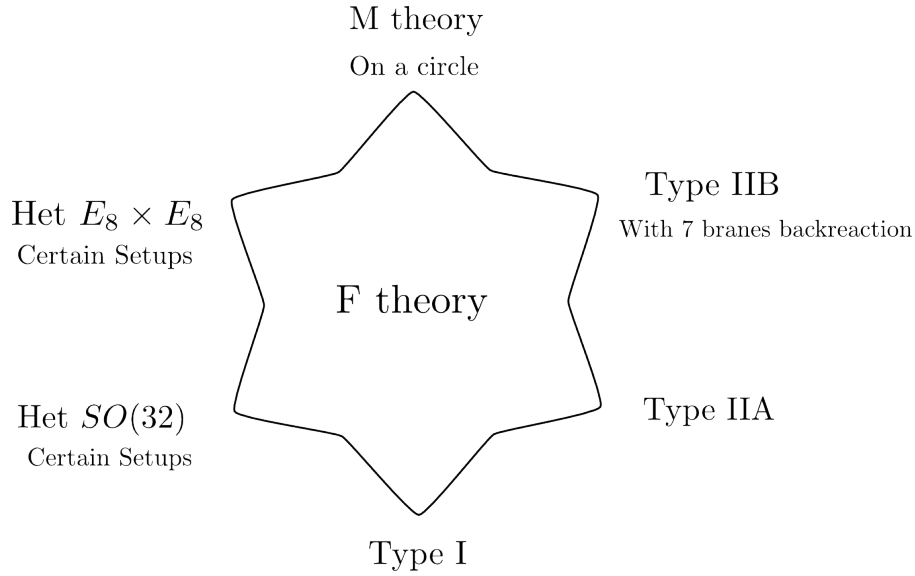


Figure 2.2: Web of dualities in String Theory with F-theory at its center.

## 2.2 F-theory

Why F-theory? Because F-theory [114, 101, 102] is powerful. It allows us to explore regions of the string landscape that were not accessible before, with elegant simplicity. The F(ather) theory was discovered in the mid 90's during the second string revolution. It has the appealing property of being local like brane constructions in type II theories, but at the same time it has the capability of allowing exceptional groups, a property of heterotic strings. In fact, it is believed that F-theory is the theory that allow us to explore the biggest part of the landscape at this time.

It is well known that F-theory does not have a Lagrangian description, however there are known limits of the theory that serve as tools to study it: the Sen limit to type IIB, the semistable degeneration to heterotic  $E_8 \times E_8$  and  $SO(32)$  and the compactification over a circle dual to M-theory. See figure 2.2. These limits help us understand the low energy theory of the compactifications and we will use them heavily in this dissertation.

F-theory is geometry. Contrary to other string theory compactifications, where we have to keep track of the geometry and other dynamic objects like branes or bundles, in F-theory

a big part of the data of the compactifications is encoded in the geometry of the space. This is not only elegant but also convenient. Well, it is almost all geometry, there is one additional important ingredient we have to add: the flux. This will be specially important in chapter 4 where we work in 4D and we need to generate chirality.

### **2.2.1 F-theory Compactifications**

Now we turn our attention to the compactifications. In figure 2.3 we show the schematic setup of all our compactifications, and although the diagram is not precise, it gives a good intuition about all the ‘moving parts’ involved.

The total geometric space is 12 real dimensional, decomposed into a Minkowski space, that represent the observable physical dimensions, and a compact Calabi-Yau (CY) space. When we refer to 4D/6D compactifications, we imply the dimension of the Minkowski space. In those cases the compact geometries will be 8D/6D respectively.

The compact CY space has a very important property: it has to be elliptically fibered, that is, locally it must look like an elliptic curve times another space that is referred as the base. See figure 2.3. An elliptic curve is basically a two real dimensional torus that includes a marked point. The point is shown schematically with a cross in the torus in figure 2.3. All the marked point points in the torus should be ‘smoothly’ connected globally, forming a section of the fibration.

Most of this dissertation is about engineering and understanding the connection between the compact CY geometries and the low energy physics. In the next subsections we will start showing how to ‘read’ the low energy physics in F-theory from the geometry.

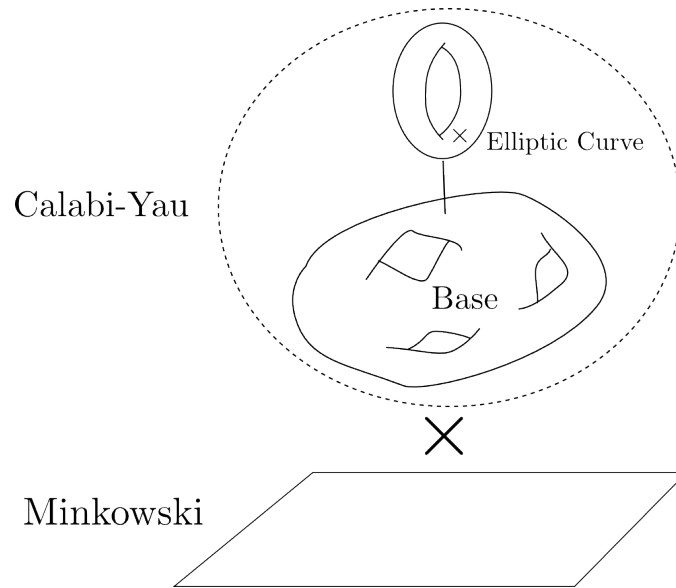


Figure 2.3: Schematics of the geometry of F-theory compactifications.

## 2.2.2 Non-Abelian Gauge Groups, Matter and Yukawas

In F-theory, most of the low-energy physics is encoded in the geometry of the compactification. More specifically, the data is encoded in the singularities of the space, i.e. the subspaces where the tangent space is locally not well defined. The most important information of the singularities are its dimension, its type and how many of them exist in the compactification.

An schematic drawing of the data is shown in figure 2.4.

Codimension one singularities in the base, that is two dimensions less than the compact space, tell us about the non-abelian gauge groups. The specific group supported at this location is determined by the local behavior of the singularity. From the perspective of type IIB string theory, the fiber encodes the string coupling, then, where a singularity appears it signals strong coupling objects in the base, in fact it points to an underlying stack of branes. An M-theory interpretation also exists. However to make sense of it, first a similar space without singularities has to be found. This geometry is called the resolved CY and the price that has to be paid is the addition of more surfaces and curves. The beautiful connection

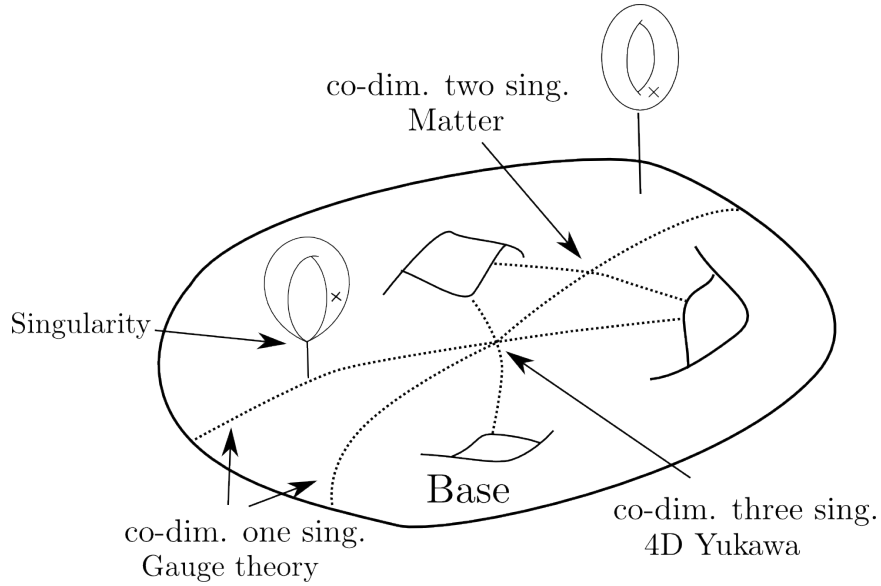


Figure 2.4: Schematics of the compact geometry and the low energy physics in F-theory compactifications.

is that if we look at the curves and their intersections, they form the dynkin diagram of the Lie Group.

Matter representations are encoded at codimension two singularities in the base, see figure 2.4. These are the places where the codimension one singularities get enhanced. From the type IIB perspective, these are the places where two stacks of branes intersect and new light modes appear realized as open strings between them. From the M-theory point of view, in the resolved geometry a new isolated curve will be added at these locations. M2 branes will wrap them and their excitations are the hypermultiplets.

Finally at codimension three singularities in the base, we find the Yukawa couplings of the theory, see figure 2.4. This is a 4D phenomenon. The 8 internal dimensions of the compact space are arranged into three complex dimensions for the base and two for the fiber. The Yukawa points then occur naturally at the triple intersection of three codimension one singularities.

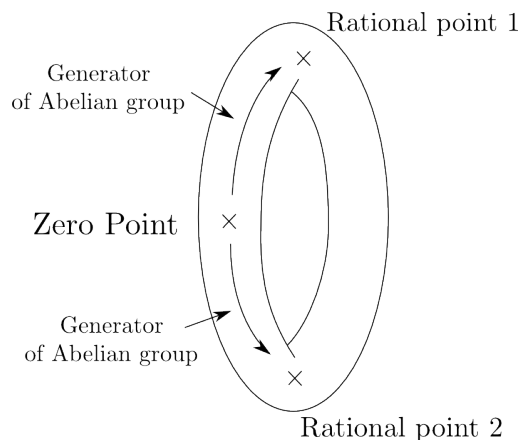


Figure 2.5: Generic elliptic fiber with rank two Mordell-Weil group.

### 2.2.3 Abelian Symmetries

Surprisingly, abelian groups, that in principle are simpler, are much less understood in F-theory. In fact, they have received less attention than the non-abelian groups. Interest in the field has only recently been rekindled and now it is a very active field of research.

Abelian gauge groups are associated to the group of sections of the elliptic fibrations. This is a little unexpected because it implies that the information about  $U(1)$ s is global, and not localized in the base, as in the case of non-abelian groups. Now, the group of sections should be observed in any fiber, as long as the elliptic curve is generic. An example of a generic fiber is shown in figure 2.5 where the sections are the marked points in the torus. These points form an abelian group in the elliptic fiber known as the Mordell-Weil group. The generators of the group, constructed as the differences between the rational points and a zero point, are associated to the abelian group of the low energy theory. The formal procedure to extract the right generators is known as the Shioda map. The decision of which point to use as the zero point is arbitrary and should not affect the low energy physics.

We should notice that abelian gauge groups do not make the space singular at codimension one in the base. However charged matter still appears as codimension two singularities in the base and the Yukawa couplings still show up as codimension three singularities.

## 2.2.4 Discrete Symmetries

Discrete gauge symmetries are even less studied in F-theory. However in the last couple of years (2014 and 2015) there has been tremendous progress and interest in understanding their origin. The workhorse of this progress has been the Higgsing mechanism of non-minimal charged hypermultiplets in abelian theories.

One fascinating aspect of the discrete symmetries is that they are not encoded in the Mordell-Weil group, but instead in a more obscure (at least for physicists) object: the Tate-Shafarevich group. The data of this group is not inside the geometry of a space, instead, each element of the group is a different space on its own. In chapters 6 and 7 we will go deeper in the understanding of the group and we will explicitly construct of some discrete gauge groups.

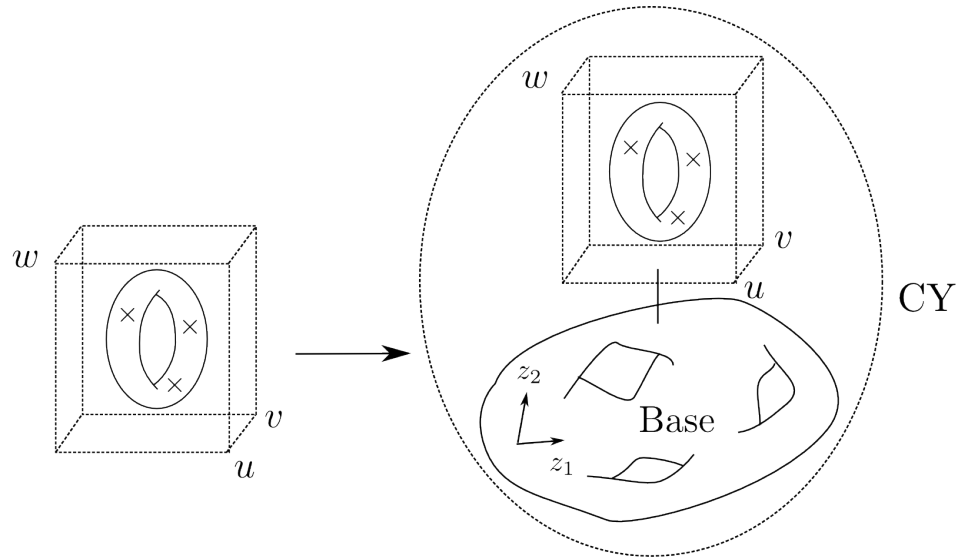
## 2.3 Geometry

As mentioned in the previous sections, the big part of the construction of the compactifications in F-theory is the engineering of the compact space. Thus, in this section we will mention our approach to the construction of geometries and the tools we use during the rest of this dissertation.

### 2.3.1 Elliptic Fibration

We need to construct compact elliptic fibrations, that is geometries that locally look like a base times an elliptic fiber. The approach we consistently take has two steps: first construct the elliptic curve with the desired properties, then create the fibration, making the elliptic fiber depend on the position of the base.

The construction of the elliptic curve is also a two step procedure. First we find a



$$p(u, v, w) = \sum a_{ijk} u^i v^j w^k \longrightarrow p(u, v, w, z_1, z_2) = \sum a_{ijk}(z_1, z_2) u^i v^j w^k$$

Figure 2.6: Construction of the elliptically fibered Calabi-Yau.

simpler higher dimensional space that is simple enough, and then we take an appropriate hyper-surface. The higher dimensional space is called ambient space. See the left side of figure 2.6. The points of the curve are then specified as the zeros of a set of equations that we called  $p(u, v, w)$  in the figure.

Once we have constructed the elliptic fiber, we proceed to construct the fibration. We need to make the coefficients of the equations,  $a_{ijk}$  in the figure, depend on the coordinates of the base,  $z_1$  and  $z_2$ . See the right hand side of figure 2.6. To find the right degrees of the coefficients, we first put together the ambient space of the fiber and the base. Then the Calabi-Yau condition forces the right degrees of the coefficients,  $a_{ijk}(z_1, z_2)$ , in the hyper-surface equation. In the following chapters we will be more precise about this procedure.

### 2.3.2 Geometry of the Elliptic Fibration

Now that we have finally constructed the geometry, we proceed to calculate things inside it. The tool that we use is intersection theory. For an introduction to the topic we refer the



readers to [47]. The motivation behind it is simple, the idea is to formalize the familiar concept of intersection of varieties that we are used to. Things like, the notion of two generic lines intersected in  $\mathbb{R}^2$  or the intersections of three generic planes in  $\mathbb{R}^3$  are points.

One problem that arises is the definition of ‘generic’. We know that two parallel lines do not intersect. The solution to this conundrum is to define classes of equivalent varieties, instead of individual varieties. Then, even if the varieties we are trying to intersect are not placed appropriately, there should exist other varieties in their corresponding classes that should intersect well. As an example, in the case of two parallel line, we can always find another rotated line that will work. All these rotated lines will then form an equivalence class. In this dissertation the equivalence relations that we use are rational equivalences. In terms of notation, the class of variety  $Y$  is denoted  $[Y]$ .

Another key inside of intersection theory, is to realize that if two varieties intersect properly, the resulting variety should have a codimension equal to the sum of the codimensions of the original varieties. As examples, we can think about the lines int the plane, or the planes in the 3D space.

Now let us define an intersection product, denoted by ‘ $\cdot$ ’. The idea is to define the class of the intersection of two varieties as the product of the of the classes of the varieties. Mathematically, it reads

$$[Y] \cdot [Z] = [Y \cap Z]. \tag{2.1}$$

We also expect that the intersection varieties whose codimensions add up to the dimension of the space, always intersect in a number of points. And if the sum of the codimensions of the intersection of varieties are bigger than the dimension of the space then the result should vanish. As and example, three lines should not intersect generically in a plane.

Coming back to our case of study, there are some natural codimension one varieties in our elliptic fibrations. We will call these varieties divisors. In our cases we will have

the following divisors: the sections, any divisor of the base together with the fiber (known as vertical divisors) and divisors in the base with a curve in the fiber (known as cartan divisors).

Finally, we need to construct higher codimension objects in our geometries. In particular, we require surfaces for the explicit construction of  $G_4$  flux in 4D compactifications. In this case we will use intersections of divisors to build a base for the surfaces. We will discuss this at length in chapter 4.

### **2.3.3 Toric Varieties**

Many of the ambient spaces we use are toric varieties. It is out of the reach of this dissertation to introduce such rich and beautiful topic. We refer the readers to [29] for a nice introduction.

Let us just mention a couple of words about them. Toric varieties are spaces that contain a torus inside them. This torus acts on itself and almost generates the full variety. Some of the properties that make these varieties so attractive are, first that they comprise a rich and extensive set of compact spaces, and second, toric varieties can be fully determined by its combinatorial structure (encoded in fans).

## Engineering $U(1) \times U(1)$ in 6D

In this chapter we explicitly construct geometries that support F-theory compactifications with low energy  $U(1) \times U(1)$  gauge groups. We restrict the analysis to six dimensions, i.e. the internal compact space is three-complex dimensional (threefold), and leave the richer four dimensional case for the next chapter.

We take most of the content from the articles [34] and [33]. The author of this dissertation is a co-author of both articles.

The content of this chapter are organized in the following way. First, we establish the machinery necessary for the analysis. Then, we construct the elliptic curve with three marked points (two rational points) and discover that the natural ambient space for this curve is the space  $\mathbb{P}^2$  blown up at two points, also known as  $dP_2$ . With this insight at hand, we proceed to construct the elliptic fibration, first over the base  $\mathbb{P}^2$  and then the general case. Voilà!, these are the geometries we were looking for. We proceed to find the spectrum of the theories i.e. the number and charges of the hypermultiplets. This task proved to be harder than expected, however, we confirmed the spectrum was anomaly free.

Let us highlight some fascinating results additional to the explicit construction of the geometry. The zero section was non-holomorphic, that means that the section behaves

badly at certain places in the geometry. This result was not fully appreciated previously in the literature. Additionally, the calculation of the spectrum required the introduction of some algebraic techniques. They are now known as the ‘resultant techniques’ and became widely used tools in the community.

One final remark about the content. The original articles included the addition of a  $SU(5)$  gauge group, some explicit toric examples and the connection between  $Bl_{(1,0,0)}\mathbb{P}^2(1,2,3)$  and  $Bl_{(0,1,0)}\mathbb{P}^2(1,1,2)$ . We decided not to include these topics in this dissertation but invite the curious readers to the articles for more details.

## 3.1 Basics of Abelian Gauge Sectors in F-theory

In this section we review the notion of the Mordell-Weil group as the group of rational points on an elliptic curve in section 3.1.1. Then we discuss the geometry of Calabi-Yau manifolds formed as elliptic fibrations with general fiber given by such an elliptic curve in section 3.1.2. The rational points are lifted to rational sections of the elliptic fibration and contribute additional cycles to the homology group of these manifolds. The Abelian sector of an F-theory compactification on these elliptically fibered Calabi-Yau manifolds, as explained in section 3.1.3, is determined by the structure of these rational sections. The reader interested in the results of our analysis can skip this section and directly proceed with section 3.2.1.

### 3.1.1 Elliptic Curves with Multiple Rational Points

To set the stage for our later discussion, we begin with the most concrete definition of an elliptic curve  $\mathcal{E}$  over a field  $K$  in terms of a Weierstrass model. The Tate form of the

Weierstrass model reads

$$y^2 + a_1xyz + a_3yz^3 = x^3 + a_2x^2z^2 + a_4xz^4 + a_6z^6 \quad (3.1)$$

with  $a_i$  denoting numbers in a field  $K$ . In elliptic fibrations of  $\mathcal{E}$  over a base  $B$ ,  $K$  will be identified with the function field of  $B$ . In the chosen projectivization (3.1) is a one-dimensional Calabi-Yau hypersurface in the weighted projective space  $\mathbb{P}^2(1, 2, 3)$  with homogeneous coordinates  $[z : x : y]$ . The Tate form can be brought into the reduced Weierstrass form

$$\tilde{y}^2 = \tilde{x}^3 + f\tilde{x}z^4 + gz^6 \quad (3.2)$$

by the variable transformation

$$\tilde{x} = x + \frac{1}{12}b_2z^2, \quad \tilde{y} = y + \frac{1}{2}a_1xz + \frac{1}{2}a_3z^3 \quad (3.3)$$

with the following definitions

$$\begin{aligned} f &= -\frac{1}{48}(b_2^2 - 24b_4), & g &= -\frac{1}{864}(-b_2^3 + 36b_2b_4 - 216b_6), \\ b_2 &= a_1^2 + 4a_2, & b_4 &= a_1a_3 + 2a_4, & b_6 &= a_3^2 + 4a_6, \\ \Delta &= -16(4f^3 + 27g^2) = -8b_4^3 + \frac{1}{4}b_2^2b_4^2 + 9b_2b_4b_6 - \frac{1}{4}b_6b_2^3 - 27b_6. \end{aligned} \quad (3.4)$$

Here the quantity  $\Delta$  defined in the last line of (3.4) is the discriminant of the Weierstrass equation (3.2). If  $\Delta = 0$  then the elliptic curve defined by (3.2) is singular.

Both the Tate form (3.1) as well as the reduced Weierstrass form (3.2) have one distinguished point  $P$  at  $[z : x : y] = [0 : 1 : 1]$ , referred to as the zero point. In general, a rational point on the elliptic curve  $\mathcal{E}$  is defined as a point with coordinates in the designated field  $K$ . The set of rational points on  $\mathcal{E}$  form an Abelian group under addition that is naturally

defined in the Weierstrass form (3.2). The group of rational points, with  $P$  as the zero, is the *Mordell-Weil group* of the curve  $\mathcal{E}$ . The Mordell-Weil group is finitely generated, i.e. it is the sum of a torsion subgroup and  $\mathbb{Z}^r$ , and  $r$  is the Mordell-Weil rank. We introduce a basis of the torsionless subgroup of the Mordell-Weil group as  $Q_m, m = 1, \dots, r$ .

We note that the presence of a rational point can imply a factorization of the Weierstrass form. A case of particular interest later in this work is a point  $Q$  of the form  $[z : \tilde{x} : \tilde{y}] = [1 : A : B]$  for given numbers  $A, B$  in  $K$ . In this case, the Weierstrass equation (3.2) factorizes as

$$(\tilde{y} - Bz^3)(\tilde{y} + Bz^3) = (\tilde{x} - Az^2)(\tilde{x}^2 + A\tilde{x}z^2 + Cz^4), \quad (3.5)$$

as is easily checked by plugging in the point  $Q$ . This implies that the coefficients  $f, g$  in (3.2) as well as the discriminant in (3.4) can be parametrized as

$$f = C - A^2, \quad g = B^2 - AC, \quad \Delta = 16(27B^2(2AC - B^2) + (A^2 - 4C)(2A^2 + C)^2) \quad (3.6)$$

This parametrization will prove useful in the discussion of matter with only charge 1 under the Abelian gauge field corresponding to the rational point  $Q$  [97], i.e. codimension two singularities only due to the presence of the point  $Q$  in the fiber  $\mathcal{E}$  alone. We add that factorization properties of the Tate form (3.1) due to rational points of the form  $z = 0$  have been discussed in [91].

### 3.1.2 Elliptic Calabi-Yau Manifolds with Rational Sections

In this section we briefly discuss the geometry of an elliptically fibered Calabi-Yau threefold  $X$ , although we note that the following holds for general complex dimension of  $X$ .

By definition an elliptic fibration over a base  $B$  is defined by a holomorphic projection  $\pi : X \rightarrow B$  to the base  $B$ . We will be interested in fibrations with general fiber  $\mathcal{E} = \pi^{-1}(pt)$

over a generic point  $pt$  in  $B$  given by elliptic curve with a zero point and a number of rational points. As mentioned before we can always describe an elliptic fibration over  $B$  by its Weierstrass model (3.2), where the field  $K$  is replaced by the function field of  $B$ . Concretely, by the Calabi-Yau condition  $f, g$  are sections of the line bundles  $K_B^{-4}$  respectively  $K_B^{-6}$ , where  $K_B$  denotes the canonical bundle of the base. If it exists globally we can also construct the Tate form<sup>1</sup> (3.1) where the coefficients  $a_i$  take values in  $K_B^{-i}$ . The holomorphic zero section in the Tate and Weierstrass form is given by  $z = 0$ .

However, when having global questions in mind, such as the global resolution of singularities of the elliptic fibration  $X$  or the construction of rational sections, it is of advantage to consider elliptic fibrations  $X$  with the general elliptic fiber  $\mathcal{E}$  given as the Calabi-Yau hypersurface in one of the 16 two-dimensional toric varieties. It is always possible, as discussed at the end of section 3.1.1, to obtain the Weierstrass form of these fibrations by a birational map. In this note we will focus on the elliptic fibration with general fiber in  $dP_2$ , cf. section 3.2.1.

When we fiber an elliptic curve  $\mathcal{E}$  over a base  $B$  its zero point  $P$  becomes the zero section  $\hat{s}_P$  and its rational points  $Q_m$  lift to rational sections  $\hat{s}_m \equiv \hat{s}_{Q_m}$  of the elliptic fibration  $\pi : X \rightarrow B$ . All of these sections define injective maps  $\hat{s}_P, \hat{s}_m : B \hookrightarrow X$  and the group generated by the  $\hat{s}_m$  is the Mordell-Weil group of the elliptic fibration  $X$ . A holomorphic section, that is in the literature typically denoted by  $\sigma$ , defines a holomorphic injection  $\sigma : B \hookrightarrow X$  on all of  $B$ . However, a rational section does in general not vary holomorphically over the base  $B$ . Indeed, over codimension two or higher the rational section can be ill-defined and wrap components of the reducible fiber over the singular loci [97, 20]. Thus, rational sections  $\hat{s}_m$  can only be defined on the blow-up  $\pi_B : \hat{B} \rightarrow B$  of  $B$  along the singular loci of  $\hat{s}_m$  with  $\pi_B$  denoting the blow-down map. Consequently, a rational section defines only a birational map  $\hat{s}_m : \hat{B} \rightarrow B \hookrightarrow X$  of the base  $B$  into  $X$ .

---

<sup>1</sup>See [75] for a reconsideration of the validity of the Tate model in global F-theory compactifications.

In sections 3.2.1 and 3.3, we study elliptic fibrations with general fiber given by an elliptic curve  $\mathcal{E}$  with two rational points  $Q$ , and  $R$  and a zero section  $P$ . As we see there, in these cases even the zero section  $\hat{s}_P$  is not defined over codimension two and wraps fiber components of the elliptic fiber. A Calabi-Yau elliptic fibration without a holomorphic zero section still defines a valid F-theory background, although these most general fibrations have only recently drawn attention in the F-theory literature. As we discuss in section 3.3, the behavior of the three rational sections  $\hat{s}_P$  and  $\hat{s}_Q, \hat{s}_R$  leads to a rich structure of charged matter.

The group of divisors, or its dual group  $H^{(1,1)}(\hat{X})$ , on the smooth elliptic Calabi-Yau manifold  $\hat{X} \rightarrow X$  arising from  $X$  by resolving all singularities, is generated by divisors  $D_A$  that fall into four different classes of divisors:

- the zero section  $\hat{s}_P$  of the fibration with homology class  $S_P$ , which in the case of a holomorphic section  $\sigma$  agrees with the class of the base  $B$ ,
- the rational sections  $\hat{s}_m, m = 1, \dots, r$ , with divisor classes  $S_m$  generating the Mordell-Weil group of rational sections of the elliptic fibration of  $X$ ,
- the vertical divisors  $D_\alpha = \pi^*(D_\alpha^b), \alpha = 1, \dots, h^{(1,1)}(B)$ , of the fibration that are inherited from divisors  $D_\alpha^b$  in the base  $B$ ,
- exceptional divisors  $D_{i_l}$  resolving singularities of  $X$  from singularities in its elliptic fibration at irreducible components  $\Delta_l = 0$  of the discriminant locus  $\Delta = 0$  in  $B$ .

We summarize this basis of divisors on  $\hat{X}$  as

$$D_A = (B, S_m, D_\alpha, D_i), \quad A = 0, 1, \dots, h^{(1,1)}(\hat{X}). \quad (3.7)$$

We conclude with some key intersection properties of the divisors  $D_A$ . The exceptional



divisors  $D_{i_l}$  over one common discriminant locus intersect as

$$D_{i_l} \cdot D_{i_j} \cdot D_\alpha = -C_{i_l j_l}^{(I)} S_{(I)} \cdot B \cdot D_\alpha \quad (3.8)$$

where  $C_{i_l j_l}^{(I)}$  denotes the Cartan matrix of an ADE-group  $G_{(I)}$  in case of an ADE-singularity in the fibration. In this case we denote the  $D_{i_l}$  as the Cartan divisors of the corresponding ADE group. Here the divisors  $S_{(I)} = \pi^*(S_{(I)}^b)$  are related to the components of the discriminant and the  $S_{(I)}^b$  are the loci in the base  $B$  wrapped by 7-branes supporting a gauge group  $G_{(I)}$  in F-theory. Upon intersecting the Cartan divisors  $D_{i_l}$  with a divisor  $\tilde{D}$  in  $B$  that intersects  $S_{(I)}$  in a point, we obtain a rational curve that is localized over  $S_{(I)}$ . The relation (3.8) teaches us that this curve is to be identified with minus the root  $\alpha_{i_l}$  of the Lie-algebra of the ADE-group under consideration, i.e.

$$C_{-\alpha_{i_l}} := D_{i_l} \cdot \tilde{D} \quad \text{for} \quad \tilde{D} \cdot S_{(I)} \cdot B = 1. \quad (3.9)$$

Next we turn to the divisors  $S_P$  and  $S_m$  of the sections. By construction the divisors corresponding to a section will intersect the general fiber  $F \cong \mathcal{E}$  as

$$S_P \cdot F = S_m \cdot F = 1. \quad (3.10)$$

In addition we note that any section of  $X$  also has to obey [97]

$$B^2 = -[c_1(B)] \cdot B, \quad S_m^2 \cdot D_\alpha = -[c_1(B)] \cdot S_m \cdot D_\alpha, \quad (3.11)$$

where the first relation holds in homology and  $c_1(B)$  is the first Chern class of the base.

### 3.1.3 Abelian Gauge Sectors in F-Theory

In an F-theory compactification on  $X$  gauge fields  $A^a$  arise by expanding the M-theory three-form  $C_3$  in the dual M-theory compactification<sup>2</sup> along appropriate  $(1,1)$ -forms  $\omega_a$ ,

$$C_3 = \sum_a A^a \omega_a. \quad (3.12)$$

These are gauge fields along the Cartan generators of all  $G_{(I)}$  and along U(1) groups. The U(1)-gauge fields correspond to rational sections  $\hat{s}_m$  and are constructed from the cohomology classes dual to the divisors  $S_m$  of the rational sections by the Shioda map.

The Shioda map roughly speaking describes an orthogonalization procedure in the (co)homology group of  $\hat{X}$ . It is defined as the map from the Mordell-Weil group to  $H^{(1,1)}(\hat{X})$  given by [97, 105, 31]

$$\sigma(\hat{s}_m) := S_m - \tilde{S}_P - (S_m \cdot \tilde{S}_P \cdot D_\alpha) \eta^{\alpha\beta} D_\beta + \sum_I (S_m \cdot \mathcal{C}_{-\alpha_i}) (C_{(I)}^{-1})^{ij} D_{jI}, \quad (3.13)$$

where the curves  $\mathcal{C}_{-\alpha}$  have been defined in (3.9) and  $C_{(I)}^{-1}$  is the inverse of the Cartan matrix determined in (3.8). The divisor  $\tilde{S}_P = S_P + \frac{1}{2} \pi^* c_1(B)$  has been introduced for convenience, and is of relevance for the match of the F- and M-theory dual effective actions [56, 12]. The matrix  $\eta^{\alpha\beta}$  is the inverse of the intersection form of the divisors on the base,

$$\eta_{\alpha\beta} = D_\alpha^b \cdot D_\beta^b. \quad (3.14)$$

The Shioda map (3.13) maps into the orthogonal complement<sup>3</sup> in  $H^{(1,1)}(\hat{X})$  generated by the zero section  $S_P$ , the vertical divisors  $D_\alpha$  and the Cartan divisors  $D_{iI}$ . Thus it ensures that the gauge field associated to  $\sigma(\hat{s}_m)$  by the reduction (3.12) along the  $(1,1)$ -form  $\omega_m$

<sup>2</sup>See [53] for a general discussion of this and a derivation of the full F-theory effective action.

<sup>3</sup>The inner product is the Néron-Tate height pairing [115].

defined as the Poincare dual of  $\sigma(\hat{s}_m)$  is a U(1)-gauge field.

Having defined the Shioda map (3.13) it is straightforward to calculate U(1)-charges of matter fields in F-theory. The matter fields arise from M2-branes wrapping rational curves  $c$  in the fiber of the elliptic fibration that are localized in codimension two in the base  $B$ . Under the assumption of a holomorphic zero section with  $S_P = B$ , the charge of the M2-brane state under the U(1)-gauge field corresponding to the rational section  $\sigma_m$  is then calculated as [97]

$$\sigma(\hat{s}_m) \cdot c = (S_m \cdot c) + \sum_I (S_m \cdot \mathcal{C}_{-\alpha_{i_I}}) (C_{(I)}^{-1})^{i_I j_I} (D_{j_I} \cdot c). \quad (3.15)$$

This follows readily using the definition of the Shioda map (3.13) and the fact, that the isolated curves  $c$  neither intersect vertical divisors nor the holomorphic zero section.

We note that the intersection matrix between the  $\sigma(\hat{s}_m)$  projected into the homology of the base by  $\pi : \hat{X} \rightarrow B$  is

$$\pi(\sigma(\hat{s}_m) \cdot \sigma(\hat{s}_n)) = \pi(S_m \cdot S_n) + [K_B] - \pi(S_m \cdot B) - \pi(S_n \cdot B) + (C_{(I)}^{-1})^{i_I j_I} (S_m \cdot \mathcal{C}_{-\alpha_{i_I}}) (S_n \cdot \mathcal{C}_{-\alpha_{j_I}}) S_{(I)}^b. \quad (3.16)$$

Here, we introduced the definition

$$\pi(\mathcal{C}) = (\mathcal{C} \cdot D_\alpha) \eta^{\alpha\beta} D_\alpha^b \quad (3.17)$$

of the Néron-Tate height pairing for a curve  $\mathcal{C}$  and employed the normalized coroot matrix of the  $I$ -th 7-brane gauge group

$$C_{i_I j_I}^{(I)} = \frac{2}{\lambda_I \langle \alpha_{i_I}, \alpha_{j_I} \rangle} C_{i_I j_I}^{(I)}. \quad (3.18)$$

In this expression we denote the inner product on the Lie-algebra by  $\langle \cdot, \cdot \rangle$  and introduced the length squared  $\lambda_I = \frac{2}{\langle \alpha_0, \alpha_0 \rangle}$  of the maximal root  $\alpha_0$ . The intersections (3.16) will be relevant for the discussion of anomaly cancellation in section 3.4.

We conclude by noting that if the zero section  $\hat{s}_P$  is only rational, the formula for the U(1)-charge has to be modified. The reason for this is that we have to relax the condition  $B \cdot c = 0$  and in general assume a non-trivial intersection

$$S_P \cdot c \neq 0, \quad (3.19)$$

where  $S_P$  denotes the homology class of the rational zero section. Then (3.15) has to be replaced by

$$\sigma(\hat{s}_m) \cdot c = (S_m \cdot c) - (S_P \cdot c) + \sum_I (S_m \cdot \mathcal{C}_{-\alpha_{I_i}}) (C_{(I)}^{-1})^{i_j j_i} (D_{j_i} \cdot c). \quad (3.20)$$

In contrast, the formula (3.16) for the intersections of sections does not have to be modified. We note that (3.20) has also been used in [20].

## 3.2 Elliptic Fibrations with Two Rational Sections

In this section we determine an elliptic fibration with two rational sections and a zero section, i.e. an elliptic curve with Mordell-Weil group of rank two. This curve serves as the model for the general elliptic fiber in an elliptically fibered Calabi-Yau manifold. As discussed in section 3.1 the F-theory compactification on such a Calabi-Yau admits two U(1)-gauge groups.

We first find in section 3.2.1 that any elliptic curve  $\mathcal{E}$  with three marked points (two rational and the zero point) has a representation as a non-generic cubic in  $\mathbb{P}^2$ . We argue further that this elliptic curve should be properly viewed as the generic Calabi-Yau onefold in the del Pezzo surface  $dP_2$ , which is the blow up of  $\mathbb{P}^2$  at two generic points. However, we first focus on the singular model of  $\mathcal{E}$  by neglecting the blow-ups in  $\mathbb{P}^2$ . This allows us

to compute the Weierstrass model for  $\mathcal{E}$  with respect to one of the three rational points on it and derive the location of the two other rational points in Weierstrass coordinates.

Then, in section 3.2.2, we discuss the resolution geometry of  $\mathcal{E}$  in  $dP_2$  that we obtain by performing the two blow-ups in  $\mathbb{P}^2$ . The understanding of the resolved geometry is relevant to resolve elliptic fibrations with general fiber being the curve  $\mathcal{E}$ . We conclude by constructing elliptic fibrations with  $\mathcal{E}$  and find that all elliptic fibrations with base  $B = \mathbb{P}^2$  are classified by two integers  $n_2$  and  $n_{12}$ . We will consequently denote the families of  $dP_2$ -fibrations over  $\mathbb{P}^2$  we have found as  $dP_2(n_2, n_{12})$ .

Our discussion partly follows and extends the techniques of appendix B of [97].

### 3.2.1 Constructing an Elliptic Curve with two Rational Points

Our discussion in this section is based on the following basic mathematical fact: Given an algebraic variety  $X$  with a very ample line bundle<sup>4</sup>  $M$  defined over it, we can find an embedding of  $X$  into projective space. If this is the case, we will have enough independent global sections  $a_0, \dots, a_n$  such that for every point  $x \in X$  there exists at least one section not vanishing at this point. Thus, there is an immersion

$$f: X \rightarrow \mathbb{P}^n \quad x \mapsto [a_0(x) : \dots : a_n(x)] \quad (3.21)$$

with  $M \cong f^*(\mathcal{O}(1))$ .

The algebraic variety we are interested in is an elliptic curve  $\mathcal{E}$  over a field  $K$ . We find the embedding of the curve  $\mathcal{E}$  into projective space, or more generally a toric variety, explicitly as a hypersurface. For this purpose we consider the global sections of powers of  $M^k$ . For sufficiently large  $k$ , in our case  $k = 3$ , not all sections are independent and the relation between them yield the desired hypersurface equation.

---

<sup>4</sup>A very ample line bundle is a line bundle that has “enough” global sections so that its base variety is embedable into projective space.

As a warm-up we use this logic to derive the Tate form (3.1) of an elliptic curve  $\mathcal{E}$  with only the zero point  $P$  as follows. We introduce the degree one line bundle  $M = \mathcal{O}(P)$  over  $\mathcal{E}$  and consider the homogeneous coordinates  $[z : x : y]$  on  $\mathbb{P}^2(1, 2, 3)$  as sections of the line bundles  $M$ ,  $M^2$  and  $M^3$ , respectively. We recall that in the case of an elliptic curve  $\mathcal{E}$  the Riemann-Roch theorem tells us that the number of independent global holomorphic sections of a line bundle  $M$  of degree  $d$  is  $h^0(X, M) = d$ . Then the bundle  $M^6$  has six independent holomorphic sections, however, we can construct seven sections from  $z, x, y$ . Thus, there has to be a relation between these sections which yields precisely the Tate form (3.1) in  $\mathbb{P}^2(1, 2, 3)$ .

The same strategy applies to finding the equation that describes an elliptic curve with rational points  $Q_m$ . Concretely, we first find the sections  $[z : x : y]$  of  $\mathcal{O}(kP)$ ,  $k = 1, 2, 3$ , and then determine the relation between sections of higher degree generated from  $[z : x : y]$ . We perform this procedure in the following for an elliptic curve  $\mathcal{E}$  with a zero point  $P$  and two rational points denoted  $Q$  and  $R$ . In the same spirit as before we first start with a general line bundle  $M$  of degree three that we then specialize to  $M = \mathcal{O}(P + Q + R)$ . The group of holomorphic section  $H^0(M)$  is generated by three sections denoted  $u, v, w$ . The space  $H^0(2M)$  has dimension six with sections  $u^2, v^2, w^2, uv, vw$  and  $wu$ . The space  $H^0(3M)$  must have nine independent sections, however we know ten of them. Consequently, there has to be a linear relation of the form

$$s_1u^3 + s_2u^2v + s_3uv^2 + s_4v^3 + s_5u^2w + s_6uvw + s_7v^2w + s_8uw^2 + s_9vw^2 + s_{10}w^3 = 0, \quad (3.22)$$

with coefficients  $s_i$  in the field  $K$ . This equation can be interpreted as the cubic hypersurface in  $\mathbb{P}^2$ . Even more it is a section of its anti-canonical bundle  $\mathcal{O}(3H)$ , see figure 3.1, where  $H$  denotes the hyperplane class in  $\mathbb{P}^2$ . Thus the zero of this section defines the

one-dimensional Calabi-Yau manifold, i.e. the torus<sup>5</sup>.

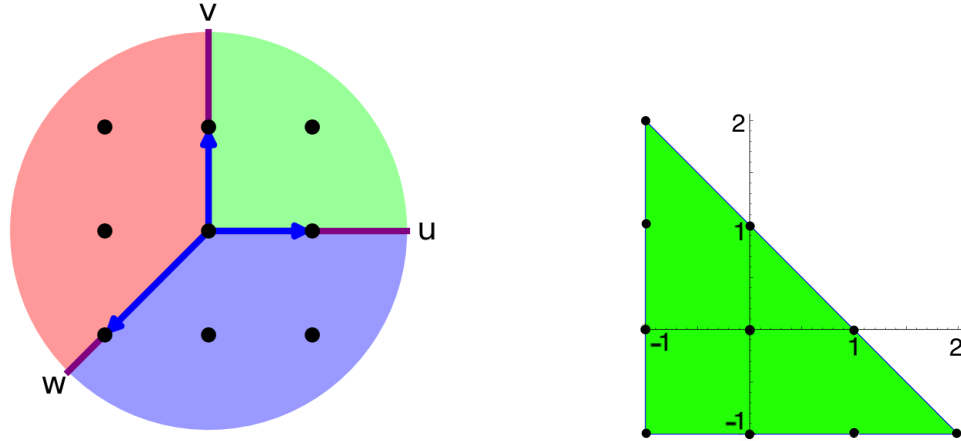


Figure 3.1: Fan of  $\mathbb{P}^2$  on the left and its dual polytope on the right.

Now we specialize to  $M = \mathcal{O}(P + Q + R)$ . Let us assume that the section  $u$  vanishes at the three points  $P$ ,  $Q$  and  $R$ , then equation (3.22) simplifies to

$$s_4 v^3 + s_7 v^2 w + s_9 v w^2 + s_{10} w^3 = 0. \quad (3.23)$$

Performing appropriate shifts of the coordinates  $v$  and  $w$  we can always get rid of the coefficients  $s_4$  and  $s_{10}$ . However, these variable transformations involve square roots of the coefficients  $s_i$  that are generically not defined over the field  $K$ . Thus, we specialize the constraint (3.22) by setting the coefficients  $s_4$  and  $s_{10}$  to zero. This specialization can also be viewed as changing the toric ambient variety such that the coefficients  $s_4$  and  $s_{10}$  are automatically absent by means of the toric construction. This is achieved by going from  $\mathbb{P}^2$  to  $dP_2$ , which is the blow-up of  $\mathbb{P}^2$  at two generic points. In figure 3.2 we have depicted the polytope of  $dP_2$  for the blow-up at  $[u : v : w] = [0 : 0 : 1]$  and  $[u : v : w] = [0 : 1 : 0]$ . We note that the blow-ups introduces new exceptional divisors  $E_i$  with coordinates  $e_i$ ,  $i = 1, 2$ .

This latter perspective on the specialization of the constraint (3.22) as the Calabi-Yau

---

<sup>5</sup>There is a one-to-one correspondence between elliptic curves and two-tori.

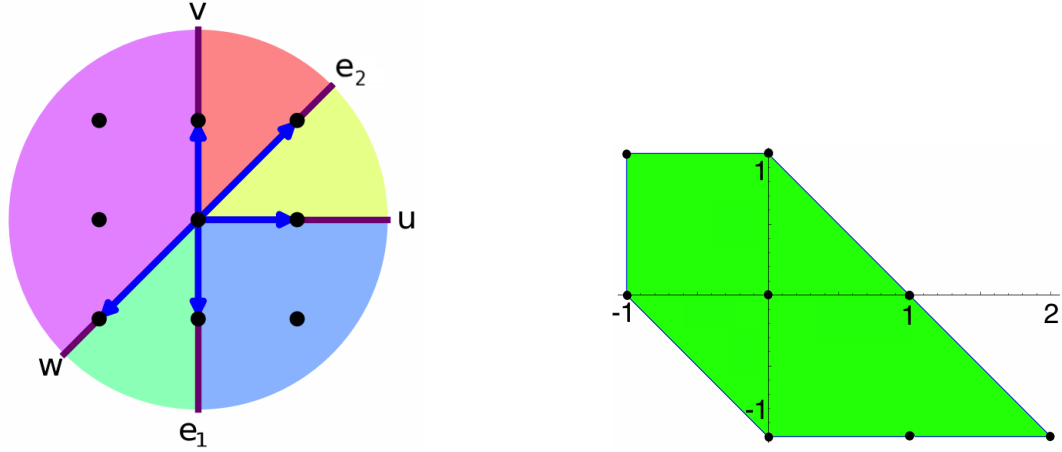


Figure 3.2: Fan of  $dP_2$  on the left and its dual polytope on the right.

hypersurface in  $dP_2$  is of particular relevance for the construction of smooth elliptic fibrations in F-theory. However, the blown-up geometry  $dP_2$  is of no importance for the determination of the Weierstrass model of the curve elliptic curve  $\mathcal{E}$  with the rational points  $Q$  and  $R$ , with which we proceed in the remainder of this section. Thus, we discuss the resolved geometry of  $dP_2$  with all divisor classes including the exceptional divisors  $E_i$  separately in section 3.2.2 and work for the following in the patch  $e_1 = 1, e_2 = 1$ .

The restricted hypersurface following from (3.22) with  $s_4 = s_{10} = 0$  takes now the form

$$p \equiv s_1 u^3 + s_2 u^2 v + s_3 u v^2 + s_5 u^2 w + s_6 u v w + s_7 v^2 w + s_8 u w^2 + s_9 v w^2 = 0. \quad (3.24)$$

Then, this hypersurface constraint specializes at  $u = 0$  to

$$v w (s_7 v + s_9 w) = 0, \quad (3.25)$$

which vanishes at the three different points with coordinates

$$P = [0 : 0 : 1], \quad Q = [0 : 1 : 0], \quad R = [0 : s_9 : -s_7]. \quad (3.26)$$



We emphasize that the points  $P$  and  $Q$  coincide with precisely those points at which we blow up  $\mathbb{P}^2$  into  $dP_2$ , see section 3.2.2 for a more detailed discussion.

We note that we could set even more coefficients  $s_i$  to zero or to one by using the automorphisms of the ambient space, e.g. by shifting or rescaling variables and the equation, if we were interested in the properties of the elliptic curve alone. For example the shift symmetry of  $w$  by an appropriate factor of  $u$  is still unbroken in the presence of the rational points  $Q$  and  $R$  since these are left invariant. For example, we can perform the transformation  $w \rightarrow w' - \frac{s_5}{2s_8}u$  to eliminate the term  $u^2w$  in (3.24)<sup>6</sup>. However, we use later in sections the elliptic curve defined by (3.24) as the general elliptic fiber in an elliptically fibered Calabi-Yau manifold. Then the coefficients  $s_i$  are lifted to sections over the base of the fibration. In this case the embedding of the fiber into the Calabi-Yau manifold will in general forbid eliminating more  $s_i$  than those in (3.24). Therefore, we work with the most general form (3.24) of an elliptic curve with two rational points.

To obtain the Weierstrass equation with respect to  $P$ , we need to find the three sections of  $H^0(kP) = H^0(kM - kQ - kR)$  for  $k = 1, 2, 3$ . These sections are precisely the projective coordinates  $z, \tilde{x}, \tilde{y}$  of the Weierstrass model in  $\mathbb{P}^2(1, 2, 3)$ . For the purpose of constructing these sections we determine sections of  $H^0(kM)$  on the ambient space  $dP_2$  that simultaneously vanish  $k$  times both at  $Q$  and  $R$ <sup>7</sup> when restricted to  $\mathcal{E}$ .

The general derivation of this birational transformation from the cubic (3.24) to the Tate model (3.1) and then the Weierstrass form (3.2) is quite lengthy. Therefore we first

---

<sup>6</sup>The coefficients will take the form

$$s'_1 = s_1 - \frac{s_5^2}{4s_8}, \quad s'_2 = s_2 - \frac{s_5s_6}{2s_8} + \frac{s_5^2s_9}{4s_8^2}, \quad s'_3 = s_3 - \frac{s_5s_7}{2s_8}, \quad s'_6 = s_6 - \frac{s_5s_9}{s_8}, \quad (3.27)$$

with the other coefficients unchanged.

<sup>7</sup>We note that this somewhat counter-intuitive fact follows from the fact that we implicitly divide by a function  $g$  vanishing at  $P + Q + R$ . Indeed, we recall the definition of the line bundle associated to a Cartier divisor  $D$ ,  $\mathcal{O}(D) := \{\frac{f}{g} \mid \text{div}(\frac{f}{g}) + D \geq 0\}$  for local functions  $f, g$ , cf. [52]. Applying this for  $\mathcal{O}(P + Q + R)$  we obtain that  $g$  has three zeros precisely at  $P, Q, R$ , with  $f$  of degree three vanishing elsewhere. For  $\mathcal{O}(P)$  we obtain  $g$  has to vanish at  $P$  and  $f$  is of degree one. Then, sections of  $\mathcal{O}(P)$  are a subset of sections of  $\mathcal{O}(P + Q + R)$  by demanding that  $f$  in the latter vanishes precisely at  $Q$  and  $R$ .

summarize the results and present the proof in the remainder of the section for the interested reader. The birational map from the projective coordinates  $[u : v : w]$  of  $dP_2$  to  $[z : \tilde{x} : \tilde{y}]$  in the Weierstrass model (3.2) reads

$$\begin{aligned}
z &= u, \\
\tilde{x} &= s_3 s_9 u v + (s_6 s_9 - s_7 s_8) u w + s_7 s_9 v w + s_9^2 w^2 + \left(\frac{1}{12} s_6^2 - \frac{1}{3} s_3 s_8 - \frac{1}{3} s_5 s_7 + \frac{2}{3} s_2 s_9\right) z^2 \\
\tilde{y} &= \frac{1}{2} \left[ s_3 (s_6 s_9 - 2 s_7 s_8) u^2 v + (s_6^2 s_9 - s_6 s_7 s_8 + 2 s_9 (-s_5 s_7 - s_3 s_8 + s_2 s_9)) u^2 w \right. \\
&\quad + (s_6 s_7 s_9 - 2 s_7^2 s_8 + 2 s_3 s_9^2) u v w + (3 s_6 s_9^2 - 4 s_7 s_8 s_9) u w^2 + s_7 s_9^2 v w^2 + 2 s_9^3 w^3 \\
&\quad \left. + (s_2 s_6 s_9 - s_2 s_7 s_8 - s_3 s_5 s_9 - s_1 s_7 s_9) z^3 \right]. \tag{3.28}
\end{aligned}$$

The sections defined like this obey the Weierstrass constraint (3.2),

$$\tilde{y}^2 = \tilde{x}^3 + f \tilde{x} z^4 + g z^6 \tag{3.29}$$

with the parameters  $f$  and  $g$  determined via (3.4) in terms of the three polynomials

$$\begin{aligned}
b_2 &= s_6^2 - 4 s_5 s_7 - 4 s_3 s_8 + 8 s_2 s_9, \\
b_4 &= 2 s_2^2 s_9^2 + s_1 s_7 (2 s_7 s_8 - s_6 s_9) + s_2 (s_6^2 s_9 - s_6 s_7 s_8 - 2 s_5 s_7 s_9) \\
&\quad + s_3 (2 s_5 s_7 s_8 - s_5 s_6 s_9 - 2 s_2 s_8 s_9 + 2 s_1 s_9^2), \\
b_6 &= (s_2 s_7 s_8 + s_3 s_5 s_9 - s_2 s_6 s_9 + s_1 s_7 s_9)^2 \\
&\quad - 4 s_1 s_3 (s_7^2 s_8^2 + s_9^2 (s_3 s_8 - s_2 s_9) + s_7 s_9 (s_5 s_9 - s_6 s_8)). \tag{3.30}
\end{aligned}$$

We have summarized the somewhat lengthy expressions for  $f$ ,  $g$  along with the Tate coefficient  $a_i$  and the discriminant in the appendix of [34].

Along similar lines outlined below, we obtain the coordinates for the generators of the Mordell-Weil group of  $\mathcal{E}$  given by the rational points  $Q$  and  $R$  in Weierstrass form. The

result reads

$$Q = [\tilde{x}_Q : \tilde{y}_Q : z_Q] = \left[ \frac{1}{12}(s_6^2 - 4s_5s_7 + 8s_3s_8 - 4s_2s_9), \frac{1}{2}(s_3s_6s_8 - s_2s_7s_8 - s_3s_5s_9 + s_1s_7s_9) : 1 \right] \quad (3.31)$$

for  $Q$  and analogously for  $R = [\tilde{x}_R : \tilde{y}_R : z_R]$ ,

$$\begin{aligned} \tilde{x}_R &= \frac{1}{12}(12s_7^2s_8^2 + s_9^2(s_6^2 + 8s_3s_8 - 4s_2s_9) + 4s_7s_9(-3s_6s_8 + 2s_5s_9)), \\ \tilde{y}_R &= \frac{1}{2}(2s_7^3s_8^3 + s_3s_9^3(-s_6s_8 + s_5s_9) + s_7^2s_8s_9(-3s_6s_8 + 2s_5s_9) \\ &\quad + s_7s_9^2(s_6^2s_8 + 2s_3s_8^2 - s_5s_6s_9 - s_2s_8s_9 + s_1s_9^2)), \\ z_R &= s_9. \end{aligned} \quad (3.32)$$

In the remainder of the section we derive the final results (3.28) and (3.30). The reader less interest in these details can safely skip to section 3.2.2. Beginning with  $H^0(M)$ , we already know that the section  $u = 0$ , by assumption, vanishes at the three points  $P$ ,  $Q$  and  $R$ . Thus we set

$$z := u. \quad (3.33)$$

Next we need two find a section of  $H^0(2M)$  with double zeros at  $Q$  and  $R$  on  $\mathcal{E}$ . There are two such sections, one of which is given by the section  $u^2 = z^2$ . The other one is constructed from an appropriate linear combination of the other elements of  $H^0(2M)$ . We make the ansatz

$$x := av^2 + buv + cw^2 + dvw + euw. \quad (3.34)$$

The coefficients are fixed requiring that the section  $x$  vanishes at degree two on both points  $Q$  and  $R$ . This gives us four equations. The other coefficient can be rescaled away using the scaling of  $x$ .

A nice pictorial way to think about these conditions on the coefficients in  $x$  is to realize

that  $x = 0$  and  $p = 0$  in (3.24) are two curves in the ambient space  $dP_2$ . Then the first two of the four conditions on the coefficients enforce that  $x$  vanishes at the points  $P, Q$ , which are also automatically the intersections of  $p = 0$  and  $x = 0$ . The other two conditions on the coefficients then make  $Q, R$  a double zero or equivalently let the curves intersect tangentially.

A systematic way of finding the coefficients is to solve for one of the variables  $u, v, w$  in one of the equations  $p = 0, x = 0$  and then to use the other one to determine the unknown coefficients in (3.34) in order to obtain the right order of vanishing. First we note that both  $Q$ , and  $R$  can be described in the affine patch  $v = 1$ . To solve for one of the remaining variables  $u, w$  instead of dealing with radicals we can approximate the curve  $\mathcal{E}$  by a Taylor expansion. We solve for  $w \equiv w(u)$  order by order in  $u$  by considering  $f(u, 1, w(u)) = 0$  as an implicit function for  $w$  in terms of  $u$ . Expanding the curve  $p = 0$  first around  $Q$ , then around  $R$  with coordinates (3.26) we obtain, omitting terms of third order and higher in  $u$ ,

$$\begin{aligned} Q: w &= -\frac{s_3}{s_7}u - \frac{1}{s_7} \left( s_2 - \frac{s_3 s_6}{s_7} + \frac{s_3^2 s_9}{s_7^2} \right) u^2, \\ R: w &= -\frac{s_7}{s_9} + \left( \frac{s_3}{s_7} + \frac{s_7 s_8 - s_6 s_9}{s_9^2} \right) u + \left( \frac{s_2}{s_7} - \frac{s_3 s_6}{s_7^2} + \frac{s_3^2 s_9}{s_7^3} - \frac{s_7 s_8^2 - s_6 s_8 s_9 + s_5 s_9^2}{s_9^3} \right) u^2. \end{aligned} \tag{3.35}$$

Now we can pull back the section  $x$  to the curve  $\mathcal{E}$  by simply plugging the solution for  $w(u)$  into the ansatz (3.34) for  $x$ . Since we require an order of vanishing of two we have to set the coefficients of  $u^0$  and  $u^1$  to zero. Employing the expansion (3.35) at  $Q$  yields

$$a = 0, \quad b - \frac{s_3}{s_7}d = 0. \tag{3.36}$$

Proceeding similarly around  $R$  using (3.35), we obtain two further equations

$$a + \frac{s_7^2}{s_9^2}c - \frac{s_7}{s_9}d = 0, \quad b + \frac{s_7^2s_8 - s_6s_7s_9 + s_3s_9^2}{s_7s_9^2}d + 2\frac{s_6s_7s_9 - s_7^2s_8 - s_3s_9^2}{s_9^3}c - \frac{s_7}{s_9}e = 0. \quad (3.37)$$

Solving these equations, setting  $c = 1$  by rescaling and cleaning denominators in  $x$ , we finally get the section

$$x = s_3s_9uv + (s_6s_9 - s_7s_8)uw + s_7s_9vw + s_9^2w^2. \quad (3.38)$$

Next, we need three elements of  $H^0(3M)$  with triple zeros at  $Q$  and  $R$  on the curve  $\mathcal{E}$ . We know ten sections of this bundle, only nine are independent and we already know two combinations that vanish appropriately, namely  $u^3$  and  $ux$ . The other possible section has to be a linear combination of the remaining seven sections and we make the ansatz

$$y := au^2v + bv^3 + cw^3 + dv^2w + euw^2 + fvw^2 + guvw. \quad (3.39)$$

Proceeding in the same way as before, we use the solutions (3.35) to pull the section  $y$  to the curve  $\mathcal{E}$ , but now require that it vanishes at order  $u^3$  both at  $Q$  and  $R$ . This yields three conditions for each point, i.e. a total of six conditions, by demanding that the terms  $u^0$ ,  $u^1$  and  $u^2$  are absent. Setting  $c = 1$  by rescaling  $y$  and cleaning some denominators, we obtain

$$\begin{aligned} y = & \frac{s_3(s_7^2s_8^2 - s_6s_7s_8s_9 + s_5s_7s_9^2 + s_3s_8s_9^2 - s_2s_9^3)}{s_6s_9 - s_7s_8}u^2v \\ & + \frac{s_7^3s_8^2 - s_6s_7^2s_8s_9 + s_5s_7^2s_9^2 + s_3s_6s_9^3 - s_2s_7s_9^3}{s_6s_9 - s_7s_8}uvw + s_7s_9^2vw^2 \\ & + \frac{s_9(2s_7^2s_8^2 - 3s_6s_7s_8s_9 + s_6^2s_9^2 + s_5s_7s_9^2 + s_3s_8s_9^2 - s_2s_9^3)}{s_6s_9 - s_7s_8}uw^2 + s_9^3w^3. \end{aligned} \quad (3.40)$$

Now that we know the form of the sections  $x, y$  we can determine the Tate model (3.1)

by plugging in the solutions (3.38), (3.40) and solving for the Tate coefficients  $a_i$ . We note that in order to find a solution we have to reduce the Tate form, which is a degree six polynomial in  $u, v, w$ , in the ideal generated by the original cubic constraint (3.24). We present the results for the  $a_i$  in equation (A.2) in the appendix of [34], from which we immediately calculate the coefficients  $b_2, b_4$  and  $b_6$  in (3.30). From the Tate model, the Weierstrass form (3.2) can be obtained by the variable transformation (3.3) that takes the form of (3.28) as claimed. We readily obtain the functions  $f$  and  $g$  in the Weierstrass model and the discriminant.

Next, we focus on finding the rational points  $Q$  and  $R$  in Weierstrass form. Recalling that there is an implicit multiplication by a meromorphic function with poles of degree  $k$  in each case, we obtain the coordinates for  $Q$  ( $R$ ) if we look for a section  $x'$  of degree two that vanishes three times at  $Q$  ( $R$ ). We have to include all elements of  $H^0(2M)$ :

$$x' := av^2 + buv + cw^2 + dvw + euw + \tilde{f}u^2, . \quad (3.41)$$

The new parameter  $\tilde{f}$  is fixed by the additional constraint from the vanishing of the coefficient of  $u^2$ , while all the other coefficients take the same values as before. Noting that  $z \equiv u$ , we then obtain

$$x' = x - (s_3s_8 - s_2s_9)z^2 \stackrel{!}{=} 0 \quad (3.42)$$

at  $Q$  which fixes the  $x$ -coordinate of  $Q$ . After scaling and going to the Weierstrass coordinates we obtain the generator as in (3.31), where the  $\tilde{y}$ -coordinate of  $Q$  is obtained by solving (3.29) for  $\tilde{y}$  given  $\tilde{x}_Q$ . Following the same procedure for the point  $R$  we confirm the result (3.32).

### 3.2.2 Resolved Elliptic Curve in $dP_2$ and its Elliptic Fibrations

In this section we discuss the key geometric properties of the resolution of the elliptic curve (3.24) in  $dP_2$ . To this end we have to take into account the exceptional divisors  $E_i$  and their sections  $e_i$ ,  $i = 1, 2$  that we have set to one in the previous discussion. Then, smoothness of  $\mathcal{E}$  is ensured by the toric construction since the curve (3.24) lifts to the generic Calabi-Yau onefold in  $dP_2$ . The smoothness property even holds in elliptic fibrations  $X$  with general fiber given by  $dP_2$ , if the most generic toric Calabi-Yau hypersurface is considered. Indeed, as we discuss explicitly in section 3.3 the divisors  $E_1, E_2$  resolve the singularities of the fibration at codimension two and higher. In particular, this allows us to determine the matter spectrum in F-theory from the splitting of the elliptic curve in  $dP_2$  over codimension two from the presence of the new projective coordinates  $e_i$ .

We construct  $dP_2$  as follows. We blow up  $\mathbb{P}^2$  at the two points  $[u : v : w] = [0 : 1 : 0]$  and  $[u : v : w] = [0 : 0 : 1]$  by introducing two new projective coordinates  $e_1, e_2$  as

$$u = u' e_1 e_2, \quad v = v' e_2, \quad w = w' e_1. \quad (3.43)$$

This is the blow-down map  $\pi : dP_2 \rightarrow \mathbb{P}^2$ , where  $e_1, e_2$  are holomorphic sections vanishing at the exceptional divisors  $E_1, E_2$ . We see that the original codimension two loci  $u = w = 0$ , respectively,  $u = v = 0$  in  $\mathbb{P}^2$  are replaced by  $e_1 = 0$ , respectively,  $e_2 = 0$ , i.e. by entire divisors  $E_i$  with the geometry of  $\mathbb{P}^1$ . We summarize the toric realization of  $dP_2$  encoded in

its polytope  $\Delta_{dP_2}$  and its homogeneous coordinates as

	vertices			divisor class
$v_1$	1	0	$u'$	$H - E_1 - E_2$
$v_2$	0	1	$v'$	$H - E_2$
$v_3$	-1	-1	$w'$	$H - E_1$
$v_4$	0	-1	$e_1$	$E_1$
$v_5$	1	1	$e_2$	$E_2$

(3.44)

Here we denote the vertices of  $\Delta_{dP_2}$  by  $v_i$  in the first row and write them explicitly as two-dimensional row-vectors in the second and third column as depicted in the polytope in figure 3.2. The only integral internal point is the origin. In the third and fourth column we summarize the homogeneous coordinates on  $dP_2$  and their divisor classes, where  $H$  is the pullback of the hyperplane class on  $\mathbb{P}^2$  and the  $E_i$  are the exceptional divisors. This in particular implies that the anti-canonical bundle  $K_{dP_2}^{-1}$  of  $dP_2$ , which is computed as the negative of the sum of all toric divisors, has changed to  $K_{dP_2}^{-1} = \mathcal{O}(3H - E_1 - E_2)$ , compared to  $K_{\mathbb{P}^2}^{-1} = \mathcal{O}(3H)$  before the blow-ups.

We note the intersections in the star triangulation of  $\Delta_{dP_2}$  with star given by the origin as

$$H^2 = 1, \quad H \cdot E_i = 0, \quad E_i \cdot E_j = -\delta_{ij}. \quad (3.45)$$

Here we made use of the exceptional set, the Stanley-Reissner ideal  $SR$  of all vertices not sharing a two dimensional cone, reading

$$SR = \{u'v', u'w', e_1e_2, e_1v', e_2w'\}. \quad (3.46)$$

We observe that the polytope of  $\mathbb{P}^2$  is embedded by the first three points  $v_1, v_2$  and



$v_3$ . The addition of the vertices  $v_4, v_5$  not only introduces the divisors  $E_i$  but also removes the corners  $(-1, 2)$  and  $(-1, -1)$  of the dual polytope of  $\mathbb{P}^2$ , compare figures 3.1 and 3.2. These corners correspond precisely to the monomials  $s_4v^3$  and  $s_{10}w^3$  in  $\mathbb{P}^2$ , that are no longer admissible sections of the anti-canonical bundle on  $dP_2$ . As one can see by either looking at dual polytope 3.2 or by writing down all sections of the anti-canonical bundle  $\mathcal{O}(3H - E_1 - E_2)$  of  $dP_2$  by hand with the charge assignments in (3.44), the generic Calabi-Yau hypersurface  $p'$  on  $dP_2$  reads

$$p' = u'(s_1u'^2e_1^2e_2^2 + s_2u'v'e_1e_2^2 + s_3v'^2e_2^2 + s_5u'w'e_1^2e_2 + s_6v'w'e_1e_2 + s_8w'^2e_1^2) + s_7v'^2w'e_2 + s_9v'w'^2e_1. \quad (3.47)$$

Now we investigate the pullback under  $\pi$  of the points  $P, Q$  and  $R$  in (3.26) that we by abuse of notation denote by the same symbols. We readily infer from the map (3.43) that the section  $u \in \mathcal{O}(P + Q + R)$  splits into three components as expected and we identify  $P$  as  $e_2 = 0$ ,  $Q$  as  $e_1 = 0$  and the image of  $R$  as  $D_{u'} := \{u' = 0\}$ . The value of all coordinates in the notation  $[u' : v' : w' : e_1 : e_2]$  is obtained by inserting these components into the hypersurface equation (3.47) and setting all coordinates to 1 that do not intersect the component under consideration due to the exceptional set (3.46). This yields

$$\begin{aligned} P : E_2 \cap p' &= [-s_9 : s_8 : 1 : 1 : 0], & Q : E_1 \cap p' &= [-s_7 : 1 : s_3 : 0 : 1], \\ R : D_{u'} \cap p' &= [0 : 1 : 1 : -s_7 : s_9] \end{aligned} \quad (3.48)$$

for the coordinates of the points  $P, Q$  and  $R$  on the resolved curve in  $dP_2$ .

We emphasize the dependence of the points  $P, Q, R$  on the  $s_i$ , in particular the situation when certain  $s_i$  vanish. Note that it is manifest in the form (3.48), that the points  $P, Q$  and  $R$  are ill-defined if  $s_i = s_j = 0$  simultaneously for the combinations  $(i, j)$  in (3.48) due to the Stanley-Reissner ideal (3.46). In particular, when considering elliptic fibrations  $\hat{X}$

with elliptic fiber given by (3.47) this translates to a special behavior of the corresponding sections  $\hat{s}_P, \hat{s}_Q, \hat{s}_R$  at codimension two loci  $s_i = s_j = 0$ . Note that the  $s_i$  lift to sections on the base  $B$  of the fibration  $\hat{X}$ , see the next paragraph, and can generically vanish. As we discuss in detail in the next section 3.3 this behavior is the key to understand the matter spectrum of an F-theory compactification on  $\hat{X}$ .

We would like to conclude by discussing the general construction of an elliptic fibration  $\hat{X}$  over a base  $B$ . For concreteness we focus on fibrations over  $B = \mathbb{P}^2$  noting that the following can readily be generalized to different bases. First, we construct all fibrations of  $dP_2$  over  $\mathbb{P}^2$ . The total space of this fibration of toric varieties is classified only by two integers, that we denote by  $n_2$  and  $n_{12}$  for reasons that will become clear below. We denote the total space as

$$dP_2 \rightarrow dP_2(n_2, n_{12}) \rightarrow \mathbb{P}^2. \quad (3.49)$$

It is clear that the fibration  $dP_2(n_2, n_{12})$  is only specified by two integers because we can associate each projective coordinates  $u', v', w', e_1, e_2$  to a different line bundle  $\mathcal{O}(k_i H_B)$ ,  $i = 1, \dots, 5$  on  $\mathbb{P}^2$ , where  $H_B$  is the hyperplane of the  $\mathbb{P}^2$ -base. However, by means of the three  $\mathbb{C}^*$ -actions on  $dP_2$  we can always eliminate three  $k_i$  and denote remaining two degrees as  $n_2, n_{12}$ . Then, a possible assignment is

$$u' \in \mathcal{O}((n_2 - 3)H_B), \quad v' \in \mathcal{O}((n_2 - n_{12})H_B), \quad (3.50)$$

with all other coordinates taking values in the trivial bundle on  $\mathbb{P}^2$ . Next, we note that the anti-canonical bundle of  $dP_2(n_2, n_{12})$  is calculated by adjunction as

$$K_{dP_2(n_2, n_{12})}^{-1} = \mathcal{O}(3H - E_1 - E_2 + (2n_2 - n_{12})H_B). \quad (3.51)$$

From this and the Calabi-Yau constraint (3.47) we can finally read off the degrees of the

coefficients  $s_i$ , that now lift to sections of  $\mathbb{P}^2$  as well:

$s_1$	$s_2$	$s_3$	$s_5$	$s_6$	$s_7$	$s_8$	$s_9$
$9 - n_2 - n_{12}$	$6 - n_2$	$3 + n_{12} - n_2$	$6 - n_{12}$	$3$	$n_{12}$	$3 + n_2 - n_{12}$	$n_2$

(3.52)

Here the second line denotes the first Chern class or in other words the degree of the section  $s_i$  with respect to the hyperplane class  $H_B$  on the base.

Finally, (3.52) illuminates the meaning of the integers  $n_2$  and  $n_{12}$ . The sections  $s_7$  and  $s_9$  vanish at curves of degree  $n_2$  respectively  $n_{12}$  in  $\mathbb{P}^2$ . But as we see from (3.48) these are precisely the loci where the points  $Q$  and  $R$ , now lifted to rational sections  $\hat{s}_Q$ ,  $\hat{s}_R$ , respectively the points  $P$ , also lifted to a section  $\hat{s}_P$ , and  $R$  coincide. In other words, these integers calculate the following intersections, cf. (3.17),

$$n_2 = \pi(S_P \cdot S_R) = S_P \cdot S_R \cdot H_B, \quad n_{12} = \pi(S_Q \cdot S_R) = S_Q \cdot S_R \cdot H_B, \quad (3.53)$$

where we denoted the divisor classes of the sections by capital letters following the conventions of section 3.1.2.

### 3.3 Matter Spectrum: Codimension Two Singularities

In this section we determine the generic matter spectrum of a six-dimensional F-theory compactification on the elliptic threefold  $\hat{X}$  over  $B$  with the general elliptic fiber  $\mathcal{E}$  in  $dP_2$  found in section 3.2.1. We mostly consider the case  $B = \mathbb{P}^2$ , although our discussion is readily generalizable to other geometries.

Determining the matter spectrum requires an analysis of the codimension two singularities of this three-section elliptic fibration<sup>8</sup>. We see that the singularity structure that is

---

<sup>8</sup>We thank Antonella Grassi for helpful discussions on the general study of codimension two singularities of elliptic fibrations and related properties of the discriminant.

generic to these fibrations is completely governed by the behavior of the three sections. This study of the behavior of the sections can be conveniently performed in the Weierstrass model (3.29) of the elliptic curve  $\mathcal{E}$ . We determine the charges in three steps in subsections 3.3.1, 3.3.2 and 3.3.3. The multiplicities of matter fields are found in 3.3.4. This analysis requires a careful counting of the codimension two points since the loci in the base  $B$  supporting matter fields of different charges intersect. The right counting requires subtraction of multiplicities of intersecting loci according to their mutual order of vanishing, which is determined by the resultant of the polynomial systems determining the intersecting codimension two loci. Since the matter is a codimension two effect, the matter charges we find immediately carry over to four-dimensional F-theory compactifications on Calabi-Yau fourfolds. Our analysis extends the methods of [97] to elliptic fibrations with two-section models.

The following discussion is organized by the three qualitatively different codimension two singularities that can occur. The codimension two loci of the first two types are readily found in the Weierstrass model, whereas the third type has to be addressed in the birationally related  $dP_2$ -model of section 3.2.2. The three types we distinguish correspond to the following behavior of the sections:

- Away from the collision of a section  $\hat{s}$  with the zero section  $z = 0$  in the Weierstrass form, the existence of the section implies the factorization (3.5) of the Weierstrass form. This factorization makes manifest the presence of conifold singularities in  $X$ . Their resolution leads to matter of charge 1 under the  $U(1)$  associated to  $\sigma(\hat{s})$ . We discuss the factorized Weierstrass form for the two sections  $\hat{s}_Q, \hat{s}_R$  in section 3.3.1.
- Two rational sections  $\hat{s}, \hat{s}'$  both away from the zero section  $z = 0$  can collide and contribute charge  $(1, 1)$ -matter under the two associated  $U(1) \times U(1)$ -symmetry. This behavior is discussed in section 3.3.2.

- A section  $\hat{s}$  can be ill-defined at codimension two. This is easily seen in the  $dP_2$ -model of section 3.2.2. The section  $\hat{s}$  is ill-defined if its corresponding point (3.48) in the fiber passes through the Stanley-Reissner ideal (3.46) of  $dP_2$ . This happens at codimension two loci  $s_i = s_j = 0$  and we have to blow-up the base  $B$  at these loci. Our discussion in section 3.3.3 is organized according to which of these combinations vanish. Then the section wraps a  $\mathbb{P}^1$  fiber component, which is precisely the toric divisor in  $dP_2$  corresponding to the ray that subdivides the 2d-cone corresponding to the two coordinates in the Stanley-Reissner ideal (3.46) .

All these singularities have in common that their resolved fiber is of  $I_2$ -type, i.e. an  $SU(2)$ -fiber with the original singular curve and one isolated  $\mathbb{P}^1$ . The matter hypermultiplets in six dimensions arise from the isolated rational curve  $\mathbb{P}^1$  at the resolved codimension two singularities of the Calabi-Yau manifold. The intersection structure of the resolved fibers with the sections  $\hat{s}_P, \hat{s}_Q, \hat{s}_R$  determines the pattern of  $U(1)$ -charges of the matter. The multiplicities of matter fields is computed by counting the number of solutions to the codimension two constraints as demonstrated in section 3.3.4. We summarize our findings in table 3.1.

$(q_1, q_2)$	Multiplicity
$(1, 0)$	$54 - 15n_2 + n_2^2 + (12 + n_2)n_{12} - 2n_{12}^2$
$(0, 1)$	$54 + 2(6n_2 - n_2^2 + 6n_{12} - n_{12}^2)$
$(1, 1)$	$54 + 12n_2 - 2n_2^2 + (n_2 - 15)n_{12} + n_{12}^2$
$(-1, 1)$	$n_{12}(3 - n_2 + n_{12})$
$(0, 2)$	$n_2 n_{12}$
$(-1, -2)$	$n_2(3 + n_2 - n_{12})$

Table 3.1: Matter spectrum with  $U(1) \times U(1)$ -charges  $(q_1, q_2)$  in the first and multiplicities in the second column. The integers  $n_2, n_{12}$  are defined in (3.53).

We begin our analysis by summarizing the basics of the construction of a (singular) elliptic fibration  $X$  over  $B = \mathbb{P}^2$  in Weierstrass form (3.2). We follow the general discussion

of section 3.1.2. The Weierstrass form of  $X$  is considered as the Calabi-Yau hypersurface in the total space of projective bundle  $\mathbb{P}^2(\mathcal{O}_B \oplus \mathcal{L}^2 \oplus \mathcal{L}^3)$  with coordinates  $[z : x : y]^9$ . By the Calabi-Yau condition we identify  $\mathcal{L} = K_B^{-1} = \mathcal{O}_{\mathbb{P}^2}(3)$  as the anti-canonical bundle and  $\mathcal{O}_B = \mathcal{O}_{\mathbb{P}^2}(0)$  as the trivial line bundle on  $\mathbb{P}^2$ . The parameters  $f$  and  $g$  in (3.2) lift to sections of  $\mathcal{O}_{\mathbb{P}^2}(12)$  and  $\mathcal{O}_{\mathbb{P}^2}(18)$ . The zero section is located at  $[z : x : y] = [0 : 1 : 1]$ . The two Mordell-Weil generators (3.31) and (3.32) are of the form

$$\hat{s} : [x, y, z] = [g_{2n+6}, g_{3n+9}, g_n], \quad (3.54)$$

where the subscript indicates the degree of the polynomials on  $\mathbb{P}^2$ . The intersection of the section  $\hat{s}$  with the zero section  $z = 0$  in the Weierstrass model is the integer  $n$ , and we denote it by  $n_1, n_2$  for the sections  $\hat{s}_Q$  and  $\hat{s}_R$  respectively<sup>10</sup>. The intersection of  $\hat{s}_Q, \hat{s}_R$  is denoted as  $n_{12}$ , cf. (3.53).

### 3.3.1 Factorized Weierstrass Form: charges $(1, 0)$ and $(0, 1)$

Charge one loci occur when the singular point of the degenerated fiber coincides with the point marked by a section  $\hat{s}$ , see figure 3.3. This ensures, that on the resolution the exceptional  $\mathbb{P}^1$  in the fiber intersects the section  $\hat{s}$  and render the hypermultiplet charged under the  $U(1)$  corresponding to  $\hat{s}$ . In our case, each of the sections  $\hat{s}_Q, \hat{s}_R$  can pass separately through the singular point and its resolving  $\mathbb{P}^1$ , thus, giving rise to matter of charge  $(1, 0)$  respectively  $(0, 1)$  under  $U(1) \times U(1)$ . See section 3.3.2 for the case when both sections go through the singular point simultaneously.

We begin by spelling out the general strategy for the identification of these loci and specialize to  $\hat{s}_Q, \hat{s}_R$  below. We emphasize that the structure of the Weierstrass model of the fibration  $X$  with fiber  $\mathcal{E}$  with two sections implies a particular factorization. This facilitates

<sup>9</sup>In contrast to section 3.1, we denote here the coordinates in Weierstrass form by  $(x, y) \equiv (\tilde{x}, \tilde{y})$ .

<sup>10</sup> $n_1 = 0$  in our class of models.

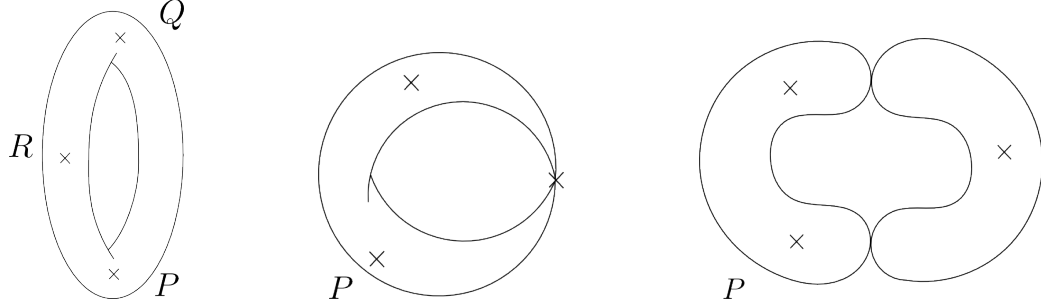


Figure 3.3: On the left it is shown a regular fiber with rational sections at generic points. In the center, a singular fiber is displayed with a section crossing the singularity where charged matter sits. On the right, the curve is shown after resolution. The isolated curve gives rise to an hypermultiplet charged under the corresponding Abelian gauge field.

the search for codimension two singularities in the fiber in  $X$  that coincide with the point marked by the section  $\hat{s}$ . As we have seen in section 3.1.1 the presence of a rational point on  $\mathcal{E}$  with  $z = 1$  implies the factorization (3.5). Noting the form (3.54) of a section in Weierstrass form, we expect this factorization where  $g_n \neq 0$ . Indeed, the  $\mathbb{C}^*$ -action on  $[x : y : z]$  then allows us to cast the Mordell-Weil (MW) generator (3.54) as

$$\hat{s} : [x, y, z] = [g_6, g_9, 1], \quad (3.55)$$

where we set  $g_6 = \frac{g_{6+2n}}{g_n^2}$ ,  $g_9 = \frac{g_{9+3n}}{g_n^3}$ . Then, the Weierstrass model factors in the form

$$p_1 := -(y^2 - g_9^2) + (x - g_6)(x^2 + g_6x + g_{12}) = 0, \quad (3.56)$$

with appropriate  $g_{12}$ , cf. (3.6).

This is a singular Weierstrass model with singularities located at the points satisfying  $p_1 = dp_1 = 0$ , where  $d$  denotes the exterior derivative. The solutions to these equations are

$$y = 0, \quad x = g_6, \quad g_9 = 0, \quad \hat{g}_{12} = g_{12} + 2g_6^2 = 0. \quad (3.57)$$

We readily confirm that the discriminant (3.6) vanishes quadratically at  $g_9 = \hat{g}_{12} = 0$ . The

singularities are conifold singularities<sup>11</sup> that are resolved by the birational transformation (3.28). The original singularity at  $y = (x - g_6) = 0$  is replaced by a rational curve  $\mathbb{P}^1$  and the whole fiber factors into two rational curves intersecting at two points, i.e. an  $I_2$ -curve. The original singular fiber is identified as the rational curve intersected by the zero section  $\hat{s}_P$ . Then the other curve has to be the isolated exceptional  $\mathbb{P}^1$ . We can confirm this identification by using the birational transformation to the Weierstrass form (3.56) and by checking explicitly which curve is mapped to the singular point (3.57) at  $y = (x - g_6) = 0$ . Let us study this explicitly for the two sections  $\hat{s}_Q, \hat{s}_R$  of  $X$ .

### Factorization at the $\hat{s}_Q$ section

The MW-generator of this section has been worked out in equation (3.31). In this case, the section is located at  $z = 1$  and therefore  $z \neq 0$  globally. The Weierstrass equation thus factorizes with

$$g_{12} = \frac{1}{72} \left[ -s_6^4 + 4s_6^2(2s_5s_7 + 5s_3s_8 + 2s_2s_9) - 36s_6(s_2s_7s_8 + s_3s_5s_9 + s_1s_7s_9) \right. \\ \left. - 8(2s_5^2s_7^2 - s_3^2s_8^2 + s_2s_3s_8s_9 + 2s_2^2s_9^2 + s_5s_7(s_3s_8 - 5s_2s_9) - 9s_1(s_7^2s_8 + s_3s_9^2)) \right] \quad (3.58)$$

and the singular loci (3.57) at codimension two are given by

$$g_9^Q = \frac{1}{2}(s_3s_6s_8 - s_2s_7s_8 - s_3s_5s_9 + s_1s_7s_9) \stackrel{!}{=} 0, \quad (3.59)$$

$$\hat{g}_{12}^Q = \frac{1}{2}(2s_3^2s_8^2 + s_7(-s_2s_6s_8 + 2s_1s_7s_8 + 2s_2s_5s_9 - s_1s_6s_9) \\ + s_3(s_6^2s_8 - 2s_5s_7s_8 - s_5s_6s_9 - 2s_2s_8s_9 + 2s_1s_9^2)) \stackrel{!}{=} 0. \quad (3.60)$$

We can use these two constraints to solve for any two coefficients  $s_i, s_j$ , as long as the solutions are rational. Plugging these solutions into the resolved elliptic fiber (3.24) reveals

---

<sup>11</sup>In the case that  $g_n = 1$  these are the 108 points in the  $\mathcal{T}_0$  theory found in [97].



its  $I_2$  nature. In fact, solving and replacing  $s_1$  and  $s_2$  yields a split of the fiber class as  $\mathcal{E} = c_1 + c_2$  for two rational curves  $c_1, c_2$ . The equations of the rational curves read

$$c_1 : s_3u + s_7w = 0, \quad (3.61)$$

$$c_2 : s_5s_7u^2 - s_3s_8u^2 + s_6s_7uv - s_3s_9uv + s_7^2v^2 + s_7s_8uw + s_7s_9vw = 0, \quad (3.62)$$

from which it is clear that the curve  $c_2$  intersects the zero section,  $\hat{s}_P = [u = 0 : v = 0 : w = 1]$  and the rational section  $\hat{s}_R = [u = 0 : v = s_9 : w = -s_7]$ . Thus  $c_2$  is identified with the original singular fiber, which is also confirmed by the fact that it maps to the original singular curve (3.56) by the birational map (3.28). The curve  $c_1$  does not intersect  $\hat{s}_P$  nor  $\hat{s}_R$  and is the isolated rational curve, see figure 3.3 for a depiction of this situation. This is also confirmed by noting that  $c_1$  is blown-down to the singular point (3.57) by the map (3.28). It thus gives rise to a massless hypermultiplet. Since  $c_1$  clearly intersects the rational section  $\hat{s}_Q = [u = 0 : v = 1 : w = 0]$  once, the hypermultiplet, according to (3.20) in the absence of Cartan divisors  $D_{i_l}$ , has  $U(1) \times U(1)$ -charges  $(q_1, q_2) = (1, 0)$  as claimed. We note that we could have performed the same analysis on the resolved geometry (3.47) with the same result.

### Factorization at the $\hat{s}_R$ section

The coordinates of this section in Weierstrass form are given in (3.32). We have to take into account that the  $z$ -coordinate of the section reads  $z = s_9$  and can vanish. When it is

non-zero, the Weierstrass equation factorizes as (3.56) along the loci

$$g_{9+3n_2}^R = \frac{1}{2} [2s_7^3 s_8^3 + s_3 s_9^3 (-s_6 s_8 + s_5 s_9) + s_7^2 s_8 s_9 (-3s_6 s_8 + 2s_5 s_9) + s_7 s_9^2 (s_6^2 s_8 + 2s_3 s_8^2 - s_5 s_6 s_9 - s_2 s_8 s_9 + s_1 s_9^2)] \stackrel{!}{=} 0, \quad (3.63)$$

$$\begin{aligned} \hat{g}_{12+4n_2}^R &= \frac{1}{2} [6s_7^4 s_8^4 + 4s_7^3 s_8^2 s_9 (2s_5 s_9 - 3s_6 s_8) + s_3 s_9^4 (s_6^2 s_8 + 2s_3 s_8^2 - s_5 s_6 s_9 - 2s_2 s_8 s_9 + 2s_1 s_9^2) \\ &- s_7 s_9^3 (s_6^3 s_8 - s_5 s_6^2 s_9 + 2s_5 s_9 (-3s_3 s_8 + s_2 s_9) + s_6 (8s_3 s_8^2 + s_9 (-3s_2 s_8 + s_1 s_9))) \\ &+ s_7^2 s_9^2 (7s_6^2 s_8^2 - 8s_5 s_6 s_8 s_9 + 2(4s_3 s_8^3 + s_9 (-2s_2 s_8^2 + s_5^2 s_9 + s_1 s_8 s_9))) ] \stackrel{!}{=} 0. \end{aligned} \quad (3.64)$$

We find the rational solutions of these equations for  $s_1$  and  $s_2$ . By plugging this into (3.24), we see that the fiber again splits into  $\mathcal{E} = c_1 + c_2$  with

$$c_1 : -s_3 s_9^2 u + s_7^2 (-s_8 u + s_9 v) + s_7 s_9 (s_6 u + s_9 w) = 0, \quad (3.65)$$

$$c_2 : s_7^2 s_8^2 u^2 + s_3 s_9^2 u (s_8 u + s_9 v) + s_7 s_9 (-s_6 s_8 u^2 + s_9 (s_5 u^2 + s_8 u w + s_9 v w)) = 0. \quad (3.66)$$

The curve  $c_2$  intersects the zero section,  $\hat{s}_P$  and also  $\hat{s}_Q$ , but not  $\hat{s}_R$ . It is the original singular fiber as can also be checked using the birational map (3.28). The curve  $c_1$  intersects the rational section  $\hat{s}_R$  at one point but does not intersect  $\hat{s}_P$  and  $\hat{s}_Q$ . It is blown-down to the singular point (3.57) in the birational map (3.28). Thus it is an isolated rational curve and contributes a hypermultiplet of charges  $(q_1, q_2) = (0, 1)$  according to (3.20).

### 3.3.2 Doubly-Factorized Weierstrass Form: charge (1, 1)

Hypermultiplets charged under both sections can and should exist, both from a geometric point of view and for anomaly cancellation, see section 3.4. Their location in the base can be found by determining singular points of the elliptic fiber  $\mathcal{E}$  due to a factorization (3.56) of the Weierstrass form, where in addition both sections  $\hat{s}_Q, \hat{s}_R$  coincide. As we will demonstrate next, this indeed is a codimension two phenomenon.

From the perspective of the  $dP_2$  fiber, the collision of the two sections happens when  $s_7 = 0$ . In the Weierstrass form there are even more loci, where the two sections collide and at which the Weierstrass model becomes automatically singular. We first summarize the structure that we find at these loci, before going into specifics. In the appropriate patch,  $z = s_9$ , we first require the coincidence condition  $\hat{s}_Q = \hat{s}_R$ , that reads

$$s_9^2 g_6^Q - g_{6+2n_2}^R = 0. \quad (3.67)$$

If this is true, then also  $s_9^3 g_9^Q = g_{9+3n_2}^R$  because the  $y$ -coordinates of the sections  $\hat{s}_Q, \hat{s}_R$  have been determined in section 3.2.1 by plugging in the  $x$ - and  $z$ -coordinates into the Weierstrass form and solving for  $y$ . But since  $s_9^2 x_Q := s_9^2 g_6^Q = g_{6+2n_2}^R =: x_R$ , the equality  $s_9^3 g_9^Q = g_{9+3n_2}^R$  is automatic. For the loci under consideration, it requires only a single further constraint to make the Weierstrass model singular, which reads

$$g_9 := s_9^3 g_9^Q = g_{9+3n_2}^R \stackrel{!}{=} 0. \quad (3.68)$$

These two conditions (3.67) and (3.68) bring the Weierstrass equation (3.56), using the notation  $g_6 \equiv s_9^2 g_6^Q = g_{6+2n_2}^R$ , into the form

$$y^2 = (x - g_6)^2 (x - f_6), \quad (3.69)$$

for  $f_6 = -2g_6$ , where the double zero at  $x = g_6, y = 0$  is manifest. We note that the polynomial  $\hat{g}_{12+4n_2}^Q = s_9^4 \hat{g}_{12}^R = 0$  in (3.59) respectively (3.63) and we see that fiber is automatically singular if the sections coincide and  $g_9 = 0$ . Here we denote the third root in  $x$  by  $f_6$ , however the fiber is smooth  $x = f_6$ .

In our concrete situation, the difference between the polynomials can be read off from

(3.31) and (3.32) and takes the form

$$\delta g_6 := s_9^2 g_6^Q - g_{6+2n_2}^R = 0 = s_7(s_7 s_8^2 + s_9(-s_6 s_8 + s_5 s_9)). \quad (3.70)$$

We see that  $s_7 = 0$  is a solution as expected, but also the vanishing of the polynomial in parenthesis makes the sections collide. In the first case,  $s_7 = 0$ , the fiber becomes singular iff in addition either  $s_3 = 0$  or  $s_9 = 0$ . However, these cases have to be treated differently, as discussed in section 3.3.3, because the rational sections are ill-defined at these loci. Thus, we assume  $s_7 \neq 0$  in the following and explore the second possibility, the vanishing of the expression in the parenthesis in (3.70). By solving  $\delta g_6 = 0$  we see explicitly that  $g_9 \equiv s_9^3 g_9^Q = g_{9+3n_2}^R$  now take the same form. Solving  $\delta g_6 = 0$  e.g. for  $s_6$  we determine

$$g_9 = \frac{1}{2} s_7 s_9^2 (s_3 s_8^2 - s_2 s_8 s_9 + s_1 s_9^2). \quad (3.71)$$

Noting that  $s_9 \neq 0$  by assumption, we drop now the coefficients of  $s_7$  and  $s_9$  in front of  $\delta g_6$  and  $g_9$ . Then the codimension two loci for matter read

$$\delta g_6' := s_7 s_8^2 + s_9(-s_6 s_8 + s_5 s_9) = 0, \quad g_9' := s_3 s_8^2 - s_2 s_8 s_9 + s_1 s_9^2 = 0. \quad (3.72)$$

To check the order of vanishing of the discriminant along the codimension two locus we consider a small neighborhood around (3.67) and (3.68) defined as

$$\delta g_6' = \varepsilon, \quad g_9' = \varepsilon, \quad s_9 \neq 0, \quad s_7 \neq 0. \quad (3.73)$$

for a small  $\varepsilon > 0$ . Again by solving for two of the  $s_i$  coefficients we see that the discriminant factors as

$$\Delta = \varepsilon^2 \Delta', \quad (3.74)$$

with  $\Delta' \neq 0$  in the limit  $\varepsilon \rightarrow 0$ , which is equivalent to the observation  $\hat{g}_{12}^Q \sim \hat{g}_{12+4n_2}^R = 0$  if (3.73) is obeyed. This is an indication for an  $I_2$  singularity at  $\varepsilon = 0$ . Indeed, by solving the conditions (3.73) for  $s_3$  and  $s_6$  and by plugging back into (3.24) on the resolution, we obtain a split of the elliptic curve as  $\mathcal{E} = c_1 + c_2$  with

$$c_1 : \quad s_8 u + s_9 v = 0. \quad (3.75)$$

$$c_2 : \quad s_1 s_8 s_9 u^2 + s_2 s_8 s_9 uv - s_1 s_9^2 uv + s_5 s_8 s_9 uw + s_7 s_8^2 vw + s_8^2 s_9 w^2 = 0. \quad (3.76)$$

From this we see that the zero section  $\hat{s}_P = [0 : 0 : 1]$  intersects  $c_1$  at a point and does not intersect  $c_2$ , while the other two sections,  $\hat{s}_Q = [0 : 1 : 0]$  and  $\hat{s}_R = [0 : s_9, -s_7]$ , intersect  $c_2$  at a point but not  $c_1$ . This implies as before that the curve  $c_1$  is the proper transform of the original singular curve under the birational map (3.28) while the curve  $c_2$  is blown down to a point. It is the isolated rational curve and contributes a hypermultiplet of charges  $(q_1, q_2) = (1, 1)$  according to (3.20).

### 3.3.3 Singular Rational Sections: charges $(-1, 1)$ , $(-1, -2)$ , $(0, 2)$

There is another way of looking for singularities of the elliptic fibration, that contribute charged matter in F-theory, which is the third type mentioned at the beginning of this section. Qualitatively, the strategy is as follows. For non-trivial sections  $s_9$  and  $s_7$  over  $B$ , the section  $\hat{s}_R = [0 : -s_9 : s_7]$  can 'move' on the fiber  $\mathcal{E}$  when varying the point on the base  $B$ . This implies that there are loci in  $B$  where two or more sections intersect in the fiber  $\mathcal{E}$ . This is achieved when  $s_7 = 0$  or  $s_9 = 0$  as can be seen from (3.26) in the  $\mathbb{P}^2$ -model for  $\mathcal{E}$ , see figure 3.4. Plugging this ansatz into the discriminant  $\Delta$  admits a factorization. The results of this analysis, that are precisely the loci not discussed in section 3.3.2, are summarized in table 3.2.

We emphasize that at each of these loci one section  $\hat{s}_P, \hat{s}_Q, \hat{s}_R$  is ill-defined. This can be

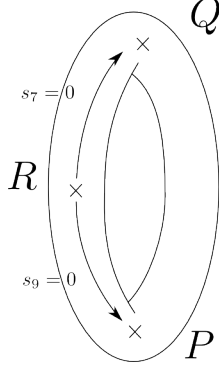


Figure 3.4: Fibers where two out of the three sections collide. The intersections occur when  $s_7$  or/and  $s_9$  vanish on the base  $B$ .

Locus	Isolated Curve	Charge $(U(1)_Q, U(1)_R)$
$s_3 = s_7 = 0$	$e_1 = 0$	$(-1, 1)$
$s_7 = s_9 = 0$	$u = 0$	$(0, 2)$
$s_8 = s_9 = 0$	$c_2$	$(-1, -2)$

Table 3.2: Codimension two loci with singular behavior of the sections. The identifications of the isolated curves are explained in (3.80), (3.83) and (3.87).

seen most easily on the resolved model of the elliptic curve  $\mathcal{E}$  in  $dP_2$  introduced in section 3.2.2. For the convenience of the reader we recall the relevant properties of the resolved geometry. After resolutions along  $u = w = 0$  and  $u = v = 0$  the sections take the values

$$\hat{s}_P = [-s_9 : s_8 : 1 : 1 : 0], \quad \hat{s}_Q = [-s_7 : 1 : s_3 : 0 : 1], \quad \hat{s}_R = [0 : 1 : 1 : -s_7 : s_9], \quad (3.77)$$

cf. (3.48). We also recall the Stanley-Reissner ideal, of the resolution<sup>12</sup>

$$SR = \{uv, uw, e_1e_2, e_1v, e_2w\}. \quad (3.78)$$

Indeed, at each locus in table 3.2 one of the sections (3.77) is ill-defined since it passes through the Stanley-Reissner ideal (3.78). This requires additional blow-ups in the base  $\pi_B : \hat{B} \rightarrow B$  as advertised in section 3.1.2 precisely along the loci where the sections are not

<sup>12</sup>In the following we denote the coordinates on  $dP_2$  as  $[u : v : w : e_1 : e_2]$  in contrast to section 3.2.2.

well-defined. We emphasize that this implies that the birational map (3.28) is not enough to completely understand and resolve the fibration  $X$ , in contrast to the codimension two loci discussed in sections 3.3.1 and 3.3.2.

To understand what is happening when one of the sections  $\hat{s}_P, \hat{s}_Q, \hat{s}_R$ , collectively denoted as  $\hat{s}$  for the following paragraph, is singular, we first look at the sections at a location in the base where the fiber is not singular. In this case, after performing the blowups in the ambient space to  $dP_2$ , the exceptional  $\mathbb{P}^1$ 's intersect the Calabi-Yau polynomial at exactly one point in the fiber with coordinates shown in (3.77). At any of the loci of table 3.2, when two coefficients,  $s_i$  and  $s_j$  vanish simultaneously, the two coordinates of the exceptional  $\mathbb{P}^1$  vanish simultaneously and the coordinates stop making sense. This is another way of saying that the section passes through the Stanley-Reissner ideal (3.78). To resolve this problem we blow up the base at this locus by introducing coordinates  $[\ell_1 : \ell_2] \in \mathbb{P}^1$  and writing

$$\ell_1 s_i - \ell_2 s_j = 0. \tag{3.79}$$

The coordinates (3.77) of the section  $\hat{s}$  will be now given by the point  $[s_j : s_i] = [\ell_1 : \ell_2]$  in  $\mathbb{P}^1$ . When the two coordinates vanish simultaneously,  $s_i = s_j = 0$ , the values of  $\ell_1$  and  $\ell_2$  in (3.79) become unrestricted and we obtain the entire  $\mathbb{P}^1$  in the fiber.

Another way of seeing this is to notice that the section  $\hat{s}$  takes different values at the singular locus  $s_i = s_j = 0$  depending on the direction (parametrized by  $[\ell_1 : \ell_2]$ ) at which we approach the locus in the base. Coming in all possible directions makes the section take all possible values at the same locus: the section becomes the entire  $\mathbb{P}^1$  of slopes.

Now that we understand that the sections can become entire  $\mathbb{P}^1$ 's, we demonstrate the factorization of the equation (3.47) into two rational curves along all codimension two loci in table 3.2. We discuss these loci successively and refer to figure 3.5 to keep track of which of the three sections wraps a  $\mathbb{P}^1$  in the resolved fiber.

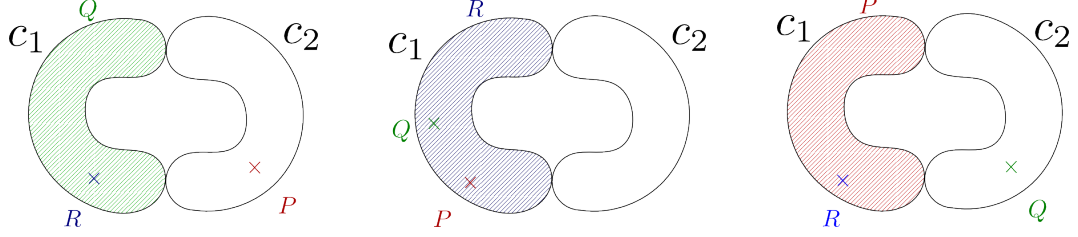


Figure 3.5: How the fiber degenerates at the three loci  $(-1,1)$ ,  $(0,2)$  and  $(-1,-2)$  respectively.

**Singularity of  $\hat{s}_Q$  & blow-up at  $s_3 = s_7 = 0$ : charge  $(-1, 1)$**

As can be seen from (3.77) at the loci  $s_3 = s_7 = 0$  the section  $\hat{s}_Q$  passes through the ideal (3.78) and is ill-defined. It has to be blown-up and wraps an entire  $\mathbb{P}^1$ -component of the fiber, which is given by the divisor  $E_1 := \{e_1 = 0\}$  in  $dP_2$ . In addition, the polynomial (3.47) factorizes into two rational curves, i.e.  $\mathcal{E} = c_1 + c_2$ , reading

$$c_1 : \quad e_1 = 0, \quad (3.80)$$

$$c_2 : \quad s_1 e_1 e_2^2 u^3 + s_2 e_2^2 u^2 v + s_5 e_1 e_2 u^2 w + s_6 e_2 uvw + s_8 e_1 uw^2 + s_9 vw^2 = 0. \quad (3.81)$$

We notice using (3.77), (3.78) and the toric intersections (3.45) on  $dP_2$  the intersections of the rational sections with the two curves as

$$S_P \cdot c_1 = 0, \quad S_P \cdot c_2 = 1, \quad S_Q \cdot c_1 = -1, \quad S_Q \cdot c_2 = 0, \quad S_R \cdot c_1 = 1, \quad S_R \cdot c_2 = 0, \quad (3.82)$$

where we denoted the homology classes of the sections by capital letters  $S_\bullet$  as before. Here we note that the last two intersections follow, besides from the toric intersections (3.45), also from the defining property of a section,  $1 = S_R \cdot \mathcal{E} = S_R \cdot (c_1 + c_2)$ , which with  $S_R \cdot c_2 = 0$  immediately yields  $S_R \cdot c_1 = 1$ .

We note that the intersections (3.82) imply that  $c_2$  is the original singular curve since it intersects the zero section  $\hat{s}_P$  and  $c_1$  is the exceptional  $\mathbb{P}^1$  contributing a hypermultiplet. Thus it follows from (3.20) that the  $U(1)_Q \times U(1)_R$ -charges are  $(q_1, q_2) = (-1, 1)$ .



**Singularity of  $\hat{s}_R$  & blow-up at  $s_7 = s_9 = 0$ : charge  $(0, 2)$**

Proceeding in a similar way as before we see that the section  $\hat{s}_R$  is blown up in a  $\mathbb{P}^1$ , which we identify with the toric divisor  $D_u := \{u = 0\}$  in  $dP_2$ . Furthermore, the polynomial (3.47) factorizes at  $s_7 = s_9 = 0$  into two rational curves given by

$$c_1 : \quad u = 0, \quad (3.83)$$

$$c_2 : \quad s_1 e_1^2 e_2^2 u^2 + s_2 e_1 e_2^2 uv + s_3 e_2^2 v^2 + s_5 e_1^2 e_2 uw + s_6 e_1 e_2 vw + s_8 e_1^2 w^2 = 0. \quad (3.84)$$

The intersections of the sections are evaluated as before employing (3.77), (3.78) and the toric intersections (3.45) on  $dP_2$  as

$$S_P \cdot c_1 = 1, \quad S_P \cdot c_2 = 0, \quad S_Q \cdot c_1 = 1, \quad S_Q \cdot c_2 = 0, \quad S_R \cdot c_1 = -1, \quad S_R \cdot c_2 = 2. \quad (3.85)$$

Here we have determined the intersections of  $S_R$  by noting that due to the blow-up in the base at  $s_7 = s_9 = 0$ , cf. (3.77), it wraps the entire  $\mathbb{P}^1$  corresponding to the ray subdividing the cone formed  $e_1, e_2$ . As we see by recalling figure 3.2 this is nothing else but the toric divisor with  $D_u$  section  $u$ . This then implies that  $S_P \cdot c_2 = 2$  because the equation for  $c_2$  has two solutions with  $u = 0$ . From the defining property  $1 = S_P \cdot \mathcal{E} = S_P \cdot (c_1 + c_2) = S_P \cdot c_1 + 2$  we infer  $S_P \cdot c_1 = -1$  as claimed in (3.85).

From the location of the zero section we infer that  $c_1$  is the original singular fiber and  $c_2$  the isolated rational curve contributing a hypermultiplet. Its charges are calculated employing (3.20) as  $(q_1, q_2) = (0, 2)$ .

**Singularity of  $\hat{s}_P$  & blow-up at  $s_8 = s_9 = 0$ : charge  $(-1, -2)$**

At this locus, the zero section  $\hat{s}_P$  is ill-defined and is blown up into a rational fiber component. It is identified with the toric divisor  $E_2 := \{e_2 = 0\}$  in  $dP_2$ . The constraint (3.47) of

the elliptic curve implies a split  $\mathcal{E} = c_1 + c_2$  at these loci with

$$c_1 : \quad e_2 = 0, \quad (3.86)$$

$$c_2 : \quad s_1 e_1^2 e_2 u^3 + s_2 e_1 e_2 u^2 v + s_3 e_2 u v^2 + s_5 e_1^2 u^2 w + s_6 e_1 u v w + s_7 v^2 w = 0. \quad (3.87)$$

As before the intersections of the sections are computed from (3.77), (3.78) and the toric intersections (3.45) on  $dP_2$  as

$$S_P \cdot c_1 = -1, \quad S_P \cdot c_2 = 2, \quad S_Q \cdot c_1 = 0, \quad S_Q \cdot c_2 = 1, \quad S_R \cdot c_1 = 1, \quad S_R \cdot c_2 = 0, \quad (3.88)$$

where the intersection  $S_P \cdot c_2 = 2$  can be obtained by setting  $e_2 = 0$  in (3.87). Alternatively, it can also be calculated using  $1 = S_P \cdot \mathcal{E} = S_P \cdot (c_1 + c_2) = -1 + S_P \cdot c_2$ .

Here we have used that the blow-up in the base along  $s_8 = s_9 = 0$  has blown-up the zero section with coordinates (3.77) into  $E_2$ , which is the toric divisor of the ray subdividing the cone spanned by  $u$  and  $v$ . The curve  $c_1$  is part of the zero section  $c_1$ , thus it is the original singular fiber, whereas  $c_2$  maps to the singular point of the original fiber. Thus  $c_2$  is the isolated curve and it contributes according to (3.20) a hypermultiplet of total charge  $(q_1, q_2) = (-1, -2)$ . We note that this locus is special in the sense that it supports the only matter multiplet where the second term in (3.20) contributes to the charge due to the ill-defined zero section  $\hat{s}_P$ .

### 3.3.4 Calculating Matter Multiplicities

Now that we have determined the full matter representations and their codimension two loci in the base  $B$ , we can count their multiplicities. The main complication that arises in these calculations is due to the intersection of different codimension two loci. In order to avoid double-counting we thus have to appropriately subtract the number of intersection

points of a codimension two loci under consideration with other codimension two loci.

For this analysis, we first have to recall the counting of the multiplicity of a root in a system of two polynomials with two independent variables. Given two polynomials

$$f(x, y) = 0, \quad g(x, y) = 0, \quad (3.89)$$

we define

$$h(y) := \text{Res}_x(f, g) \quad (3.90)$$

as the resultant of  $f, g$  with respect to  $x$ . The degree of a root  $(x_0, y_0)$  of (3.89) is given by the multiplicity of  $y_0$  as a zero of  $h(y)$ <sup>13</sup>.

Now that we know how to count roots of a polynomial system, the strategy is simple: take the degrees of the polynomials for the codimension two loci we are interested, multiply them and then subtract all intersecting loci we are not interested in with the appropriate multiplicity. As a warm up and a demonstration of this technique we rederive the multiplicity of the charge one loci of the elliptic fibration over  $\mathbb{P}^2$  with elliptic fiber  $Bl_{(0,1,0)}\mathbb{P}^{1,1,2}$  considered in [97].

**Example: Charge one multiplicity of the  $Bl_{(0,1,0)}\mathbb{P}^2(1, 1, 2)$  model**

The loci of the charge one hypermultiplets were given in equations (5.64) of [97]

$$\begin{aligned} f_{3+n}^3 - 3f_6 f_{3+n} b_n^2 + b_n^4 f_{9-n} &= 0, \\ f_{3+n}^4 - 6f_6 f_{3+n}^2 b_n^2 + 9f_6^2 b_n^4 - f_{12-2n} b_n^6 &= 0, \end{aligned} \quad (3.91)$$

---

<sup>13</sup>The degree can also be defined with respect to the variable  $x$ , however, yielding the same multiplicity.

with  $b_n \neq 0$  and  $f_{3+n} \neq 0$  because those were identified as the charge two loci. We see that  $f_{3+n} = b_n = 0$  obviously solves the system.

Viewing now the equations (3.91) as polynomials in the variables  $f_{3+n}$  and  $b_n$ , the resultant with respect to the variable  $f_{3+n}$  is given by

$$h(b_n) = b_n^{16}(b_n^2 f_{12-2n}^3 - 9f_{12-2n}^2 f_6^2 + 6f_{12-2n} f_6 f_{9-n}^2 - f_{9-n}^4), \quad (3.92)$$

from where it can be seen that  $f_{3+n} = b_n = 0$  is a root of degree 16 of the system (3.91). Now we can calculate the multiplicity of the charge one hypermultiplets. The degrees of (3.91) are  $(9 + 3n)$  and  $(12 + 4n)$  respectively and there are  $n(3 + n)$  roots we are not interested in and that have to be subtracted, each of which of degree 16. Thus we obtain

$$(9 + 3n)(12 + 4n) - 16n(3 + n) = 4(9 - n)(3 + n) \quad (3.93)$$

charge one hypermultiplets.

### **Matter multiplicities of the $dP_2$ model**

In this subsection we will finally apply the resultant technique to determine the multiplicity of all six codimension two matter loci found in sections 3.3.1, 3.3.2 and 3.3.3. We denote the multiplicities by the same variables  $x_i$ ,  $i = 1, \dots, 6$ , as in (3.104) to facilitate a straightforward comparison with results from anomaly cancellation.

The basis of our analysis are the degrees of the coefficients  $s_i$  calculated in (3.52) for the base  $B = \mathbb{P}^2$ . Let us recall that the degree of  $s_9$  is equal to the intersection number  $n_2$  of the zero section  $\hat{s}_P$  and the section  $\hat{s}_R$  and the degree  $n_{12}$  of  $s_7$  equals the intersection number of  $\hat{s}_Q$  and  $\hat{s}_R$ , cf. (3.53). With these degrees, the multiplicities of the hypermultiplets of section 3.3.3 are straightforward: they are simply the multiplication of the degrees of the

two coefficient that vanish, see table 3.3. For the other hypermultiplets we have to work a little more.

Locus	Charge $(U(1)_Q, U(1)_R)$	Multiplicity
$s_3 = s_7 = 0$	$(-1, 1)$	$x_4 = (3 - n_2 + n_{12})n_{12}$
$s_7 = s_9 = 0$	$(0, 2)$	$x_5 = n_{12}n_2$
$s_8 = s_9 = 0$	$(-1, -2)$	$x_6 = (3 + n_2 - n_{12})n_2$

Table 3.3: Matter multiplicities.

### Charge (1,1)

The charge  $(1, 1)$  hypermultiplets are located at the roots of equations (3.72), that we recall for convenience of the reader as

$$\delta g'_6 = s_7 s_8^2 + s_9(-s_6 s_8 + s_5 s_9) \stackrel{!}{=} 0, \quad g'_9 = s_3 s_8^2 - s_2 s_8 s_9 + s_1 s_9^2 \stackrel{!}{=} 0.$$

They have degrees

$$\begin{aligned} \deg(\delta g'_6) &= n_{12} + 2(3 + n_2 - n_{12}) = 6 + 2n_2 - n_{12}, \\ \deg(g'_9) &= (3 - n_2 + n_{12}) + 2(3 + n_2 - n_{12}) = 9 + n_2 - n_{12}. \end{aligned} \quad (3.94)$$

The loci  $s_8 = s_9 = 0$  are obviously roots of these equations. The degree of this root is four as we see by working out the resultant of these constraints with respect to  $s_8$  and  $s_9$ . No other codimension two loci satisfy the equations (3.94). Thus, the multiplicity of the hypermultiplets with charges  $(1, 1)$  is

$$x_3 = (6 + 2n_2 - n_{12})(9 + n_2 - n_{12}) - 4n_2(3 + n_2 - n_{12}) = 54 + 12n_2 - 2n_2^2 + (n_2 - 15)n_{12} + n_{12}^2 \quad (3.95)$$

### Charge (1,0)

We proceed with the calculation of the multiplicity of charge (1,0) hypermultiplets. The constraints of the corresponding codimension two loci is given by equation (3.59), that takes the schematic form

$$g_9^Q = 0, \quad \hat{g}_{12}^Q = 0. \quad (3.96)$$

Recalling table 3.2 we notice that all hypermultiplets with charges (1,1), (-1,1) and (-1,-2) satisfy these equations. The multiplicity is calculated from the resultant as one in each case. Thus, the multiplicity of the loci supporting charge (1,0) hypermultiplets is then

$$\begin{aligned} x_1 &= 108 - (54 + 12n_2 - 2n_2^2 + (n_2 - 15)n_{12} + n_{12}^2) - n_{12}(3 - n_2 + n_{12}) - n_2(3 + n_2 - n_{12}) \\ &= 54 - 15n_2 + n_2^2 + 12n_{12} + n_2n_{12} - 2n_{12}^2. \end{aligned} \quad (3.97)$$

### Charge (0,1)

The defining equations for the loci supporting these hypermultiplets are given by the equations in (3.63), that schematically read as

$$g_{9+3n_2}^R = 0, \quad \hat{g}_{12+4n_2}^R = 0. \quad (3.98)$$

Again by looking at table 3.2 we see that all hypermultiplets with charge (1,1), (-1,1), (0,2) and (-1,-2) satisfy the equations with multiplicities. Their multiplicities are 1, 1, 16 and 16, respectively, and by subtracting from the degree of (3.98) we obtain the multiplicity

as

$$\begin{aligned}
x_2 &= (9 + 3n_2)(12 + 4n_2) - x_3 - x_4 - 16x_5 - 16x_6 \\
&= 54 + 12n_2 - 2n_2^2 + 12n_{12} - 2n_{12}^2.
\end{aligned}
\tag{3.99}$$

### 3.4 Anomaly Cancellation: a Consistency Check

In this section we check the consistency of the matter spectrum determined in the previous section via constraints arising from anomaly cancellation. We demonstrate that anomaly cancellation allows us to classify all F-theory compactifications with base  $B = \mathbb{P}^2$  and the two section elliptic fiber determined in section 3.2.1. This confirms the geometric analysis of the previous section that has led to determination of the charges of matter fields. We also see that the computed multiplicities agree with the ones predicted by anomaly cancellation. This analysis ensure a consistent low-energy theory of F-theory in six dimensions with two Abelian gauge fields.

Anomaly cancellation in six-dimensional F-theory vacua, based on general results on 6d anomaly cancellation [45, 66], has been discussed in [105, 97], whose notations and conventions we follow here. See also the analysis in [31] of anomaly cancellation in four dimensional F-theory compactifications. We note that the following discussion holds more generally for any Abelian gauge theory.

We are interested in anomaly cancellation in an Abelian gauge theory with matter arising from F-theory compactifications. In this case, there are only the purely gravitational anomaly, the mixed Abelian-gravitational and the pure Abelian gauge anomalies. We assume that there are  $H$  hypermultiplets,  $T$  tensor multiplets and  $V$  vector multiplets. The gauge and mixed anomalies induced by the six-dimensional charged matter in hypermultiplets have to be canceled by a classical effect, the generalized Green-Schwarz mecha-

nism [107]. These cancellation conditions are the anomaly equations. The mixed Abelian-gravitational, purely Abelian and purely gravitational anomaly equations read

$$\begin{aligned}
K_B \cdot b_{mn} &= -\frac{1}{6} \sum_{\underline{q}} x_{q_m, q_n} q_m q_n, \\
b_{mn} \cdot b_{kl} + b_{mk} \cdot b_{nl} + b_{ml} \cdot b_{nk} &= \sum_{\underline{q}} x_{q_m, q_n, q_k, q_l} q_m q_n q_k q_l, \\
273 = H - V + 29T, \quad K_B \cdot K_B &= 9 - T.
\end{aligned} \tag{3.100}$$

Here we have labeled the  $r$   $U(1)$ -fields in our theory by  $A^m$ , where  $r$  denotes the rank of the Mordell-Weil group of the Calabi-Yau threefold  $X$ . On the right hand side of (3.100), the sum runs over all hypermultiplets with charge vector  $\underline{q} = (q_1, \dots, q_r)$ . The integers  $x_{q_m, q_n}$  respectively  $x_{q_m, q_n, q_k, q_l}$  denote the number of hypermultiplets with charges  $(q_m, q_n)$  under  $U(1)_m \times U(1)_n$  respectively charges  $(q_m, q_n, q_k, q_l)$  under  $U(1)_m \times U(1)_n \times U(1)_k \times U(1)_l$ . The left hand side of (3.100) is to be evaluated in the cohomology of the base  $B$  of the fibration.  $K_B$  denotes the canonical class of  $B$ ,  $\cdot$  is the intersection pairing on  $B$  and the expressions  $b_{mn}$  are defined as the curves

$$\begin{aligned}
b_{mn} &= -\pi(\sigma(\hat{s}_m) \cdot \sigma(\hat{s}_n)) \\
&= -\pi(S_m \cdot S_n) - [K_B] + \pi(S_m \cdot S_P) + \pi(S_n \cdot S_P).
\end{aligned} \tag{3.101}$$

We recall that  $S_m$  denotes the divisors class of a section  $\hat{s}_m$  and the homology class  $S_P$  of the zero section  $\hat{s}_P$ . Here the first line has been evaluated employing (3.16) in the presence of only Abelian gauge fields. We note that the pure gravitational anomaly even without further specification of the spectrum puts an upper bound on a theory with  $T = 0$ , which is the case for  $B = \mathbb{P}^2$ , as

$$\sum_f N_f \leq 275. \tag{3.102}$$



We now analyze the anomaly constraints (3.100) for the F-theory compactification on the elliptic fibration over  $\mathbb{P}^2$  with two U(1) gauge fields and the matter content determined in section 3.3. We see that anomaly cancellation fixes the possible matter multiplicities in terms of two integers. We first evaluate the anomaly coefficients  $b_{mn}$  in (3.100). In the case of  $\mathbb{P}^2$  as the base, there is only one element generating  $H_2(B)$ , the hyperplane class  $H_B$ . The anti-canonical line bundle is  $K_{\mathbb{P}^2} = -3H_B$ . Then the coefficients are just numbers, namely the coefficients of  $H_B$ , and evaluated to

$$b_{kl} = \begin{cases} 2(n_k + 3), & k = l \\ 3 + n_k + n_l - n_{kl}, & k \neq l, \end{cases} \quad (3.103)$$

where we defined  $n_{kl} = \pi(S_k \cdot S_l)$  and  $n_k = \pi(S_k \cdot B)$ . In addition, we have employed the second relation in (3.11) to replace  $\pi(S_k \cdot S_k) = (S_k \cdot S_k \cdot H_B)H_B = K = 3H_B$ . Then, we evaluate the right hand side of (3.100) using the spectrum found in section 3.3 with arbitrary multiplicities  $x_i$  assigned as

$(q_1, q_2)$	$(1, 0)$	$(0, 1)$	$(1, 1)$	$(-1, 1)$	$(0, 2)$	$(-1, -2)$	(3.104)
multiplicity	$x_1$	$x_2$	$x_3$	$x_4$	$x_5$	$x_6$	

Upon inserting this into the anomaly constraints (3.100) for two sections  $S_1 \equiv S_Q, S_2 \equiv S_R$

and the zero section  $S_P$  we obtain a set of linear equations for the  $x_i$  reading

$$\begin{aligned}
36(3+n_1) &= 12(3+n_1)^2 = x_1 + x_3 + x_4 + x_6, \\
18(3+n_1-n_{12}+n_2) &= 6(3+n_1)(3+n_1-n_{12}+n_2) = x_3 - x_4 + 2x_6, \\
12(3+n_2)^2 &= x_2 + x_3 + x_4 + 16x_5 + 16x_6, \\
6(3+n_2)(3+n_1-n_{12}+n_2) &= x_3 - x_4 + 8x_6, \\
36(3+n_2) &= x_2 + x_3 + x_4 + 4x_5 + 4x_6, \\
4(3+n_1)(3+n_2) + 2(3+n_1-n_{12}+n_2)^2 &= x_3 + x_4 + 4x_6. \tag{3.105}
\end{aligned}$$

We see that the first equation in this system immediately requires  $n_1 = \pi(S_Q \cdot S_P) = 0$ . This nicely agrees with the finding of (3.31) respectively (3.48) that the section  $S_Q$  does not intersect the zero section  $S_P$ . The solutions of (3.105) then take the form

$$\begin{aligned}
x_1 &= 54 - 15n_2 + n_2^2 + (12+n_2)n_{12} - 2n_{12}^2, & x_4 &= n_{12}(3-n_2+n_{12}), \\
x_2 &= 54 + 2(6n_2 - n_2^2 + 6n_{12} - n_{12}^2), & x_5 &= n_2n_{12}, \\
x_3 &= 54 + 12n_2 - 2n_2^2 + (n_2-15)n_{12} + n_{12}^2, & x_6 &= n_2(3+n_2-n_{12}) \tag{3.106}
\end{aligned}$$

This provides a full classification of the possible matter multiplicities with two U(1)-gauge fields in terms of the intersections

$$n_2 = \pi(S_Q \cdot S_P), \quad n_{12} = \pi(S_Q \cdot S_R) \tag{3.107}$$

of the two sections  $S_Q$ ,  $S_R$  and of  $S_P$  introduced in (3.17). It is satisfying that the matter multiplicities found in section 3.3.4 are reproduced by (3.106).

We conclude by evaluating two special cases. First we consider  $n_2 = n_{12} = 0$  where we

obtain

$(q_1, q_2)$	(1,0)	(0,1)	(1,1)	(-1,1)	(0,2)	(-1,-2)	(3.108)
multiplicity	54	54	54	0	0	0	

In this case, charge two loci are completely absent. A less trivial example can be constructed by setting  $n_2 = n_{12} = 1$  in which case we obtain

$(q_1, q_2)$	(1,0)	(0,1)	(1,1)	(-1,1)	(0,2)	(-1,-2)	(3.109)
multiplicity	51	74	51	3	1	3	

The global geometries of both examples are constructed in the example section. See [34] for more details.

### 3.5 Compactifications for a General Base: $U(1) \times U(1)$

In this Section we work out the spectrum of a general F-theory compactification to six dimensions on elliptically fibered Calabi-Yau threefolds,  $\pi : \hat{X} \rightarrow B$ , with arbitrary base. The low energy theory realizes a rank two Abelian sector. Consistency of the theory is shown at the level of anomaly cancellation.

#### 3.5.1 Construction of the Fibration

The general elliptic fiber with a rank two Mordell-Weil group is given by the generic elliptic curve  $\mathcal{E}$  in  $dP_2$ , see section 3.2.1 and [74], which takes the following form:

$$p = u(s_1 u^2 e_1^2 e_2^2 + s_2 u v e_1 e_2^2 + s_3 v^2 e_2^2 + s_5 u v e_1^2 e_2 + s_6 v w e_1 e_2 + s_8 w^2 e_1^2) + s_7 v^2 w e_2 + s_9 v w^2 e_1, \quad (3.47)$$

where  $[u : v : w : e_1 : e_2]$  are the homogeneous coordinates on  $dP_2$  and the  $s_i$ 's are numbers in  $\mathbb{C}$ .

The elliptic fibrations of this curve over the base  $B = \mathbb{P}^2$  have been constructed in this chapter. In this Section, we extend the construction to an arbitrary base  $B$ . Here we closely follow the derivation and the notation of [30]. These elliptic threefolds  $\hat{X}$  can be described as a hypersurface in a four-dimensional ambient space.

We begin by constructing this ambient space. It is given by a  $dP_2$ -fibration over the two-dimensional base  $B$ ,

$$\begin{array}{ccc} dP_2 & \longrightarrow & dP_2^B(\mathcal{S}_7, \mathcal{S}_9) \\ & & \downarrow \\ & & B \end{array} \quad (3.110)$$

In this fibration the homogeneous coordinates of  $dP_2$  are lifted to sections of line bundles over the base  $B$ . Using the three  $\mathbb{C}^*$ -actions on  $dP_2$  three of these coordinates can be chosen to transform in the trivial line bundle on the base without loss of generality. We can choose the following assignments of line bundles for the remaining two homogeneous coordinates:

$$u \in \mathcal{O}_B(\mathcal{S}_9 + [K_B]), \quad v \in \mathcal{O}_B(\mathcal{S}_9 - \mathcal{S}_7), \quad (3.111)$$

where  $[K_B]$  is the canonical bundle on  $B$  and  $\mathcal{S}_7, \mathcal{S}_9$  are arbitrary divisors on  $B$ . We note that (3.110) is the natural generalization of eq. (3.30) in [34].

Next, we construct an elliptically fibered Calabi-Yau threefold with its general elliptic fiber in  $dP_2$ . It is described as the hypersurface (3.47) in the ambient space (3.110). The Calabi-Yau condition enforces that the coefficients  $s_i$  are lifted to sections of appropriate line bundles on  $B$ . To see this, we calculate the total Chern class of the ambient space via

adjunction,

$$c(dP_2^B) = c(B)(1 + H - E_1 - E_2 + \mathcal{S}_9 - [K_B^{-1}])(1 + H - E_2 + \mathcal{S}_9 - \mathcal{S}_7)(1 + H - E_1)(1 + E_1)(1 + E_2), \quad (3.112)$$

where  $H$ ,  $E_1$  and  $E_2$  are the three divisor classes on  $dP_2$ , c.f., eq. (3.24) in [34] as well as eq. (2.2) of [30]. This yields the following anti-canonical bundle:

$$K_{dP_2^B}^{-1} = \mathcal{O}(3H - E_1 - E_2 + 2\mathcal{S}_9 - \mathcal{S}_7), \quad (3.113)$$

where for brevity of notation we suppressed the dependence on  $\mathcal{S}_7$ ,  $\mathcal{S}_9$  on the left side of (3.112) and (3.113). Requiring that the hypersurface (3.47) is a section of the anti-canonical bundle, we obtain the following assignment of line bundles for the coefficients  $s_i$ :

Section	Bundle	Section	Bundle
$u$	$\mathcal{O}(H - E_1 - E_2 + \mathcal{S}_9 + [K_B])$	$s_1$	$\mathcal{O}(3[K_B^{-1}] - \mathcal{S}_7 - \mathcal{S}_9)$
$v$	$\mathcal{O}(H - E_2 + \mathcal{S}_9 - \mathcal{S}_7)$	$s_2$	$\mathcal{O}(2[K_B^{-1}] - \mathcal{S}_9)$
$w$	$\mathcal{O}(H - E_1)$	$s_3$	$\mathcal{O}([K_B^{-1}] + \mathcal{S}_7 - \mathcal{S}_9)$
$e_1$	$\mathcal{O}(E_1)$	$s_5$	$\mathcal{O}(2[K_B^{-1}] - \mathcal{S}_7)$
$e_2$	$\mathcal{O}(E_2)$	$s_6$	$\mathcal{O}([K_B^{-1}])$
		$s_7$	$\mathcal{O}(\mathcal{S}_7)$
		$s_8$	$\mathcal{O}([K_B^{-1}] + \mathcal{S}_9 - \mathcal{S}_7)$
		$s_9$	$\mathcal{O}(\mathcal{S}_9)$

(3.114)

Here, in the first column, we have also summarized the line bundles of the homogeneous coordinates on  $dP_2$ .

The rational sections  $\hat{s}_P$ ,  $\hat{s}_Q$  and  $\hat{s}_R$  are given by  $e_2 = 0$ ,  $e_1 = 0$  and  $u = 0$  in  $\hat{X}$ . From

this it follows that their classes, denoted by capital letters, are given by:

$$S_P = E_2, \quad S_Q = E_1, \quad S_R = H - E_1 - E_2 + \mathcal{S}_9 + [K_B], \quad (3.115)$$

as in [34]. We choose  $\hat{s}_P$  as the zero section of the elliptic fibration of  $\hat{X}$ .

From the assignments (3.114) we see that the divisors  $\mathcal{S}_7, \mathcal{S}_9$  are precisely the vanishing loci of the sections  $s_7, s_9$  in (3.110), which is the reason for the choice of their labels. As mentioned before, these two divisors geometrically encode the intersections of the rational sections. Indeed, we observe the following intersections:

$$\mathcal{S}_7 = \pi(S_Q \cdot S_R), \quad \mathcal{S}_9 = \pi(S_P \cdot S_R), \quad 0 = \pi(S_P \cdot S_Q), \quad (3.116)$$

where  $\pi$  denotes the projection to the (co-)homology of the base  $B$ .

The assignment of sections for the base  $B = \mathbb{P}^2$  can be recovered from (3.114) by making the replacements  $[K_B^{-1}] \rightarrow 3H_B, \mathcal{S}_9 \rightarrow n_2 H_B$  and  $\mathcal{S}_7 \rightarrow n_{12} H_B$ , where  $H_B$  is the hyperplane class of the base.

### 3.5.2 Hypermultiplet Matter Representations and Multiplicities

To find the matter content we track the codimension two singularities. Locally the fiber degenerates in the same fashion as for the case  $B = \mathbb{P}^2$ . Furthermore, the intersections of the rational sections with the components of the reducible fiber do not depend on the global geometry of  $B$ . This implies that the  $U(1)$ -charges of matter fields are independent of the base  $B$ , as can be seen from the charge formula

$$q_m = (S_m - S_P) \cdot c_{\text{mat}}, \quad (3.117)$$

where  $c_{\text{mat}}$  is an isolated  $\mathbb{P}^1$  in the fiber corresponding to a matter field and where we collectively labeled the divisor classes  $S_m = (S_Q, S_R)_m$ , with  $m = 1, 2$ .

Furthermore, the functional dependencies of the polynomials describing the codimension two loci supporting matter on the sections  $s_i$  are base-independent. However, the multiplicities of matter do depend on  $B$  because the line bundles in which the  $s_i$ 's take values are base dependent, see (3.114). Nevertheless, in the following we can still calculate the matter multiplicities directly for an arbitrary base by applying the results in Section 4 of [34] and the intersection theory on  $B$ .

First, we calculate the multiplicities of the singlets in Section 4.3 of [34]. These arise at codimension two singularities of the fibration due to the rational sections being ill-defined. These codimension two loci are complete intersections in the base  $B$  and their multiplicities are the number of intersection points given by

Loci	Representation	Multiplicity
$s_7 = s_3 = 0$	$\mathbf{1}_{(-1,1)}$	$\mathcal{S}_7 \cdot ([K_B^{-1}] + \mathcal{S}_7 - \mathcal{S}_9)$
$s_7 = s_9 = 0$	$\mathbf{1}_{(0,2)}$	$\mathcal{S}_7 \cdot \mathcal{S}_9$
$s_9 = s_8 = 0$	$\mathbf{1}_{(-1,-2)}$	$\mathcal{S}_9 \cdot ([K_B^{-1}] + \mathcal{S}_9 - \mathcal{S}_7)$

(3.118)

where we used (3.114). Here  $\cdot$  denotes the intersection product on  $B$ .

Second, we calculated the multiplicities of the singlets in Sections 3.3.1 and 3.3.2. These arised at codimension two singularities where a rational section collides with a singularity in the Weierstrass fibration. We first calculate the line bundles of the polynomials

of the complete intersections that contain the respective codimension two loci. They read

Polynomial	Bundle	Polynomial	Bundle
$\delta g'_6$	$\mathcal{O}(2[K_B^{-1}] + 2\mathcal{S}_9 - \mathcal{S}_7)$	$g'_9$	$\mathcal{O}(3[K_B^{-1}] + \mathcal{S}_9 - \mathcal{S}_7)$
$g_9^{\mathcal{O}}$	$\mathcal{O}(3[K_B^{-1}])$	$\hat{g}_{12}^{\mathcal{O}}$	$\mathcal{O}(4[K_B^{-1}])$
$g_{9+3n_2}^R$	$\mathcal{O}(3[K_B^{-1}] + 3\mathcal{S}_9)$	$\hat{g}_{12+4n_2}^R$	$\mathcal{O}(4[K_B^{-1}] + 4\mathcal{S}_9)$

(3.119)

The polynomials  $\delta g'_6$  and  $g'_9$  were defined in eq. 3.72. Their zero loci contain the loci of the representation  $\mathbf{1}_{(1,1)}$ . Similarly,  $g_9^{\mathcal{O}}$  and  $\hat{g}_{12}^{\mathcal{O}}$  were defined in eqs. 3.59. Their zero loci contain the loci of the representation  $\mathbf{1}_{(1,0)}$ . Finally, the loci of  $\mathbf{1}_{(0,1)}$  are contained in the zero loci of  $g_{9+3n_2}^R$  and  $\hat{g}_{12+4n_2}^R$  defined in eqs. 3.63, respectively.

The polynomials (3.119) also have zeros at the loci corresponding to the fields in (3.118) that have already been counted. We have to subtract these zeros with the appropriate order in order to obtain the multiplicities of  $\mathbf{1}_{(1,1)}$ ,  $\mathbf{1}_{(1,0)}$  and  $\mathbf{1}_{(0,1)}$ . Because the functional dependencies of the polynomials in (3.119) on the  $s_i$ 's are the same as for the case  $B = \mathbb{P}^2$ , the order of the zeroes determined in Section 3.3.4, using resultant techniques, still holds. Invoking these results, the rest of the multiplicities are

Representation	Multiplicity
$\mathbf{1}_{(1,0)}$	$6[K_B^{-1}]^2 + [K_B^{-1}] \cdot (4\mathcal{S}_7 - 5\mathcal{S}_9) - 2\mathcal{S}_7^2 + \mathcal{S}_7 \cdot \mathcal{S}_9 + \mathcal{S}_9^2$
$\mathbf{1}_{(0,1)}$	$6[K_B^{-1}]^2 + [K_B^{-1}] \cdot (4\mathcal{S}_7 + 4\mathcal{S}_9) - 2\mathcal{S}_7^2 - 2\mathcal{S}_9^2$
$\mathbf{1}_{(1,1)}$	$6[K_B^{-1}]^2 + [K_B^{-1}] \cdot (-5\mathcal{S}_7 + 4\mathcal{S}_9) + \mathcal{S}_7^2 + \mathcal{S}_7 \cdot \mathcal{S}_9 - 2\mathcal{S}_9^2$

(3.120)

We note that the results for the special base  $B = \mathbb{P}^2$  are recovered by making the identifications  $[K_B^{-1}] \rightarrow 3H_B$ ,  $\mathcal{S}_7 \rightarrow n_{12}H_B$ ,  $\mathcal{S}_9 \rightarrow n_2H_B$  and  $H_B^2 \rightarrow 1$ , where again  $H_B$  is the hyperplane class of the base  $B$ .



### 3.5.3 Anomaly Cancellation

With the hypermultiplet representations and their multiplicities at hand, six-dimensional anomaly cancellation can be verified. For the convenience of the reader we summarize below the expressions for the respective mixed Abelian-gravitational, pure Abelian and pure gravitational anomaly cancellation:

$$\begin{aligned}
K_B \cdot b_{mn} &= -\frac{1}{6} \sum_{\underline{q}} x_{q_m, q_n} q_m q_n, \\
b_{mn} \cdot b_{kl} + b_{mk} \cdot b_{nl} + b_{ml} \cdot b_{nk} &= \sum_{\underline{q}} x_{q_m, q_n, q_k, q_l} q_m q_n q_k q_l, \\
273 = H - V + 29T, \quad K_B \cdot K_B &= 9 - T.
\end{aligned} \tag{3.121}$$

Here  $x_{q_m, q_n}$  and  $x_{q_m, q_n, q_k, q_l}$  denote the number of matter hypermultiplets with charges  $(q_m, q_n)$  and  $(q_m, q_n, q_k, q_l)$  under  $U(1)_m \times U(1)_n$ , respectively,  $U(1)_m \times U(1)_n \times U(1)_k \times U(1)_l$ . In addition,  $H$ ,  $V$  and  $T$  denote the total number of hyper-, vector- and tensor-multiplets, respectively. The  $b_{mn}$  denote curves in the base  $B$  defined as

$$b_{mn} = -\pi(\sigma(\hat{s}_m) \cdot \sigma(\hat{s}_n)) = \begin{pmatrix} -2[K_B] & \mathcal{S}_9 - \mathcal{S}_7 - [K_B] \\ \mathcal{S}_9 - \mathcal{S}_7 - [K_B] & 2(\mathcal{S}_9 - [K_B]) \end{pmatrix}_{mn}. \tag{3.122}$$

Here we have collectively denoted rational sections  $\hat{s}_m = (\hat{s}_Q, \hat{s}_R)_m$  and their divisor classes  $S_m = (S_Q, S_R)_m$ , with  $m = 1, 2$  as before. The Shioda map of rational sections  $\hat{s}_m$  to corresponding divisor classes  $\sigma(\hat{s}_m)$  gives:

$$\sigma(\hat{s}_Q) = S_Q - S_P - [K_B^{-1}], \quad \sigma(\hat{s}_R) = S_R - S_P - [K_B^{-1}] - \mathcal{S}_9. \tag{3.123}$$

In (3.122) we have further used (3.116).

Inserting (3.122) as well as the multiplicities (3.118) and (3.120) into the anomaly can-

cellation equations (3.121), we see that all equations are satisfied and thus all anomalies are cancelled. This verifies the six-dimensional anomaly cancellation for the general F-theory compactification with  $U(1) \times U(1)$  gauge symmetry over an arbitrary base  $B$ .<sup>14</sup>

---

<sup>14</sup>The base  $B$  has to admit a generic elliptic fibration of the form (3.47), i.e. all line bundles in (3.114) have to have generic sections  $s_i$ . See the discussion in Section 2 of [30].

# Engineering $U(1) \times U(1)$ in 4D - Adding $G_4$ Flux

Encouraged by the results of the previous chapter, we push toward more realistic scenarios and construct  $U(1) \times U(1)$  F-theory compactifications in four dimensions. To achieve this goal, we need to construct four-complex dimensional geometries (fourfolds). The appearance of Yukawa couplings at codimension three is expected. Finally, in order to obtain chiral matter in 4D,  $G_4$  flux have to be engineered on top of the geometry.

In this chapter, most of the content have been taken from [30], where the author of this dissertation is a co-author.

The content of this chapter is organized as follows. First, we leverage the knowledge from the previous chapter and construct the four-complex dimensional fibration using the  $dP_2$  ambient space for the fiber. As in the previous chapter, we proceed to find the spectrum of the theory. We realize that the charges of the hypermultiplets under  $U(1) \times U(1)$  remain unchanged. The number of chiral matter, however, requires the specification of the flux and the matter surfaces. As advertised, we find the Yukawa couplings at codimension three in the base, located at the intersection of three matter curves.

We continue with the construction of the  $G_4$  flux. Given that this flux is an element of  $H_V^{(2,2)}$ , we require the cohomology ring of the fourfold. The calculation of chiralities can then in principle be done with the integrating the flux over the matter surfaces. However, one problem appears, we do not have the explicit description of all matter surfaces. In order to achieve our goal we make use of the 4D/3D F- M-theory duality. The trick is to read the chirality from the Chern-Simons terms of the 3D theory. There is an interesting twist in the story here given that the section is not holomorphic. Finally we check anomaly cancellation of the spectrum.

Let us point to some results beyond the construction of the geometry. In order to calculate the Yukawa points we again made use of algebraic techniques, in particular, we had to describe the varieties as the zero locus of ideals. In order to obtain the varieties associated to each charged curve, we have to decompose the ideals in its prime ideals using primary decomposition. This technique has been adopted by the community and it has been dubbed as the ‘ideal technique’. Additionally, the existence of a non-holomorphic zero section had non-trivial implications in the F-theory M-theory duality. This was a very important result and this is why it is explained at length in a full section.

In the original article [30], almost half of the paper is dedicated to the  $SU(5)\times U(1)\times U(1)$  case. During the full study of this non-abelian example we found a non-flat fibration. The non-flat fiber can be wrapped by a M5 brane giving rise to stringy excitations in the low energy theory. It was an interesting discovery, however, we decided not to include this topic in this dissertation. We point the curious reader to the article for more information.

## 4.1 The Elliptic Curve in $dP_2$ And Its Fibrations

In this section we review the construction of the elliptic curve  $\mathcal{E}$  in  $dP_2$  and its Calabi-Yau elliptic fibrations over a general  $B$ . These Calabi-Yau manifolds have a rank two Mordell-Weil group, that gives rise to  $U(1) \times U(1)$  gauge symmetry in F-theory.

In section 4.1.1 we construct resolved elliptically fibered Calabi-Yau manifolds  $\hat{\pi} : \hat{X} \rightarrow X$  over an arbitrary base  $B$  with this elliptic curve  $\mathcal{E}$  as the general fiber. The singular Calabi-Yau manifold is denoted by  $X$ . We show that these Calabi-Yau manifolds  $\hat{X}$  are classified by the choice of two divisors  $\mathcal{S}_7, \mathcal{S}_9$  in the base  $B$ . In particular, we work out all the line bundles that are relevant to formulate the Calabi-Yau constraint of  $\hat{X}$ , which is the analog of the Tate model for elliptic fibrations with  $dP_2$ -elliptic fiber.

The content of section 4.1.1 is a direct extension of the discussion in [34], where the possibility of a full classification of all Calabi-Yau elliptic fibrations with general fiber  $\mathcal{E}$  was pointed out, but demonstrated explicitly only for  $B = \mathbb{P}^2$ .

### 4.1.1 General Calabi-Yau Fibrations with $dP_2$ -Elliptic Fiber

In this section we discuss the construction of resolved elliptically fibered Calabi-Yau manifolds  $\hat{X}$  with general elliptic fiber in  $dP_2$ . The following results hold for general complex dimension of  $\hat{X}$ , in particular for Calabi-Yau three- and fourfolds. We end this section with the concrete example of  $B = \mathbb{P}^3$ .

#### Classifying $dP_2$ -fibrations and their Calabi-Yau hypersurfaces $\hat{X}$

In general an elliptically fibered Calabi-Yau manifold  $\mathcal{E} \rightarrow \hat{X} \xrightarrow{\pi} B$  with  $\pi$  denoting the projection to the base  $B$  is constructed by first considering the defining equation for the desired elliptic curve  $\mathcal{E}$  alone and then by lifting the coefficients in this equation to sections over the base  $B$ . In the case at hand, the elliptic curve is described by (3.47). Thus, all we

have to do to obtain an elliptic fibration is to promote the coefficients  $s_i$  to sections of line bundles on the base  $B$ . Finally, the Calabi-Yau condition for (3.47) fixes the respective line bundles for the sections  $s_i$ .

The procedure of lifting the  $s_i$  to sections of  $B$  is described as follows. First, we have to define the ambient space in which the elliptically fibered manifold  $\hat{X} \rightarrow B$  is embedded. Since the constraint (3.47) merely cuts the elliptic curve  $\mathcal{E}$  out of  $dP_2$ , the ambient space is simply a  $dP_2$ -fibration over the base  $B$  of  $\hat{X}$ . It takes the form

$$\begin{array}{ccc} dP_2 & \longrightarrow & dP_2^B(\mathcal{S}_7, \mathcal{S}_9) \\ & & \downarrow \\ & & B \end{array} \quad (4.1)$$

which can be viewed as a generalization of a projective bundle. Here  $\mathcal{S}_7$  and  $\mathcal{S}_9$  are two divisors on  $B$  associated to the vanishing loci of the sections  $s_7$  and  $s_9$  in (3.47). The total space is denoted  $dP_2^B(\mathcal{S}_7, \mathcal{S}_9)$  since it is uniquely determined by these divisors  $\mathcal{S}_7$  and  $\mathcal{S}_9$  if we demand that the constraint (3.47) defines a Calabi-Yau manifold  $\hat{X}$ . In fact, we first note that any the  $dP_2$ -fibration is specified by only two divisors on  $B$ . This can be seen by noting that in a general such fibrations the homogeneous coordinates  $[u : v : w : e_1 : e_2]$  on  $dP_2$  are sections of five different line bundles on the base  $B$ , respectively. However, we can always use the three  $\mathbb{C}^*$ -actions to eliminate three of these line bundles, so that only two of the five coordinates on  $dP_2$  take values in non-trivial line bundles. We use the assignment of line bundles on  $B$  to the coordinates from the previous chapter,

$$u \in \mathcal{O}_B(\mathcal{S}_9 + [K_B]), \quad v \in \mathcal{O}_B(\mathcal{S}_9 - \mathcal{S}_7), \quad (3.111)$$

where  $K_B$  denotes the canonical bundle on  $B$  and  $[K_B]$  the associated divisor. All other coordinates on  $dP_2$  transform as the trivial bundle on  $B$ . We note that this parametrization

of the two line bundles for  $u$  and  $v$  is completely general, because  $\mathcal{S}_7$  and  $\mathcal{S}_9$  are completely general divisors on  $B$  at the moment.

Next, we use these results to readily calculate the total Chern class of  $dP_2^B(\mathcal{S}_7, \mathcal{S}_9)$  from adjunction from which we obtain its anti-canonical bundle, c.f. 3.113,

$$K_{dP_2^B}^{-1} = \mathcal{O}(3H - E_1 - E_2 + 2\mathcal{S}_9 - \mathcal{S}_7), \quad (4.2)$$

where we suppressed the dependence on  $\mathcal{S}_7, \mathcal{S}_9$  for brevity of our notation. Then the Calabi-Yau condition implies that the constraint (3.47) has to be a section of  $K_{dP_2^B}^{-1}$ . This immediately fixes the line bundles of all the sections  $s_i$  on  $B$ . We summarize the sections defining the elliptically fibered Calabi-Yau manifold  $\hat{X}$  as follows, c.f. 3.114,

section	bundle	section	bundle
$u$	$\mathcal{O}(H - E_1 - E_2 + \mathcal{S}_9 + [K_B])$	$s_1$	$\mathcal{O}(3[K_B^{-1}] - \mathcal{S}_7 - \mathcal{S}_9)$
$v$	$\mathcal{O}(H - E_2 + \mathcal{S}_9 - \mathcal{S}_7)$	$s_2$	$\mathcal{O}(2[K_B^{-1}] - \mathcal{S}_9)$
$w$	$\mathcal{O}(H - E_1)$	$s_3$	$\mathcal{O}([K_B^{-1}] + \mathcal{S}_7 - \mathcal{S}_9)$
$e_1$	$\mathcal{O}(E_1)$	$s_5$	$\mathcal{O}(2[K_B^{-1}] - \mathcal{S}_7)$
$e_2$	$\mathcal{O}(E_2)$	$s_6$	$\mathcal{O}([K_B^{-1}])$
		$s_7$	$\mathcal{O}(\mathcal{S}_7)$
		$s_8$	$\mathcal{O}([K_B^{-1}] + \mathcal{S}_9 - \mathcal{S}_7)$
		$s_9$	$\mathcal{O}(\mathcal{S}_9)$

(4.3)

In particular we see that with the parametrization (3.111) the divisors  $\mathcal{S}_7$  and  $\mathcal{S}_9$  are indeed associated to  $s_7$  and  $s_9$  as claimed at the beginning.

## Basic geometry of Calabi-Yau manifolds with $dP_2$ -elliptic fiber

Having constructed the general elliptically fibered Calabi-Yau manifolds  $\hat{X}$  over  $B$ , we discuss next the group of divisors on  $\hat{X}$ . By construction, the basis of divisors on a generic<sup>1</sup>  $\hat{X}$  is induced by a basis of divisors on the ambient space  $dP_2^B(\mathcal{S}_7, \mathcal{S}_9)$ , which consists of divisors of the base  $B$  and the fiber  $dP_2$ . The divisors induced from a basis of divisors  $D_\alpha^b$  of the base  $B$  are the vertical divisors  $D_\alpha = \pi^*(D_\alpha^b)$  of the elliptic fibration  $\pi : \hat{X} \rightarrow B$ . Similarly, the classes  $H, E_1, E_2$  of the fiber  $dP_2$  become divisors on  $\hat{X}$ . Then, the points  $P, Q$  and  $R$  in (3.48) lift to, in general, *rational sections* of the fibration of  $\pi : \hat{X} \rightarrow B$ , denoted  $\hat{s}_P, \hat{s}_Q$  and  $\hat{s}_R$ , with  $\hat{s}_P$  the zero section. We denote the homology classes of the associated divisors by capital letters,

$$S_P = E_2, \quad S_Q = E_1, \quad S_R = H - E_1 - E_2 + \mathcal{S}_9 + [K_B]. \quad (4.4)$$

In general, a rational section is a non-holomorphic map of the base  $B$  into  $\hat{X}$ , such as  $\hat{s}_P : B \rightarrow \hat{X}$  for example. A rational section  $B \rightarrow \hat{X}$  is ill-defined over codimension two loci to the effect that it wraps entire fiber components over these loci. From a given rational section, one can easily obtain a *holomorphic section*, i.e. a holomorphic map  $\hat{B} \rightarrow \hat{X}$ , by a birational transformation, namely a blow-up  $\hat{B} \rightarrow B$  at those codimension two loci of  $B$ . Usually the zero section  $\hat{s}_P$  has been assumed to be holomorphic in F-theory. Only lately, the possibility of a non-holomorphic zero section  $\hat{s}_P$  in F-theory has been studied [20, 34, 60]. The group of sections excluding the zero section  $\hat{s}_P$  is the *Mordell-Weil group* of rational sections on  $\hat{X}$ , which in the case at hand is rank two and generated by  $\hat{s}_Q, \hat{s}_R$ . For brevity of our notation, we will occasionally denote the generators of the Mordell-Weil

---

<sup>1</sup>By generic we mean the absence of Cartan divisors  $D_i$  from resolutions of codimension one singularities of the fibration of  $\hat{X}$ . We will briefly discuss the geometry of  $\hat{X}$  in the presence of  $D_i$  at the end of this section.



group and their divisor classes collectively as

$$\hat{s}_m = (\hat{s}_Q, \hat{s}_R), \quad S_m = (S_Q, S_R). \quad (4.5)$$

There are some characteristic intersections involving the divisors  $S_P, S_Q$  and  $S_R$  in (4.4) that immediately follow from the defining properties of a section. We list them in the following and refer to [105, 97, 31, 34] for a more thorough discussion. We also give a simple criterion to distinguish between rational and holomorphic sections. A more detailed account on intersections in the presence of a rational zero section can be found in [60]. Here, we content ourselves with noting that  $\hat{s}_P$  is holomorphic if  $\mathcal{S}_9 = 0$  or  $\mathcal{S}_8 = 0$ ,  $\hat{s}_Q$  is holomorphic if  $\mathcal{S}_3 = 0$  or  $\mathcal{S}_7 = 0$  and  $\hat{s}_R$  is holomorphic if  $\mathcal{S}_7 = 0$  or  $\mathcal{S}_9 = 0$ , cf. the paragraph following (3.48) and [34].

The following intersections and definitions will be crucial in the rest of this work:

<b>Universal intersection:</b>	$S_P \cdot F = S_m \cdot F = 1$ with general fiber $F \cong \mathcal{E}$ , <span style="float: right;">(4.6)</span>
<b>Rational sections:</b>	$\pi(S_P^2 + [K_B^{-1}] \cdot S_P) = \pi(S_m^2 + [K_B^{-1}] \cdot S_m) = 0$ , <span style="float: right;">(4.7)</span>
	$\mathcal{S}_7 = \pi(S_P \cdot S_R), \quad \mathcal{S}_9 = \pi(S_Q \cdot S_R)$ , <span style="float: right;">(4.8)</span>
<b>Holomorphic sections:</b>	$S_P^2 + [K_B^{-1}] \cdot S_P = S_m^2 + [K_B^{-1}] \cdot S_m = 0$ , <span style="float: right;">(4.9)</span>
<b>Shioda maps:</b>	$\sigma(\hat{s}_Q) = S_Q - S_P - [K_B^{-1}]$ , <span style="float: right;">(4.10)</span>
	$\sigma(\hat{s}_R) = S_R - S_P - [K_B^{-1}] - \mathcal{S}_9$ ,
<b>Height pairing:</b>	$\begin{pmatrix} 2[K_B] & [K_B] - \mathcal{S}_7 + \mathcal{S}_9 \\ [K_B] + \mathcal{S}_7 - \mathcal{S}_9 & 2[K_B] - 2\mathcal{S}_9 \end{pmatrix}_{mn}$ <span style="float: right;">(4.11)</span>

Let us briefly comment on these intersections in the order of their appearance. The intersection (4.6) is an immediate consequence of the definition of a section: its divisor class intersects the general class of the fiber  $F \cong \mathcal{E}$  at a point. The relation (4.7) can be shown by an adjunction argument, see section 4.2.2 for direct cohomology computations. Here we have defined the a projection onto the homology  $H^4(B)$  of the base as

$$\pi(\mathcal{C}) = (\mathcal{C} \cdot \Sigma^\alpha) D_\alpha^b, \quad \Sigma_b^\alpha \cdot D_\beta^b = \delta_\beta^\alpha \quad (4.12)$$

for every complex surface  $\mathcal{C}$  in  $\hat{X}$ . The intersection pairings on  $\hat{X}$ , respectively,  $B$  are denoted  $\cdot$  and the  $\Sigma^\alpha = \pi^*(\Sigma_b^\alpha)$  arise from a basis of curves  $\Sigma_b^\alpha$  dual to the divisors  $D_\alpha^b$  on  $B$  as indicated in the last equation in (4.12). We emphasize that in the case of a holomorphic section, the relations (4.7) hold in the full homology of  $\hat{X}$  as indicated in (4.9). The divisors  $\mathcal{S}_7, \mathcal{S}_9$  are the codimension one loci where the sections collide in the fiber  $\mathcal{E}$ , as discussed below (3.48). They are encoded in the intersections (4.8). Next, we introduce the divisors  $\sigma(\hat{s}_Q), \sigma(\hat{s}_R)$  in (4.10). The map  $\sigma$  is the Shioda map that takes here the form

$$\sigma(\hat{s}_m) := S_m - \tilde{S}_P - \pi(S_m \cdot \tilde{S}_P), \quad (4.13)$$

where we introduced the combination [56, 12]

$$\tilde{S}_P = S_P + \frac{1}{2}[K_B^{-1}]. \quad (4.14)$$

We refer to [110, 105, 97, 31, 34] for more details on the Shioda map. We note that the divisors (4.10) support U(1)-gauge fields in F-theory due to their vanishing intersections with vertical divisors  $D_\alpha$  and the zero-section, as well as potential Cartan divisors  $D_i$  of non-Abelian groups. Finally, we have calculated the intersection matrix of the Shioda map of  $\hat{s}_Q, \hat{s}_R$  in (4.11).

We finish this section by some concluding definitions and remarks on the general structure of the fibrations (4.1) and  $\hat{X}$ . First, we summarize the basis of divisors on  $\hat{X}$  as

$$D_A = (\tilde{S}_P, D_\alpha, D_i, \sigma(\hat{s}_m)), \quad A = 0, 1, \dots, h^{(1,1)}(\hat{B}) + \text{rk}(G) + 3, \quad (4.15)$$

where we have collectively denoted the basis (4.10) as  $\sigma(\hat{s}_m)$ . We have also introduced one set of Cartan divisors  $D_i$  with  $i = 1, \dots, \text{rk}(G)$  in order to prepare for the presence of a non-Abelian group  $G$ . These divisors  $D_i$  are present for non-generic  $\hat{X}$  with a resolved singularity of type  $G$  of the elliptic fibration over codimension one in  $B$ . The  $D_i$  admit a fibration

$$\begin{array}{ccc} c_{-\alpha_i} & \longrightarrow & D_i \\ & & \downarrow \\ & & \mathcal{S}_G^b \end{array} \quad (4.16)$$

where the general fiber is a rational curve  $c_{-\alpha_i} \cong \mathbb{P}^1$  that corresponds to the simple root  $-\alpha_i$  of  $G$ . The divisor  $\mathcal{S}_G^b$  in  $B$  physically supports 7-branes that give rise to the non-Abelian gauge symmetry  $G$  in F-theory [101, 102, 9].

Next, we expand the canonical bundle  $K_B$  of the base  $B$  in terms of the vertical divisors  $D_\alpha$  as

$$[K_B] = K^\alpha D_\alpha \quad (4.17)$$

with coefficients  $K^\alpha$ . Similarly, we expand the divisors

$$\mathcal{S}_7 = n_7^\alpha D_\alpha^b, \quad \mathcal{S}_9 = n_9^\alpha D_\alpha^b, \quad (4.18)$$

with general positive integral coefficients  $n_7^\alpha, n_9^\alpha, \alpha = 1, \dots, h^{(1,1)}(B)$ . It is important to emphasize that the coefficients  $n_7^\alpha, n_9^\alpha$  are in general further bounded from above by the requirement that all sections  $s_i$  in (4.3) are generic, i.e. that the line bundle of  $s_i$  admits

sufficiently many holomorphic sections. If this is not the case we expect additional singularities in  $\hat{X}$ , potentially corresponding to a minimal (non-Abelian) gauge symmetry in F-theory. For this reason, we will in the rest of this work assume that  $\hat{X}$  can be constructed with generic  $s_i$ .

Despite these restrictions on the integers  $n_7^\alpha$  and  $n_9^\alpha$  we would like to point out that the constructions of the fibration (4.1) and of  $\hat{X}$  hold in general for an arbitrary base  $B$  and arbitrary complex dimension. In particular this analysis applies to an arbitrary choice of divisors  $\mathcal{S}_7$  and  $\mathcal{S}_9$  within these bounds. In particular the general construction here reproduce immediately the classification in [34] with  $B = \mathbb{P}^2$  as a special case.

### **$dP_2$ -fibrations over $B = \mathbb{P}^3$ with generic Calabi-Yau hypersurfaces $\hat{X}$**

We conclude with the discussion of the special case  $B = \mathbb{P}^3$ , which will be considered in later sections of this work. In this case, there is only one divisor in the base, the hyperplane  $H_B$ , so that the  $dP_2$ -fibration (4.1) is specified only by two integers  $n_7 \equiv n_7^1, n_9 \equiv n_9^1$ . In this case we use the notation

$$\begin{array}{ccc} dP_2 & \longrightarrow & dP_2(n_7, n_9) \\ & & \downarrow \\ & & \mathbb{P}^3 \end{array} \quad (4.19)$$

where we suppress the base  $B = \mathbb{P}^3$  when denoting the total space (4.1) of the fibration if the context is clear.

We note that  $K_{\mathbb{P}^3}^{-1} = \mathcal{O}_{\mathbb{P}}(4)$ . In this case all sections  $s_i$  exist iff all bundles in the second table in (4.3) have non-negative degree. This puts the following conditions on the integers  $n_7, n_9$ ,

$$0 \leq n_7, n_9 \leq 8, \quad n_7 + n_9 \leq 12, \quad 0 \leq 4 + n_7 - n_9, \quad 0 \leq 4 + n_9 - n_7. \quad (4.20)$$

The domain of allowed values for  $n_7$  and  $n_9$  are displayed in figure 4.1. The general strategy to build the corresponding reflexive polytopes is outlined in the appendix of [30]. It is satisfying, that in the toric context the conditions (4.20) are enforced by reflexivity of the toric polytope, i.e. for values  $n_7, n_9$  exceeding the bounds (4.20) the toric polytope is no longer reflexive.

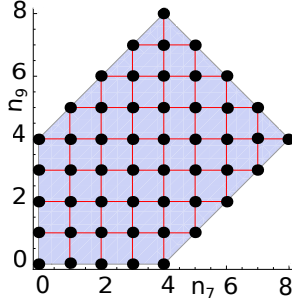


Figure 4.1: Each dot corresponds to a  $dP_2$ -fibration over  $\mathbb{P}^3$  with generic Calabi-Yau  $\hat{X}$ .

## 4.2 Calabi-Yau Fourfolds with Rank Two Mordell-Weil

In this section we analyze F-theory compactifications to four dimensions on a generic elliptically fibered Calabi-Yau fourfold  $\hat{X}$  over a base  $B$  with general fiber  $\mathcal{E}$  in  $dP_2$ . These compactifications have a gauge theory with  $U(1) \times U(1)$  gauge group and a number of chiral matter fields in representations  $\mathbf{1}_{(q_1, q_2)}$ . The possible  $U(1) \times U(1)$ -charges  $(q_1, q_2)$  have been determined recently in [74, 34] and the full 6D anomaly-free spectrum including matter multiplicities has been derived for  $B = \mathbb{P}^2$  in [34].

Here we extend this geometric analysis to fourfolds. The main difference to the 6D case is that matter is not localized anymore at points in  $B$ , but on in general rather complicated matter curves. The determination of these matter curves and some of their associated matter surfaces, along with the Yukawa points, is presented in section 4.2.1. Then, in section 4.2.2 we present a method to determine the cohomology ring of the fourfold  $\hat{X}$ . We use these

techniques to derive general expressions for the Euler number of  $\hat{X}$  and its second Chern class. For the example of  $B = \mathbb{P}^3$  we finally compute the full vertical cohomology group. These calculations serve as a preparation for the computation of 4D chiralities in section 4.4, which requires both the knowledge of matter surfaces and the construction of  $G_4$ -flux.

## 4.2.1 Singularities of the Fibration: Matter Surfaces & Yukawa Points

We organize this section into a detailed discussion of codimension two singularities in section 4.2.1 and a very brief account on codimension three singularities in section 4.2.1.

### Matter: Codimension Two

In general, the determination of the matter sector in F-theory vacua with general gauge group requires a detailed analysis of singularities of the elliptic fibration of the Calabi-Yau fourfold at codimension two in the base  $B$ , where the elliptic fiber  $\mathcal{E}$  becomes reducible. Then one has to identify the isolated rational curve  $c_{\mathbf{w}}$  in the fiber over these loci, since these correspond in F-theory to matter in a representation  $\mathbf{R}$  from wrapped M2-brane states. These curves are in one-to-one correspondence to the weights  $\mathbf{w}$  of the representations  $\mathbf{R}$  and accordingly labeled. In the case of elliptically fibered Calabi-Yau fourfolds, the codimension two matter loci are Riemann surfaces of genus  $g$ , the so-called matter curves  $\Sigma_{\mathbf{R}}$  in  $B$  conveniently labeled by the corresponding matter representation  $\mathbf{R}$ . In addition, for the determination of four-dimensional chirality, compare section 4.4, we have to know the homology classes of the associated matter surfaces

$$\begin{array}{ccc}
 c_{\mathbf{w}} & \longrightarrow & C_{\mathbf{R}}^{\mathbf{w}} \\
 & & \downarrow \\
 & & \Sigma_{\mathbf{R}}
 \end{array} \tag{4.21}$$

which are constructed as the fibration of the rational curve  $c_{\mathbf{w}}$  corresponding to a given weight  $\mathbf{w}$  of the representation  $\mathbf{R}$  fibered over  $\Sigma_{\mathbf{R}}$ .

In this section we determine the matter curves  $\Sigma_{\mathbf{R}}$  and the matter surfaces  $C_{\mathbf{R}}^{\mathbf{w}}$  for the six representations occurring in the Calabi-Yau fourfold  $\hat{X}$ . As we demonstrate, their determination is complicated by the fact that three of the six the codimension two loci in the base  $B$  where the elliptic fiber  $\mathcal{E}$  becomes reducible are themselves reducible curves. Their irreducible components are multiple different matter curves  $\Sigma_{\mathbf{R}}$ . Some of these matter curves, denoted  $\Sigma_{\mathbf{R}'}$ , fail to be complete intersection and can only be described in terms of their prime ideals. These prime ideals are straightforwardly constructed from the two equations of the original reducible codimension two locus. However, the isolation of rational curves  $c_{\mathbf{w}}$  over those matter curves  $\Sigma_{\mathbf{R}'}$  is very involved. Thus, in these cases we can not determine the corresponding matter surfaces (4.21) explicitly. Fortunately, we can obtain the other three matter surfaces straightforwardly, and are still able to determine the full F-theory matter spectrum for the fourfold  $\hat{X}$ , as outlined in section 4.4. It would be desirable, however, to reproduce the results obtained there invoking M-/F-theory duality by direct geometric computation based on a better understanding of the matter surfaces  $C_{\mathbf{R}'}$  in general.

In any case, we can qualitatively describe all the matter surfaces  $C_{\mathbf{R}}^{\mathbf{w}}$  by recalling the construction of the resolved fourfold  $\hat{X}$ . The smooth fourfold  $\hat{X}$  is formed by two consecutive blow-ups of a singular Weierstrass model  $X$ . We depict this schematically as

$$\begin{array}{ccc}
 \hat{X} \subset dP_2^B(\mathcal{S}_7, \mathcal{S}_9) & \xrightarrow{\hat{\pi}} & X \subset (\mathbb{P}^2(1, 2, 3) \rightarrow B) \\
 \text{generic CY} & & \text{non-generic WSF} \\
 \swarrow \pi_2 & & \nearrow \pi_1 \\
 & \hat{X} \subset (\mathbb{P}^2 \rightarrow B) & \\
 & \text{non-generic cubic} & 
 \end{array} \tag{4.22}$$

where the full blow-down map  $\hat{\pi} : \hat{X} \rightarrow X$  is consequently a composition  $\hat{\pi} = \pi_1 \circ \pi_2$ . On the left we have the smooth geometry with elliptic fiber constructed in section 4.1. It can be understood as a toric blow-up  $\pi_2 : \hat{X} \rightarrow \tilde{X}$  from a non-generic cubic in  $\mathbb{P}^2$ , with corresponding fourfold denoted by  $\tilde{X}$ . A final blow-down  $\pi_1$  yields the singular Weierstrass form (WSF)  $X$  with  $\mathbb{P}^2(1, 2, 3)$ -fiber. The birational map  $\pi_1$  is derived in detail in [34], see its defining equations Eqs. (3.18) and (3.20) therein.

Having the diagram (4.22) in mind, the three matter surfaces  $\mathcal{C}_{\mathbf{R}}$  which have a simple description are those generated in the blow-up  $\pi_2$ . There are three simple codimension two singularities in  $\tilde{X}$ , which are precisely the three simple matter curves  $\Sigma_{\mathbf{R}}$ . Their pull-backs under  $\pi_2$  are precisely the matter surfaces  $\mathcal{C}_{\mathbf{R}} = \pi_2^*(\Sigma_{\mathbf{R}})$ . Because of the simplicity of both  $\Sigma_{\mathbf{R}}$  and the blow-up  $\pi_2$ , these surfaces have a description as a simple complete intersection in the ambient space  $dP_2(\mathcal{S}_7, \mathcal{S}_9)$ . In contrast, the other three matter curves  $\Sigma_{\mathbf{R}'}$  are the loci of codimension two singularities in the WSF  $X$ , which are resolved by the map  $\pi_1$ . However, these curves  $\Sigma_{\mathbf{R}'}$  have a description only in terms of prime ideals and the map  $\pi_1$  is not a simple toric blow-up but a fully-fledged birational map [34]. These two complications make an explicit determination of the surfaces  $\mathcal{C}_{\Sigma_{\mathbf{R}'}}^{\mathbf{w}}$  hard. Nevertheless, the matter surfaces are again abstractly given by  $\mathcal{C}_{\mathbf{R}'} = \pi_1^*(\Sigma_{\mathbf{R}'})$ , which are ruled surfaces over  $\Sigma_{\mathbf{R}'}$ . Thus, the determination of the exceptional loci of the map  $\pi_1$  might be a first step towards an understanding of these matter surfaces.

## Summary of Matter Representations & Their Matter Curves

Before going into technical calculations of matter curves and surfaces, let us briefly summarize the matter content as it has been determined in [74, 34].

There are six different matter representations  $\mathbf{R} = \mathbf{1}_{(q_1, q_2)}$  in the F-theory compactification on the fourfold  $\hat{X}$ . The list of realized  $U(1) \times U(1)$ -charges, together with the



cohomology class of the corresponding matter curves  $\Sigma_{\mathbf{R}}$  determined below, reads

Matter	Homology class of $\Sigma_{\mathbf{R}}$ in $B$
$\mathbf{1}_{(1,0)}$	$6[K_B^{-1}]^2 + 4[K_B^{-1}] \cdot \mathcal{S}_7 - 5[K_B^{-1}] \cdot \mathcal{S}_9 + \mathcal{S}_9^2 + \mathcal{S}_7 \cdot \mathcal{S}_9 - 2\mathcal{S}_7^2$
$\mathbf{1}_{(0,1)}$	$6[K_B^{-1}]^2 + 4[K_B^{-1}] \cdot (\mathcal{S}_7 + \mathcal{S}_9) - 2\mathcal{S}_7^2 - 2\mathcal{S}_9^2$
$\mathbf{1}_{(1,1)}$	$6[K_B^{-1}]^2 + 4[K_B^{-1}] \cdot \mathcal{S}_9 - 5[K_B^{-1}] \cdot \mathcal{S}_7 + \mathcal{S}_7^2 + \mathcal{S}_7 \cdot \mathcal{S}_9 - 2\mathcal{S}_9^2$
$\mathbf{1}_{(-1,1)}$	$([K_B^{-1}] + \mathcal{S}_7 - \mathcal{S}_9) \cdot \mathcal{S}_7$
$\mathbf{1}_{(0,2)}$	$\mathcal{S}_7 \cdot \mathcal{S}_9$
$\mathbf{1}_{(-1,-2)}$	$\mathcal{S}_9 \cdot ([K_B^{-1}] + \mathcal{S}_9 - \mathcal{S}_7)$

(4.23)

Here we used as before the notation  $[K_B^{-1}]$  for the anti-canonical divisor of the base and denoted the intersection on  $B$  as  $\cdot$ . These representations of matter fields are model-independent and in particular do not depend on the choice of base  $B$ . The last three matter representations arise from rational curves created in the blow-up  $\pi_2^{-1}$  in (4.22). Their matter curves are simply described by  $s_3 = s_7 = 0$ ,  $s_7 = s_9 = 0$  and  $s_8 = s_9 = 0$  in the order of their appearance in (4.23). The first three representations arise from rational curves from the blow-up  $\pi_1^{-1}$  in (4.22). The determination of their matter curves is more involved and presented below.

All the matter representations in (4.22) arise from M2-branes on rational curves  $c_{\mathbf{w}}$  with wight  $\mathbf{w} = (q_1, q_2)$ . These charges are calculated by the intersection of the curve  $c_{\mathbf{w}}$  with the Shioda maps  $\sigma(\hat{s}_Q)$ ,  $\sigma(\hat{s}_R)$  defined in (4.10) as

$$q_m \equiv \sigma(\hat{s}_m) \cdot c_{\mathbf{w}} = (S_m \cdot c_{\mathbf{w}}) - (S_P \cdot c_{\mathbf{w}}), \quad (4.24)$$

All curves  $c_{\mathbf{w}}$  are part of an  $I_2$ -fiber. Along the matter surfaces in (4.23) the general elliptic fiber  $\mathcal{E}$  splits into two rational curves  $c_1, c_2 \cong \mathbb{P}^1$  intersecting in two points with one curve,

say  $c_1$ , the original singular fiber and the other curve  $c_2 \equiv c_w$ . We write this as

$$I_2\text{-fiber} : \quad \mathcal{E} = c_1 + c_2, \quad c_1 \cdot c_2 = 2. \quad (4.25)$$

A cartoon of such a reducible fiber together with possible locations of the points  $P$ ,  $Q$  and  $R$  is depicted in figure 4.2. In terms of the Calabi-Yau constraint (3.47) the split of  $\mathcal{E}$  into

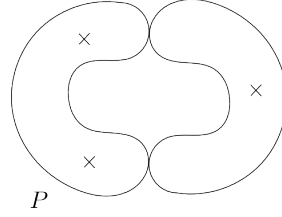


Figure 4.2:  $I_2$ -fiber from resolving a codimension two singularity of the fibration of  $\hat{X}$ .

an  $I_2$ -fiber is visible as a factorization at a point  $pt \in \Sigma_{\mathbf{R}}$  as

$$p|_{pt} = p_1 \cdot p_2. \quad (4.26)$$

Here the two rational curves in (4.25) are described by one of these two factors, for example  $c_1 = \{p_1 = 0, pt \in \Sigma_{\mathbf{R}}\}$  and  $c_2 = \{p_2 = 0, pt \in \Sigma_{\mathbf{R}}\}$ .

### **Matter Surfaces $\mathcal{C}_{(-1,1)}, \mathcal{C}_{(0,2)}, \mathcal{C}_{(-1,-2)}$ and their Homology Classes**

Next, we determine the matter surfaces  $\mathcal{C}_{\mathbf{R}}^w$  for the last three representations in (4.23). As we will see, this is straightforward since the matter curves  $\Sigma_{\mathbf{R}}$  in these cases are irreducible varieties of the simple form  $s_i = s_j = 0$  for appropriate  $i, j$ . This implies that the factorization of the elliptic fiber  $\mathcal{E} = c_1 + c_2$  is manifest over the entire matter curve  $\Sigma_{\mathbf{R}}$  and the matter surfaces  $\mathcal{C}_{\mathbf{R}}^w$  can be described by a complete intersection of three constraints in the ambient space  $dP_2^B(\mathcal{S}_7, \mathcal{S}_9)$ . Then its homology class is given simply by the product of the divisor classes of each of these constraints.

The resulting homology classes of matter surfaces read

Matter surface	Homology class
$\mathcal{C}_{\mathbf{1}_{(-1,1)}}$	$([K_B^{-1}] + \mathcal{S}_7 - \mathcal{S}_9) \cdot \mathcal{S}_7 \cdot E_1$
$\mathcal{C}_{\mathbf{1}_{(0,2)}}$	$\mathcal{S}_7 \cdot \mathcal{S}_9 \cdot ([K_B^{-1}] + \mathcal{S}_9 - \mathcal{S}_7 + 2H)$
$\mathcal{C}_{\mathbf{1}_{(-1,-2)}}$	$([K_B^{-1}] + \mathcal{S}_9 - \mathcal{S}_7) \cdot \mathcal{S}_9 \cdot (3H - E_1 - 2E_2 + 2\mathcal{S}_9 - \mathcal{S}_7)$

(4.27)

Here we suppressed the weight  $\mathbf{w}$  since it is identical to the charges  $(q_1, q_2)$ . We obtain the homology class of the first matter surface  $\mathcal{C}_{\mathbf{1}_{(-1,1)}}$  by noting its description as the complete intersection

$$\mathcal{C}_{\mathbf{1}_{(-1,1)}} = \{s_3 = s_7 = 0, e_1 = 0\} \quad (4.28)$$

in the ambient space  $dP_2^B(\mathcal{S}_7, \mathcal{S}_9)$ . Here the first two equations describe the matter curve  $\Sigma_{\mathbf{1}_{(-1,1)}} = \{s_3 = s_7 = 0\}$  over which the Calabi-Yau constraint (3.47) factorizes as  $p = p_1 p_2$  with one factor given by  $e_1$ , cf. section 4.3 of [34]. Thus, the rational isolated curve is described as  $c_{(-1,1)} = \{e_1 = 0, pt \in \Sigma_{(-1,1)}\}$  over all the points of  $\Sigma_{(-1,1)}$ . The homology class in the first line of (4.27) for  $\mathcal{C}_{\mathbf{1}_{(-1,1)}}$  in the ambient space  $dP_2^B(\mathcal{S}_7, \mathcal{S}_9)$  is then easily obtained from (4.28) employing the assignments (4.3) of line bundles to  $s_3, s_7$  and  $e_1$ .

Similarly we obtain the homology classes of the matter surfaces  $\mathcal{C}_{\mathbf{1}_{(0,2)}}$  and  $\mathcal{C}_{\mathbf{1}_{(-1,-2)}}$ . In the former case the matter curve is  $\Sigma_{\mathbf{1}_{(0,2)}} = \{s_7 = s_9 = 0\}$  over which the Calabi-Yau constraint (3.47) factorizes globally with the isolated rational curve given by [34]

$$c_{(0,2)} = \{s_1 e_1^2 e_2^2 u^2 + s_2 e_1 e_2^2 uv + s_3 e_2^2 v^2 + s_5 e_1^2 e_2 uw + s_6 e_1 e_2 vw + s_8 e_1^2 w^2 = 0\}. \quad (4.29)$$

Here it is understood that the sections  $s_i$  are evaluated on  $\Sigma_{\mathbf{1}_{(0,2)}}$ . The homology class of this complete intersection is the product of the class of  $c_{(0,2)}$  and of  $\Sigma_{\mathbf{1}_{(0,2)}}$  and we immediately reproduce the second line in (4.27) using (4.3). Finally, the matter curve for  $\mathbf{1}_{(-1,-2)}$  is

given by  $\Sigma_{\mathbf{1}_{(-1,-2)}} = \{s_8 = s_9 = 0\}$  and the isolated rational curve is [34]

$$c_{(-1,-2)} = \{s_1 e_1^2 e_2 u^3 + s_2 e_1 e_2 u^2 v + s_3 e_2 u v^2 + s_5 e_1^2 u^2 w + s_6 e_1 u v w + s_7 v^2 w = 0\}, \quad (4.30)$$

where as before the  $s_i$  are evaluated on  $\Sigma_{\mathbf{1}_{(-1,-2)}}$ . Then, the matter surface is again a complete intersection in the ambient space (4.1) and its homology class, employing the line bundles (4.3), is indeed given by the third line in (4.27).

### **Matter Curves $\Sigma_{(1,0)}$ , $\Sigma_{(0,1)}$ , $\Sigma_{(1,1)}$ and their Prime Ideals**

As mentioned before, the three remaining matter curves  $\Sigma_{\mathbf{R}'}$  are themselves no simple complete intersections, but contained in a reducible codimension two subvarieties in  $B$  that are complete intersections. To isolate the component  $\Sigma_{\mathbf{R}'}$  of interest we have to determine its prime ideal. This prime ideal is generated by more than two constraints, but still describes a codimension two variety in  $B$ . In addition, the factorization (4.26) describing the split  $\mathcal{E} = c_1 + c_2$  of the elliptic curve does not occur globally over the matter curves  $\Sigma_{\mathbf{R}'}$ , but is manifest only at generic points of  $\Sigma_{\mathbf{R}'}$ . These combined effects render the determination of the homology class of the matter surfaces  $\mathcal{C}_{\mathbf{R}'}$  unfeasible. However, we can obtain the homology class of the matter curves  $\Sigma_{\mathbf{R}'}$  as shown next. For completeness we will also present the prime ideal for one illustrative example. In general the prime ideals are needed for a thorough analysis of codimension three singularities presented in section 4.2.1.

We begin with the determination of the homology classes of the matter curves  $\Sigma_{\mathbf{R}'}$ . They can be obtained by first determining the homology class of the two equations for the reducible codimension two locus in  $B$  and by then subtracting the classes of those components  $\Sigma_{\mathbf{R}}$  we are not interested in. As in the six-dimensional case [34] we have to subtract the components  $\Sigma_{\mathbf{R}}$  with the right multiplicity, which is computed by the resultant<sup>2</sup>

---

<sup>2</sup>In general, the resultant gives the order of a root of two polynomials in two variables.

of the two equations at the root corresponding to  $\Sigma_{\mathbf{R}}$ . The resulting homology classes of this computations give the first three lines of (4.23). We work out these homology classes in detail in the remainder of this section.

First we present the equations for the reducible codimension two loci in  $B$  that contain the three matter curves  $\Sigma_{\mathbf{R}}$  that we are interested in as irreducible components. These codimension two loci read [34]

$$\text{loc}_1 = \{s_7s_8^2 + s_9(s_5s_9 - s_6s_8) = s_3s_8^2 - s_2s_8s_9 + s_1s_9^2 = 0\}, \quad (4.31)$$

$$\begin{aligned} \text{loc}_2 = \{ & s_3s_6s_8 - s_2s_7s_8 - s_3s_5s_9 + s_1s_7s_9 = s_3^2s_8^2 + s_7(s_1s_7s_8 + s_2s_5s_9 - s_2s_6s_8) \\ & + s_3(s_6^2s_8 - s_5s_7s_8 - s_5s_6s_9 - s_2s_8s_9 + s_1s_9^2) = 0\}, \end{aligned}$$

$$\begin{aligned} \text{loc}_3 = \{ & 2s_7^3s_8^3 + s_3s_9^3(s_5s_9 - s_6s_8) + s_7^2s_8s_9(2s_5s_9 - 3s_6s_8) - s_7s_9^2(s_5s_6s_9 + s_2s_8s_9 - s_6^2s_8 \\ & - 2s_3s_8^2 - s_1s_9^2) = s_7^4s_8^4 + 2s_7^3s_8^2s_9(s_5s_9 - s_6s_8) + s_7s_9^3(2s_3s_8 - s_2s_9)(s_5s_9 - s_6s_8) \\ & - s_7^2s_9^2(2s_5s_6s_8s_9 + s_2s_8^2s_9 - s_6^2s_8^2 - 2s_3s_8^3 - s_5^2s_9^2) + s_3s_9^4(s_3s_8^2 + s_9(s_1s_9 - s_2s_8)) = 0\} \end{aligned}$$

By calculating the associated prime ideals<sup>3</sup> of  $\text{loc}_1$  we see that it has two irreducible components. One is obviously the matter curve  $\Sigma_{\mathbf{1}_{(-1,-2)}} = \{s_8 = s_9 = 0\}$  and the other one is the matter curve  $\Sigma_{\mathbf{1}_{(1,1)}}$ . Then we determine the homology class of the reducible variety  $\text{loc}_1$ . We further recall from [34] that the order of the root  $(s_8, s_9) = (0, 0)$  of the two polynomials in  $\text{loc}_1$  is 4. Thus, decompose the class of  $\text{loc}_1$  as

$$\begin{aligned} [\text{loc}_1] &= (2[K_B^{-1}] + 2\mathcal{S}_9 - \mathcal{S}_7) \cdot (3[K_B^{-1}] + \mathcal{S}_9 - \mathcal{S}_7) \cong \Sigma_{(1,1)} + 4\Sigma_{(-1,-2)} \\ \Rightarrow \Sigma_{(1,1)} &\cong 6[K_B^{-1}]^2 + 4[K_B^{-1}] \cdot \mathcal{S}_9 - 5[K_B^{-1}] \cdot \mathcal{S}_7 + \mathcal{S}_7^2 + \mathcal{S}_7 \cdot \mathcal{S}_9 - 2\mathcal{S}_9^2, \end{aligned} \quad (4.32)$$

where we used (4.3) and denote the equivalence relation in homology as ' $\cong$ '. Here we also

---

<sup>3</sup>The ideal generated by  $\text{loc}_1$  is the intersection of its associated primary ideals. An ideal  $I$  is primary ideal if  $ab \in I$  implies  $a \in I$  or  $b^n \in I$  for some  $n > 0$ . If  $n = 1$ , the ideal  $I$  is a prime ideal.

used that the homology class of  $\Sigma_{\mathbf{1}_{(-1,-2)}}$  as given in the third line of (4.27) by the first two factors. Thus, we have obtained the homology class of  $\Sigma_{\mathbf{1}_{(1,1)}}$  as in (4.23).

Similarly, we obtain the homology class of  $\Sigma_{\mathbf{1}_{(1,0)}}$ . We calculate four associated prime ideals of  $\text{loc}_2$  in (4.31) that correspond to four different irreducible components. These components are the curves  $\Sigma_{\mathbf{1}_{(-1,1)}} = \{s_3 = s_7 = 0\}$ ,  $\Sigma_{\mathbf{1}_{(-1,-2)}} = \{s_8 = s_9 = 0\}$ ,  $\Sigma_{\mathbf{1}_{(1,1)}}$  and finally  $\Sigma_{\mathbf{1}_{(1,0)}}$ . By calculating the resultants of  $\text{loc}_2$  at the relevant roots, we obtain multiplicities one for all irreducible components. Thus, we obtain the homology class of  $\Sigma_{(1,0)}$  from decomposition of the class of  $\text{loc}_2$  as

$$\begin{aligned} [\text{loc}_2] &= 12[K_B^{-1}]^2 = \Sigma_{(-1,1)} + \Sigma_{(-1,-2)} + \Sigma_{(1,1)} + \Sigma_{(1,0)} \\ \Rightarrow \Sigma_{(1,0)} &\cong 6[K_B^{-1}]^2 + 4[K_B^{-1}] \cdot \mathcal{S}_7 - 5[K_B^{-1}] \cdot \mathcal{S}_9 + \mathcal{S}_9^2 + \mathcal{S}_7 \cdot \mathcal{S}_9 - 2\mathcal{S}_7^2, \end{aligned} \quad (4.33)$$

where we have used (4.3), the homology classes of matter curves in (4.27) as well as in (4.32). This is the result in (4.23).

Finally, we determine the homology class of the matter curve  $\Sigma_{\mathbf{1}_{(0,1)}}$ . The ideal  $\text{loc}_3$  in (4.31) has five prime ideals corresponding to the matter curves  $\Sigma_{\mathbf{1}_{(-1,1)}}$ ,  $\Sigma_{\mathbf{1}_{(0,2)}}$ ,  $\Sigma_{\mathbf{1}_{(-1,-2)}}$ ,  $\Sigma_{\mathbf{1}_{(1,1)}}$  and the matter curve  $\Sigma_{\mathbf{1}_{(0,1)}}$  we are interested in. The multiplicities of the irreducible components we are not interested are calculated as one, 16, 16, one, respectively, by the corresponding resultants of  $\text{loc}_3$ . Thus, we calculate the homology class of the curve  $\Sigma_{\mathbf{1}_{(0,1)}}$  from the homology class of  $\text{loc}_3$  as

$$\begin{aligned} \text{loc}_3 &= 12[K_B^{-1}]^2 = \Sigma_{(-1,1)} + 16 \cdot \Sigma_{(0,2)} + 16 \cdot \Sigma_{(-1,-2)} + \Sigma_{(1,1)} + \Sigma_{(0,1)} \\ \Rightarrow \Sigma_{(0,1)} &= 6[K_B^{-1}]^2 + 4[K_B^{-1}] \cdot (\mathcal{S}_7 + \mathcal{S}_9) - 2\mathcal{S}_7^2 - 2\mathcal{S}_9^2, \end{aligned} \quad (4.34)$$

where we used the homology class of the matter curves in (4.27) and (4.32). This is the homology class in (4.23).

We conclude this discussion by presenting the associated prime ideal of selected matter surfaces as an instructive preparation of section 4.2.1. The prime ideal of  $\Sigma_{\mathbf{1}(1,1)}$  reads

$$\begin{aligned}
\mathcal{P} = & \{s_3^2 s_5^2 + s_7 (s_2^2 s_5 - s_1 s_2 s_6 + s_7^2 s_7) + s_3 (-s_2 s_5 s_6 + s_1 (s_6^2 - 2s_5 s_7)) , \\
& s_3 s_5^2 s_9 + s_2 s_5 (s_7 s_8 - s_6 s_9) + s_1 (-s_6 s_7 s_8 + s_6^2 s_9 - s_5 s_7 s_9) , \\
& s_3 s_5 s_8 - s_1 s_7 s_8 - s_2 s_5 s_9 + s_1 s_6 s_9, s_3 s_6 s_8 - s_2 s_7 s_8 - s_3 s_5 s_9 + s_1 s_7 s_9, \\
& s_3 s_8^2 + s_9 (-s_2 s_8 + s_1 s_9), s_7 s_8^2 + s_9 (-s_6 s_8 + s_5 s_9)\} . \tag{4.35}
\end{aligned}$$

The dimension of  $\mathcal{P}$  is calculated to be six in the ring generated by the  $s_i$  which confirms that the irreducible variety described by it is codimension two in  $B$  as expected. It is evident from (4.35) that the two irreducible components  $\Sigma_{\mathbf{1}(1,1)}$  and  $\Sigma_{\mathbf{1}(-1,-2)} = \{s_8 = s_9 = 0\}$  of  $\text{loc}_1$  intersect at points in  $B$ . These points may correspond to Yukawa points in F-theory since the fiber in the resolved space  $\hat{X}$  splits further into three components, as can be seen by a prime ideal analysis. We also determine the prime ideal of the matter curve  $\Sigma_{\mathbf{1}(1,0)}$  as

$$\begin{aligned}
\mathcal{P} = & \{-s_2^2 s_8^2 + s_2 (s_5 s_6 s_8 - s_5^2 s_9 + 2s_1 s_8 s_9) - s_1 (s_6^2 s_8 - s_5 s_6 s_9 + s_1 s_9^2) , \\
& s_2 s_5 s_7 - s_1 s_6 s_7 - s_2 s_3 s_8 + s_1 s_3 s_9, s_3 s_5 s_7 - s_1 s_7^2 - s_3^2 s_8, \\
& s_3 s_6 s_7 - s_2 s_7^2 - s_3^2 s_9, s_3 s_6 s_8 - s_2 s_7 s_8 - s_3 s_5 s_9 + s_1 s_7 s_9\} . \tag{4.36}
\end{aligned}$$

From this ideal we see that  $\Sigma_{\mathbf{1}(1,0)}$  intersects the matter curve  $\Sigma_{\mathbf{1}(-1,1)}$ , where again there is an additional split of the fiber.

### Yukawa Couplings: Codimension Three

At codimension three the singularities of the fibration enhance further signaling the presence of a Yukawa point. In the case at hand we find an enhancement to an  $I_3$ -singularity, which is resolved into three intersecting  $\mathbb{P}^1$ 's in  $\hat{X}$ . The loci of  $I_3$ -fibers are determined by

looking at zeros of higher order of the discriminant and by checking whether the fiber in the resolution  $\hat{X}$  splits further. We find the following loci,

Loci	Yukawa
$s_8 = s_9 = s_7 = 0$	$\mathbf{1}_{(-1,-2)} \times \mathbf{1}_{(0,2)} \times \mathbf{1}_{(1,0)}$
$s_3 = s_7 = s_9 = 0$	$\mathbf{1}_{(0,2)} \times \bar{\mathbf{1}}_{(1,-1)} \times \bar{\mathbf{1}}_{(-1,-1)}$
$\Sigma_{1(1,0)} \cap \Sigma_{1(1,0)} \cap \Sigma_{1(1,0)}$	$\bar{\mathbf{1}}_{(-1,-1)} \times \mathbf{1}_{(1,0)} \times \mathbf{1}_{(0,1)}$
$\Sigma_{1(1,0)} \cap \{s_3 = s_7 = 0\}$	$\bar{\mathbf{1}}_{(1,-1)} \times \bar{\mathbf{1}}_{(-1,0)} \times \mathbf{1}_{(0,1)}$
$\Sigma_{1(1,1)} \cap \{s_8 = s_9 = 0\}$	$\mathbf{1}_{(1,1)} \times \mathbf{1}_{(-1,-2)} \times \mathbf{1}_{(0,1)}$

(4.37)

We note that the first three agree with earlier results, see [74]. The last two loci also produce reducible fibers with three irreducible components that can be described in terms of the prime ideals. The study of these new Yukawa points, along with a more thorough discussion of the use of prime ideals, will be postponed to future work.

## 4.2.2 The Cohomology Ring and the Chern Classes of $\hat{X}$

In this section we abstractly calculate the cohomology ring of the fourfold  $\hat{X}$ . The central result of these computations is the basis of surfaces or dual  $(2,2)$ -forms in  $H^{(2,2)}(\hat{X})$ , which is relevant for the construction of  $G_4$ -flux, see section 4.4.1. Furthermore, for the calculation of the D3-brane tadpole and the quantization of the  $G_4$ -flux, we use these techniques to calculate the general expression for the Euler number and the second Chern class of  $\hat{X}$  for a general base  $B$ . In addition, we derive the full cohomology ring explicitly for  $B = \mathbb{P}^3$ , leaving the straightforward generalization to other bases for future works.

We note that the presentation of the cohomology of  $\hat{X}$  used here has been employed in the context of toric mirror symmetry for a long time and is in this sense not new. For an F-theory context see e.g. [59, 79] and references therein. We refer also to [89] for cohomol-



ogy calculations in the same spirit. However, we emphasize that, except for the language that we borrow from toric geometry, the following discussion is based only on reasonable assumptions on the intersections of  $\hat{X}$ . Thus, we expect the following procedure to work also in the non-toric case. In particular, not all fourfolds considered here have, to our knowledge, a description in terms of a reflexive polytope, which does, however, not keep us from using them for F-theory and computing their full chiral 4D spectrum.

The basic idea to calculate the cohomology ring  $H_V^{(*,*)}(\hat{X})$  of a general elliptically fibered Calabi-Yau fourfold  $\hat{X}$  over a base  $B$  with general fiber the elliptic curve in  $dP_2$  is to exploit the Stanley-Reissner (SR) ideal<sup>4</sup>  $SR$  of the ambient space  $dP_2^B(\mathcal{S}_7, \mathcal{S}_9)$  together with the linear equivalences of divisors. After dividing out the linear equivalences, the cohomology ring  $H_V^{(*,*)}(\hat{X})$  can be represented as the quotient ring  $R$  of the form<sup>5</sup>

$$H_V^{(*,*)}(\hat{X}) \cong \frac{\mathbb{C}[D_\alpha, S_P, S_Q, S_R] \cdot [\hat{X}]}{SR}, \quad (4.38)$$

where the basis (4.4) together with the vertical divisors  $D_\alpha$  are the variables of the free polynomial ring  $\mathbb{C}[D_\alpha, S_P, S_Q, S_R]$  and  $SR$  is considered as an ideal in this ring. For this purpose, the ideal  $SR$  has to be translated into intersection relations of those divisors. Note that we have to multiply by the homology class of  $\hat{X}$  in  $dP_2^B(\mathcal{S}_7, \mathcal{S}_9)$  in (4.2) to restrict the intersections on the ambient space  $dP_2^B(\mathcal{S}_7, \mathcal{S}_9)$  to  $\hat{X}$ .<sup>6</sup> By the Calabi-Yau condition this class is precisely given as  $\mathcal{O}(\hat{X}) = K_{dP_2^B}^{-1}$ .

The quotient ring (4.38) is graded with each graded piece being finitely generated by

---

<sup>4</sup>We merely borrow this term from toric geometry. In general,  $SR$  can be any ideal containing all vanishing intersections of divisors on  $dP_2^B(\mathcal{S}_7, \mathcal{S}_9)$ , which not necessarily has to be a toric variety.

<sup>5</sup>We note that this polynomial ring is only the primary vertical cohomology  $H_V^{(*,*)}(\hat{X})$  [51]. This is the subspace of  $H^{(*,*)}(\hat{X})$  relevant for  $G_4$ -flux inducing chirality in F-theory. Its complement in  $H^{(2,2)}(\hat{X})$  is the horizontal cohomology  $H_H^{(2,2)}(\hat{X})$  that encodes complex structure moduli of  $\hat{X}$ . See e.g. [59] for an analysis of  $G_4$ -flux in  $H_H^{(2,2)}(\hat{X})$  in F-theory.

<sup>6</sup>Generally, not all divisors on  $\hat{X}$  arise as restrictions of divisors on the ambient space. However, for generic  $\hat{X}$  with elliptic fiber in  $dP_2$ , only divisors in  $B$  can potentially miss this assumption. We exclude those  $B$  in the following. Note that non-generic  $\hat{X}$  can have additional divisors, see the footnote 7.

monomials in the divisors  $D_\alpha$ ,  $S_P$  and  $S_m$  of appropriate degree. We denote this ring by  $R$ . The  $k$ -th graded piece is then identified with

$$H_V^{(k,k)}(\hat{X}) = R^{(k)}, \quad (4.39)$$

after restriction to  $\hat{X}$ , i.e. after dropping the overall factor  $K_{dP_2}^{-1}$  in (4.38). More precisely, at grade zero we obtain  $H^{(0,0)}(\hat{X}) = \langle 1 \rangle$ , at grade one we have  $H^{(1,1)}(\hat{X}) = \langle D_\alpha, S_P, S_Q, S_R \rangle$ . At higher grade we obtain naively as many generators as homogeneous monomials of appropriate degree in the divisors in (4.38). However, due to equivalence relation in  $R$  the number of independent monomials is in general smaller. In fact, by Poincaré duality the rings  $R^{(3)}$ , and  $R^{(4)}$  are fixed, i.e. the corresponding Hodge numbers are related as  $h^{(3,3)}(\hat{X}) \stackrel{!}{=} h^{(1,1)}(\hat{X}) = 3 + h^{(1,1)}(B)$  and  $h^{(4,4)}(\hat{X}) \stackrel{!}{=} h^{(0,0)}(\hat{X}) = 1$ . At degree  $k \geq 5$  we trivially have  $R^{(k)} = \{0\}$  by reasons of dimensionality. In this sense the only non-trivial piece is  $R^{(2)} \cong H_V^{(2,2)}(\hat{X})$ , and the corresponding Hodge-number  $h_V^{(2,2)}(\hat{X})$ . Furthermore, it is precisely the elements  $H_V^{(2,2)}(\hat{X})$  of independent surfaces on  $\hat{X}$  into which the general  $G_4$ -flux on  $\hat{X}$  has to be expanded, as discussed in section 4.4.1.

The main advantage of the representation (4.38) compared to concrete toric models is that it allows us to determine the cohomology ring for all fibrations  $dP_2^B(\mathcal{S}_7, \mathcal{S}_9)$  in (4.1) over a given base  $B$  with general divisors  $\mathcal{S}_7$ ,  $\mathcal{S}_9$ . Of course the relevant computations depend on the geometry of the base  $B$  since the ideal  $SR$  in (4.38) in general is generated by the  $SR$ -ideal (3.46) of the fiber  $dP_2$  and of the base  $B$ , which differs from case to case. Nevertheless, as we demonstrate next, it is possible to calculate the total Chern class  $c(\hat{X})$  and Euler number  $\chi(\hat{X})$  of  $\hat{X}$  for any base  $B$  using minimal assumptions.

## Second Chern Class and Euler Number of $\hat{X}$ : General Formulas

For the purpose of finding the general expression for  $c(\hat{X})$  and, thus, the Euler number  $\chi(\hat{X})$ , it suffices to know, that the intersections of more than three vertical divisors  $D_\alpha$  in both  $dP_2^B(\mathcal{S}_7, \mathcal{S}_9)$  and  $\hat{X}$  are zero. The latter is true because of the properties of fibrations. Thus, we are working in the following with the ideal of vanishing intersections on  $dP_2^B(\mathcal{S}_7, \mathcal{S}_9)$  generated by the ideal of the fiber  $dP_2$  supplemented by the vanishing of quartic intersection of vertical divisors,

$$SR' = \{S_R \cdot (S_R + S_Q - \mathcal{S}_7 - [K_B]), S_R \cdot (S_R + S_P - \mathcal{S}_9 - [K_B]), S_Q \cdot S_P, \quad (4.40)$$

$$S_Q \cdot (S_R + S_Q - \mathcal{S}_7 - [K_B]), S_P \cdot (S_R + S_P - \mathcal{S}_9 - [K_B]), D_\alpha \cdot D_\beta \cdot D_\gamma \cdot D_\delta\}.$$

Here we have employed (4.3) in combination with (4.4) to translate (3.46) into intersection relations. The prime in  $SR'$  reminds us that we are not working with the full SR-ideal of the base  $B$ , but just assume vanishing quartic intersections. As before ‘ $\cdot$ ’ denotes the intersections product in  $dP_2^B(\mathcal{S}_7, \mathcal{S}_9)$ .

Next we can perform the calculation of the total Chern class of  $\hat{X}$ . For this purpose we first compute the formal expression of the Chern class  $c(\hat{X})$  by adjunction,

$$c(\hat{X}) = \frac{c(dP_2^B)}{1 + c_1(\mathcal{O}(\hat{X}))}. \quad (4.41)$$

The numerator denotes the total Chern class of  $dP_2^B(\mathcal{S}_7, \mathcal{S}_9)$  and the denominator is the Chern class of its anti-canonical bundle (4.2), which is the class of  $\hat{X}$  as mentioned above.

Then, we reduce this expression in the quotient ring (4.38) with  $SR$  replaced by the reduced ideal  $SR'$  in (4.40). We refer to appendix in [30] for the detailed calculations leading to the following results, as well as for the general expression of the total Chern classes  $c(dP_2^B)$  and  $c(\hat{X})$  for Calabi-Yau two-, three- and fourfolds. We obtain for the

second Chern class  $c_2(\hat{X})$  of  $\hat{X}$  the expression

$$\begin{aligned} c_2(\hat{X}) = & 3c_1^2 + c_2 - 2S_Q^2 - 3S_P^2 + c_1(2S_Q + S_P + 4S_R - 2(\mathcal{S}_7 + \mathcal{S}_9)) \\ & + 2\mathcal{S}_7(S_Q - S_P) + \mathcal{S}_9(3S_P - 2S_Q - S_R + \mathcal{S}_7), \end{aligned} \quad (4.42)$$

where we have expressed all cohomology classes in terms of the basis of divisors (4.4) on the fiber  $dP_2$  and the first and second Chern classes  $c_1 \equiv c_1(B)$ , respectively,  $c_2 \equiv c_2(B)$  of the base  $B$ . By abuse of notation we denote a divisor and its Poincaré dual  $(1, 1)$ -form by the same symbol.

As a first sanity check we note that (4.42) is consistent with the formula for the second Chern class of a fourfold with a generic  $E_6$ -elliptic fiber, i.e. with the elliptic curve in  $\mathbb{P}^2$ . In fact, in the limit  $\mathcal{S}_7 = \mathcal{S}_9 = 0$ , the total space  $dP_2^B(\mathcal{S}_7, \mathcal{S}_9)$  formally turns into  $\mathbb{P}(\mathcal{O}_B \oplus K_B^{-1} \oplus K_B^{-1})$ , the sections  $S_P$ ,  $S_Q$  and  $S_R$  become indistinguishable and fuse into a single holomorphic three-section  $\sigma$ , following conventions in the literature. Then the second line in (4.42) vanishes and we use the relation (4.9) for  $\sigma^2$  to rewrite the first line as

$$c_2(\hat{X}) \rightarrow c_2(X_{E_6}) = 3c_1^2 + c_2 + 12\sigma c_1, \quad (4.43)$$

where we denote by  $X_{E_6}$  the fourfold with  $E_6$ -elliptic fiber. This expression is in line with the results obtained in [78].

Similarly, the Euler number of  $\hat{X}$  is calculated from the integration of the fourth Chern class  $c_4(\hat{X})$  as

$$\chi(\hat{X}) = 3 \int_B [24c_1^3 + 4c_1c_2 - 16c_1^2(\mathcal{S}_7 + \mathcal{S}_9) + c_1(8\mathcal{S}_7^2 + \mathcal{S}_7\mathcal{S}_9 + 8\mathcal{S}_9^2) - \mathcal{S}_7\mathcal{S}_9(\mathcal{S}_7 + \mathcal{S}_9)]. \quad (4.44)$$

Here the integral over  $\hat{X}$  has been reduced to an integral over the base  $B$  by first consecutive application of the relation (4.7) and then by employing (4.6), which can be rewritten for

Calabi-Yau fourfolds as the intersection relation

$$S_P \cdot D_\alpha \cdot D_\beta \cdot D_\gamma = S_m \cdot D_\alpha \cdot D_\beta \cdot D_\gamma = (D_\alpha \cdot D_\beta \cdot D_\gamma)|_B. \quad (4.45)$$

Here  $S_m$  collectively denotes the divisors  $S_Q, S_R$  of the sections  $\hat{s}_Q, \hat{s}_R$  and  $D_\alpha, D_\beta, D_\gamma$  are general vertical divisors. We emphasize that our expression of the Euler number (4.44) reproduces the Euler number of [78] as the special case  $S_7 = S_9 = 0$ . As before  $S_P, S_Q$  and  $S_R$  become homologous and we obtain

$$\chi(\hat{X}_{E_6}) = 72 \int_B c_1^3 + 12 \int_B c_1 c_2. \quad (4.46)$$

As another consistency check, and also for the sake of the discussion of general flux quantization and the D3-brane tadpole in section 4.4.1, we calculate the arithmetic genus  $\chi_0(\hat{X})$  on  $\hat{X}$ . It is calculated from the Todd class  $\text{Td}_4(\hat{X})$  by the Hirzebruch-Riemann-Roch index theorem. Since  $\hat{X}$  is a simply-connected Calabi-Yau fourfold, its arithmetic genus has to be two,

$$\chi_0(\hat{X}) := \sum_p (-1)^p h^{(p,0)}(\hat{X}) \stackrel{!}{=} 2. \quad (4.47)$$

This immediately follows from  $h^{(0,0)}(\hat{X}) = h^{(4,0)}(\hat{X}) = 1$  and  $h^{(p,0)}(\hat{X}) = 0$  otherwise. From index theory, however, we obtain

$$\chi_0(\hat{X}) = \int_{\hat{X}} \text{Td}_4(\hat{X}) = \frac{1}{720} \int_{\hat{X}} (3c_2(\hat{X})^2 - c_4(\hat{X})) = \frac{1}{720} \left( 3 \int_{\hat{X}} c_2(\hat{X})^2 - \chi(\hat{X}) \right). \quad (4.48)$$

Evaluating this integral using our expressions (4.42), (4.44) for the second Chern class and Euler number on  $\hat{X}$  we obtain

$$\chi_0(\hat{X}) = \frac{1}{12} \int_B c_1 c_2 = 2\chi_0(B) \stackrel{!}{=} 2. \quad (4.49)$$

Here the first equality is due to a remarkable cancellation of all terms containing the divisors  $\mathcal{S}_7, \mathcal{S}_9$  in the second Chern class and Euler number of  $\hat{X}$ . In the second equality we used the index theorem for the arithmetic genus of the base

$$\chi_0(B) = \frac{1}{24} \int_B c_1 c_2, \quad (4.50)$$

and the last equality follows from the constraint (4.47). Thus we see, that the arithmetic genus  $\chi_0(\hat{X}) = 2$  precisely iff  $\chi_0(B) = 1$ . In general, one demands the stronger conditions  $h^{(1,0)}(B) = h^{(2,0)}(B) = h^{(3,0)}(B) = 0$  since non-trivial  $(p,0)$ -forms of the base  $B$  would pull back to  $(p,0)$ -forms on  $\hat{X}$  under the projection  $\pi : \hat{X} \rightarrow B$ , which we excluded by assumption.

We note that our result (4.49) for the arithmetic genus is in line with the computations in [109, 77], whose analysis we followed. We also refer to [89] for an application of these techniques to F-theory with  $SU(5)$  gauge group.

### **The Full Cohomology Ring of $\hat{X}$ : Base $B = \mathbb{P}^3$**

As we demonstrate next, the representation (4.38) for a concrete base  $B$  allows us to calculate the full cohomology ring for a general Calabi-Yau fourfold  $\hat{X}$  in  $dP_2^B(\mathcal{S}_7, \mathcal{S}_9)$  with general divisors  $\mathcal{S}_7, \mathcal{S}_9$ . We exemplify this in the following for the base  $B = \mathbb{P}^3$ , but note that this analysis can be generalized to other bases. For all details of the intersection calculations as well as the quartic intersections, we refer the reader to appendix in [30].

In the case  $B = \mathbb{P}^3$  the cohomology  $H^{(1,1)}(\hat{X})$  is generated according to (4.15) by the divisors  $D_A$ . We choose the following basis,

$$H^{(1,1)}(\hat{X}) = \langle H_B, \mathcal{S}_P, \mathcal{S}_Q, \mathcal{S}_R \rangle, \quad (4.51)$$

where  $H_B$  is the only vertical divisor of the fibration, which is pullback of the hyperplane

of  $\mathbb{P}^3$  to  $\hat{X}$ . The three other divisors are related to the in general rational sections  $\hat{s}_P, \hat{s}_Q$  and  $\hat{s}_R$ . Employing (4.3) and (4.4), their associated divisor classes are

$$S_P = E_2, \quad S_Q = E_1, \quad S_R = H - E_1 - E_2 + (n_9 - 4)H_B, \quad (4.52)$$

where we have used  $c_1(K_{\mathbb{P}^3}) = -c_1(\mathbb{P}^3) = -4H_B$ . We recall that the divisors  $S_7, S_9$  on  $\mathbb{P}^3$  are specified by integers  $n_7, n_9$  in the region in figure 4.1 specifying the total space (4.19) of the  $dP_2$ -fibration over  $\mathbb{P}^3$ .

We set up the construction of the cohomology ring of  $\pi : \hat{X} \rightarrow \mathbb{P}^3$  via (4.38) by specifying the ideal  $SR$ . We note that the  $SR$ -ideal in the case of  $B = \mathbb{P}^3$  is generated by the Stanley-Reissner ideal (3.46) of the fiber  $dP_2$  and the base, which is just  $H_B^4 = 0$ . Thus, using the divisor classes (4.51), the resulting ideal is identical to (4.40) with all vertical divisors equal to  $H_B$  and with  $K_{\mathbb{P}^3}^{-1} = \mathcal{O}_{\mathbb{P}^3}(4)$ . Then, we need the anti-canonical bundle  $K_{dP_2(n_7, n_9)}^{-1}$  of  $dP_2(n_7, n_9)$ . It is given in general in (4.2) and easily specialized to  $B = \mathbb{P}^3$  using  $S_7 = n_7 H_B$  and  $S_9 = n_9 H_B$  as well as expressed in the basis (4.52). Now we are equipped with all the necessary quantities to construct the quotient ring representation (4.38) of the cohomology ring  $H_V^{(*,*)}(\hat{X})$ .

We begin by summarizing the Hodge numbers of the vertical cohomology of  $\hat{X}$  as

$$h^{(0,0)}(\hat{X}) = h^{(4,4)}(\hat{X}) = 1, \quad h^{(1,1)}(\hat{X}) = h^{(3,3)}(\hat{X}) = 4, \quad h_V^{(2,2)}(\hat{X}) = 5 \quad (4), \quad (4.53)$$

where the subscript  $V$  indicates that we are considering the vertical subspace, and the number in the bracket denotes the non-generic case with  $(n_7, n_9)$  on the boundary<sup>7</sup> of the al-

---

<sup>7</sup>We note that for the two special values  $(n_7, n_9) = (4, 8), (8, 4)$  there is one additional divisor on  $\hat{X}$  that is not induced from the ambient space. For these special values we see from (4.3) that  $\hat{X}$  is not generic since  $s_1, s_2, s_3$ , respectively,  $s_1, s_5, s_8$  are constants. Then, we can perform a variable transformation on the fiber coordinates to achieve  $s_1 = 0$ , i.e. the elliptic curve will have an additional section at  $u = 1, v = w = 0$ . The elliptic fiber can then be embedded into  $dP_3$  with all sections toric. We thank Jan Keitel for pointing out the existence of a non-toric divisor for non-generic  $\hat{X} \rightarrow \mathbb{P}^3$ .

lowed region in figure 4.1. These are the lines  $n_7 = 0$ ,  $n_9 = 0$ ,  $n_9 = 4 + n_7$  for  $n_7 \leq 4$ ,  $n_9 = n_7 - 4$  and  $n_9 = 12 - n_7$ , both of the latter two for  $4 < n_7$ .

Indeed, we obtain these Hodge numbers as follows from the ring (4.38). At degree zero, which is  $H^{(0,0)}(\hat{X})$ , the only generator is the trivial element 1. The graded piece  $R^{(1)} \cong H^{(1,1)}(\hat{X})$  is generated by the four divisors  $D_A$ . At degree two, i.e.  $H_V^{(2,2)}(\hat{X})$ , there are ten different combinations  $D_A \cdot_X D_B$ , of which, however, only five are generically inequivalent. A choice of basis, denoted in general by  $\mathcal{C}_r$  with  $r = 1, \dots, h_V^{(2,2)}(\hat{X})$ , for  $H_V^{(2,2)}(\hat{X})$  is given by

$$H_V^{(2,2)}(\hat{X}) = \langle H_B^2, H_B \cdot S_P, H_B \cdot \sigma(\hat{s}_Q), H_B \cdot \sigma(\hat{s}_R), S_P^2 \rangle. \quad (4.54)$$

Here  $\sigma(\hat{s}_Q)$ , respectively,  $\sigma(\hat{s}_R)$  are the Shioda maps (4.10) of the sections  $\hat{s}_Q, \hat{s}_R$ . In the case at hand these take the form

$$\sigma(\hat{s}_Q) = S_Q - S_P - 4H_B, \quad \sigma(\hat{s}_R) = S_R - S_P - (4 + n_9)H_B \quad (4.55)$$

We can evaluate the  $5 \times 5$ -intersection matrix  $\eta^{(2)}$  in the basis (4.54) using the quartic intersections as

$$\eta^{(2)} = \begin{pmatrix} 0 & 1 & 0 & 0 & -4 \\ 1 & -4 & 0 & 0 & 16 + (n_7 - n_9 - 4)n_9 \\ 0 & 0 & -8 & n_7 - n_9 - 4 & n_9(4 - n_7 + n_9) \\ 0 & 0 & \eta_{34}^{(2)} & -2(4 + n_9) & 2n_9(4 - n_7 + n_9) \\ -4 & \eta_{25}^{(2)} & \eta_{35}^{(2)} & \eta_{45}^{(2)} & -64 - (8 + n_7 - 2n_9)(n_7 - n_9 - 4)n_9 \end{pmatrix}. \quad (4.56)$$

Here entries  $\eta_{rs}^{(2)}$  that are determined by symmetry are omitted and denoted by  $\eta_{sr}^{(2)}$ . We note that for values of  $(n_7, n_9)$  on the boundary of figure 4.1, there are only four inequivalent such surfaces. A quick way to see this is by calculating the rank of the matrix (4.56) which



is generically five, but decreases to four in these cases. In all these cases we can drop the basis element  $S_P^2$  in (4.54) since it becomes homologous to the other four basis elements. The corresponding intersection matrix  $\eta^{(2)}$  is then obtained from (4.56) by deleting the last row and column. We note that both the knowledge of the basis (4.54) as well as of the intersections (4.56) is essential for the construction of  $G_4$ -flux in section 4.4.1.

At degree three, there are 20 combinations of three divisors  $D_A$ , however, there are only four inequivalent ones, which is expected by duality of  $H^{(3,3)}(\hat{X})$  and  $H^{(1,1)}(\hat{X})$ . Finally, at degree four, which is  $H^{(4,4)}(\hat{X})$ , there are 35 different quartic monomials in the  $D_A$ , of which there is only one inequivalent combination. This combination is precisely the quartic intersections on  $\hat{X}$ . The higher graded pieces of  $H^{(k,k)}(\hat{X})$ ,  $k > 4$  vanish, which is intuitively clear since there are at most quartic intersections on a Calabi-Yau fourfold.

We conclude by summarizing some key intersections on  $\hat{X}$  which are discussed in section 4.1.1 as general properties of the fibrations, that can, however, be proven explicitly using the representation (4.38). Of the complete quartic intersections we highlight the following intersections,

$$S_P \cdot S_R \cdot H_B^2 = n_9 S_* \cdot H_B^3, \quad S_Q \cdot S_R \cdot H_B^2 = n_7 S_* \cdot H_B^3, \quad S_* \cdot H_B^3 = 1, \quad S_*^2 \cdot H_B^2 = -4, \quad (4.57)$$

where  $S_*$  collectively denotes all the divisor classes  $S_P$ ,  $S_Q$  and  $S_R$  of the sections. Here the first two relations are the versions of (4.8), respectively, on  $B = \mathbb{P}^3$ . The third relation implies that a section of the elliptic fibration of  $\hat{X}$  intersects the generic fiber  $F = \pi^*(pt)$  for a generic point  $pt$  in  $B$  precisely at one point, cf. (4.6). Finally, the last relation is the analog of (4.7) on  $B = \mathbb{P}^3$ . We note that for a holomorphic section, this relation holds without intersection with  $H_B^2$ . Indeed, this is confirmed by the concrete cohomology calculation in the appendix [30] for the zero-section  $S_P$ .

### 4.3 $G_4$ -Flux Conditions in F-Theory from CS-Terms: Kaluza-Klein States on the 3D Coulomb Branch

In this section we discuss the construction of  $G_4$ -flux in F-theory compactifications on general elliptically fibered Calabi-Yau fourfolds  $\hat{X}$  with a non-trivial Mordell-Weil group and a non-holomorphic zero section.

We define  $G_4$ -flux in F-theory through the *M-theory* compactification on the resolved fourfold  $\hat{X}$ , that is dual to F-theory reduced on a circle to 3D. The general constraints on  $G_4$ -flux in M-theory compactifications are reviewed in section 4.3.1. In addition to these conditions,  $G_4$ -flux that is admissible for an *F-theory* compactification has to obey additional constraints. The form of  $G_4$ -flux that yields a consistent F-theory has been derived first in [38] by requiring a Lorentz-invariant uplift to four dimensions. Here we discuss a different logic to obtain constraints on the  $G_4$ -flux. As we point out in section 4.3.2, these constraints are appropriately formulated as the requirement of the vanishing of certain Chern-Simons (CS) terms on the Coulomb branch of the effective three-dimensional theory<sup>8</sup>. In particular, consistent conditions on the  $G_4$ -flux are obtained only if one-loop corrections of both massive states on the 3D Coulomb branch as well as *Kaluza-Klein* (KK) states are taken into account. Most importantly, the presence of a non-holomorphic zero section is linked to the existence of new CS-terms for the KK-vector, that are generated by KK-states, whereas other CS-terms receive additional shifts.

We present for the first time a consistent set of conditions on  $G_4$ -flux in F-theory compactifications with a non-holomorphic zero section. We also evaluate explicitly the corrections of massive states to 3D CS-levels for the F-theory/M-theory compactification on the fourfold  $\hat{X}$  with  $dP_2$ -elliptic fiber.

---

<sup>8</sup>See also [25, 26] for recent related studies of connections between CS-terms and contact terms in 3D effective field theories with background fields in the context of F-maximization.

The following discussion is an extension of [31], where KK-states have first been discussed in the context of 4D anomaly cancellation, and inspired by the analogous six-dimensional analysis in [60]<sup>9</sup>, see also [13] for the relevance of KK-states in the description of self-dual two-forms in 6D/5D.

### 4.3.1 A Brief Portrait of $G_4$ -Flux in M-Theory

Let  $\hat{X}$  denote an arbitrary smooth Calabi-Yau fourfold. In general,  $G_4$ -flux in M-theory can only be defined on such a smooth manifold, that in the context of F-theory typically arises from resolutions of both codimension one singularities from non-Abelian gauge groups or, as in the case considered here, from higher codimension singularities in the presence of a non-trivial Mordell-Weil group.

Then,  $G_4$ -flux in F-theory is defined as  $G_4$ -flux in M-theory with as set of additional F-theoretic restrictions discussed in the next section 4.3.2.  $G_4$ -flux in M-theory is consistent if it obeys two basic conditions. First,  $G_4$  has to be quantized as [116]

$$G_4 + \frac{c_2(\hat{X})}{2} \in H^4(\hat{X}, \mathbb{Z}), \quad (4.58)$$

which depends on the second Chern class  $c_2(\hat{X})$  of  $\hat{X}$ . In addition, the M2-brane tadpole has to be cancelled [109, 62],<sup>10</sup>

$$\frac{\chi(\hat{X})}{24} = n_3 + \frac{1}{2} \int_{\hat{X}} G_4 \wedge G_4, \quad (4.59)$$

where  $\chi(\hat{X})$  is the Euler characteristic of  $\hat{X}$  and  $n_3$  the number of spacetime-filling M2-

---

<sup>9</sup>We are grateful to Thomas W. Grimm for explanations and comments on the importance of  $\Theta_{00}$ .

<sup>10</sup>We are working here in the carefully checked conventions of [10], where also comparison with other, inconsistent sign choices in the literature can be found.

branes. This tadpole lifts to the D3-brane tadpole in F-theory with  $n_3$  denoting the number of D3-branes.

In addition, one can distinguish  $G_4$ -flux further by decomposing  $H^4(\hat{X})$  into its primary vertical and horizontal subspaces  $H^4(\hat{X}) = H_V^4(\hat{X}) \oplus H_H^4(\hat{X})$  [51]. As mentioned before, only  $G_4$ -flux in the vertical homology induces 4D chirality as well as gaugings of axions in F-theory and is considered here. A general  $G_4$ -flux in the vertical cohomology  $H_V^{(2,2)}(\hat{X})$  than has an expansion as

$$G_4 = m^r \mathcal{C}_r, \quad (4.60)$$

where  $\mathcal{C}_r$  with  $r = 1, \dots, h_V^{(2,2)}(\hat{X})$  denotes an integral basis of  $H_V^{(2,2)}(\hat{X})$  and  $m^r$  are the flux-quanta with integrality fixed by the quantization condition (4.58).<sup>11</sup> Such a basis can be constructed explicitly, as demonstrated in sections 4.2.2, for concrete examples.

### 4.3.2 Deriving Conditions on $G_4$ -Flux in F-theory

The additional constraints on the  $G_4$ -flux in F-theory compactifications are most conveniently formulated in the three-dimensional theory obtained after compactification of the 4D  $\mathcal{N} = 1$  effective action of F-theory on  $S^1$ . Then we can use the basic duality between three-dimensional F-theory on  $\hat{X} \times S^1$  and M-theory on  $\hat{X}$ . Consideration of the resolved fourfold  $\hat{X}$  means in terms of the 3D  $\mathcal{N} = 2$  effective theory obtained in the circle reduction to go to the 3D Coulomb. The corresponding fields acquiring a VEV are the adjoint valued scalars  $\zeta^A$ ,  $A = 0, \dots, h^{(1,1)}(B) + \text{rk}(G) + n_{U(1)}$ , along the Cartan directions of the 4D gauge group  $G \times U(1)^{n_{U(1)}}$ . The zeroth component denotes the scalar in the multiplet of the KK-vector. Then the 3D gauge group is broken in an ordinary Higgs effect to the

---

<sup>11</sup>In general,  $c_2(\hat{X})$  has to be decomposed into the integral basis of  $H_V^{(2,2)}(\hat{X})$ . However, the determination of this basis is very involved and requires more sophisticated techniques that would exceed the scope of this work. We refer to [59] for the application of mirror symmetry to fix the integral basis. See also [73] for a discussion of potential conflicts between the split of  $H^4(\hat{X})$  into vertical and horizontal subspace and the choice of an integral basis.

maximal torus  $U(1)^{h^{(1,1)}(B)+\text{rk}(G)+n_{U(1)}+1}$  and in addition the charged fermions, in particular those from the 4D massless matter multiplets, obtain a mass (shift) as  $m = q_A \cdot \zeta^A$ , where  $q_A$  denotes the full 3D charge vector.

This Coulomb branch then describes the IR dynamics of the dual M-theory compactification on the fourfold  $\hat{X}$  in the supergravity approximation. It is the key point of the following analysis that the matching of the two dual descriptions works only on the level of the quantum effective action after massive degrees of freedom have been integrated out on the F-theory side. As we emphasize in the following, also corrections due to KK-states have to be considered. In fact, consistent conditions on the  $G_4$ -flux in the presence of a non-holomorphic zero section are only obtained if new CS-terms for the KK-vector are taken into account.

The general approach of matching F- and M-theory in 3D initiated in [53] has been exploited recently in [54, 61, 31, 20] to study various aspects of the F-theory effective action. We refer to these references for the background of the following discussion.

### F-Theory Conditions from KK-States Corrected CS-Terms

First we recall that  $G_4$ -flux in M-theory induces CS-terms for the  $U(1)$ -gauge fields  $A^A$  on the 3D Coulomb branch that read

$$S_{CS}^{(3)} = -\frac{1}{2} \int \Theta_{AB}^M A^A \wedge F^B \quad \Theta_{AB}^M = \frac{1}{2} \int_{\hat{X}} G_4 \wedge \omega_A \wedge \omega_B. \quad (4.61)$$

This can be shown by reducing the M-theory three-form  $C_3$  along  $(1,1)$ -forms  $\omega_A$  on the fourfold  $\hat{X}$  that are dual to the basis of divisors  $D_A$ ,  $A = 0, 1, \dots, h^{(1,1)}(\hat{X}) - 1$ . We recall, cf. (4.15) for the case  $n_{U(1)} = 2$ , that this basis is given by  $h^{(1,1)}(B)$  vertical divisors  $D_\alpha$ , the divisor  $\tilde{S}_P = S_P + \frac{1}{2}[K_B^{-1}]$ , see (4.14), associated to the zero section, the Shioda maps

$\sigma(\hat{s}_m)$  for a rank  $n_{U(1)}$  Mordell-Weil group and  $\text{rk}(G)$  Cartan divisors  $D_i$  in the presence of a four-dimensional non-Abelian gauge group  $G$ .

Now the strategy to formulate conditions on the  $G_4$ -flux for a valid F-theory compactification is as follows. We require that the CS-levels on the F-theory side, denoted  $\Theta_{AB}^F$ , have to agree with the M-theory CS-levels, denoted  $\Theta_{AB}^M$  and given by the flux integral in (4.61),

$$\Theta_{AB}^F \stackrel{!}{=} \Theta_{AB}^M. \quad (4.62)$$

This means, whenever a non-vanishing CS-level  $\Theta_{AB}^F$  is there on the F-theory side, as a classical CS-level or generated by loops of massive matter on the 3D Coulomb branch, then the same CS-level has to be there on the M-theory side, i.e. it has to be generated by the  $G_4$ -flux. In contrast, when a CS-term is not there on the F-theory effective field theory side, the corresponding flux integral in (4.61) for the same CS-term in M-theory has to vanish. However, the critical point is to allow in the corresponding F-theory loop-computation also for loops with an infinite tower of KK-states. If KK-states are not included, the  $G_4$ -flux is in general over-constrained, in particular in the presence of a non-holomorphic zero section. In addition, certain CS-levels get shifted by KK-states and a consistent match of CS-terms in F- and M-theory is only possible if these corrections are included.

The general form for the correction to the classical CS-level on the F-theory side, denoted by  $\Theta_{\text{cl},AB}^F$ , has been worked out in [104, 106, 1]. The correction is one-loop exact with all 3D massive fermions contributing in the loop. Assuming a fermion with charge vector  $q_A$ , the loop corrected CS-term takes the simple form

$$\Theta_{AB}^F = \Theta_{\text{cl},AB}^F + \frac{1}{2} \sum_{\underline{q}} n(\underline{q}) q_A q_B \text{sign}(q_A \zeta^A), \quad (4.63)$$

where  $n(\underline{q})$  is the number of fermions with charge vector  $\underline{q}$  and the sum runs over all these charge vectors. We note that since real masses can be negative in 3D, the sign-function

is non-trivial. We can rewrite this expression further by noting the general form of the charge vector

$$q_A = (n, q_\alpha, q_i, q_m), \quad (4.64)$$

where we recall the 3D gauge group  $U(1)^{h^{(1,1)}(B)+\text{rk}(G)+n_{U(1)}+1}$  on the Coulomb branch and that the charge under the KK-vector  $A^0$  is just the KK-label of KK-states,  $q_0 \equiv q_{KK} = n$ .

Next, we assume that in a theory obtained by circle reduction from 4D, there are no states with charge under the  $A^\alpha$ , since these do not correspond to a 4D gauge symmetry, i.e. we assume  $q_\alpha = 0$ .<sup>12</sup> We consider in the following the massive charged states obtained from the reduction of four-dimensional massless chiral matter to 3D, along with their KK-states. Denoting their charge vectors as  $q_A = (n, 0, q_i, q_m)$  with  $q_i$  the Dynkin labels of their non-Abelian representations  $\mathbf{R}$  under  $G$ , we write the loop-correction (4.63) as

$$\begin{aligned} \Theta_{00}^F &= \frac{1}{2} \sum_{\mathbf{R}_{q_m}} \sum_{\underline{q} \in \mathbf{R}_{q_m}} \chi(\mathbf{R}_{q_m}) \sum_{n=-\infty}^{\infty} n^2 \text{sign}(m_{CB} + n \cdot m_{KK}), \\ \Theta_{0\Lambda}^F &= \frac{1}{2} \sum_{\mathbf{R}_{q_m}} \sum_{\underline{q} \in \mathbf{R}_{q_m}} q_\Lambda \chi(\mathbf{R}_{q_m}) \sum_{n=-\infty}^{\infty} n \text{sign}(m_{CB} + n \cdot m_{KK}), \\ \Theta_{\Sigma\Lambda}^F &= \frac{1}{2} \sum_{\mathbf{R}_{q_m}} \sum_{\underline{q} \in \mathbf{R}_{q_m}} q_\Sigma q_\Lambda \chi(\mathbf{R}_{q_m}) \sum_{n=-\infty}^{\infty} \text{sign}(m_{CB} + n \cdot m_{KK}), \end{aligned} \quad (4.65)$$

where we invoked the absence of classical CS-terms. Here we have suppressed a labeling of the KK-charges  $n$  by the weights  $\mathbf{w}$  of the representation  $\mathbf{R}_{q_m}$  and unified the labels  $i$  and  $m$  as  $\Lambda = (i, m)$  and  $\chi(\mathbf{R}_{q_m})$  denote the *4D chiralities* of chiral matter fields. We have also defined the Coulomb branch mass  $m_{CB} = q_\Sigma \zeta^\Sigma$  and the KK-mass  $m_{KK} = \frac{1}{R_{KK}}$  with  $R_{KK}$  the radius of the  $S^1$ . The terms (4.65) are, bearing our assumptions on the spectrum of massive fermions in mind, the only CS-terms receiving loop-corrections via (4.63). Other CS-terms are classically generated, either in 4D or in the 3D reduction.

---

<sup>12</sup>One might wonder whether these states correspond, on the M-theory side, to M2-branes wrapping curves in the base  $B$ , e.g. generated from resolved conifolds in  $B$ .

We summarize all CS-terms, the presence of classical terms, the potential correction via loop-effects, their physical interpretation and a related reference in the following,

$\Theta_{AB}^F$	$\Theta_{cl,AB}^F$	loop-corr.	$G_4$ -condition	interpretation
$\Theta_{00}^F$	-	yes	-	4D chiralities
$\Theta_{0\alpha}^F$	yes	-	$\stackrel{!}{=} 0$	$S^1$ -circle fluxes [56]
$\Theta_{0i}^F$	-	yes	-	4D chiralities
$\Theta_{0m}^F$	-	yes	-	4D anomaly cancellation [31] (for holomorphic $\hat{s}_P$ )
$\Theta_{\alpha\beta}^F$	- (?)	-	$\stackrel{!}{=} 0$	non-geometric flux?
$\Theta_{\alpha i}^F$	yes	-	$\stackrel{!}{=} 0$	4D gaugings by GUT Cartans
$\Theta_{\alpha m}^F$	yes	-	-	4D gaugings by $U(1)_m$ (4D GS-mechanism)
$\Theta_{\Sigma\Lambda}^F$	-	yes	-	4D chiralities

(4.66)

Here we also mention in one column whether the corresponding CS-term is used to impose a condition on the  $G_4$ -flux. Indeed, the effect of CS-terms  $\Theta_{0\alpha}^F$  is the induction of circle fluxes along the  $S^1$  in compactification from 4D and, thus, not a physical effect in 4D. Therefore, we impose these CS-terms to vanish. Then, the CS-terms  $\Theta_{\alpha\beta}^F$  obstruct the lift back to 4D [53], potentially by non-geometric effects, and are required to vanish. Finally, the CS-terms  $\Theta_{\alpha i}$  correspond to 4D gaugings of axions via the maximal torus of the GUT and are thus set to zero. Thus, using the M-/F-theory duality relation (4.62) we formulate the F-theory conditions on the  $G_4$ -flux in terms of 3D CS-levels  $\Theta_{AB}$  as

**$G_4$ -flux conditions:**  $\Theta_{0\alpha} = \Theta_{\alpha\beta} = \Theta_{i\alpha} = 0$

(4.67)

We note that these conditions on the  $G_4$ -flux look much weaker than the ones considered in



the literature before. We claim that these conditions are the appropriate ones, in particular in cases with a non-holomorphic the zero section  $\hat{s}_P$ . In contrast, however, in compactifications with a holomorphic zero section, the vanishing of the CS-levels in (4.67) implies the vanishing of other, dependent CS-levels. We discuss this in the following and contrast it to the situation with a non-holomorphic  $\hat{s}_P$ .

### KK-Corrected 3D CS-Terms: Field Theory Computations

In certain cases, the loop-corrections (4.65) can vanish, leading to additional vanishing CS-terms. In particular, for a holomorphic zero-section, the CS-term  $\Theta_{00}^F$  in field theory vanishes, and consistently also the geometric CS-term  $\Theta_{00}^M$  in M-theory. The latter can be seen easily using the conditions (4.67) in the relation

$$\Theta_{00} = \frac{1}{4} K^\alpha K^\beta \Theta_{\alpha\beta}, \quad (4.68)$$

which is derived employing the definition (4.14), the intersection property (4.9), and  $K^\alpha$  introduced in (4.17). In order to see the same from the field theory side and, in general, to compute the loop-corrections to the CS-terms, we first have to evaluate the sign-function in (4.65).

We calculate the sign-function geometrically, recalling from the discussion of section 4.2.1 that to every weight  $\mathbf{w}$  of a representation  $\mathbf{R}_{q_m}$  realized in F-theory there is a corresponding curve  $c_{\mathbf{w}}$ , cf. (4.21). The sign-function in (4.65) is then determined by testing whether the curve  $c_{\mathbf{w}}$  associated to a given weight  $\mathbf{w}$  with Dynkin labels  $q_\Lambda$  and KK-charge  $n$  is in the Mori cone  $M(\hat{X})$  of effective curves on  $\hat{X}$ . We define

$$\text{sign}(q_A \zeta^A) = \begin{cases} 1, & c_{\mathbf{w}} \in M(\hat{X}), \\ -1, & \text{otherwise.} \end{cases} \quad (4.69)$$

Here the KK-charge  $q_0 = n$  of a curve  $c_{\mathbf{w}}$  is obtained geometrically as

$$n = c_{\mathbf{w}} \cdot \tilde{S}_P. \quad (4.70)$$

In general, a curve is in the Mori cone if it is described by holomorphic equations and an analysis of the geometry allows in general to find all holomorphic curves corresponding to matter, cf. section 4.2.1 as well as [34].<sup>13</sup> In the toric context, the relevant parts of the Mori cone can be constructed systematically as recently demonstrated in [60].

Now, in the presence of a holomorphic zero section the sign-function is centered around 0 because no curve  $c_{\mathbf{w}}$  has KK-charge. This follows from the simple geometric fact that by definition any rational curve  $c_{\mathbf{w}}$  does not intersect  $S_P$ , which always goes through the original singular curve, cf. figure 4.2. This implies that the loop-corrections in (4.65) that are odd in the KK-level  $n$  vanish since KK-states with charge  $-|n|$  cancel those with charge  $|n|$ . In particular,  $\Theta_{00}^F = 0$ , confirming the geometric result (4.68). In addition, the sum over KK-states in  $\Theta_{\Lambda\Sigma}^F$  reduces to

$$\Theta_{\Lambda\Sigma}^F = \frac{1}{2} \sum_{\mathbf{R}_{q_m}} \sum_{\underline{q} \in \mathbf{R}_{q_m}} q_{\Sigma} q_{\Lambda} \chi(\mathbf{R}_{q_m}) \text{sign}(m_{CB}), \quad (4.71)$$

which has been used in [54, 31].

In contrast, the CS-levels  $\Theta_{0\Lambda}$  receive an infinite loop-correction that has to be regularized by zeta-function regularization. In [31] this zeta function regularization has been performed and it was shown that the field theory result for  $\Theta_{0m}$  agrees with the 4D mixed

---

<sup>13</sup>In general, the values of the sign-function on a given representation  $\mathbf{R}_{q_m}$  depend on the phase of  $\hat{X}$ , respectively, of the 3D gauge theory. See [65] for a detailed discussion of phases structure of Calabi-Yau fourfolds and 3D SU(5) gauge theories. However, it can be shown by a similar argument as in [117] that 4D observables like the chiralities  $\chi(\mathbf{R}_{q_m})$  are not expected to depend on the phase.

Abelian-gravitational anomaly,

$$\Theta_{0m}^F = -\frac{1}{12} \sum_{\underline{q}} n(\underline{q}) q_m, \quad (4.72)$$

with  $n(\underline{q})$  denoting the number of fermions in 4D with U(1)-charge vector  $\underline{q}$ . In particular, anomaly cancellation follows then using the M-/F-theory relation (4.62) and the geometric result

$$\Theta_{0\Lambda}^M = \frac{1}{2} K^\alpha \Theta_{\alpha\Lambda}^M, \quad (4.73)$$

where the right side is immediately identified with the 4D Green-Schwarz term for  $\Lambda = m$ , cf. section 4.4.3. Here we used the general result  $S_P \cdot D_\Lambda = 0$  for a holomorphic zero section. We also infer from (4.73) that the CS-terms  $\Theta_{0i}$  are set to zero recalling (4.67).

In the presence of a non-holomorphic section  $\hat{s}_P$  the only thing that changes on the field theory side is a shift of the sign function in (4.69). It is no longer centered symmetrically around the origin of the sum over KK-labels  $n$ . This is geometrically clear because there are now rational curves  $c_w$  in the Mori cone that have non-zero intersection with the rational zero section  $\hat{s}_P$ , i.e. that have non-zero KK-charge (4.70). These curves have to be located precisely at the loci where the rational zero section is ill-defined and wraps a whole  $\mathbb{P}^1$  in the fiber, which is the original singular curve. Everywhere else in the base  $B$  the zero section is only a point on the original singular fiber and does not intersect curves  $c_w$ .

The effect of the shift of the sign-function is dramatic because now KK-states with positive and negative KK-label  $|n|$ , respectively,  $-|n|$  do no longer cancel in corrections (4.65) that are odd in  $n$ . The infinite parts of the sums over KK-states still cancel, but with a non-zero remainder. Thus, the CS-term  $\Theta_{00}^F$  that was zero for a holomorphic zero section is now generated by a contribution of a finite number of KK-states. For example, assuming,

with  $k$  denoting an integer, a sign-function of the form

$$\text{sign}(m_{CB} + n \cdot m_{KK}) = \begin{cases} 1, & \text{for } n \geq -k, \\ -1, & \text{for } n < -k, \end{cases} \quad (4.74)$$

for only one weight of a single matter multiplet  $\mathbf{R}_{q_m}$  the loop induced CS-term in (4.65) reads

$$\Theta_{00}^F = \frac{k(k+1)(2k+1)}{6} \chi(\mathbf{R}_{q_m}). \quad (4.75)$$

See e.g. [60] for a formal derivation or the following for an intuitive understanding,

Integers	$-k-1$	$-k$	$-k+1$	$\dots$	$0$	$1$	$\sum_n n^2 \text{sign}$	
$n^2 \text{sign}(n)$	$-(k+1)^2$	$-k^2$	$-(k-1)^2$	$\dots$	$0$	$1$	$0$	(4.76)
$n^2 \text{sign}(n+k)$	$-(k+1)^2$	$k^2$	$(k-1)^2$	$\dots$	$0$	$1$	$\frac{k(k+1)(2k+1)}{3}$	

Here the unshifted sum was normalized to zero, then the shifted sum differs only by the amount obtained as the finite sum over the differences between the first and second row in (4.76) for each column.

Thus we see that  $\Theta_{00}^F$  in (4.75) is directly proportional to one chirality. Consequently, imposing  $\Theta_{00}^M = 0$ , as done in the literature with holomorphic zero sections, also in the non-holomorphic case would unnecessarily set this chirality to zero. We will see that the loop-correction to  $\Theta_{00}^F$  precisely takes the form (4.75) for  $dP_2$ -elliptic fibrations, cf. section 4.4.2, since only one singlet has a non-trivial KK-charge  $n = 2$  and, thus, a shifted sign-function (4.74) with  $k = -2$ .

We conclude by mentioning that the CS-terms  $\Theta_{\Lambda\Sigma}$  are shifted in a similar way, where as in (4.76) the shift originates from a finite number of KK-states. We note that this shift has to be taken into account when we determine certain 4D chiralities via 3D CS-terms in

sections 4.4.2. In addition, also the relation (4.72) is modified by a finite correction due to KK-states. Assuming again that only one weight in the representation  $\mathbf{R}_{q_m}$  has a non-trivial KK-charge with shifted sign-function (4.74), we obtain the corrected expression

$$\Theta_{0m}^F = -\frac{1}{12} \sum_{\underline{q}} n(\underline{q}) q_m - \frac{k(k+1)}{2} \chi(\mathbf{R}_{q_m}) q_m. \quad (4.77)$$

Thus, we see that these CS-levels are no longer directly related to the 4D mixed Abelian-gravitational anomaly as in (4.72) with a holomorphic zero section. Geometrically this is also clear since in general  $S_P \cdot \sigma(\hat{s}_m) \neq 0$  in compactifications with rational zero sections. Thus, (4.73) does not hold and the cancellation of 4D mixed Abelian-gravitational anomaly is not geometrically implied. However, after subtracting the contribution of KK-states in (4.77), 4D anomaly cancellation requires the remaining piece to again equal  $\frac{1}{2} K^\alpha \Theta_{\alpha m}$ . In other words, we can formulate the relation

$$\frac{1}{4} \int_{\hat{X}} S_P \cdot \sigma(\hat{s}_m) \cdot G_4 = \frac{k(k+1)}{2} q_m \chi(\mathbf{R}_{q_m}) \quad (4.78)$$

on the fourfold  $\hat{X}$  as a necessary and sufficient condition for 4D anomaly cancellation. It would be nice to proof this relation purely geometrically. Finally, we note that also the CS-terms  $\Theta_{0i}^F$  need no longer vanish, since geometrically  $\Theta_{0i}^M \neq \frac{1}{2} K^\alpha \Theta_{\alpha i}^M$ .

## 4.4 $G_4$ -Flux & Chiralities on Fourfolds with Two U(1)s

In this section we analyze chirality-inducing  $G_4$ -flux in F-theory on the fourfolds  $\hat{X}$  with  $dP_2$ -elliptic fiber and a non-holomorphic zero section. In section 4.4.1 we first construct the general  $G_4$ -flux for the fourfold  $\pi : \hat{X} \rightarrow \mathbb{P}^3$ , where we also comment on the general D3-brane tadpole. Then in section 4.4.2 we outline first our general strategy to obtain chiralities on Calabi-Yau fourfolds with higher rank Mordell-Weil group and a rational zero section,

before applying it again to the fourfold  $\hat{X}$  with  $B = \mathbb{P}^3$ . Then in section 4.4.3 we first review anomaly cancellation conditions in general 4D effective field theories. Then we show that the general spectrum obtained for the Calabi-Yau fourfold  $\hat{X}$  is anomaly-free for the entire allowed region of figure 4.1.

#### 4.4.1 $G_4$ -Flux on Fourfolds with Two Rational Sections

In this section we first show that on a general fourfold  $\hat{X}$  with  $dP_2$ -elliptic fiber the D3-brane tadpole can always be solved by adding a sufficient amount of  $n_{D3}$  of integral D3-brane charge. Then we construct viable  $G_4$ -flux for F-theory on a general fourfold  $\hat{X}$  with base  $B = \mathbb{P}^3$ . We show that for different elliptic fibrations, i.e. for different values of the integers  $n_7, n_9$ , the number of independent  $G_4$ -flux quanta changes.

##### Integral D3-Tadpole on General Fourfolds with $U(1) \times U(1)$

In the following we prove the necessary condition for D3-tadpole cancellation on  $\hat{X}$ , namely that the induced D3-brane charge from the combination of the Euler number and the quantized  $G_4$ -flux in the tadpole equation (4.59) is always integral. The following discussion is an application of the arguments in [109, 116, 77], that immediately carry over to elliptic fibrations  $\hat{X}$  with  $dP_2$ -elliptic curve.

To this end, we use the relation (4.48) between the arithmetic genus  $\chi_0(\hat{X})$  and the Euler number  $\chi(\hat{X})$  to rewrite the tadpole (4.59) as

$$n_{D3} = \frac{\chi(\hat{X})}{24} - \frac{1}{2} \int_{\hat{X}} G_4^2 = -60 + \frac{1}{2} \int_{\hat{X}} \left( \frac{1}{4} c_2(\hat{X})^2 - G_4^2 \right). \quad (4.79)$$

Here we have also employed that  $\chi_0(\hat{X}) = 2$ , cf. (4.49). Using the flux quantization condi-

tion (4.58) this can be written as

$$n_{D3} = -60 - \frac{1}{2} \int_{\hat{X}} (x^2 - x \wedge c_2(\hat{X})) , \quad (4.80)$$

where we used  $x = G_4 + \frac{1}{2}c_2(\hat{X})$ . By flux quantization (4.58) we know that  $x$  is integral, i.e. an element in  $H^4(\hat{X}, \mathbb{Z})$ . This implies by Wu's theorem that  $x^2 \cong c_2(\hat{X}) \wedge x \pmod{2}$  [116], so that the integrand in (4.80) is divisible by two. Thus, the number  $n_{D3}$  of D3-branes is integral for every elliptically Calabi-Yau fourfold  $\hat{X}$  with general elliptic fiber in  $dP_2$ .

### The $G_4$ -Flux on $\hat{X}$ with $B = \mathbb{P}^3$

Next we explicitly determine the  $G_4$ -flux on  $\hat{X}$  for a general elliptic fibration over the base  $B = \mathbb{P}^3$ , i.e. for all integers  $n_7, n_9$  in the allowed region in figure 4.1.

We begin by expanding the  $G_4$ -flux according to (4.60) into the basis of  $H_V^{(2,2)}(\hat{X})$  determined in (4.54),

$$G_4 = a_1 H_B^2 + a_2 H_B \cdot S_P + a_3 H_B \cdot \sigma(\hat{s}_Q) + a_4 H_B \cdot \sigma(\hat{s}_R) + a_5 S_P^2, \quad (4.81)$$

for general coefficients  $a_i$ , where as before the application of Poincaré duality is understood. Then we calculate the CS-levels (4.61) employing the intersection ring in the basis of divisors (4.51), but with  $\tilde{S}_P = S_P + 2H_B$  as defined in (4.14) replacing the zero section  $S_P$ . The generic solution is a three-parameter family of  $G_4$ -flux given by

$$G_4 = a_5 n_9 (4 - n_7 + n_9) H_B^2 + 4a_5 H_B \cdot S_P + a_3 H_B \cdot \sigma(\hat{s}_Q) + a_4 H_B \cdot \sigma(\hat{s}_R) + a_5 S_P^2, \quad (4.82)$$

which is valid for all values of  $n_7$  and  $n_9$  in the allowed region figure 4.1.

This generic three-parameter solution for the  $G_4$ -flux is expected since there are generically five different surfaces in (4.81) and two independent conditions (4.67), namely

$\Theta_{0\alpha} = \Theta_{\alpha\beta} = 0$  with  $\alpha, \beta = 1$ . However, the situation becomes more interesting at special values for  $(n_7, n_9)$ . First, we recall that for  $(n_7, n_9)$  on the boundary of the region in figure 4.1, the dimensionality of  $H_V^{(2,2)}(\hat{X})$  decreases to 4. The surface  $S_P^2$  becomes linearly dependent in homology on the four other surfaces, as noted below (4.56). At the same time, the number of independent conditions on the  $G_4$ -flux remains two. Thus, we find two independent  $G_4$ -fluxes on the boundary. We have depicted this situation in figure 4.2

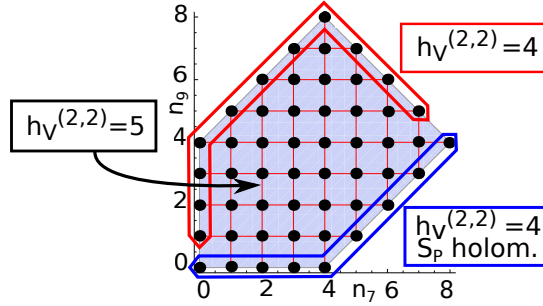


Figure 4.3: The region of allowed values for  $(n_7, n_9)$  from figure 4.1. On the entire region, there are two conditions on the flux. In the interior of this region, (4.82) holds. On the red and the blue boundary, there are only four independent  $(2, 2)$ -forms in the expansion (4.81). On the blue boundary,  $\hat{s}_P$  is holomorphic.

In all these cases we can obtain the expression for the  $G_4$ -flux by specializing (4.82). This ensures that all quantities, in particular the chiralities of 4D charged matter, that are calculated from the most general  $G_4$ -flux specialize correctly for non-generic values of  $(n_7, n_9)$ . We discuss this specialization at the end of this subsection, but note that the reader may want to skip these details on a first read and proceed with the chirality formulas in section 4.4.2.

Before delving into the details of this analysis, we evaluate the D3-brane tadpole (4.59) for the Calabi-Yau fourfold  $\hat{X} \rightarrow \mathbb{P}^3$  and the  $G_4$ -flux (4.82). First, we calculate the individual terms in the D3-brane tadpole. We obtain the Euler number for  $\hat{X}$  with  $B = \mathbb{P}^3$  from the general formula (4.44) as

$$\chi(\hat{X}) = 4896 + 3 \left[ -256(n_7 + n_9) + 4(8n_7^2 + n_7n_9 + 8n_9^2) - n_7n_9(n_7 + n_9) \right], \quad (4.83)$$



where we employed  $c_1(\mathbb{P}^3) = 4H_B$ ,  $c_2(\mathbb{P}^3) = 6H_B^2$ . We note that this expression is manifestly positive due to the bounds on  $n_7$  and  $n_9$  in (4.20), respectively, figure 4.3. Then we calculate the contribution of the  $G_4$ -flux (4.82) to the D3-tadpole as

$$\begin{aligned} \int_{\hat{X}} G_4^2 &= -8a_3^2 + 2a_3a_4(n_7 - n_9 - 4) + a_5^2n_9(2n_9 - n_7)(n_7 - n_9 - 4) - 2a_4^2(4 + n_9) \\ &\quad + 2a_5(a_3 + 2a_4)n_9(4 - n_7 + n_9). \end{aligned} \quad (4.84)$$

Finally, for the purpose of  $G_4$ -flux quantization via (4.58) we note the following expression for the second Chern-class of  $\hat{X}$ ,

$$\begin{aligned} c_2(\hat{X}) &= (182 + 3n_9(n_7 - n_9 - 4))H_B^2 + 28H_B \cdot S_P + 2(8 - n_9)H_B \cdot \sigma(\hat{s}_Q) \\ &\quad + (16 + 2n_7 - 3n_9)H_B \cdot \sigma(\hat{s}_R) - 5S_P^2, \end{aligned} \quad (4.85)$$

where we expanded the general expression (4.42) for a better comparison with the  $G_4$ -flux (4.82) in the basis (4.54) of the vertical cohomology. Also for completeness we calculate the square of the second Chern-class from the general formula as

$$\int_{\hat{X}} c_2(\hat{X})^2 = 2112 - 256(n_7 + n_9) + 4(8n_7^2 + n_7n_9 + 8n_9^2) - n_7n_9(n_7 + n_9). \quad (4.86)$$

Comparing this with the Euler number (4.83) we reconfirm the general relation (4.48) between the arithmetic genus and the Euler number of a Calabi-Yau fourfold.

Finally, we conclude by a discussion of (4.82) for non-generic values of  $(n_7, n_9)$ . Along each component of the boundary we have to use the homology relations between  $S_P^2$  and the four remaining basis elements (4.54) of  $H_V^{(2,2)}(\hat{X})$ . The relevant relations are worked out in the appendix of [30]. In all these cases the general formula (4.82) for the  $G_4$ -flux can

be shown to reduce to the two-parameter

$$G_4 = \tilde{a}_3 H_B \cdot \sigma(\hat{s}_Q) + \tilde{a}_4 H_B \cdot \sigma(\hat{s}_R). \quad (4.87)$$

Here the coefficients  $\tilde{a}_3$  and  $\tilde{a}_4$  are the following linear combination of  $a_3$ ,  $a_4$  and  $a_5$  on the three boundary components,

$$\begin{aligned} \{n_7 = 0\} : \tilde{a}_3 = a_3, \tilde{a}_4 = a_4 - n_9 a_5, \quad \{n_9 = n_7 + 4\} : \tilde{a}_3 = a_3 - n_7 a_5, \tilde{a}_4 = a_4 - 4a_5, \\ \{n_9 = 12 - n_7\} : \tilde{a}_3 = a_3 + (n_7 - 8)a_5, \tilde{a}_4 = a_4 + (n_7 - 8)a_5, \\ \{n_9 = n_7 - 4\} \cup \{n_9 = 0\} : \tilde{a}_3 = a_3, \tilde{a}_4 = a_4. \end{aligned} \quad (4.88)$$

It is satisfying to see that the parameters  $\tilde{a}_3$ ,  $\tilde{a}_4$  are continuous at the intersection points of boundary components. We note that the blue boundaries in figure 4.3,  $n_9 = 0$  and  $n_9 = n_7 - 4$ , are special because  $\hat{s}_P$  is holomorphic.

We conclude with one remark on the form of the  $G_4$ -flux obtained here. In some cases, Type IIB seven-brane gauge fluxes  $F^{(1)}$ ,  $F^{(2)}$  of two single D7-branes can be lifted into F-theory by considering a  $G_4$ -flux of the type

$$G_4 = F^{(1)} \cdot \sigma(\hat{s}_Q) + F^{(2)} \cdot \sigma(\hat{s}_R). \quad (4.89)$$

We note that the flux (4.87) is precisely of this form. In contrast, the interpretation of the general  $G_4$ -flux in (4.82) in terms of Type IIB quantities, if possible, is less clear and would be very interesting to investigate.

## 4.4.2 4D Chiralities from Matter Surfaces & 3D CS-Terms

Finally we are prepared to calculate the chirality of matter in four-dimensional F-theory compactifications on  $\hat{X}$  with  $U(1) \times U(1)$  gauge group. We demonstrate that the chirality of all six matter representations discussed in section 4.2 can be determined uniquely. Half of the chiralities are determined by integration of the  $G_4$ -flux over matter surfaces  $\mathcal{C}_{\mathbf{R}}^{\mathbf{w}}$ , the other half from the 3D CS-terms  $\Theta_{\Sigma\Lambda}$ . As we see explicitly, the 3D CS-terms  $\Theta_{\Lambda\Sigma}$  are not sufficient to fix all chiralities, in contrast to earlier works with a holomorphic zero section. However, supplemented by new CS-terms present only for non-holomorphic zero sections, see section 4.3.2, the chiralities can be obtained also exclusively via 3D CS-terms. We emphasize that this analysis requires the inclusion of KK-charges for all curves  $c_{\mathbf{w}}$ . In the fourfold  $\hat{X}$  only the representation  $\mathbf{1}_{(-1,-2)}$  has non-trivial KK-charge  $q_{KK} = 2$ .

We outline the general strategy to obtain 4D chiralities in section 4.4.2 before we determine them explicitly in section 4.4.2. The concrete calculations are performed for the Calabi-Yau fourfold  $\hat{X}$  with base  $B = \mathbb{P}^3$  for the entire allowed region in figure (4.1).

### General Strategy to Determine 4D Chiralities

We begin our discussion by recalling how to extract the chiral index of 4D matter in a representation  $\mathbf{R}$  under a gauge group  $G$  in a global F-theory compactification on an arbitrary resolved elliptically fibered Calabi-Yau fourfold  $\hat{X}$ .

As explained in section 4.2, each matter representation  $\mathbf{R}$  possesses an associated ruled surface, the matter surface  $\mathcal{C}_{\mathbf{R}}^{\mathbf{w}}$ , where  $\mathbf{w}$  denotes a weight of  $\mathbf{R}$ . Then, the chiral index of charged matter in this representation  $\mathbf{R}$  is given by the flux integral<sup>14</sup> [42, 64, 16, 89]

$$\chi(\mathbf{R}) = -\frac{1}{4} \int_{\mathcal{C}_{\mathbf{R}}^{\mathbf{w}}} G_4, \quad (4.90)$$

---

<sup>14</sup>The factor  $-\frac{1}{4}$  has been introduced to be consistency with the conventions of [31]. It can be reabsorbed into the  $G_4$ -flux.

where the  $G_4$ -flux is a quantized M-theory flux subject to the conditions (4.67). It is important to note that these conditions, more precisely the conditions  $\Theta_{i\beta} = 0$ , imply that the integral (4.90) is independent on the choice of a particular weight  $\mathbf{w}$ , since different weights  $\mathbf{w}, \mathbf{w}'$  of the same representation  $\mathbf{R}$  are related by a root  $\alpha_i$ ,  $\mathbf{w} - \mathbf{w}' = \alpha_i$ .

In cases where all the matter surfaces  $\mathcal{C}_{\mathbb{R}}^{\mathbf{w}}$  are known, the integral (4.90) is the most direct and geometric way of calculating the chirality  $\chi(\mathbf{R})$ . However, for the fourfold  $\hat{X}$  at hand, the homology class of all matter surfaces  $\mathcal{C}_{\mathbb{R}}^{\mathbf{w}}$  is not known. Fortunately, since we know the expected matter spectrum from the geometric analysis there is to determine the missing chiralities  $\chi(\mathbf{R})$  indirectly via 3D CS-terms.

For this purpose we recall the three-dimensional M-/F-duality explained in section 4.3.2. There we have seen that the 3D CS-terms (4.61) for the U(1)-vector fields  $A^\Lambda = (A^i, A^m)$  on the Coulomb branch can be calculated in two independent ways. On the one hand, after solving the  $G_4$ -flux condition (4.67), one can calculate all CS-terms  $\Theta_{\Lambda\Sigma}^M$  on the M-theory side by evaluating the classical flux integrals in (4.61). On the other hand, the CS-levels  $\Theta_{AB}^F$  on the F-theory side are generated and corrected at one-loop from integrating out charged matter and, thus, contain, as shown in section 4.3.2, cf. (4.65), the 4D chiral indices  $\chi(\mathbf{R}_{q_m})$  of all 4D matter. Since we know which representations  $\mathbf{R}_{q_m}$  are there from our geometric analysis in section 4.2.1, we can solve the matching condition (4.62) for the chiralities  $\chi(\mathbf{R}_{q_m})$ .

We note that in the fourfold  $\hat{X}$  we know the homology classes for a number of matter surfaces  $\mathcal{C}_{\mathbb{R}}^{\mathbf{w}}$ , but not for all. For these matter surfaces, we can evaluate the index (4.90) directly. The remaining chiralities can be fixed, as demonstrated in section 4.4.2 by the matching of the CS-terms  $\Theta_{\Lambda\Sigma}$ , that are given on the F-theory side by the loop-expression given in (4.65). However, we can also obtain *all* 4D chiralities by taking into account the CS-terms  $\Theta_{00}$  and  $\Theta_{0m}$  in (4.65), respectively, in (4.75) and (4.77). As we will see concretely, the obtained results agree with the direct computations via (4.90), confirming

the validity of application of the M-/F-theory duality (4.62) to the determination of 4D chiralities.

We conclude by noting that the matching (4.62) of CS-terms  $\Theta_{\Sigma\Lambda}$  has been used in [54, 31, 20] to calculate successfully the chiralities of F-theory compactifications with  $SU(5)$  and  $SU(5)\times U(1)$  gauge symmetry. In this work, however, we encounter the novel situation that the conditions arising from  $\Theta_{\Sigma\Lambda}$  are not sufficient to determine the chiralities of the full spectrum with  $U(1)\times U(1)$  gauge symmetry, as outlined in the following. The reason for this is precisely the existence of a non-holomorphic zero section. However, either supplemented by the chiralities that can be directly determined by the flux integrals (4.90) or by the CS-terms  $\Theta_{00}$  and  $\Theta_{0m}$ , we obtain all chiralities. For an application of the latter resolution, see also the analogous analysis of [60] in 6D.

One might wonder whether the CS-terms always provide enough conditions to solve for the chiralities of a known F-theory spectrum. By a simple counting argument assuming a rank  $n_{U(1)}$  Mordell-Weil group, we enumerate the number of conditions arising from the matching of these CS-terms as

$$\#(\text{CS-terms}) = \frac{(n_{U(1)} + 2)(n_{U(1)} + 1)}{2}. \quad (4.91)$$

If all these conditions remain independent, the CS-terms might indeed be sufficient to determine the chiralities in F-theory compactifications with more  $U(1)$ -symmetries. This can be seen by a similar estimate on the growth of the number of different representations as a function of the rank  $n_{U(1)}$  of the Mordell-Weil group.

### **Chiralities on $\hat{X}$ with $B = \mathbb{P}^3$ : Matter Surfaces & CS-Terms**

In the following we calculate for the first time 4D chiralities  $\chi(\mathbf{R})$  of an F-theory compactification on a general elliptically fibered Calabi-Yau fourfold  $\hat{X}$  with rank two Mordell-Weil

group and with the full matter spectrum analyzed in section 4.2. The following is a direct extension of the six-dimensional analysis in [34] to a 4D chiral theory.

As mentioned before, the 4D chirality of a given representation  $\mathbf{R}$  is computed by the flux integrals (4.90) given the  $G_4$ -flux and the corresponding matter surfaces  $\mathcal{C}_{\mathbf{R}}^{\mathbf{w}}$ . The matter surfaces for the matter fields  $\mathbf{1}_{(q_1, q_2)}$  with the three different  $U(1)^2$ -charges  $(q_1, q_2) = (-1, 1), (0, 2), (-1, -2)$  have been determined in (4.27). Using the general  $G_4$ -flux (4.82) on  $\hat{X} \rightarrow \mathbb{P}^3$  we obtain the following chiralities

$$\begin{aligned}\chi(\mathbf{1}_{(-1,1)}) &= -\frac{1}{4} \int_{\mathcal{C}_{(-1,1)}} G_4 = \frac{1}{4} (a_3 - a_4) n_7 (4 + n_7 - n_9), \\ \chi(\mathbf{1}_{(0,2)}) &= -\frac{1}{4} \int_{\mathcal{C}_{(0,2)}} G_4 = \frac{1}{4} n_7 n_9 (-2a_4 + a_5 (4 - n_7 + n_9)), \\ \chi(\mathbf{1}_{(-1,-2)}) &= -\frac{1}{4} \int_{\mathcal{C}_{(-1,-2)}} G_4 = \frac{1}{4} n_9 (4 - n_7 + n_9) (a_3 + 2a_4 + a_5 (n_7 - 2n_9)).\end{aligned}\quad (4.92)$$

In order to evaluate the involved intersections we have made use of the topological metric  $\eta^{(2)}$  on the cohomology  $H_V^{(2,2)}(\hat{X})$  calculated in (4.56).

In order to obtain the chiralities for the matter fields  $\mathbf{1}_{(q_1, q_2)}$  with charges  $(q_1, q_2) = (1, 0), (0, 1), (1, 1)$ , we have to use the 3D CS-levels and the matching condition (4.62). For this purpose we have to determine the KK-charges of all six matter representations on  $\hat{X}$ . As mentioned before, a non-trivial KK-charge is calculate by the intersection (4.70) of the curve  $c_{\mathbf{w}}$  and the zero section  $\tilde{S}_P$ . Such a non-trivial intersection can only occur at loci, where the zero section is ill-defined and wraps fiber components. This is precisely the case at the loci  $s_8 = s_9 = 0$ , where  $\mathbf{1}_{(-1,-2)}$  is supported. Since the fiber is an  $I_2$ -fiber over all matter loci, we obtain a KK-charge

$$q_{KK}(\mathbf{1}_{(-1,-2)}) = c_{(-1,-2)} \cdot \tilde{S}_P = 2, \quad (4.93)$$

and zero for all other matter representations. We note that (4.93) implies that the sign-

function (4.69) is given by the shifted sign-function (4.74) with  $k = -2$  whereas the other matter fields retain a point-symmetric sign-function.

We can immediately cross-check this result using the field theory computations of sections 4.3.2. We first calculate the CS-level  $\Theta_{00}^F$  for the 3D KK-vector on the field theory side. Using the general expression (4.75) for  $k = -2$  we obtain

$$\Theta_{00}^F = -\chi(\mathbf{1}_{(-1,-2)}), \quad (4.94)$$

with the chirality  $\chi(\mathbf{1}_{(-1,-2)})$  determined in (4.92). We readily calculate the corresponding flux integral  $\Theta_{00}^M$  via (4.61) and immediately reproduce (4.94). Next we check the relation (4.77) for the CS-level  $\Theta_{0m}$ , respectively, (4.78). Again we start with the field theory result for the right hand side of (4.78) which requires

$$\frac{1}{4} \int_{\hat{X}} S_P \cdot \sigma(\hat{s}_Q) \cdot G_4 \stackrel{!}{=} -\chi(\mathbf{1}_{(-1,-2)}), \quad \frac{1}{4} \int_{\hat{X}} S_P \cdot \sigma(\hat{s}_R) \cdot G_4 \stackrel{!}{=} -2\chi(\mathbf{1}_{(-1,-2)}). \quad (4.95)$$

We confirm this relation easily by calculating the intersections on the left hand side directly from the  $G_4$ -flux (4.82). Thus, as we have just demonstrated the results for the chiralities in (4.92) obtained from the matter surface integrals can be employed as an independently check of the field theory expressions for the CS-levels in 4.3.2 and the M-/F-theory duality relation (4.62).

Next we proceed with the computation of the other CS-levels  $\Theta_{mn}$ ,  $m, n = 1, 2$ , for the two U(1) gauge fields  $A^m$  corresponding to the divisors  $\sigma(\hat{s}_Q)$ , respectively,  $\sigma(\hat{s}_R)$ . Beginning with the M-theory expressions, we obtain using the Shioda maps (4.55), (4.61)

and the general  $G_4$ -flux (4.82),

$$\begin{aligned}
\Theta_{11}^M &= \frac{1}{2} [a_3(96 - n_7(4 + n_7) + n_9(4 + n_9)) + a_5(4 - n_7 + n_9)n_9(n_7 - 12 - 2n_9)) \\
&\quad + a_4(n_7^2 + 2(4 + n_9)(6 + n_9) - n_7(8 + 3n_9))] , \\
\Theta_{12}^M &= \frac{1}{2} [a_3(n_7^2 + 2(4 + n_9)(6 + n_9) - n_7(8 + 3n_9)) + (4 - n_7 + n_9)(a_5(-12 + 3n_7 - 5n_9)n_9 \\
&\quad + a_4(12 + 5n_9))] , \\
\Theta_{22}^M &= \frac{1}{2} [96a_4 + a_3(4 - n_7 + n_9)(12 + 5n_9) + 2a_4n_9(32 - 4n_7 + 5n_9) \\
&\quad - 2a_5n_9(4 - n_7 + n_9)(12 - 2n_7 + 5n_9)] , \tag{4.96}
\end{aligned}$$

with  $\Theta_{21}^M = \Theta_{12}^M$ .

Then we compute the one-loop CS-terms  $\Theta_{mn}^F$  in (4.65) on the F-theory side. For the matter spectrum at hand, cf. (4.23), we obtain

$$\begin{aligned}
\Theta_{11}^F &= \frac{1}{2} (\chi(\mathbf{1}_{(1,0)}) + \chi(\mathbf{1}_{(1,1)}) + \chi(\mathbf{1}_{(-1,1)}) - 3\chi(\mathbf{1}_{(-1,-2)})) , \\
\Theta_{12}^F &= \frac{1}{2} (\chi(\mathbf{1}_{(1,1)}) - \chi(\mathbf{1}_{(-1,1)}) - 6\chi(\mathbf{1}_{(-1,-2)})) , \\
\Theta_{22} &= \frac{1}{2} (\chi(\mathbf{1}_{(0,1)}) + \chi(\mathbf{1}_{(1,1)}) + \chi(\mathbf{1}_{(-1,1)}) + 4(\chi(\mathbf{1}_{(0,2)}) - 3\chi(\mathbf{1}_{(-1,-2)}))) . \tag{4.97}
\end{aligned}$$

We note that the factor of  $-3$  in front of  $\chi(\mathbf{1}_{(-1,-2)})$  occurs due to the shifted sign-function (4.74) with  $k = -2$ . Indeed, the relevant sum over KK-states in this case yields

$$\sum_n \text{sign}(n+k) = -3. \tag{4.98}$$

We note that the matching of 3D CS-terms (4.62) only using the  $\Theta_{mn}$  yields three conditions for the six a priori unknown chiralities in (4.97). Thus, it is impossible to determine the full matter spectrum from these CS-terms alone, which is in contrast to earlier studies in the literature with holomorphic zero sections. However, we can either use the results



(4.92) from the integral of the  $G_4$ -flux over the matter surfaces or have to incorporate the CS-terms  $\Theta_{00}$  and  $\Theta_{0m}$  to obtain three further conditions and to fix all six chiralities.

Consequently, taking into account the results (4.92), we apply the matching condition (4.62) for the dual CS-terms (4.96) and (4.97) we obtain the remaining three chiralities as

$$\begin{aligned}\chi(\mathbf{1}_{(1,0)}) &= \frac{1}{4} [a_5 n_7 n_9 (4 - n_7 + n_9) + a_3 (2n_7^2 - (12 - n_9)(8 - n_9) - n_7(16 + n_9))] , & (4.99) \\ \chi(\mathbf{1}_{(0,1)}) &= \frac{1}{2} [a_5 n_9 (4 - n_7 + n_9) (12 - n_9) - a_4 (n_7 (8 - n_7) + (12 - n_9) (4 + n_9))] , \\ \chi(\mathbf{1}_{(1,1)}) &= \frac{1}{4} [2a_5 n_9 (4 - n_7 + n_9) (12 - n_9) - (a_3 + a_4) (n_7^2 + n_7 (n_9 - 20) + 2(12 - n_9) (4 + n_9))] .\end{aligned}$$

We conclude by noting that the chiralities we obtain include factors of  $\frac{1}{2}$  and  $\frac{1}{4}$ . These factors should disappear once the  $G_4$ -flux has been quantized appropriately according to (4.58). The precise quantization will, however, depend on the values of  $n_7$ ,  $n_9$  and has to be done in a case by case analysis. In addition, for concrete  $n_7$ ,  $n_9$  the factors in the numerator (4.92) and (4.99) have different divisibility properties and can cancel the denominators. Therefore, in order to not obscure these cancellation effects, we keep the normalization in (4.92), (4.99) and the mild fractions of  $\frac{1}{2}$  and  $\frac{1}{4}$ . In concrete toric examples, they can be cancelled appropriately.

#### 4.4.3 4D Anomaly Cancellation: F-Theory with Multiple U(1)s

Finally, after having calculated the matter spectrum of an F-theory compactification, we check consistency of the obtained low-energy effective physics. One check is anomaly cancellation. In the following we introduce the necessary quantities to analyze anomalies and refer to [31] for more details on anomalies in general and, in particular, in F-theory. Then we use these techniques to show that the general spectrum found in section 4.4.2 for F-theory compactifications on  $\hat{X} \rightarrow \mathbf{P}^3$  with gauge group  $U(1)^2$  is anomaly-free.

## 4D Anomaly Cancellation: General Discussion

In the following we assume a 4D gauge group  $G$  with a single non-Abelian factors, see for example [31] for the general case, and with a number  $n_{U(1)}$  of Abelian factors. Charges are summarized by a charge vector  $\underline{q} = (q_m)$  and the number of left Weyl fermions in a matter representation  $\mathbf{R}_{\underline{q}}$  are denoted in general by  $n(\mathbf{R}_{\underline{q}})$ . The number of fermions in a representation  $\mathbf{R}$  irrespective of their  $U(1)$ -charges is denoted by  $n(\mathbf{R})$ , whereas  $n(\underline{q})$  indicates the number of fermions with charges  $\underline{q}$  regardless of their non-Abelian representation. All these numbers can be expressed in terms of the chiralities  $\chi(\mathbf{R}_{\underline{q}})$ .

The conditions for 4D anomaly cancellation via the generalized Green-Schwarz (GS) mechanism [50, 108] yield a system of linear equations involving the spectrum of the theory as well as parameters encoding the GS-counter terms and the gaugings of axions. These conditions for cancellation of 4D purely non-Abelian, purely Abelian, mixed Abelian-non-Abelian and mixed Abelian-gravitational anomalies read, in the same order,

$$\begin{aligned}
\text{purely non-Abelian anomaly} & : \sum_{\mathbf{R}} n(\mathbf{R})V(\mathbf{R}) = 0, \\
U(1)_k \times U(1)_l \times U(1)_m\text{-anomaly} & : \frac{1}{6} \sum_{\underline{q}} n(\underline{q})q_{(m}q_nq_{k)} = \frac{1}{4} b_{(mn}^{\alpha} \Theta_{k)\alpha}, \\
U(1)_m\text{-non-Abelian anomaly} & : \frac{1}{2} \sum_{\mathbf{R}} \sum_{\underline{q}} n(\mathbf{R}_{\underline{q}})U(\mathbf{R})q_m = \frac{1}{4\lambda} b^{\alpha} \Theta_{\alpha m}, \\
U(1)_m\text{-gravitational anomaly} & : \frac{1}{48} \sum_{\underline{q}} n(\underline{q})q_m = -\frac{1}{16} a^{\alpha} \Theta_{m\alpha}. \tag{4.100}
\end{aligned}$$

Here  $V(\mathbf{R})$  and  $U(\mathbf{R})$  denote group theoretical constants that arise when rewriting traces in the representation  $\mathbf{R}$  as traces in the fundamental representation  $\mathbf{f}$ . Letting  $F$  denote the non-Abelian field strength, we set

$$\text{tr}_{\mathbf{R}} F^3 = V(\mathbf{R}) \text{tr}_{\mathbf{f}} F^3, \quad \text{tr}_{\mathbf{R}} F^2 = U(\mathbf{R}) \text{tr}_{\mathbf{f}} F^2. \tag{4.101}$$

Similarly, we note that  $\lambda = 2c_G/V(\mathbf{adj})$  with  $c_G$  the dual Coxeter number of  $G$  and  $\mathbf{adj}$  its adjoint representation. Note that  $\lambda = 1$  for  $G = \mathrm{SU}(N)$ , the case of interest here.

There are some remarks in order. The left hand sides of (4.100) are the actual one-loop triangle anomalies of the field theory. These are determined entirely by the spectrum. The right hand sided of (4.100) are the contribution of the anomalous tree-level GS-counter terms. In an F-theory compactification on a Calabi-Yau fourfold  $\hat{X}$  over a base  $B$  they are identified as follows [57, 31]

$$\Theta_{m\alpha} = \Theta_{m\alpha}^M, \quad b_{mn}^\alpha = -\pi(\sigma(\hat{s}_m) \cdot \sigma(\hat{s}_n)) \cdot \Sigma_b^\alpha, \quad b^\alpha = S_G^b \cdot \Sigma_b^\alpha, \quad a^\alpha = K^\alpha. \quad (4.102)$$

Here the CS-terms  $\Theta_{AB}^M$  are defined in (4.61), the Néron-Tate height pairing has been introduced in (4.11) for two sections and can be straightforwardly generalized to an arbitrary number of sections,  $\Sigma_b^\alpha$  denotes a basis of curves defined in (4.12),  $S_G^b$  is the divisor in the base  $B$  supporting the gauge symmetry  $G$ , cf. 4.16, and  $K^\alpha$  is the coefficient (4.17) in the expansion of  $K_B$ .

### Anomaly Cancellation in 4D F-Theory with a $\mathrm{U}(1)^2$ -Sector: $B = \mathbb{P}^3$

The spectrum of the F-theory compactification to four dimensions on the fourfold  $\hat{X} \rightarrow \mathbb{P}^3$  has been calculated in (4.92) and (4.99). The various anomalies for this spectrum read

$$\begin{aligned} A_{111}^{\mathrm{U}(1)} &: 2[a_3(n_9 - n_7 - 12) + a_5 n_7(4 - n_7 + n_9)], & A_{222}^{\mathrm{U}(1)} &: n_7(a_3 + a_5(4 - n_9))(4 + n_9), \\ A_{112}^{\mathrm{U}(1)} &: \frac{1}{6} [a_5 n_7(48 + n_7^2 + n_9^2 - 2n_7(4 + n_9)) + a_3(n_7^2 - 2n_7(n_9 - 8) + (n_9 - 12)(4 + n_9))], \\ A_{122}^{\mathrm{U}(1)} &: \frac{1}{6} (a_5 n_7(n_7 - n_9 - 4)(n_9 - 12) + a_3(-2n_7^2 + n_7(4 + n_9) + (n_9 - 12)(4 + n_9))), \\ A_1^{\mathrm{U}(1)\text{-grav}} &: a_3(n_9 - n_7 - 12) + a_5 n_7(4 - n_7 + n_9), & A_2^{\mathrm{U}(1)\text{-grav}} &: 2n_7(a_3 + a_5(4 - n_9)), \end{aligned} \quad (4.103)$$

where we brought all numerical factors in (4.100) to the left hand sides. We denoted by  $A_{klm}^{\mathrm{U}(1)}$  the  $\mathrm{U}(1)_k \times \mathrm{U}(1)_l \times \mathrm{U}(1)_m$ - and by  $A_k^{\mathrm{U}(1)\text{-grav}}$  the  $\mathrm{U}(1)$ -gravitational anomalies.

Clearly, there are no non-Abelian anomalies due to the absence of a non-Abelian group  $G$ . Thus, since the anomalies (4.103) are all non-vanishing, a non-trivial GS-mechanism is required for consistency of the theory.

Therefore, all that is left to check cancellation to prove anomaly cancellation of these F-theory compactifications is to calculate the quantities on the right of (4.102) that encode the GS-mechanism. First, we obtain

$$\begin{aligned} \Theta_{\alpha m} &= \left( \frac{1}{4}[(-12 - n_7 + n_9)a_3 + n_7(4 - n_7 + n_9)a_5], \frac{1}{2}n_7[a_3 + (4 - n_9)a_5] \right)_m, \\ b_{mn}^\alpha &= \begin{pmatrix} 8 & 4 - n_7 + n_9 \\ 4 - n_7 + n_9 & 8 + 2n_9 \end{pmatrix}, \quad a^\alpha = -4. \end{aligned} \quad (4.104)$$

where we evaluated the CS-terms (4.61) for the flux (4.82), computed the height pairing (4.11) and (4.17) for  $K_{\mathbb{P}^3} = \mathcal{O}_{\mathbb{P}^3}(-4)$ . We note that the index  $\alpha = 1$  since the only vertical divisor is the hyperplane  $H_B$  and  $m = 1, 2$  for the two rational sections  $\hat{s}_Q, \hat{s}_R$ . Equipped with the coefficients in (4.104) we finally calculate the GS-terms on the right side of (4.100), which precisely yield (4.103). Thus, we see that all anomalies are cancelled by the GS-mechanism.

We conclude note that the spectrum calculated in section 4.4.2 is the uniquely determined anomaly-free spectrum if only one chirality  $\chi(\mathbf{1}_{(q_1, q_2)})$  is calculated independently. Anomaly cancellation is not sufficient to fix the spectrum completely, since the  $U(1)_1^3$ -anomaly is proportional to the  $U(1)_1$ -gravitational anomaly as is evident from (4.103).

## Engineering $U(1)^3$ in 6D

In this chapter we return to six dimensions, but now we turn our attention to the exploration higher rank abelian groups. In this chapter we explicitly construct geometries that support F-theory compactifications with the gauge group  $U(1) \times U(1) \times U(1)$ .

The article [35] is the source of the content of this chapter. The author of this dissertation is a co-author of such source.

This chapter is organized as follows. First, we construct the elliptic curve with four marked points (three rational points). To our surprise we find that the natural ambient space is the three dimensional space  $\mathbb{P}^3$  blown up at three points. The elliptic curve is given by the vanishing of two polynomials, i.e. it is a complete intersection. We also discover that the curve can be embedded, in two different ways, into the familiar  $dP_2$ , i.e. the ambient space of the two rational points elliptic curve. The price we pay is non generic coefficients. However this approach help us understand the singularity structure of the geometry, pointing us to the charge and location of the matter spectrum. We continue constructing the fibration, calculating the matter spectrum and checking the vanishing of anomalies.

There is another unexpected and fascinating finding in this chapter: the appearance of

matter charged under the three  $U(1)$ s. Geometrically, for this to happen, six polynomials have to vanish simultaneously in the base. This is rare. In a two dimensional space it does not happen generically. Also, from the field theory point of view, it is unexpected. Matter charged under three  $U(1)$ s happens naturally after breaking exceptional groups, however no such structure has been imposed in the construction of the geometry.

## 5.1 Three Ways to the Elliptic Curve with Three Rational Points

In this section we construct explicitly the general elliptic curve  $\mathcal{E}$  with a rank three Mordell-Weil group of rational points, denoted  $Q$ ,  $R$  and  $S$ .

We find three different, but equivalent representations of  $\mathcal{E}$ . First, in section 5.1.1 we find that  $\mathcal{E}$  is naturally embedded into  $\mathbb{P}^3$  as the complete intersection of two non-generic quadrics, i.e. two homogeneous equations of degree two. Equivalently, we embed  $\mathcal{E}$  in section 5.1.2 as the generic complete intersection Calabi-Yau into the blow-up  $\text{Bl}_3\mathbb{P}^3$  of  $\mathbb{P}^3$  at three generic points, which is effectively described via a nef-partition of the corresponding 3D toric polytope. In this representation the three rational points of  $\mathcal{E}$  and the zero point  $P$  descend from the four inequivalent divisors of the ambient space  $\text{Bl}_3\mathbb{P}^3$ . Thus, the Mordell-Weil group of  $\mathcal{E}$  is *toric*. Finally, we show in section 5.1.3 that  $\mathcal{E}$  can also be represented as a non-generic Calabi-Yau hypersurface in  $dP_2$ . In contrast to the generic elliptic curve in  $dP_2$  that has a rank two Mordell-Weil group [74, 34] which is toric, the onefold in  $dP_2$  we find here exhibits a third rational point, say  $S$ , and has a rank three Mordell-Weil group. This third rational point, however, is *non-toric* in the presentation of  $\mathcal{E}$  in  $dP_2$ . We note that there are three different maps of the quadric intersection in  $\text{Bl}_3\mathbb{P}^3$  to an elliptic curve in  $dP_2$  corresponding to the different morphisms from  $\text{Bl}_3\mathbb{P}^3$  to  $dP_2$ .

We emphasize that in the presentation of  $\mathcal{E}$  as a complete intersection in  $\text{Bl}_3\mathbb{P}^3$  the

rank four Mordell-Weil group is toric. Thus, as we will demonstrate in section 5.2 this representation is appropriate for the construction of resolved elliptic fibrations of  $\mathcal{E}$  over a base  $B$ .

### 5.1.1 The Elliptic Curve as Intersection of Two Quadrics in $\mathbb{P}^3$

In this section we derive the embedding of  $\mathcal{E}$  with a zero point  $P$  and the rational points  $Q$ ,  $R$  and  $S$  into  $\mathbb{P}^3$  as the intersection of two non-generic quadrics. We follow the methods described in chapter 3 and in [97, 34] used for the derivation of the general elliptic curves with rank one and two Mordell-Weil groups.

We note that the presence of the four points on  $\mathcal{E}$  defines a degree four line bundle  $\mathcal{O}(P+Q+R+S)$  over  $\mathcal{E}$ . Let us first consider a general degree four line bundle  $\mathcal{M}$  over  $\mathcal{E}$ . Then the following holds, as we see by employing the Riemann-Roch theorem:

1.  $H^0(\mathcal{E}, \mathcal{M})$  is generated by four sections, that we denote by  $u', v', w', t'$ .
2.  $H^0(\mathcal{E}, \mathcal{M}^2)$  is generated by eight sections. However we know ten sections of  $\mathcal{M}^2$ , the quadratic monomials in  $[u' : v' : w' : t']$ , i.e.  $u'^2, v'^2, w'^2, t'^2, u'v', u'w', u't', v'w', v't', w't'$ .

The above first bullet point shows that  $[u' : v' : w' : t']$  are of equal weight one and can be viewed as homogeneous coordinates on  $\mathbb{P}^3$ . The second bullet point implies that  $H^0(2\mathcal{M})$  is generated by sections we already know and that there have to be two relations between the ten quadratic monomials in  $[u' : v' : w' : t']$ , that we write as

$$s_1 t'^2 + s_2 u'^2 + s_3 v'^2 + s_4 w'^2 + s_5 t' u' + s_6 u' v' + s_7 u' w' + s_8 v' w' = s_9 v' t' + s_{10} w' t', \quad (5.1)$$

$$s_{11} t'^2 + s_{12} u'^2 + s_{13} v'^2 + s_{14} w'^2 + s_{15} u' t' + s_{16} u' v' + s_{17} u' w' + s_{18} v' w' = s_{19} v' t' + s_{20} w' t',$$

Now specialize to  $\mathcal{M} = \mathcal{O}(P+Q+R+S)$  and assume  $u'$  to vanish at all points  $P, Q, R, S$ .

By inserting  $u' = 0$  into (5.1) we should then get four rational solutions corresponding to the four points, i.e. other words (5.1) should factorize accordingly. However, this is not true for generic  $s_i$  taking values e.g. in the ring of functions of the base  $B$  of an elliptic fibration<sup>1</sup>. Thus, we have to set the following coefficients  $s_i$  to zero,

$$s_1 = s_3 = s_4 = s_{11} = s_{13} = s_{14} = 0. \quad (5.3)$$

As we see below in section 5.1.2, this can be achieved globally, by blowing up  $\mathbb{P}^3$  at three generic points.

For the moment, let us assume that (5.3) holds and determine  $P, Q, R, S$ . First we note that the presentation (5.1) for the elliptic curve  $\mathcal{E}$  now reads

$$\begin{aligned} s_2 u'^2 + s_5 u' t' + s_6 u' v' + s_7 u' w' &= s_9 v' t' + s_{10} w' t' - s_8 v' w', \\ s_{12} u'^2 + s_{15} u' t' + s_{16} u' v' + s_{17} u' w' &= s_{19} v' t' + s_{20} w' t' - s_{18} v' w', \end{aligned} \quad (5.4)$$

which is an intersection of two *non-generic* quadrics in  $\mathbb{P}^3$ . Setting  $u' = 0$  we obtain

$$0 = s_9 v' t' + s_{10} w' t' - s_8 v' w', \quad 0 = s_{19} v' t' + s_{20} w' t' - s_{18} v' w', \quad (5.5)$$

---

<sup>1</sup>In contrast, if we were considering an elliptic curve over an algebraically closed field, we could set some  $s_i = 0$  by using the  $\mathbb{P}GL(4)$  symmetries of  $\mathbb{P}^3$  to eliminate some coefficients  $s_i$ . For example,  $s_3 = 0$  can be achieved by making the transformation

$$u' \mapsto u' + kv', \quad \text{with } k \text{ obeying } (s_2 k^2 + s_6 k + s_3) = 0. \quad (5.2)$$

Solving this quadratic equation in  $k$  will, however, involve the square roots of  $s_i$ , which is only defined in an algebraically closed field. In particular, when considering elliptic fibrations the coefficients  $s_i$  will be represented by polynomials, of which a square root is not defined globally.



which has in the coordinates  $[u' : v' : w' : t']$  the four solutions

$$\begin{aligned} P &= [0 : 0 : 0 : 1], & Q &= [0 : 1 : 0 : 0], & R &= [0 : 0 : 1 : 0], \\ S &= [0 : |M_1^S| |M_3^S| : -|M_1^S| |M_2^S| : -|M_3^S| |M_2^S|]. \end{aligned} \quad (5.6)$$

Here we introduced the determinants  $|M_i^S|$  of all three  $2 \times 2$ -minors  $M_i^S$  reading

$$|M_1^S| = s_9 s_{20} - s_{10} s_{19}, \quad |M_2^S| = s_8 s_{19} - s_9 s_{18}, \quad |M_3^S| = s_8 s_{20} - s_{10} s_{18}, \quad (5.7)$$

that are obtained by deleting the  $(4 - i)$ -th column in the matrix

$$M^S = \begin{pmatrix} s_9 & s_{10} & -s_8 \\ s_{19} & s_{20} & -s_{18} \end{pmatrix}, \quad (5.8)$$

where  $M^S$  is the matrix of coefficients in (5.5).

It is important to realize that the coordinates of the rational point  $S$  are products of determinants in (5.7), in particular when studying elliptic fibrations at higher codimension in the base  $B$ , cf. section 5.3. On the one hand, the vanishing loci of the determinant of a single determinant  $|M_i^S|$  with  $i = 1, 2, 3$  indicates the collisions of  $S$  with  $P$ ,  $Q$  and  $R$ , respectively, i.e.

$$|M_1^S| = 0 : S = P, \quad |M_2^S| = 0 : S = Q, \quad |M_3^S| = 0 : S = R. \quad (5.9)$$

On the other hand the simultaneous vanishing of all  $|M_i^S|$  is equivalent to the two constraints in (5.4) getting linearly dependent. Then, the elliptic curve  $\mathcal{E}$  degenerates to an  $I_2$ -curve, i.e. two  $\mathbb{P}^1$ 's intersecting at two points, see the discussion around (5.27), with the point  $S$

becoming the entire  $\mathbb{P}^1 = \{u = s_9 v' t' + s_{10} w' t' - s_8 v' w' = 0\}^2$ . We note that this behavior of  $S$  indicates that in an elliptic fibration the point  $S$  will only give rise to a rational, not a holomorphic section of the fibration.

In summary, we have found that the general elliptic curve  $\mathcal{E}$  with three rational points  $Q, R, S$  and a zero point  $P$  is embedded into  $\mathbb{P}^3$  as the intersection of the two non-generic quadrics (5.4).

### 5.1.2 Resolved Elliptic Curve as Complete Intersection in $\text{Bl}_3 \mathbb{P}^3$

In this section we represent the elliptic curve  $\mathcal{E}$  with a rank three Mordell-Weil group as a *generic* complete intersection Calabi-Yau in the ambient space  $\text{Bl}_3 \mathbb{P}^3$ . As we demonstrate here, the three blow-ups in  $\text{Bl}_3 \mathbb{P}^3$  remove globally the coefficients in (5.3). In addition, the three blow-ups resolve all singularities of  $\mathcal{E}$ , that can appear in elliptic fibrations. Finally, we emphasize that the elliptic curve  $\mathcal{E}$  is a complete intersection associated to the nef-partition of the polytope of  $\text{Bl}_3 \mathbb{P}^3$ , where we refer to the appendix in [35] for more details on nef-partitions.

First, we recall the polytope of  $\mathbb{P}^3$  and its nef-partition describing a complete intersection of quadrics. The polytope  $\nabla_{\mathbb{P}^3}$  of  $\mathbb{P}^3$  is the convex hull  $\nabla_{\mathbb{P}^3} = \langle \rho_1, \rho_2, \rho_3, \rho_4 \rangle$  of the four vertices

$$\rho_1 = (-1, -1, -1), \quad \rho_2 = (1, 0, 0), \quad \rho_3 = (0, 1, 0), \quad \rho_4 = (0, 0, 1), \quad (5.10)$$

corresponding to the homogeneous coordinates  $u', v', w'$  and  $t'$ , respectively. The anti-canonical bundle of  $\mathbb{P}^3$  is  $K_{\mathbb{P}^3}^{-1} = \mathcal{O}(4H)$ , where  $H$  denotes the hyperplane class of  $\mathbb{P}^3$ . Two generic degree two polynomials in the class  $\mathcal{O}(2H)$  are obtained from the nef-partition of

---

<sup>2</sup>This curve can be seen to define a  $\mathbb{P}^1$  either using adjunction or employing the Segre embedding of  $\mathbb{P}^1 \times \mathbb{P}^1$  into  $\mathbb{P}^3$ .

the polytope of  $\mathbb{P}^3$  into  $\nabla_1, \nabla_2$  reading

$$\nabla_{\mathbb{P}^3} = \langle \nabla_1 \cup \nabla_2 \rangle, \quad \nabla_1 = \langle \rho_1, \rho_2 \rangle, \quad \nabla_2 = \langle \rho_3, \rho_4 \rangle, \quad (5.11)$$

where  $\cup$  denotes the union of sets of a vector space. This complete intersection defines the elliptic curve in (5.1) with only the origin  $P$ .

Next, we describe the elliptic curve  $\mathcal{E}$  as a generic complete intersection associated to a nef-partition of  $\text{Bl}_3\mathbb{P}^3$ , the blow-up of  $\mathbb{P}^3$  at three generic points, that we choose to be  $P$ ,  $Q$  and  $R$  in (5.6). We first perform these blow-ups and determine the proper transform of  $\mathcal{E}$  by hand, before we employ toric techniques and nef-partitions.

The blow-up from  $\mathbb{P}^3$  to  $\text{Bl}_3\mathbb{P}^3$  is characterized by the blow-down map

$$u' = e_1 e_2 e_3 u, \quad v' = e_2 e_3 v, \quad w' = e_1 e_3 w, \quad t' = e_1 e_2 t. \quad (5.12)$$

It maps the coordinates  $[u : v : w : t : e_1 : e_2 : e_3]$  on  $\text{Bl}_3\mathbb{P}^3$  to the coordinates on  $[u : v : w : t]$  on  $\mathbb{P}^3$ . Here the  $e_i = 0$ ,  $i = 1, 2, 3$ , are the exceptional divisors  $E_i$  of the the blow-ups at the points  $Q, R$  and  $P$ , respectively. We summarize the divisor classes of all homogeneous coordinates on  $\text{Bl}_3\mathbb{P}^3$  together with the corresponding  $\mathbb{C}^*$ -actions that follow immediately from (5.12) as

	divisor class	$\mathbb{C}^*$ -actions			
$u$	$H - E_1 - E_2 - E_3$	1	1	1	1
$v$	$H - E_2 - E_3$	1	0	1	1
$w$	$H - E_1 - E_3$	1	1	0	1
$t$	$H - E_1 - E_2$	1	1	1	0
$e_1$	$E_1$	0	-1	0	0
$e_2$	$E_2$	0	0	-1	0
$e_3$	$E_3$	0	0	0	-1

(5.13)

Here  $H$  denotes the pullback of the hyperplane class  $H$  on  $\mathbb{P}^3$ . The coordinates  $[u : w : t]$ ,  $[u : v : t]$  and  $[u : v : w]$  are the homogeneous coordinates on each  $E_i \cong \mathbb{P}^2$ , respectively, and can not vanish simultaneously. Together with the pullback of the Stanley-Reissner ideal of  $\mathbb{P}^3$  this implies the following Stanley Reisner ideal on  $\text{Bl}_3\mathbb{P}^3$ ,

$$SR = \{uvt, uwt, uvw, e_1v, e_2w, e_3t, e_1e_2, e_2e_3, e_1e_3\}. \quad (5.14)$$

This implies the following intersections of the four independent divisors on  $\text{Bl}_3\mathbb{P}^3$ ,

$$H^3 = E_i^3 = 1, \quad E_i \cdot H = E_i \cdot E_j = 0, \quad i \neq j. \quad (5.15)$$

The proper transform under the map (5.12) of the constraints (5.4) describing  $\mathcal{E}$  read

$$\begin{aligned} p_1 &:= s_2e_1e_2e_3u^2 + s_5e_1e_2ut + s_6e_2e_3uv + s_7e_1e_3uw - s_9e_2vt - s_{10}e_1wt + s_8e_3vw, \\ p_2 &:= s_{12}e_1e_2e_3u^2 + s_{15}e_1e_2ut + s_{16}e_2e_3uv + s_{17}e_1e_3uw - s_{19}e_2vt - s_{20}e_1wt + s_{18}e_3vw. \end{aligned} \quad (5.16)$$

We immediately see that this complete intersection defines a Calabi-Yau onefold in  $\text{Bl}_3\mathbb{P}^3$  employing (5.13), adjunction and noting that the anti-canonical bundle of  $\text{Bl}_3\mathbb{P}^3$  reads

$$K_{\text{Bl}_3\mathbb{P}^3} = \mathcal{O}(4H - 2E_1 - 2E_2 - 2E_3). \quad (5.17)$$

From (5.6), (5.12) and (5.16) we readily obtain the points in  $P$ ,  $Q$ ,  $R$  and  $S$  on  $\text{Bl}_3\mathbb{P}^3$ . They are given by the intersection of (5.16) with the four inequivalent toric divisors on

$\text{Bl}_3\mathbb{P}^3$ , the divisor  $D_u := \{u = 0\}$  and the exceptional divisors  $E_i$ . Their coordinates read

$$\begin{aligned}
E_3 \cap \mathcal{E} : P &= [s_{10}s_{19} - s_{20}s_9 : s_{10}s_{15} - s_{20}s_5 : s_{19}s_5 - s_{15}s_9 : 1 : 1 : 1 : 0], \\
E_1 \cap \mathcal{E} : Q &= [s_{19}s_8 - s_{18}s_9 : 1 : -s_{19}s_6 + s_{16}s_9 : -s_{18}s_6 + s_{16}s_8 : 0 : 1 : 1], \\
E_2 \cap \mathcal{E} : R &= [s_{10}s_{18} - s_{20}s_8 : -s_{10}s_{17} + s_{20}s_7 : 1 : s_{18}s_7 - s_{17}s_8 : 1 : 0 : 1], \\
D_u \cap \mathcal{E} : S &= [0 : 1 : 1 : 1 : s_{19}s_8 - s_{18}s_9 : s_{10}s_{18} - s_{20}s_8 : s_{10}s_{19} - s_{20}s_9].
\end{aligned} \tag{5.18}$$

Here we made use of the Stanley-Reissner ideal (5.14) to set the coordinates to one that can not vanish simultaneously with  $u = 0$ , respectively,  $e_i = 0$ .

We emphasize that the coordinates (5.18) are again given by determinants of  $2 \times 2$ -minors. Indeed, we can write (5.18) as

$$\begin{aligned}
P &= [-|M_3^P| : |M_2^P| : -|M_1^P| : 1 : 1 : 1 : 0], \quad Q = [-|M_3^Q| : 1 : |M_2^Q| : -|M_1^Q| : 0 : 1 : 1], \\
R &= [|M_3^R| : -|M_2^R| : 1 : |M_1^R| : 1 : 0 : 1], \quad S = [0 : 1 : 1 : 1 : -|M_3^Q| : |M_3^R| : -|M_3^P|]
\end{aligned} \tag{5.19}$$

Here we defined the matrices

$$M^P = \begin{pmatrix} -s_5 & s_9 & s_{10} \\ -s_{15} & s_{19} & s_{20} \end{pmatrix}, \quad M^Q = \begin{pmatrix} -s_6 & -s_8 & s_9 \\ -s_{16} & -s_{18} & s_{19} \end{pmatrix}, \quad M^R = \begin{pmatrix} -s_7 & -s_8 & s_{10} \\ -s_{17} & -s_{18} & s_{20} \end{pmatrix} \tag{5.20}$$

with their  $2 \times 2$ -minors  $M_i^{P,Q,R}$  defined by deleting the  $(4-i)$ -th column. We emphasize that the minors of the matrix  $M^S$  in (5.7) can be expressed by the minors of the matrices in (5.20) and, thus,  $M^S$  does not appear in (5.19). The matrices  $M^{P,Q,R}$  describe the two linear equations that we obtain by setting  $e_3 = 0$ ,  $e_2 = 0$  and  $e_1 = 0$  in (5.16), respectively.

It is important to realize that the points  $P$ ,  $Q$  and  $R$  are always distinct, as can be seen from (5.19) and the Stanley-Reissner ideal (5.14) since the exceptional divisors do not

mutually intersect. However, the point  $S$  can agree with all other points, if the appropriate minors in (5.19) vanish. In fact, we see the following pattern,

$$|M_3^P| = 0 : S = P, \quad |M_3^Q| = 0 : S = Q, \quad |M_3^R| = 0 : S = R, \quad (5.21)$$

which will be relevant to keep in mind for the study of elliptic fibrations.

We note that the elliptic curve  $\mathcal{E}$  degenerates into an  $I_2$ -curve if, as explained before below (5.8), the rank of one of the matrices in (5.8) and (5.20) is one<sup>3</sup>. In addition, one particular intersection in (5.18) no longer yields a point in  $\mathcal{E}$ , but an entire  $\mathbb{P}^1$ . As discussed below in section 5.3 the points on  $\mathcal{E}$ , thus, will only lift to rational sections of an elliptic fibration of  $\mathcal{E}$ .

Finally, we show that the presentation of  $\mathcal{E}$  as the complete intersection (5.16) can be obtained torically from a nef-partition of the  $\text{Bl}_3\mathbb{P}^3$ . For this purpose we only have to realize that the blow-ups (5.12) can be realized torically by adding the following rays to the polytope of  $\mathbb{P}^3$  in (5.10),

$$\rho_{e_1} = (-1, 0, 0), \quad \rho_{e_2} = (0, -1, 0), \quad \rho_{e_3} = (0, 0, -1). \quad (5.22)$$

The rays of the polytope of  $\text{Bl}_3\mathbb{P}^3$  are illustrated in the center of figure (5.1).

Here the ray  $\rho_{e_i}$  precisely corresponds to the exceptional divisor  $E_i = \{e_i = 0\}$ . Then we determine the nef-partitions of this polytope  $\nabla_{\text{Bl}_3\mathbb{P}^3}$  of  $\text{Bl}_3\mathbb{P}^3$ . We find that it admits a single nef-partition into  $\nabla_1, \nabla_2$  reading

$$\nabla_{\text{Bl}_3\mathbb{P}^3} = \langle \nabla_1 \cup \nabla_2 \rangle, \quad \nabla_1 = \langle \rho_1, \rho_4, \rho_{e_1}, \rho_{e_2} \rangle \quad \nabla_2 = \langle \rho_2, \rho_3, \rho_{e_3} \rangle. \quad (5.23)$$

It is straightforward to check that the general formula, see equation (B.2) in the appendix

---

<sup>3</sup>We emphasize that the complete intersection (5.4) in  $\mathbb{P}^3$  degenerates into only one  $\mathbb{P}^1$  and becomes singular if one matrices in (5.20) has rank one, in contrast to the smooth  $I_2$ -curve obtained from (5.16).

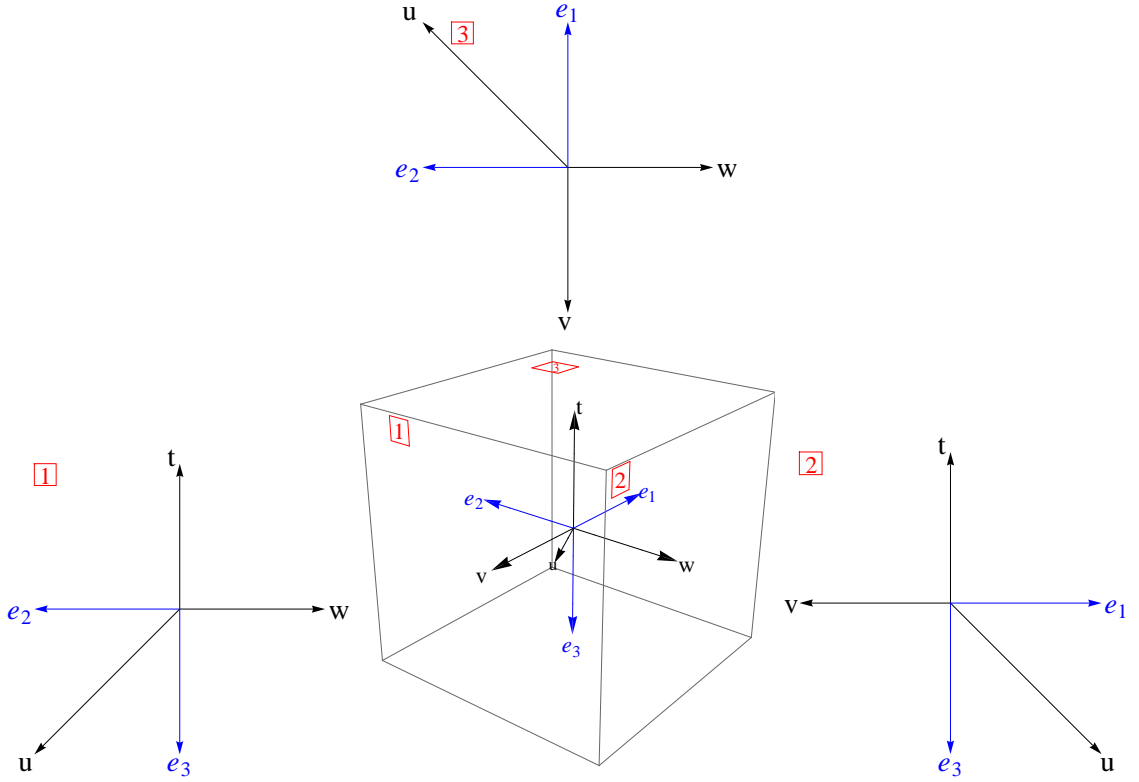


Figure 5.1: Toric fan of  $\text{Bl}_3\mathbb{P}^3$  and the 2D projections to the three coordinate planes, each of which yielding the polytope of  $dP_2$ .

of [35], for the nef-partition at hand reproduces precisely the constraints (5.16).

### 5.1.3 Connection to the cubic in $dP_2$

In this section we construct three equivalent maps of the elliptic curve  $\mathcal{E}$  given as the intersection (5.16) in  $\text{Bl}_3\mathbb{P}^3$  to the Calabi-Yau onefold in  $dP_2$ . The elliptic curve we obtain will not be the generic elliptic curve in  $dP_2$  found in [74, 34] with rank two Mordell-Weil group, but non-generic with a rank three Mordell-Weil group with one *non-toric generator*. The map of the toric generator of the Mordell-Weil group in  $\text{Bl}_3\mathbb{P}^3$  to a non-toric generator in  $dP_2$  will be manifest.

The presentation of  $\mathcal{E}$  as a non-generic hypersurface in  $dP_2$  with a non-toric Mordell-Weil group allows us to use the results of [34] from the analysis of the generic  $dP_2$ -curve.

On the one hand, we can immediately obtain the birational map of  $\mathcal{E}$  in (5.16) to the Weierstrass model by first using the map to  $dP_2$  and then by the map from  $dP_2$  to the Weierstrass form. We present this map separately in section 5.1.4. On the other hand, the study of codimension two singularities in section 5.3 will essentially reduce to the analysis of codimension two singularities in fibrations with elliptic fiber in  $dP_2$ . However, the additional non-toric Mordell-Weil generator as well as the non-generic hypersurface equation in  $dP_2$  will give rise to a richer structure of codimension two singularities.

### Mapping the Intersection of Two Quadrics in $\mathbb{P}^3$ to the Cubic in $\mathbb{P}^2$

As a preparation, we begin with a brief digression on the map of an elliptic curve with a single point  $P_0$  given as a complete intersection of two quadrics in  $\mathbb{P}^3$  to the cubic in  $\mathbb{P}^2$ , where we closely follow [23, 27].

Let us assume that there is a rational point  $P_0$  on the complete intersection of two quadrics with coordinates  $[x_0 : x_1 : x_2 : x_3] = [0 : 0 : 0 : 1]$  in  $\mathbb{P}^3$ .<sup>4</sup> This implies the quadrics must have the form

$$Ax_3 + B = 0, \quad Cx_3 + D = 0, \quad (5.24)$$

where  $A, C$  are linear and  $B, D$  are quadratic polynomials in the variables  $x_0, x_1, x_2$ . Assuming that  $A, C$  are generic, we obtain a cubic equation in  $\mathbb{P}^2$  with coordinates  $[x_0 : x_1 : x_2]$ <sup>5</sup> by solving (5.24) for  $x_3$ ,

$$AD - BC = 0, \quad (5.25)$$

Here we have to require that  $[x_0 : x_1 : x_2] \neq [0, 0, 0]$ , because  $x_3 = -\frac{B}{A} = -\frac{D}{C}$  has to be well-defined. Then, the inverse map from the cubic in  $\mathbb{P}^2$  to the complete intersection (5.24)

---

<sup>4</sup>We choose coordinates  $[x_0 : x_1 : x_2 : x_3]$  on  $\mathbb{P}^3$  in order to keep our discussion here general. We will identify the  $x_i$  with the coordinates used in sections 5.1.1 and (5.1.2) in section 5.1.3.

<sup>5</sup>We can think of this  $\mathbb{P}^2$  as being obtained from  $\mathbb{P}^3$  via a toric morphism defined by projection along one toric ray. In the case at hand this is the ray corresponding to  $x_3 = 0$ .



reads

$$[x_0 : x_1 : x_2] \mapsto [x_0 : x_1 : x_2 : x_3 = -\frac{B}{A} = -\frac{D}{C}]. \quad (5.26)$$

The original point  $P_0 = [0 : 0 : 0 : 1]$  is mapped to the rational point given by the intersection of the two lines  $A = 0, C = 0$ . This can be seen by noting that  $A = C = 0$  in (5.24) implies also  $B = D = 0$  which is only solved if  $[x_0 : x_1 : x_2] = [0 : 0 : 0]$ .

We note that the case when  $A$  and  $C$  are co-linear, i.e.  $A \sim C$ , is special because the curve (5.24) describes no longer a smooth elliptic curve, but a  $\mathbb{P}^1$ . Indeed, if  $A = aC$  for a number  $a$  we can rewrite (5.24) as

$$B - aD = 0, \quad Cx_3 + D = 0, \quad (5.27)$$

where we can solve the second constraint for  $x_3$ , given  $C \neq 0$ , so that we are left with the quadratic constraint  $B - aD = 0$  in  $\mathbb{P}^2$ , which is a  $\mathbb{P}^1$ . This type of degeneration of the complete intersection (5.24) will be the prototype for the degenerations of the elliptic curve (5.16), that we find in section 5.3.

### **Mapping the Intersection in $\text{Bl}_3\mathbb{P}^3$ to the Calabi-Yau Onefold in $dP_2$**

Next we apply the map of section 5.1.3 to the elliptic curve  $\mathcal{E}$  with three rational points. Since (5.4) is linear in all three coordinates  $v', w'$  and  $t'$  we will obtain according to the discussion below (5.24) three canonical maps to a cubic in  $\mathbb{P}^2$ . In fact, these maps lift to maps of the elliptic curve (5.16) in  $\text{Bl}_3\mathbb{P}^3$  to elliptic curves presented as Calabi-Yau hypersurfaces in  $dP_2$ , as we demonstrate in the following.

We construct the map from the complete intersection (5.16) to the elliptic curve in  $dP_2$  explicitly for the point  $R$  in (5.6), i.e. we identify  $P_0 \equiv R$  and  $[x_0 : x_1 : x_2 : x_3] = [u' : v' : t' : w']$  in the coordinates on  $\mathbb{P}^3$  before the blow-up for the discussion in section 5.1.3. Next, we compare (5.24) to the complete intersection (5.16). After the blow-up (5.12), the point  $R$

is mapped to  $e_2 = 0$  as noted earlier in (5.18). This allows us to identify  $A, C$  in (5.24) as those terms in (5.16) that do not vanish, respectively,  $B, D$  as the terms that vanish for  $e_2 = 0$ . Thus we effectively rewrite (5.16) in the form (5.24) with  $x_3 \equiv w$  after the blow-up, since  $w = 1$  follows from (5.14) for  $e_2 = 0$ , and obtain

$$A = s_7 e_1 e_3 u + s_8 e_3 v - s_{10} e_1 t, \quad C = s_{17} e_1 e_3 u + s_{18} e_3 v - s_{20} e_1 t, \quad (5.28)$$

$$B = e_2 (s_2 e_1 e_3 u^2 + s_5 e_1 u t + s_6 e_3 u v - s_9 v t), \quad D = e_2 (s_{12} e_1 e_3 u^2 + s_{15} e_1 u t + s_{16} e_3 u v - s_{19} v t).$$

In particular, this identification implies that  $R = \{e_2 = 0\}$  is mapped to  $A = C = 0$  on  $dP_2$  as required. Then, we solve both equations for  $w$  and obtain the hypersurface equation of the form

$$u(\tilde{s}_1 u^2 e_1^2 e_3^2 + \tilde{s}_2 u v e_1 e_3^2 + \tilde{s}_3 v^2 e_3^2 + \tilde{s}_5 u t e_1^2 e_3 + \tilde{s}_6 v t e_1 e_3 + \tilde{s}_8 t^2 e_1^2) + \tilde{s}_7 v^2 t e_3 + \tilde{s}_9 v t^2 e_1 = 0, \quad (5.29)$$

where we have set  $e_2 = 1$  using one  $\mathbb{C}^*$ -action on  $\text{Bl}_3 \mathbb{P}^3$  as  $B, D \sim e_2$  and  $e_2 = 0$  implies  $w = -\frac{B}{A} = -\frac{D}{C} = 0$  which is inconsistent with the SR-ideal (5.14). The coefficients  $\tilde{s}_i$  in (5.29) read

	coefficients in $dP_2$ -curve projected along $[w : e_2]$	
$\tilde{s}_1$	$-s_{17}s_2 + s_{12}s_7$	
$\tilde{s}_2$	$-s_{18}s_2 - s_{17}s_6 + s_{16}s_7 + s_{12}s_8$	
$\tilde{s}_3$	$- M_1^Q  = s_{16}s_8 - s_{18}s_6$	
$\tilde{s}_5$	$-s_{10}s_{12} + s_2s_{20} - s_{17}s_5 + s_{15}s_7$	(5.30)
$\tilde{s}_6$	$-s_{10}s_{16} - s_{18}s_5 + s_{20}s_6 - s_{19}s_7 + s_{15}s_8 + s_{17}s_9$	
$\tilde{s}_7$	$ M_3^Q  = s_{18}s_9 - s_{19}s_8$	
$\tilde{s}_8$	$- M_2^P  = -s_{10}s_{15} + s_{20}s_5$	
$\tilde{s}_9$	$- M_3^P  = s_{10}s_{19} - s_{20}s_9$	

Here we have used the minors introduced in (5.7) and in (5.19), (5.20).

We note that the ambient space of (5.29) is  $dP_2$  with homogeneous coordinates  $[u : v : w : t : e_1 : e_3]$ . The relevant  $dP_2$  is obtained from  $\text{Bl}_3\mathbb{P}^3$  by a toric morphism that is defined by projecting the polytope of  $\text{Bl}_3\mathbb{P}^3$  generated by (5.10), (5.22) onto the plane that is perpendicular to the line through the rays  $\rho_3$  and  $\rho_{e_2}$ . The rays of the fan are shown in the figure on the right of 5.1 that is obtained by the projection of the rays on the face number two of the cube. This can also be seen from the unbroken  $\mathbb{C}^*$ -actions in (5.13) and the SR-ideal (5.14) for  $e_2 = 1$  and  $w = 0$ , or  $e_2 = 0$  and  $w = 1$ . Then, the cubic (5.29) is a section precisely of the anti-canonical bundle of this  $dP_2$  surface.

The general elliptic curve in  $dP_2$  was studied in [34, 74] and shown to have a rank two Mordell-Weil group. However, the elliptic curve (5.29) has by construction a rank three Mordell-Weil group. Indeed, we see that the coefficients  $\tilde{s}_i$  are non-generic and precisely allow for a fourth rational point. This fourth point, however, does not descend from a divisor of the ambient space  $dP_2$  and is not toric. In fact, the mapping of the four rational points (5.18) in the coordinates on  $dP_2$  reads

$$\begin{aligned}
P &= [-|M_3^P| : |M_2^P| : -|M_1^P| : 1 : 1 : 1 : 0] \mapsto [|M_3^P| : -|M_2^P| : 1 : 1 : 0], & (5.31) \\
Q &= [-|M_3^Q| : 1 : |M_2^Q| : -|M_1^Q| : 0 : 1 : 1] \mapsto [-|M_3^Q| : 1 : -|M_1^Q| : 0 : 1], \\
R &= [|M_3^R| : -|M_2^R| : 1 : |M_1^R| : 1 : 0 : 1] \mapsto [|M_3^R| : -|M_2^R| : |M_1^R| : 1 : 1], \\
S &= [0 : 1 : 1 : 1 : -|M_3^Q| : |M_3^R| : -|M_3^P|] \mapsto [0 : 1 : 1 : -|M_3^Q| : -|M_3^P|].
\end{aligned}$$

We see, that the points  $P$ ,  $Q$  and  $S$  are mapped to the three toric points on the elliptic curve in  $dP_2$  studied in [34], whereas the points  $R$  is mapped to a non-toric point.

The map from the complete intersection in  $\text{Bl}_3\mathbb{P}^3$  to the elliptic curve (5.29) in  $dP_2$  implies that the results from the analysis of [34], where the generic elliptic curve in  $dP_2$  was considered, immediately apply. More precisely, renaming the coordinates  $[u : v : t : e_1 : e_3]$

in (5.29) as  $[u : v : w : e_1 : e_2]$  we readily recover equation (3.4) of [34]. Furthermore, the points  $P$ ,  $Q$  and  $S$  in (5.31) immediately map to the origin and the two rational points of the rank two elliptic curve in  $dP_2$ , that we denote in the following as  $\tilde{P}$ ,  $\tilde{Q}$  and  $\tilde{R}$ . In the notation of [34] we thus rewrite (5.31) using (5.30) as

$$\begin{aligned} P \mapsto \tilde{P} &:= [-\tilde{s}_9 : \tilde{s}_8 : 1 : 1 : 0], & Q \mapsto \tilde{Q} &:= [-\tilde{s}_7 : 1 : \tilde{s}_3 : 0 : 1], \\ S \mapsto \tilde{R} &:= [0 : 1 : 1 : -\tilde{s}_7 : \tilde{s}_9]. \end{aligned} \tag{5.32}$$

We emphasize that the origin  $P$  in the complete intersection in (5.16) is mapped to the origin  $\tilde{P}$ , which implies that the Weierstrass form of the curve in  $dP_2$  will agree with the Weierstrass form of the curve (5.16), cf. section 5.1.4.

As we mentioned before, the point  $R$  is mapped to a non-toric point in  $dP_2$ . This complicates the determination of the Weierstrass coordinates for  $R$ , for example. Fortunately, there are two other maps of the elliptic curve (5.16) to a curve in  $dP_2$  in which the point  $R$  is mapped to a toric point and another point, either  $Q$  or  $P$ , are realized non-torically. Thus, we construct in the following a second map to an elliptic curve in  $dP_2$ , where  $R$  is toric. Since the logic is completely analogous to the previous construction, we will be as brief as possible.

We choose  $P_0 \equiv Q$  for the map to  $dP_2$ . We recall from (5.18) that  $Q$  is realized as  $e_1 = 0$  on the elliptic curve in  $\text{Bl}_3\mathbb{P}^3$ . Thus, we write (5.16) as

$$Av + B = 0, \quad Cv + D = 0, \tag{5.33}$$

where, as before,  $A$  and  $C$  are obtained by setting  $e_1 = 0$  and  $B, D$  are the terms proportional

to  $e_1$ ,

$$A = -s_9e_2t + s_6e_2e_3u + s_8e_3w, \quad C = -s_{19}e_2t + s_{16}e_2e_3u + s_{18}e_3w, \quad (5.34)$$

$$B = e_1(s_2e_2e_3u^2 + s_5e_2ut + s_7e_3uw - s_{10}wt), \quad D = e_1(s_{12}e_2e_3u^2 + s_{15}e_2ut + s_{17}e_3uw - s_{20}wt).$$

Thus, we obtain an elliptic curve in  $dP_2$  with homogeneous coordinates  $[u : w : t : e_2 : e_3]$  by solving (5.33) for  $v$  and by setting  $e_1 = 1$  as required by the SR-ideal (5.14). The hypersurface constraint (5.25) takes the form

$$u(\hat{s}_1u^2e_2^2e_3^2 + \hat{s}_2uwe_2e_3^2 + \hat{s}_3w^2e_3^2 + \hat{s}_5ute_2^2e_3 + \hat{s}_6wte_2e_3 + \hat{s}_8t^2e_2^2) + \hat{s}_7w^2te_3 + \hat{s}_9wt^2e_2 = 0, \quad (5.35)$$

with coefficients  $\hat{s}_i$  defined as

	coefficients in $dP_2$ -curve projected along $[v : e_1]$
$\hat{s}_1$	$-s_{16}s_2 + s_{12}s_6$
$\hat{s}_2$	$-s_{18}s_2 + s_{17}s_6 - s_{16}s_7 + s_{12}s_8$
$\hat{s}_3$	$- M_1^R  = -s_{18}s_7 + s_{17}s_8$
$\hat{s}_5$	$s_{19}s_2 - s_{16}s_5 + s_{15}s_6 - s_{12}s_9$
$\hat{s}_6$	$s_{10}s_{16} - s_{18}s_5 - s_{20}s_6 + s_{19}s_7 + s_{15}s_8 - s_{17}s_9$
$\hat{s}_7$	$ M_3^R  = s_{10}s_{18} - s_{20}s_8$
$\hat{s}_8$	$- M_1^P  = s_{19}s_5 - s_{15}s_9$
$\hat{s}_9$	$ M_3^P  = -\tilde{s}_9 = -s_{10}s_{19} + s_{20}s_9$

where we have used (5.30). Analogously to the previous map, the ambient space of the hypersurface (5.35) is the  $dP_2$  with homogeneous coordinates  $[u : w : t : e_2 : e_3]$  that is obtained from  $\text{Bl}_3\mathbb{P}^3$  by the toric morphism induced by projecting along the line through the rays  $\rho_2$  and  $\rho_{e_1}$ . The rays of the fan are shown in the left figure of 5.1 that corresponds

to the projection of the rays on the face number one. Then, the three rational points on  $\mathcal{E}$  and the origin get mapped, in the coordinates  $[u : w : t : e_2 : e_3]$  of  $dP_2$ , to

$$\begin{aligned}
P &= [-|M_3^P| : |M_2^P| : -|M_1^P| : 1 : 1 : 1 : 0] \mapsto [-|M_3^P| : -|M_1^P| : 1 : 1 : 0], \quad (5.37) \\
Q &= [-|M_3^Q| : 1 : |M_2^Q| : -|M_1^Q| : 0 : 1 : 1] \mapsto [-|M_3^Q| : |M_2^Q| : -|M_1^Q| : 1 : 1], \\
R &= [|M_3^R| : -|M_2^R| : 1 : |M_1^R| : 1 : 0 : 1] \mapsto [|M_3^R| : 1 : |M_1^R| : 0 : 1], \\
S &= [0 : 1 : 1 : 1 : -|M_3^Q| : |M_3^R| : -|M_3^P|] \mapsto [0 : 1 : 1 : |M_3^R| : -|M_3^P|].
\end{aligned}$$

As before, it is convenient to make contact to the notation of [34]. After the renaming  $[u : w : t : e_2 : e_3] \rightarrow [u : v : w : e_1 : e_2]$  we obtain the hypersurface constraint (5.35) takes the standard form of eq. (3.4) in [34]. In addition, we see that the points  $P, R$  and  $S$  get mapped to the toric points on  $dP_2$ , whereas  $Q$  maps to a non-toric point. Denoting the origin of the  $dP_2$ -curve by  $\hat{P}$  and the two rational points by  $\hat{Q}, \hat{R}$  in order to avoid confusion, we then write (5.37) as

$$\begin{aligned}
P &\mapsto \hat{P} := [-\hat{s}_9 : \hat{s}_8 : 1 : 1 : 0], \quad R \mapsto \hat{Q} = [-\hat{s}_7 : 1 : \hat{s}_3 : 0 : 1], \\
S &\mapsto \hat{R} = [0 : 1 : 1 : \hat{s}_7 : -\hat{s}_9]. \quad (5.38)
\end{aligned}$$

We note that there is a third map from (5.16) to  $dP_2$  by solving for the variable  $t$ , respectively,  $e_3$  (its fan would correspond to the upper figure in figure 5.1 that shows the projection of the rays in the face number three). Although this map is formally completely analogous to the above the maps, it is not very illuminating for our purposes since the chosen zero point  $P$  on  $\mathcal{E}$  maps to a non-toric point in  $dP_2$ . In particular, the Weierstrass model with respect to  $P$  can not be obtained from this elliptic curve in  $dP_2$  by simply applying the results of [34], where  $P$  by assumption has to be a toric point.

### 5.1.4 Weierstrass Form with Three Rational Points

Finally, we are prepared to obtain the Weierstrass model for the elliptic curve  $\mathcal{E}$  in (5.16) with respect to the chosen origin  $P$  along with the coordinates in Weierstrass form for the three rational points  $Q$ ,  $R$  and  $S$ . We present three maps to a Weierstrass model in this work, each of which yielding an identical Weierstrass form, i.e. identical  $f$ ,  $g$  in  $y^2 = x^3 + fxz^4 + gz^6$ . The details of the relevant computations as well as the explicit results can be found in the appendix of [35].

The simplest two ways to obtain this Weierstrass form is by first exploiting the two presentations of the elliptic curve  $\mathcal{E}$  as the hypersurfaces (5.29) and (5.35) in  $dP_2$  constructed in section 5.1.3 and by then using the birational map of [34] of the general elliptic curve in  $dP_2$  to the Weierstrass form in  $\mathbb{P}^2(1, 2, 3)$ . In summary, we find the following schematic coordinates for the coordinates in Weierstrass form of the rational points  $Q$ ,  $R$  and  $S$

$$Q = [g_2^Q : g_3^Q : 1], \quad R = [g_2^R : g_3^R : 1], \quad S = [g_2^S : g_3^S : (s_{10}s_{19} - s_9s_{20})] \quad (5.39)$$

with the explicit expressions for  $g_2^{Q,R,S}$  and  $g_3^{Q,R,S}$  given in (A.11-A.15) in the appendix of [35]. The explicit form for  $f$  and  $g$ , along with the discriminant follow from the formulas in [34] in combination with (5.30), respectively, (5.36). In fact, we obtain (5.39) for  $Q$  and  $S$  by using the presentation (5.29) along with the maps (5.32) of the rational points  $Q$  and  $S$  onto the two toric points in the  $dP_2$ -elliptic curve, denoted by  $\tilde{Q}$  and  $\tilde{R}$  in this context. Then, we apply Eqs. (3.11) and (3.12) of [34] for the coordinates in Weierstrass form of the two toric rational points on the elliptic curve in  $dP_2$ . For concreteness, for the curve (5.29) the coordinates in Weierstrass form of the two points read

$$[g_2^Q : g_3^Q : z_Q] = \left[ \frac{1}{12}(\tilde{s}_6^2 - 4\tilde{s}_5\tilde{s}_7 + 8\tilde{s}_3\tilde{s}_8 - 4\tilde{s}_2\tilde{s}_9), \frac{1}{2}(\tilde{s}_3\tilde{s}_6\tilde{s}_8 - \tilde{s}_2\tilde{s}_7\tilde{s}_8 - \tilde{s}_3\tilde{s}_5\tilde{s}_9 + \tilde{s}_1\tilde{s}_7\tilde{s}_9) : 1 \right] \quad (5.40)$$

for the point  $\tilde{Q} = [-\tilde{s}_7 : 1 : \tilde{s}_3 : 0 : 1]$  and

$$\begin{aligned}
g_2^S &= \frac{1}{12}(12\tilde{s}_7^2\tilde{s}_8^2 + \tilde{s}_9^2(\tilde{s}_6^2 + 8\tilde{s}_3\tilde{s}_8 - 4\tilde{s}_2\tilde{s}_9) + 4\tilde{s}_7\tilde{s}_9(-3\tilde{s}_6\tilde{s}_8 + 2\tilde{s}_5\tilde{s}_9)), \\
g_3^S &= \frac{1}{2}(2\tilde{s}_7^3\tilde{s}_8^3 + \tilde{s}_3\tilde{s}_9^3(-\tilde{s}_6\tilde{s}_8 + \tilde{s}_5\tilde{s}_9) + \tilde{s}_7^2\tilde{s}_8\tilde{s}_9(-3\tilde{s}_6\tilde{s}_8 + 2\tilde{s}_5\tilde{s}_9) \\
&\quad + \tilde{s}_7\tilde{s}_9^2(\tilde{s}_6^2\tilde{s}_8 + 2\tilde{s}_3\tilde{s}_8^2 - \tilde{s}_5\tilde{s}_6\tilde{s}_9 - \tilde{s}_2\tilde{s}_8\tilde{s}_9 + \tilde{s}_1\tilde{s}_9^2), \\
z_S &= \tilde{s}_9
\end{aligned} \tag{5.41}$$

for the point  $\tilde{R} = [0 : 1 : 1 - \tilde{s}_7 : \tilde{s}_9]$ , where we apply (5.30). The explicit result in terms of the coefficients  $s_i$  for both  $Q, S$  can be found in the appendix, see [35].

In order to obtain the Weierstrass coordinates for the point  $R$  in (5.39) we invoke the map  $R \mapsto \hat{Q}$  in (5.38) for the elliptic curve (5.35) in  $dP_2$ . Here, the coordinates of  $R \mapsto \hat{Q}$  are again given by (5.40) after replacing  $\tilde{s}_i \rightarrow \hat{s}_i$ . The explicit form for these coordinates in terms of the  $s_i$  is obtained using (5.36). We emphasize that the coordinates in Weierstrass form for  $S$  can also be obtained from the map  $S \mapsto \hat{R}$  in (5.38) in combination with (5.36). They precisely agree with those deduced from the map  $S \mapsto \tilde{R}$  and (5.30).

Alternatively, one can directly construct the birational map from (5.16) to the Weierstrass form by extension of the techniques of [97, 34], where  $x$  and  $y$  in  $\mathbb{P}^2(1, 2, 3)$  are constructed as sections of appropriate line bundles that vanish with appropriate degrees at  $Q, R$  and  $S$ . However, the corresponding calculations are lengthy and the resulting Weierstrass model is identical to the one obtained from  $dP_2$ . Thus, we have opted to relegate this analysis to the appendix in the appendix of [35].

## 5.2 Elliptic Fibrations with Three Rational Sections

In this section we construct resolved elliptically fibered Calabi-Yau manifolds  $\mathcal{E} \rightarrow \hat{X} \xrightarrow{\pi} B$  over a base  $B$  with a rank three Mordell-Weil group. The map  $\pi$  denotes the projection to



the base  $B$  and the general elliptic fiber  $\mathcal{E} = \pi^{-1}(pt)$  over a generic point  $pt$  in  $B$  is the elliptic curve with rank three Mordell-Weil group of section 5.1. An elliptic Calabi-Yau manifold  $\hat{X}$  with all singularities at higher codimension resolved is obtained by fibering  $\mathcal{E}$  in the presentation (5.16). In addition, in this representation for  $\mathcal{E}$  the generators of the Mordell-Weil group are given by the restriction to  $\hat{X}$  of the toric divisors of the ambient space  $\text{Bl}_3\mathbb{P}^3$  of the fiber, i.e. the Mordell-Weil group of the generic  $\hat{X}$  is toric.

We begin in section 5.2.1 with the construction of Calabi-Yau elliptic fibrations  $\hat{X}$  with rank three Mordell-Weil group over a general base  $B$  with the elliptic curve (5.16) as the general elliptic fiber. We see that all these fibrations are classified by three divisors in the base  $B$ . Then in section 5.2.2 we compute the universal intersections on  $\hat{X}$ , that hold generically and are valid for any base  $B$ . Finally, in section 5.2.3 we classify all generic Calabi-Yau manifolds  $\hat{X}$  with elliptic fiber  $\mathcal{E}$  in  $\text{Bl}_3\mathbb{P}^3$  over any base  $B$ . Each such F-theory vacua  $\hat{X}$  is labeled by one point in a particular polytope, that we determine.

The techniques and results in the following analysis are a direct extension to the ones used in [34, 30, 33] for the case of a rank two Mordell-Weil group.

## 5.2.1 Constructing Calabi-Yau Elliptic Fibrations

Let us begin with the explicit construction of the Calabi-Yau manifold  $\hat{X}$ . Abstractly, a general elliptic fibration of the given elliptic curve  $\mathcal{E}$  over a base  $B$  is given by defining the complete intersection (5.16) over the function field of  $B$ . In other words, we lift all coefficients  $s_i$  as well as the coordinates in (5.16) to sections of appropriate line bundles over  $B$ .

To each of the homogeneous coordinates on  $\text{Bl}_3\mathbb{P}^3$  we assign a different line bundle on the base  $B$ . However, we can use the  $(\mathbb{C}^*)^4$ -action in (5.13) to assign without loss of

generality the following non-trivial line bundles

$$u \in \mathcal{O}_B(D_u), \quad v \in \mathcal{O}_B(D_v), \quad w \in \mathcal{O}_B(D_w), \quad (5.42)$$

with all other coordinates  $[t : e_1 : e_2 : e_3]$  transforming in the trivial bundle on  $B$ . Here  $K_B$  denotes the canonical bundle on  $B$ ,  $[K_B]$  the associated divisor and  $D_u$ ,  $D_v$  and  $D_w$  are three, at the moment, arbitrary divisors on  $B$ . They will be fixed later in this section by the Calabi-Yau condition on the elliptic fibration. The assignment (5.42) can be described globally by constructing the fiber bundle

$$\begin{array}{ccc} \mathrm{Bl}_3\mathbb{P}^3 & \longrightarrow & \mathrm{Bl}_3\mathbb{P}_B^3(D_u, D_v, D_w) \\ & & \downarrow \\ & & B \end{array} \quad (5.43)$$

The total space of this fibration is the ambient space of the complete intersection (5.16), that defines the elliptic fibration of  $\mathcal{E}$  over  $B$ .

Next, we require the complete intersection (5.16) to define a Calabi-Yau manifold in the ambient space (5.43). To this end, we first calculate the anti-canonical bundle of  $\mathrm{Bl}_3\mathbb{P}_B^3(D_u, D_v, D_w)$  via adjunction. We obtain

$$K_{\mathrm{Bl}_3\mathbb{P}_B^3}^{-1} = 4H - 2E_1 - 2E_2 - 2E_3 + [K_B^{-1}] + D_u + D_v + D_w, \quad (5.44)$$

where we suppressed the dependence on the vertical divisors  $D_u$ ,  $D_v$  and  $D_w$  for brevity of our notation and  $H$  as well as the  $E_i$  are the classes introduced in (5.13). For the complete intersection (5.16) to define a Calabi-Yau manifold  $\hat{X}$  in (5.43) we infer again from adjunction that the sum of the classes of the two constraints  $p_1$ ,  $p_2$  has to be agree with  $[K_{\mathrm{Bl}_3\mathbb{P}_B^3}^{-1}]$ .

Thus, the Calabi-Yau condition reads

$$[p_1] + [p_2] \stackrel{!}{=} 4H - 2E_1 - 2E_2 - 2E_3 + [K_B^{-1}] + D_u + D_v + D_w. \quad (5.45)$$

We see from (5.13) that both constraints in (5.16) are automatically in the divisor class  $2H - E_1 - E_2 - E_3$  w.r.t. the classes on the fiber  $\text{Bl}_3\mathbb{P}^3$ . Thus, (5.45) effectively reduces to a condition on the class of (5.16) in the homology of the base  $B$ . Denoting the part of the homology classes of the  $[p_i]$  in the base  $B$  by  $[p_1]^b$  and  $[p_2]^b + D_v + D_w$ , we obtain

$$[p_1]^b + [p_2]^b \stackrel{!}{=} [K_B^{-1}] + D_u. \quad (5.46)$$

Here we shifted the class  $[p_2]^b \rightarrow D_v + D_w + [p_2]^b$  for reasons that will become clear in section 5.2.3.

Using this information we fix the line bundles on  $B$  in which the coefficients  $s_i$  take values. We infer from (5.16), (5.42) and the Calabi-Yau condition (5.46) the following assignments of line bundles,

section	line-bundle	section	line-bundle
$s_2$	$\mathcal{O}([K_B^{-1}] - D_u - [p_2]^b)$	$s_{12}$	$\mathcal{O}(-2D_u + D_v + D_w + [p_2]^b)$
$s_5$	$\mathcal{O}([K_B^{-1}] - [p_2]^b)$	$s_{15}$	$\mathcal{O}(-D_u + D_v + D_w + [p_2]^b)$
$s_6$	$\mathcal{O}([K_B^{-1}] - [p_2]^b - D_v)$	$s_{16}$	$\mathcal{O}(-D_u + D_w + [p_2]^b)$
$s_7$	$\mathcal{O}([K_B^{-1}] - [p_2]^b - D_w)$	$s_{17}$	$\mathcal{O}(-D_u + D_v + [p_2]^b)$
$s_8$	$\mathcal{O}([K_B^{-1}] - [p_2]^b + D_u - D_v - D_w)$	$s_{18}$	$\mathcal{O}([p_2]^b)$
$s_9$	$\mathcal{O}([K_B^{-1}] - [p_2]^b + D_u - D_v)$	$s_{19}$	$\mathcal{O}(D_w + [p_2]^b)$
$s_{10}$	$\mathcal{O}([K_B^{-1}] - [p_2]^b + D_u - D_w)$	$s_{20}$	$\mathcal{O}(D_v + [p_2]^b)$

(5.47)

We also summarize the complete line bundles of the homogeneous coordinates on  $\text{Bl}_3\mathbb{P}^3$

by combining the classes in (5.13) and (5.42),

section	bundle	
$u$	$\mathcal{O}(H - E_1 - E_2 - E_3 + D_u)$	
$v$	$\mathcal{O}(H - E_2 - E_3 + D_v)$	
$w$	$\mathcal{O}(H - E_1 - E_3 + D_w)$	
$t$	$\mathcal{O}(H - E_1 - E_2)$	(5.48)
$e_1$	$\mathcal{O}(E_1)$	
$e_2$	$\mathcal{O}(E_2)$	
$e_3$	$\mathcal{O}(E_3)$	

For later reference, we point out that the divisors associated to the vanishing of the coefficients  $\tilde{s}_7$ ,  $\hat{s}_7$  and  $\tilde{s}_9 = -\hat{s}_9$ , denoted as  $\tilde{\mathcal{S}}_7$ ,  $\hat{\mathcal{S}}_7$  respectively  $\mathcal{S}_9$ , in the two presentations (5.29) and (5.35) in  $dP_2$  of the elliptic curves  $\mathcal{E}$  are given by

$$\begin{aligned} \tilde{\mathcal{S}}_7 &:= [-s_{19}s_8 + s_{18}s_9] = [K_B^{-1}] + D_u - D_v, & \hat{\mathcal{S}}_7 &:= [s_{10}s_{18} - s_{20}s_8] = [K_B^{-1}] + D_u - D_w, \\ \mathcal{S}_9 &:= [\tilde{s}_9] = [\hat{s}_9] = [-s_{10}s_{19} + s_{20}s_9] = D_u + [K_B^{-1}]. \end{aligned} \quad (5.49)$$

Here we have used the definitions in (5.30), respectively, (5.36) together with (5.47) and denoted the divisor classes of a section  $s_i$  by  $[\cdot]$ .

It is important to notice that the line bundles of the  $s_i$  admit an additional degree of freedom due to the choice of the class  $[p_2]^b$ , the divisor class of the second constraint  $p_2$  in the homology of  $B$ . This is due to the fact that the Calabi-Yau condition (5.46) is a partition problem, that only fixes the sum of the classes  $[p_1]^b$ ,  $[p_2]^b$  but leaves the individual classes undetermined. For example, in complete intersections in a toric ambient space (5.43) the freedom of the class  $[p_2]^b$  is fixed by finding all nef-partitions of the toric

polytope associated to (5.43) that are consistent with the nef-partition (5.23) of the  $\text{Bl}_3\mathbb{P}^3$ -fiber. We discuss the freedom in  $[p_2]^b$  further in section 5.2.3.

## 5.2.2 Basic Geometry of Calabi-Yau Manifolds with $\text{Bl}_3\mathbb{P}^3$ -elliptic Fiber

Let us next discuss the basic topological properties of the Calabi-Yau manifold  $\hat{X}$ .

We begin by constructing a basis  $D_A$  of the group of divisors  $H^{(1,1)}(\hat{X})$  on  $\hat{X}$  that is convenient for the study of F-theory on  $\hat{X}$ . A basis of divisors on the generic complete intersection  $\hat{X}$  is induced from the basis of divisors of the ambient space  $\text{Bl}_3\mathbb{P}^3(\tilde{\mathcal{S}}_7, \hat{\mathcal{S}}_7, \mathcal{S}_9)$  by restriction to  $\hat{X}$ . There are the vertical divisors  $D_\alpha$  that are obtained by pulling back divisors  $D_\alpha^b$  on the base  $B$  as  $D_\alpha = \pi^*(D_\alpha^b)$  under the projection map  $\pi : \hat{X} \rightarrow B$ . In addition, each point  $P, Q, R$  and  $S$  on the elliptic fiber  $\mathcal{E}$  in (5.16) lifts to an in general rational section of the fibration  $\pi : \hat{X} \rightarrow B$ , that we denote by  $\hat{s}_P, \hat{s}_Q, \hat{s}_R$  and  $\hat{s}_S$ , with  $\hat{s}_P$  the zero section. The corresponding divisor classes, denoted  $S_P, S_Q, S_R$  and  $S_S$ , then follow from (5.18) and (5.48) as

$$S_P = E_3, \quad S_Q = E_1, \quad S_R = E_2, \quad S_S = H - E_1 - E_2 - E_3 + \mathcal{S}_9 + [K_B], \quad (5.50)$$

where we denote, by abuse of notation, the lift of the classes  $H, E_1, E_2, E_3$  of the fiber  $\text{Bl}_3\mathbb{P}^3$  in (5.13) to classes in  $\hat{X}$  by the same symbol. For convenience, we collectively denote the generators of the Mordell-Weil group and their divisor classes as

$$\hat{s}_m = (\hat{s}_Q, \hat{s}_R, \hat{s}_S), \quad S_m = (S_Q, S_R, S_S) \quad m = 1, 2, 3. \quad (5.51)$$

The vertical divisors  $D_\alpha$  together with the classes (5.50) of the rational points form a basis of  $H^{(1,1)}(\hat{X})$ . A basis that is better suited for applications to F-theory, however, is

given by

$$D_A = (\tilde{S}_P, D_\alpha, \sigma(\hat{s}_m)), \quad A = 0, 1, \dots, h^{(1,1)}(B) + 4, \quad (5.52)$$

where the Hodge number  $h^{(1,1)}(B)$  of the base  $B$  counts the number of vertical divisors  $D_\alpha$  in  $\hat{X}$ . Here we have introduced the class [56, 12]

$$\tilde{S}_P = S_P + \frac{1}{2}[K_B^{-1}], \quad (5.53)$$

and have applied the Shioda map  $\sigma$  that maps the Mordell-Weil group of  $\hat{X}$  to a certain subspace of  $H^{(1,1)}(\hat{X})$ . The map  $\sigma$  is defined as

$$\sigma(\hat{s}_m) := S_m - \tilde{S}_P - \pi(S_m \cdot \tilde{S}_P), \quad (5.54)$$

where  $\pi$ , by abuse of notation, denotes the projection of  $H^{(2,2)}(\hat{X})$  to the vertical homology  $\pi^*H^{(1,1)}(B)$  of the base  $B$ . For every  $\mathcal{C}$  in  $H^{(2,2)}(\hat{X})$  the map  $\pi$  is defined as

$$\pi(\mathcal{C}) = (\mathcal{C} \cdot \Sigma^\alpha) D_\alpha, \quad (5.55)$$

where we obtain the elements  $\Sigma^\alpha = \pi^*(\Sigma_b^\alpha)$  in  $H_4(\hat{X})$  as pullbacks from a dual basis  $\Sigma_b^\alpha$  to the divisors  $D_\alpha^b$  in  $B$ , i.e.  $\Sigma_b^\alpha \cdot D_\beta^b = \delta_\beta^\alpha$ .

Next, we list the fundamental intersections involving the divisors  $S_P$ ,  $S_Q$  and  $S_R$  in (5.50), that will be relevant throughout this work:

<b>Universal intersection:</b>	$S_P \cdot F = S_m \cdot F = 1$ with general fiber $F \cong \mathcal{E}$ , (5.56)
<b>Rational sections:</b>	$\pi(S_P^2 + [K_B^{-1}] \cdot S_P) = \pi(S_m^2 + [K_B^{-1}] \cdot S_m) = 0$ , (5.57) $\tilde{\mathcal{S}}_7 = \pi(S_Q \cdot S_S)$ , $\hat{\mathcal{S}}_7 = \pi(S_R \cdot S_S)$ , $\mathcal{S}_9 = \pi(S_P \cdot S_S)$ ,
<b>Holomorphic sections:</b>	$S_P^2 + [K_B^{-1}] \cdot S_P = S_m^2 + [K_B^{-1}] \cdot S_m = 0$ , (5.58)
<b>Shioda maps:</b>	$\sigma(\hat{s}_Q) = S_Q - S_P - [K_B^{-1}]$ , $\sigma(\hat{s}_R) = S_R - S_P - [K_B^{-1}]$ , (5.59) $\sigma(\hat{s}_S) = S_S - S_P - [K_B^{-1}] - \mathcal{S}_9$ ,

The first line (5.56) and the second line (5.57) are the defining property of a section of a fibration, whereas the fourth line only holds for a holomorphic section. The third line holds because the collision pattern of the points in (5.21) directly translates into intersections of their divisor classes  $S_m$ , where we made use of (5.30) and (5.36). In other words, (5.57) states that divisors  $\tilde{\mathcal{S}}_7$ ,  $\hat{\mathcal{S}}_7$ ,  $\mathcal{S}_9$  are the codimension one loci where the sections collide with each other in the fiber  $\mathcal{E}$ . Finally, the result for the Shioda maps of the sections follows from their definitions in (5.54) and the intersections in (5.57).

For later reference, we also compute the intersection matrix of the Shioda maps  $\sigma(\hat{s}_m)$ , i.e. the height pairing, as

$$\pi(\sigma(\hat{s}_m) \cdot \sigma(\hat{s}_n)) = \begin{pmatrix} 2[K_B] & [K_B] & -\mathcal{S}_9 + \tilde{\mathcal{S}}_7 + [K_B] \\ [K_B] & 2[K_B] & -\mathcal{S}_9 + \hat{\mathcal{S}}_7 + [K_B] \\ -\mathcal{S}_9 + \hat{\mathcal{S}}_7 + [K_B] & -\mathcal{S}_9 + \hat{\mathcal{S}}_7 + [K_B] & 2(-\mathcal{S}_9 + [K_B]) \end{pmatrix}_{mn} \quad (5.60)$$

which readily follows from (5.59) and (5.57).

We note that all the above intersections (5.56), (5.57), (5.58), (5.59) and (5.60) are in completely analogous to the ones found in [31, 34, 30] for the case of an elliptic Calabi-Yau manifold with rank two Mordell-Weil group, see also [105, 97, 20, 60] for a discussion of intersections in the rank one case.

### 5.2.3 All Calabi-Yau manifolds $\hat{X}$ with $\text{Bl}_3\mathbb{P}^3$ -elliptic fiber over $B$

Finally, we are equipped to classify the generic Calabi-Yau manifolds  $\hat{X}$  with elliptic fiber in  $\text{Bl}_3\mathbb{P}^3$  and base  $B$ . This task reduces to a classification of all possible assignments of line bundles to the sections  $s_i$  in (5.47) so that the Calabi-Yau manifold  $\hat{X}$  is given by the generic complete intersection (5.16). Otherwise we expect additional singularities in  $\hat{X}$ , potentially corresponding to a minimal gauge symmetry in F-theory, either from non-toric non-Abelian singularities or from non-toric sections. We prove in the following that a generic Calabi-Yau manifold  $\hat{X}$  over a base  $B$  corresponds to a point in a certain polytope, that is related to the single nef-partition of the polytope of  $\text{Bl}_3\mathbb{P}^3$  as explained below. The following discussion is similar in spirit to the one in [30, 74], that can agree with the toric classification of [19].

We begin with the basis expansion

$$D_u = n_u^\alpha D_\alpha, \quad D_v = n_v^\alpha D_\alpha, \quad D_w = n_w^\alpha D_\alpha, \quad (5.61)$$

into vertical divisors  $D_\alpha$ , where the  $n_u^\alpha$ ,  $n_v^\alpha$  and  $n_w^\alpha$  are integer coefficients. For  $\hat{X}$  to be generic these coefficients are bounded by the requirement that all the sections  $s_i$  in (5.47) are generic, i.e. that the line bundles of which the  $s_i$  are holomorphic sections admit holomorphic sections. This is equivalent to all divisors in (5.47) being effective.

First, we notice that effectiveness of the sum  $[s_i] + [s_{i+10}] \geq 0$  in (5.47) is guaranteed



if the vector of integers  $\mathbf{n}^\alpha = (n_u^\alpha, n_v^\alpha, n_w^\alpha)$  is an integral point in the rescaled polytope of  $\text{Bl}_3\mathbb{P}^3$ . Indeed, we can express the conditions of effectiveness of the divisors  $[s_i] + [s_{i+10}]$  as the following set of inequalities in  $\mathbb{R}^3$ ,

$$\frac{1}{-K^\alpha} \mathbf{n}^\alpha \cdot \mathbf{v}_i \geq -1, \quad i = 1, \dots, 7, \quad (5.62)$$

where we also expand the canonical bundle  $K_B$  of the base  $B$  in terms of the vertical divisors  $D_\alpha$  as

$$[K_B] = K^\alpha D_\alpha \quad (5.63)$$

with integer coefficients  $K^\alpha$ . The entries of the vectors  $\mathbf{v}_i$  are extracted by first summing the rows of the two tables in (5.47), requiring the sum to be effective and then taking the coefficients of the the divisors  $D_u, D_v, D_w$ . The  $\mathbf{v}_i$  span the following polytope

$$\Delta_3 := \langle \mathbf{v}_i \rangle = \left\langle \begin{pmatrix} -3 \\ 1 \\ 1 \end{pmatrix}, \begin{pmatrix} -1 \\ 1 \\ 1 \end{pmatrix}, \begin{pmatrix} -1 \\ -1 \\ 1 \end{pmatrix}, \begin{pmatrix} -1 \\ 1 \\ -1 \end{pmatrix}, \begin{pmatrix} 1 \\ -1 \\ -1 \end{pmatrix}, \begin{pmatrix} 1 \\ -1 \\ 1 \end{pmatrix}, \begin{pmatrix} 1 \\ 1 \\ -1 \end{pmatrix} \right\rangle. \quad (5.64)$$

This is precisely the dual of the polytope  $\nabla_{\text{Bl}_3\mathbb{P}^3}$  of  $\text{Bl}_3\mathbb{P}^3$ , where the latter polytope is the convex hull of the following vertices,

$$\nabla_{\text{Bl}_3\mathbb{P}^3} = \left\langle -\rho_1, \rho_{e_1}, \rho_4, \rho_3, \rho_{e_2}, \rho_{e_3}, \rho_1 \right\rangle. \quad (5.65)$$

We note that these vertices are related to the vertices in (5.10) and (5.22) by an  $\text{SL}(3, \mathbb{Z})$  transformation. Thus, we confirm that the solutions to (5.62), for which all divisors  $[s_i] + [s_{i+10}]$  are effective, are precisely given by vectors  $\mathbf{n}^\alpha$  that take values for all  $\alpha$  in the polytope of  $\text{Bl}_3\mathbb{P}^3$  rescaled by the factor  $-K^\alpha$ .

Next we determine the conditions inferred from each individual class  $[s_i]$  in (5.47) being

effective. We obtain the following *two sets of conditions*, whose solutions, given also below, yield the set of all generic elliptic fibrations  $\hat{X}$  with a general rank three Mordell-Weil group over a given base  $B$ :

$$\begin{aligned}
1) \quad & 0 \leq ([p_2]^b)^\alpha \leq -K_B^\alpha, \quad (5.66) \\
2) \quad & \mathbf{n}^\alpha \cdot \mathbf{v}_i \geq K^\alpha + ([p_2]^b)^\alpha, \quad \mathbf{v}_i \in \nabla_1, \quad \mathbf{n}^\alpha \cdot \mathbf{v}_i \geq -([p_2]^b)^\alpha, \quad \mathbf{v}_i \in \nabla_2.
\end{aligned}$$

These conditions are solved by any  $\mathbf{n}^\alpha$  being integral points in the following Minkowski sum of the polyhedra  $\nabla_1, \nabla_2$  defined in (5.70),

$$\mathbf{n}^\alpha \in -(K^\alpha + ([p_2]^b)^\alpha)\nabla_1 + ([p_2]^b)^\alpha\nabla_2, \quad \forall \alpha = 1, \dots, h^{(1,1)}(B). \quad (5.67)$$

Here the two conditions for  $[p_2]^b$  in the first line of (5.66) follow from  $[s_5], [s_{18}] \geq 0$  and the first, respectively, second set of conditions in the second line follow from the first, respectively, second table in (5.47). In addition, we have expanded the class  $[p_2]^b$  into a basis  $D_\alpha$  as

$$[p_2]^b = ([p_2]^b)^\alpha D_\alpha \quad (5.68)$$

and have introduced the points  $\mathbf{v}_i$  that define two polytopes

$$\begin{aligned}
\Delta_1 & := \langle \mathbf{v}_i \rangle_{0 \leq i \leq 6} = \left\langle \begin{pmatrix} -1 \\ 0 \\ 0 \end{pmatrix}, \begin{pmatrix} 0 \\ -1 \\ 0 \end{pmatrix}, \begin{pmatrix} 0 \\ 0 \\ -1 \end{pmatrix}, \begin{pmatrix} 1 \\ -1 \\ -1 \end{pmatrix}, \begin{pmatrix} 1 \\ -1 \\ 0 \end{pmatrix}, \begin{pmatrix} 1 \\ 0 \\ -1 \end{pmatrix} \right\rangle, \\
\Delta_2 & := \langle \mathbf{v}_i \rangle_{7 \leq i \leq 12} = \left\langle \begin{pmatrix} -2 \\ 1 \\ 1 \end{pmatrix}, \begin{pmatrix} -1 \\ 1 \\ 1 \end{pmatrix}, \begin{pmatrix} -1 \\ 0 \\ 1 \end{pmatrix}, \begin{pmatrix} -1 \\ 1 \\ 0 \end{pmatrix}, \begin{pmatrix} 0 \\ 0 \\ 1 \end{pmatrix}, \begin{pmatrix} 0 \\ 1 \\ 0 \end{pmatrix} \right\rangle. \quad (5.69)
\end{aligned}$$

Next, we show how we have constructed the solutions (5.67) to (5.66). To this end, it we only have to notice that the two polytopes  $\Delta_1, \Delta_2$  are the duals of the following two

polytopes  $\nabla_1, \nabla_2$ ,

$$\nabla_1 = \langle -\rho_1, \rho_{e_1}, \rho_4, \rho_3 \rangle, \quad \nabla_2 = \langle \rho_{e_2}, \rho_{e_3}, \rho_1 \rangle, \quad (5.70)$$

where the vectors  $\rho_i, \rho_{e_i}$  were defined in (5.10), (5.22). These two polytopes correspond to the unique nef-partition of (5.65). Now, we first fix the class  $[p_2]^b$  such that the first conditions in (5.66) are met. Second, for each allowed class for  $[p_2]^b$  we solve the second set of conditions in (5.66) for the vectors  $\mathbf{n}^\alpha$ . However, these are just the duality relations between the  $\Delta_i$  and  $\nabla_j$ , rescaled by appropriate factors. Consequently, the solutions are precisely given by the integral points in the Minkowski sum of the polyhedra in (5.67). Here we emphasize again that both coefficients in (5.67) are positive integers by means of the first condition in (5.66).

In summary, we have shown that for a given base  $B$  a generic elliptically fibered Calabi-Yau manifold  $\hat{X}$  with general elliptic fiber  $\mathcal{E}$  given by (5.16) in  $\text{Bl}_3\mathbb{P}^3$  corresponds to an integral point  $\mathbf{n}^\alpha$  in the polyhedron (5.67) for every  $\alpha$  and for every class  $[p_2]^b$  obeying  $0 \leq [p_2]^b \leq [K_B^{-1}]$ . The coordinates of the point  $\mathbf{n}^\alpha$  are the coefficients of the divisors  $D_u, D_v, D_w$  in the expansion (5.61) into vertical divisors  $D_\alpha$ .

## 5.3 Matter in F-Theory Compactifications with a Rank

### Three Mordell-Weil Group

In this section we analyze the codimension two singularities of the elliptic fibration of  $\hat{X}$  to determine the matter representations of corresponding F-theory compactifications to six and four dimensions. We find 14 different singlet representations in sections 5.3.1 and 5.3.2. Then, we determine the explicit matter multiplicities of these 14 matter fields in six-dimensional F-theory compactification on a Calabi-Yau threefold  $\hat{X}_3$  with a general

two-dimensional base  $B$  in section 5.3.3. The following discussion is based on techniques developed in [34, 30, 33] for the case of a rank two Mordell-Weil group, to which we refer for more background on some technical details.

We begin with an outline of the general strategy to determine matter in an F-theory compactification on a Calabi-Yau manifold with a higher rank Mordell-Weil group. First, we recall that in general rational curves  $c_{\text{mat}}$  obtained from resolving a singularity of the elliptic fibration at codimension two in the base  $B$  give rise to matter in F-theory due to the presence of light M2-brane states in the F-theory limit. In elliptically fibered Calabi-Yau manifolds with a non-Abelian gauge symmetry in F-theory, these codimension two singularities are located on the divisor in the base  $B$ , which supports the 7-branes giving rise to the non-Abelian gauge group. Technically, the discriminant of the elliptic fibration takes the form  $\Delta = z^n(k + \mathcal{O}(z))$ , where  $z$  vanishes along the 7-brane divisor and  $k$  is a polynomial independent of  $z$ . Then, the codimension two singularities are precisely given by the intersections of  $z = 0$  and  $k = 0$ .

This is in contrast to elliptic fibrations with only a non-trivial Mordell-Weil group, i.e. only an Abelian gauge group, since the elliptic fibration over codimension one has only  $I_1$ -singularities and the discriminant does not factorize in an obvious way. Thus, the codimension two codimension singularities are not contained in a simple divisor in  $B$  and have to be studied directly. In fact, the existence of a rational section, denoted by say  $\hat{s}_Q$ , means that there is a solution to the Weierstrass form (WSF) of the form  $[x^Q : y^Q : z^Q] = [g_2^Q : g_3^Q : 1]$ .<sup>6</sup> Here  $g_2^Q$  and  $g_3^Q$  are sections of  $K_B^{-2}$  and  $K_B^{-3}$ , respectively.<sup>7</sup> Thus, the

---

<sup>6</sup>Sections with  $z^Q = b$  for a section  $b$  of a line bundle  $\mathcal{O}([b])$  on the base  $B$  and with  $g_2^Q, g_3^Q$  sections of  $K_B^{-2} \otimes \mathcal{O}(2[b])$ , respectively,  $K_B^{-3} \otimes \mathcal{O}(3[b])$ , can be studied similarly. We only have to assume that we are at a locus with  $b \neq 0$ . Then we can employ the  $\mathbb{C}^*$ -action to set  $z^Q = 1, x^Q = \frac{g_2^Q}{b^2}, y^Q = \frac{g_3^Q}{b^3}$ .

<sup>7</sup>For concreteness and for comparison to [97, 34], in the special case of the base  $B = \mathbb{P}^2$ , the sections  $g_2^Q = g_6, g_3^Q = g_9$  are polynomials of degree 6, respectively, 9

presence of  $\hat{s}_Q$  implies the factorization

$$(y - g_3^Q z^3)(y + g_3^Q z^3) = (x - g_2^Q z^2)(x^2 + g_2^Q x z^2 + g_4^Q z^4) \quad (5.71)$$

for appropriate  $g_4^Q$ . Parametrizing the discriminant  $\Delta$  in terms of the polynomials in (5.71), we see that it vanishes of order two at the codimension two loci in  $B$  reading

$$g_3^Q = 0, \quad \hat{g}_4^Q := g_4^Q + 2(g_2^Q)^2 = 0. \quad (5.72)$$

These two conditions lead to a factorization of both sides of (5.71), so that a conifold singularity is developed at  $y = (x - g_2^Q z^2) = 0$ .

It is evident that the section  $\hat{s}_Q$  passes automatically through the singular point of the elliptic curve. Thus, in the resolved elliptic curve  $\mathcal{E}$  where the singular point  $y = (x - g_2^Q z^2) = 0$  is replaced by a Hirzebruch-Jung sphere tree of intersecting  $\mathbb{P}^1$ 's,<sup>8</sup> the section  $\hat{s}_Q$  automatically intersects at least one  $\mathbb{P}^1$ . This implies that the loci (5.72) in the base contain matter charged under  $U(1)_Q$  associated to  $\hat{s}_Q$ , as can be seen from the charge formula

$$q_Q = c_{\text{mat}} \cdot (S_Q - S_P). \quad (5.73)$$

Here  $S_Q, S_P$  denote the divisor classes of  $\hat{s}_Q$  and the zero section  $\hat{s}_P$ , respectively. In fact, the locus (5.72) contains the codimension two loci supporting *all* matter charged under  $U(1)_Q$ , without distinguishing between matter with different  $U(1)_Q$ -charges. The loci of the different matter representations correspond to the irreducible components of (5.72), that can in principle be obtained by finding all associated prime ideals of (5.72) of codimension two in  $B$ . Unfortunately, in many concrete setups this is computationally unfeasible and we have to pursue a different strategy to obtain the individual matter representations that has

---

<sup>8</sup>In F-theory compactifications with only Abelian groups the resolved elliptic fibers are expected to be  $I_2$ -curves, i.e. two  $\mathbb{P}^1$ 's intersecting at two points.

already been successful in the rank two case in [97, 34].

For the following analysis of codimension two singularities of  $\hat{X}$  we identify the irreducible components of (5.72) corresponding to different matter representations in two qualitatively different ways:

- 1) One type of codimension two singularities corresponds to singularities of the sections  $\hat{s}_m$  and  $\hat{s}_p$ . This analysis, see section 5.3.1, is performed in the presentation of  $\mathcal{E}$  as the complete intersection (5.16) in  $\text{Bl}_3\mathbb{P}^3$ , where the rational sections are given by (5.19). In fact, when a rational section  $\hat{s}_m$  or the zero section  $\hat{s}_p$  is ill-defined, the resolved elliptic curve splits into an  $I_2$ -curve with one  $\mathbb{P}^1$  representing the original singular fiber and the other  $\mathbb{P}^1$  representing the singular section.
- 2) The second type of codimension two singularities has to be found directly in the Weierstrass model. The basic idea is isolate special solutions to (5.72) by supplementing the two equations (5.72) by further constraints that have to vanish in addition in order for a certain matter representation to be present. We refer to section 5.3.2 for concrete examples. It is then possible to find the codimension two locus along which all these constraints vanish simultaneously. We note that for the geometry  $\hat{X}$  there are three rational sections, thus, three factorizations of the form (5.71) and loci (5.72), that have to be analyzed separately.

A complete analysis of codimension two singularities following the above two-step strategy should achieve a complete decomposition of (5.72) for all sections of  $\hat{X}$  into irreducible components. It would be interesting to prove this mathematical for the codimension two singularities of  $\hat{X}$  we find in this section. As a consistency check of our analysis of codimension two singularities we find, we determine the full spectrum, including multiplicities, of charged hypermultiplets of a six-dimensional F-theory compactification and check that six-dimensional anomalies are cancelled, cf. section 5.3.3.

### 5.3.1 Matter at the Singularity Loci of Rational Sections

Now that the strategy is clear, we will look for the first type of singularities in this subsection. These are the codimension two loci in the base where the rational sections are singular in  $\text{Bl}_3\mathbb{P}^3$ . This precisely happens when the coordinates (5.18), (5.19) of any of the rational sections take values in the Stanley-Reisner ideal (5.14) of  $\text{Bl}_3\mathbb{P}^3$ .

There are two reasons why codimension two loci with singular rational sections are good candidates for  $I_2$ -fibers. First, the elliptic fibration of  $\hat{X}$  is smooth<sup>9</sup>, thus, the indeterminacy of the coordinates of the sections in the fiber may imply that the section is not a point, but an entire  $\mathbb{P}^1$ . Second, as was remarked in [97] and [34], if we approach the codimension two singularity of the section along a line in the base  $B$  the section has a well defined coordinate given by the slope of the line. Thus, approaching the singularity along lines of all possible slopes the section at the singular point is identified with the  $\mathbb{P}^1$  formed by all slopes. In fact, specializing the elliptic curve to each locus yielding a singularity of a rational section we observe a splitting of the elliptic curve into an  $I_2$ -curve. We note that it is crucial to work in  $\text{Bl}_3\mathbb{P}^3$ , because only in this space the fiber is fully resolved space by the exceptional divisors  $E_i$ , in contrast to the curve (5.4) in  $\mathbb{P}^3$ .

#### The vanishing of two minors: special singularities of $\hat{s}_S$

In order to identify singularities of rational sections, let us take a close look at the Stanley-Reisner ideal (5.14). It contains monomials with two variables of the type  $e_i e_j$  and monomials with three variables of the type  $uXY$ , where  $X$  and  $Y$  are two variables out of the set  $\{v, w, t\}$ . In this subsection we look for singular sections whose coordinates are forbidden by the elements  $e_i e_j$ .

From the coordinates (5.19) of the rational sections we infer that this type of singular

---

<sup>9</sup>This is clear for toric bases  $B$ .

behavior can only occur for the section  $\hat{s}_S$ , whose coordinates in the fiber  $\mathcal{E}$  are

$$S = [0 : 1 : 1 : 1 : s_{19}s_8 - s_{18}s_9 : s_{10}s_{18} - s_{20}s_8 : s_{10}s_{19} - s_{20}s_9]. \quad (5.74)$$

There are three codimension two loci where  $S$  is singular, reading

$$\{s_8 = s_{18} = 0\}, \quad \{s_9 = s_{19} = 0\}, \quad \{s_{10} = s_{20} = 0\}. \quad (5.75)$$

It is important to note that the matrices (5.8), (5.20) retain rank two at these loci, since only two of their  $2 \times 2$ -minors, being identified with the coordinates (5.19), have vanishing determinant. Next, we inspect the constraint (5.16) of the elliptic curve at these loci.

At all these three codimension two loci, we see that the elliptic curve in (5.16) takes the common form

$$Au + BY = 0, \quad Cu + DY = 0. \quad (5.76)$$

Here  $Y$  is one of the variables  $\{v, w, t\}$  and the polynomials  $B, D$  are chosen to be independent of  $u$  and  $Y$ , which fixes the polynomials  $A, C$  uniquely. This complete intersection describes a reducible curve. This can be seen by rewriting it as

$$(AD - BC)u = 0, \quad Au + BY = Cu + DY = 0, \quad (5.77)$$

which we obtained by solving for the variable  $Y$  in the first equation of (5.76) and requiring consistency with the second equation.

Now, we directly see that one solution to (5.77) is given by  $\{u = 0, Y = 0\}$ . This is a  $\mathbb{P}^1$  as is clear from the remaining generators of the SR-ideal after setting the coordinates that are not allowed to vanish to one using the  $\mathbb{C}^*$ -actions. The second solution, which also describes a  $\mathbb{P}^1$ , is given by the vanishing of the determinant in the first equation in (5.77),



which implies that the two constraint in the second equation become dependent. Thus, the two  $\mathbb{P}^1$ 's of the  $I_2$ -curve are given by

$$c_1 = \{u = 0, Y = 0\}, \quad c_2 = \{AD - BC = 0, Cu + DY = 0\}. \quad (5.78)$$

As an example, let us look at the loci  $\{s_8 = s_{18} = 0\}$  in (5.75) in detail. In this case the elliptic curve  $\mathcal{E}$  given in (5.16) takes the form

$$\begin{aligned} u(s_2e_1e_2e_3u + s_5e_1e_2t + s_6e_2e_3v + s_7e_1e_3w) &= t(s_9e_2v + s_{10}e_1w), \\ u(s_{12}e_1e_2e_3u + s_{15}e_1e_2t + s_{16}e_2e_3v + s_{17}e_1e_3w) &= t(s_{19}e_2v + s_{20}e_1w). \end{aligned} \quad (5.79)$$

This complete intersection is in the form (5.76) by identifying  $Y = t$  and setting

$$\begin{aligned} A &= (s_2e_1e_2e_3u + s_5e_1e_2t + s_6e_2e_3v + s_7e_1e_3w), & B &= -(s_9e_2v + s_{10}e_1w), \\ C &= (s_{12}e_1e_2e_3u + s_{15}e_1e_2t + s_{16}e_2e_3v + s_{17}e_1e_3w), & D &= -(s_{19}e_2v + s_{20}e_1w). \end{aligned} \quad (5.80)$$

Then the two  $\mathbb{P}^1$ 's of the  $I_2$ -curve are given by  $c_1, c_2$  in (5.78).

Equipped with the equations for the individual curves  $c_1, c_2$  we can now calculate the intersections with the sections and the charge of the hypermultiplet that is supported there. The intersections of the curve defined  $c_1$  can be readily obtained from the toric intersections of  $\text{Bl}_3\mathbb{P}^3$ . It has intersection  $-1$  with the section  $S_S$ , intersection one with the sections  $S_Q, S_R$  and zero with  $S_P$ , where the last intersection is clear from the existence of the term  $e_3t$  in the Stanley-Reisner ideal (5.14). The intersections with  $c_2$  can be calculated either directly from (5.78) or from the fact, that the intersections of a section with the total class  $F = c_1 + c_2$  have to be one.

We summarize our findings as:

Loci	Curve	$\cdot S_P$	$\cdot S_Q$	$\cdot S_R$	$\cdot S_S$
$s_8 = s_{18} = 0$	$c_1 = \{u = t = 0\}$	0	1	1	-1
	$c_2$	1	0	0	2
$s_9 = s_{19} = 0$	$c_1 = \{u = w = 0\}$	1	1	0	-1
	$c_2$	0	0	1	2
$s_{10} = s_{20} = 0$	$c_1 = \{u = v = 0\}$	1	0	1	-1
	$c_2$	0	1	0	2

(5.81)

Here we denoted the intersection pairing by ‘ $\cdot$ ’ and we also computed the intersections of the sections with the  $I_2$ -curves at the other two codimension two loci in (5.75). In these cases, we identified  $Y = w$ , respectively,  $Y = v$ .

We proceed with the calculation of the charges in each case employing the charge formula (5.73). We note that the isolated curve  $c_{mat}$  is always the curve in the  $I_2$ -fiber that that does not intersect the zero section  $S_P$ . We obtain the charges:

Loci	$q_Q$	$q_R$	$q_S$
$s_8 = s_{18} = 0$	1	1	-1
$s_9 = s_{19} = 0$	0	1	2
$s_{10} = s_{20} = 0$	1	0	2

(5.82)

### The vanishing of three minors: singularities of all sections

The remaining singularities of the rational sections occur if the three of the determinants of the minors of the matrices (5.8), (5.20) vanish. This implies that three coordinates (5.19) of a section are forbidden by the SR-ideal (5.14), which happens also for the sections  $\hat{s}_P$ ,  $\hat{s}_Q$ ,  $\hat{s}_R$ , in addition to  $\hat{s}_S$ , due to the elements  $uXY$  with  $X, Y$  in  $\{v, w, t\}$ .

Before analyzing these loci, we emphasize that the three vanishing conditions are a codimension two phenomenon because the vanishing of the determinants of three minors of the same matrix is not independent. In fact, these codimension two loci can be viewed as determinantal varieties describing the loci where the rank of each of the matrices in (5.8), (5.20) jump from two to one, which is clearly a codimension two phenomenon.

Concretely, for the section  $\hat{s}_P$  to be singular, the three minors that have to vanish are  $|M_3^P| = |M_2^P| = |M_1^P| = 0$ , which implies the conditions

$$\frac{s_5}{s_{15}} = \frac{s_{10}}{s_{20}} = \frac{s_9}{s_{19}}. \quad (5.83)$$

Similarly, for  $\hat{s}_Q$  to be singular, we impose  $|M_3^Q| = |M_2^Q| = |M_1^Q| = 0$ , which yields

$$\frac{s_6}{s_{16}} = \frac{s_8}{s_{18}} = \frac{s_9}{s_{19}}. \quad (5.84)$$

For a singular section  $\hat{s}_R$ , we require  $|M_3^R| = |M_2^R| = |M_1^R| = 0$ , which is equivalent to

$$\frac{s_{10}}{s_{20}} = \frac{s_8}{s_{18}} = \frac{s_7}{s_{17}}. \quad (5.85)$$

Finally, the section  $\hat{s}_S$  is singular at  $|M_3^Q| = |M_3^R| = |M_3^P| = 0$ , or equivalently at

$$\frac{s_{10}}{s_{20}} = \frac{s_8}{s_{18}} = \frac{s_9}{s_{19}}. \quad (5.86)$$

We remark that the vanishing of the three minors in all these cases excludes the loci (5.75) of the previous subsection.

All these singularities imply a reducible curve of a form similar to (5.27), however, adapted to the ambient space  $\text{Bl}_3\mathbb{P}^3$ . In fact, at each of the loci (5.83)-(5.86) the complete

intersection (5.16) takes the form

$$AX + BY = 0, \quad CX + DY = 0, \quad (5.87)$$

for appropriate polynomials  $A, B, C, D$  with  $A$  and  $C$  collinear, that is  $A = aC$ , and the pair of coordinates  $[X : Y]$  forming a  $\mathbb{P}^1$ .<sup>10</sup> Then, we can multiply the second equation by  $a$  and subtract from the first equation, to obtain

$$(B - aD)Y = 0, \quad AX + BY = 0. \quad (5.88)$$

From this we see that the two solutions are given by

$$c_1 = \{Y = A = 0\}, \quad c_2 = \{B - aD = AX + BY = 0\}, \quad (5.89)$$

that describe two  $\mathbb{P}^1$ 's intersecting at two points. Thus the complete intersection (5.88) is an  $I_2$ -curve.

### One example in detail

Let us focus on the locus in (5.84) where the section  $\hat{s}_Q$  is singular. The complete intersection (5.16) then takes the form

$$\begin{aligned} v(-e_2s_9t + e_2e_3s_6u + e_3s_8w) + e_1(e_2s_5tu + e_2e_3s_2u^2 - s_{10}tw + s_7e_3uw) &= 0, \\ v(-e_2s_{19}t + e_2e_3s_{16}u + e_3s_{18}w) + e_1(e_2s_{15}tu + e_2e_3s_{12}u^2 - s_{20}tw + e_3s_{17}uw) &= 0. \end{aligned}$$

---

<sup>10</sup>When  $\hat{s}_S$  becomes singular, we identify  $Y = u$  and  $X = 1$ . However,  $A, C$  still become collinear and the argument applies.

This is of the form (5.87) as we see by identifying  $X = v$  and  $Y = e_1$  and by setting

$$A = -e_2s_9t + e_2e_3s_6u + e_3s_8w, \quad B = e_2s_5tu + e_2e_3s_2u^2 - s_{10}tw + s_7e_3uw, \quad (5.90)$$

$$C = -e_2s_{19}t + e_2e_3s_{16}u + e_3s_{18}w, \quad D = e_2s_{15}tu + e_2e_3s_{12}u^2 - s_{20}tw + e_3s_{17}uw$$

with  $A = (s_8/s_{18})C$  collinear at the locus (5.84). Then, the two  $\mathbb{P}^1$ 's in this  $I_2$ -curve are given by (5.89) with the identifications (5.90).

Next, we obtain the intersections of the curves  $c_1, c_2$  with the rational sections, that follow directly from the toric intersections of  $\text{Bl}_3\mathbb{P}^3$ . We find the intersections

Loci	Curve	$\cdot S_P$	$\cdot S_Q$	$\cdot S_R$	$\cdot S_S$
$ M_3^Q  =  M_2^Q  =  M_1^Q  = 0$	$c_1$	0	-1	0	1
	$c_2$	1	2	1	0

(5.91)

As expected, the total fiber  $F = c_1 + c_2$  has intersections  $S_m \cdot F = 1$  with all sections.

Repeating the procedure with the other codimension two loci (5.83), (5.85) and (5.86), we obtain the intersections of the split elliptic curve with the sections as

Loci	Curve	$\cdot S_P$	$\cdot S_Q$	$\cdot S_R$	$\cdot S_S$
$ M_3^R  =  M_2^R  =  M_1^R  = 0$	$c_1$	0	0	-1	1
	$c_2$	1	1	2	0
$ M_3^P  =  M_2^P  =  M_1^P  = 0$	$c_1$	-1	0	0	1
	$c_2$	2	1	1	0
$ M_3^Q  =  M_3^R  =  M_3^P  = 0$	$c_1$	1	1	1	-1
	$c_2$	0	0	0	2

(5.92)

With these intersection numbers and the charge formula (5.73) we obtain the charges

Loci	$q_Q$	$q_R$	$q_S$
$ M_3^Q  =  M_2^Q  =  M_1^Q  = 0$	-1	0	1
$ M_3^R  =  M_2^R  =  M_1^R  = 0$	0	-1	1
$ M_3^P  =  M_2^P  =  M_1^P  = 0$	-1	-1	-2
$ M_3^Q  =  M_3^R  =  M_3^P  = 0$	0	0	2

(5.93)

### Relation to $dP_2$

In section 5.1.3 we saw that the elliptic curve  $\mathcal{E}$  can be mapped to two<sup>11</sup> non-generic anti-canonical hypersurfaces in  $dP_2$ . It is expected that some of the singularities we just found map to the singularities in the  $dP_2$ -elliptic curve. We recall from [34, 74], that the Calabi-Yau hypersurfaces (5.29), (5.35) in  $dP_2$  have singular sections at the codimension two loci given by  $\tilde{s}_3 = \tilde{s}_7 = 0$  ( $\hat{s}_3 = \hat{s}_7 = 0$ ),  $\tilde{s}_8 = \tilde{s}_9 = 0$  ( $\hat{s}_8 = \hat{s}_9 = 0$ ) and  $\tilde{s}_7 = \tilde{s}_9 = 0$  ( $\hat{s}_7 = \hat{s}_9 = 0$ ), respectively.

In tables (5.30) and (5.36) we readily identified the minors of the matrices in (5.20) with the some of the coefficients  $\tilde{s}_i$  and  $\hat{s}_j$ . This implies a relationship between the singular codimension two loci of the elliptic curves in  $\text{Bl}_3\mathbb{P}^3$  and in the two  $dP_2$ -varieties, that we

---

<sup>11</sup>There are actually three  $dP_2$  maps if we are willing to give up the zero point as a toric point. See section 5.1.3 for more details.

summarize in the following table:

$\text{Bl}_3\mathbb{P}^3$ -singularity	Singularity of curve in (5.29)	Singularity of curve in (5.35)	(5.94)
$ M_3^Q  =  M_2^Q  =  M_1^Q  = 0$	$\tilde{s}_3 = \tilde{s}_7 = 0$	$Q$ non-toric	
$ M_3^R  =  M_2^R  =  M_1^R  = 0$	$R$ non-toric	$\hat{s}_3 = \hat{s}_7 = 0$	
$ M_3^P  =  M_2^P  =  M_1^P  = 0$	$\tilde{s}_8 = \tilde{s}_9 = 0$	$\hat{s}_8 = \hat{s}_9 = 0$	
$ M_3^Q  =  M_3^R  =  M_3^P  = 0$	$\tilde{s}_7 = \tilde{s}_9 = 0$	$\hat{s}_7 = \hat{s}_9 = 0$	

In each case, three out of the four singular loci (5.93) yield singularities of the toric sections in the  $dP_2$ -elliptic curve. The other singular locus in the curve in  $\text{Bl}_3\mathbb{P}^3$  is not simply given by the vanishing of two coefficients  $\tilde{s}_i$ , respectively  $\hat{s}_j$ , because the non-toric rational sections becomes singular. Nevertheless, the elliptic curve in  $dP_2$  admits a factorization at the singular locus of the non-toric section, i.e. it splits into an  $I_2$ -curve, due to the non-genericity of the corresponding coefficients  $\tilde{s}_i$  or  $\hat{s}_j$ .

### 5.3.2 Matter from Singularities in the Weierstrass Model

As mentioned in the introduction of this subsection, *all* the loci of matter charged under a section  $\hat{s}_m$  satisfy the equations  $g_3^m = 0$  and  $\hat{g}_4^m = 0$ . Since we have three rational sections  $\hat{s}_m$ , the WSF admits three possible factorizations of the form (5.71), each of which implying a singular elliptic fiber at the loci  $g_3^{Q,R,S} = \hat{g}_4^{Q,R,S} = 0$  with  $\hat{g}_4^{R,S}$  defined analogous to (5.72). In this subsection we separate solutions to these equations by requiring additional constraints to vanish.

We can isolate matter with simultaneous U(1)-charges. The idea is the following. If the matter is charged under two sections, both sections have to pass through the singularity in

the WSF. This requires the  $x$ -coordinates  $g_2^{m_1}, g_2^{m_2}$  of the sections to agree<sup>12</sup>,

$$\delta g_2^{m_1, m_2} := g_2^{m_1} - g_2^{m_2} \stackrel{!}{=} 0, \quad (5.95)$$

for any two sections  $\hat{s}_{m_1}$  and  $\hat{s}_{m_2}$ . The polynomial (5.95) has a smaller degree than the other two conditions (5.72) and in fact it will be one of the two polynomials of the complete intersection describing the codimension two locus. The other constraint will be  $g_3^m = 0$  for  $m$  either  $m_1$  or  $m_2$ .

If we solve for two coefficients in these two polynomials and insert the solution back into the elliptic curve (5.16) we observe a reducible curve of the form (5.88). In this  $I_2$ -curve, one  $\mathbb{P}^1$  is automatically intersected once by both sections  $\hat{s}_{m_1}$  and  $\hat{s}_{m_2}$ . This means that a generic solution of equations (5.72), (5.95) support matter with charges one under  $U(1)_{m_1} \times U(1)_{m_2}$ .

Let us be more specific for matter charged under the sections  $\hat{s}_Q$  and  $\hat{s}_R$ , that is matter transforming under  $U(1)_Q \times U(1)_R$ . The conditions (5.72) and (5.95) read

$$\delta g_2^{QR} := g_2^Q - g_2^R \stackrel{!}{=} 0, \quad g_3^Q = 0, \quad \hat{g}_4^Q = 0, \quad (5.96)$$

and the codimension to locus is given by the complete intersection  $\delta g_2^{QR} = g_3^Q = 0$ . In fact the constraint  $\hat{g}_4^Q, \hat{g}_4^R$  are in the ideal generate by  $\langle \delta g_2^{QR}, g_3^Q \rangle$ .

We proceed to look for matter charged under  $U(1)_Q \times U(1)_S$ . In this case, because of the section  $\hat{s}_S$  having a non-trivial  $z$ -component, the right patch of the WSF is  $z \equiv \tilde{z}^S = s_{10}s_{19} - s_{20}s_9$ , c.f. (5.39). Thus, the constrains (5.72) and (5.95) take the form

$$\delta g_2^{QS} := g_2^S - (\tilde{z}^S)^2 g_2^Q \stackrel{!}{=} 0, \quad g_3^S = 0, \quad \hat{g}_4^S = 0. \quad (5.97)$$

---

<sup>12</sup>Here we assume that the  $z$ -coordinates of both sections are  $z = 1$ , for simplicity.



Instead of using these polynomials, we will use two slightly modified polynomials that generate the same ideal. They were defined in [34] where they were denoted by  $\delta g'_6$  and  $g'_9$  and defined as

$$\delta(g_2^{QS})' := \tilde{s}_7 \tilde{s}_8^2 + \tilde{s}_9(-\tilde{s}_6 \tilde{s}_8 + \tilde{s}_5 \tilde{s}_9) = 0, \quad (g_3^{QS})' := \tilde{s}_3 \tilde{s}_8^2 - \tilde{s}_2 \tilde{s}_8 \tilde{s}_9 + \tilde{s}_1 \tilde{s}_9^2 = 0, \quad (5.98)$$

Here we have to use the map (5.30) to obtain these polynomials in terms of the coefficients  $s_i$ . We will see in section 5.3.3 that these polynomials are crucial to obtain the matter multiplicities of this type of charged matter fields.

Similarly, for matter charged under  $U(1)_R \times U(1)_S$  we demand

$$\delta g_2^{RS} := g_2^S - (\tilde{z}^S)^2 g_2^R \stackrel{!}{=} 0, \quad g_3^S = 0, \quad \hat{g}_4^S = 0. \quad (5.99)$$

For this type of locus we will also use the modified polynomials  $\delta(g_2^{RS})'$  and  $\delta(g_3^{RS})'$  that can be obtained from (5.98) by replacing all the coefficients  $\tilde{s}_i \rightarrow \hat{s}_i$  and by using (5.36).

Next, we look for matter charged under all  $U(1)$  factors  $U(1)_Q \times U(1)_R \times U(1)_S$ . This requires the three sections to collide and pass through the singular point  $y = 0$  in the WSF, at codimension two. The four polynomials that are required to vanish simultaneously are

$$\delta g_2^{QS} = 0, \quad (\tilde{z}^S)^2 \delta g_2^{RS} = 0, \quad g_3^S = 0, \quad \hat{g}_4^S = 0, \quad (5.100)$$

where the first two conditions enforce a collision of the three sections in the elliptic fiber. In order for a codimension two locus to satisfy all these constraints simultaneously, all the polynomials (5.100) should factor as

$$p = h_1 p_1 + h_2 p_2, \quad (5.101)$$

where  $h_1$  and  $h_2$  are the polynomials whose zero-locus defines the codimension two locus in question. To obtain the polynomials we use the Euclidean algorithm twice. We first divide all polynomials in (5.100) by the lowest order polynomial available, which is  $\delta g_2^{QR}$  and take the biggest common factor from all residues. This is the polynomial  $h_1$  and it reads

$$\begin{aligned}
h_1 = & (s_{10}^2 s_{15} s_{16} s_{19} + s_{10}^2 s_{12} s_{19}^2 + s_{10} s_{15} s_{18} s_{19} s_5 + s_{10} s_{17} s_{19}^2 s_5 - s_{10} s_{16} s_{19} s_{20} s_5 \\
& - s_{18} s_{19} s_{20} s_5^2 - s_{10} s_{15}^2 s_{18} s_9 - s_{10} s_{15} s_{17} s_{19} s_9 - s_{10} s_{15} s_{16} s_{20} s_9 - 2 s_{10} s_{12} s_{19} s_{20} s_9 \\
& + s_{15} s_{18} s_{20} s_5 s_9 - s_{17} s_{19} s_{20} s_5 s_9 + s_{16} s_{20}^2 s_5 s_9 + s_{15} s_{17} s_{20} s_9^2 + s_{12} s_{20}^2 s_9^2). \quad (5.102)
\end{aligned}$$

The knowledge of  $h_1$  allows us to repeat the Euclidean algorithm. We reduce the polynomials (5.100) by (5.102) and again obtain the second common factor from the residues of all polynomials reading

$$\begin{aligned}
h_2 = & s_{10}^2 s_{19} (s_{15} s_{16} + s_{12} s_{19}) - s_{10} [s_{15}^2 s_{18} s_9 + s_{19} (-s_{17} s_{19} s_5 + s_{16} s_{20} s_5 + 2 s_{12} s_{20} s_9) \\
& + s_{15} (-s_{18} s_{19} s_5 + s_{17} s_{19} s_9 + s_{16} s_{20} s_9)] + s_{20} [s_{18} s_5 (-s_{19} s_5 + s_{15} s_9) \\
& + s_9 (-s_{17} s_{19} s_5 + s_{16} s_{20} s_5 + s_{15} s_{17} s_9 + s_{12} s_{20} s_9)]. \quad (5.103)
\end{aligned}$$

To confirm that these polynomials define the codimension two locus we were looking for, we check that all the constraints (5.100) are in the ideal generated by  $\langle h_1, h_2 \rangle$ .

Finally, if there are no more smaller ideals, i.e. special solutions, of  $g_3^m = \hat{g}_4^m = 0$  we expect its remaining solutions to be generic and to support matter charged under only the section  $\hat{s}_m$ , i.e. matter with charges  $q_m = 1$ , and  $q_n = 0$  for  $n \neq m$ . In summary, we find that

matter at a generic point of the following loci has the following charges,

Generic point in locus	$q_Q$	$q_R$	$q_S$
$g_2^{QR} = g_3^Q = 0$	1	1	0
$(g_2^{QS})' = (g_3^S)' = 0$	1	0	1
$(g_2^{RS})' = (g_3^S)' = 0$	1	0	1
$h_1 = h_2 = 0$	1	1	1
$g_3^Q = \hat{g}_4^Q = 0$	1	0	0
$g_3^R = \hat{g}_4^R = 0$	0	1	0
$g_3^S = \hat{g}_4^S = 0$	0	0	1

(5.104)

In each of these six cases we checked explicitly the factorization of the complete intersection (5.27) for  $\mathcal{E}$  into an  $I_2$ -curve, then computed the intersections of the sections  $\hat{s}_P, \hat{s}_m$ ,  $m = Q, R, S$  and obtained the charges by applying the charge formula (5.73).

### 5.3.3 6D Matter Multiplicities and Anomaly Cancellation

In this section we specialize to six-dimensional F-theory compactifications on an elliptically fibered Calabi-Yau threefolds  $\hat{X}_3$  over a general two-dimensional base  $B$  with generic elliptic fiber given by (5.16). We work out the spectrum of charged hypermultiplets, that transform in the 14 different singlet representations found in sections 5.3.1 and 5.3.2. To this end, we compute the explicit expressions for the multiplicities of these 14 hypermultiplets. We show consistency of this charged spectrum by checking anomaly-freedom.

The matter multiplicities are given by the homology class of the irreducible locus that supports a given matter representation. As discussed above, some of these irreducible matter loci can only be expressed as prime ideals, of which we can not directly compute the homology classes. Thus, we have to compute matter multiplicities successively, starting

from the complete intersections  $\text{Loc}_{\text{CI}}$  in (5.104) that support multiple matter fields of different type. We found, that at the generic point of the complete intersection  $\text{Loc}_{\text{CI}}$  one type of matter is supported, but at special points  $\text{Loc}_s^i$  different matter fields are located. We summarize this as

$$\cup_i \text{Loc}_s^i \subset \text{Loc}_{\text{CI}}. \quad (5.105)$$

Thus, first we calculate all multiplicities of matter located at all these special loci  $\text{Loc}_s^i$  and then subtract them from the complete intersection  $\text{Loc}_{\text{CI}}$  in which they are contained with a certain degree. This degree is given by the order of vanishing of resultant, that has already been used in a similar context in [34]. It is defined as follows. Given two polynomials  $(r, s)$  in the variables  $(x, y)$ , if  $(0, 0)$  is a zero of both polynomials, its degree is given by the order of vanishing of the resultant  $h(y) := \text{Res}_x(r, s)$  at  $y = 0$ .

This is a straightforward calculation when the variables  $(x, y)$  are pairs of the coefficients  $s_i$ . However, for more complicated loci we will need to treat full polynomials  $(p_1, p_2)$  as these variables, for example  $x = \tilde{s}_7, y = \tilde{s}_9$  or  $x = \delta g_6, y = g_9$ . In this case we have to solve for two coefficients  $s_i, s_j$  from  $\{p_1 = x, p_2 = y\}$ , then replace them in  $(r, s)$  and finally proceed to take the resultant in  $x$  and  $y$ .

There is one technical caveat, when we are considering polynomials  $(p_1, p_2)$  that contain multiple different matter multiplets. We choose the coefficients  $s_i, s_j$  in such a way that the variables  $(x, y)$  only parametrize the locus of the hypermultiplets we are interested in. This is achieved by choosing  $s_i, s_j$  we are solving for so that the polynomials of the locus we are *not* interested in appear as denominators and are, thus, forbidden. For example, let us look at the loci  $|M_3^Q| = |M_3^P| = 0$ . This complete intersection contains the loci of the hypermultiplets with charges  $(0, 0, 2)$  at the generic point and with charges  $(0, 1, 2)$  at the special locus  $s_9 = s_{19} = 0$ , c.f. (5.82), respectively, (5.93). Let us focus on the former

hypermultiplets. We set

$$|M_3^O| = s_{18}s_9 - s_{19}s_8 \equiv x, \quad |M_3^P| = s_{10}s_{19} - s_{20}s_9 \equiv y, \quad (5.106)$$

and solve for  $s_8$  and  $s_{20}$  to obtain

$$s_8 = \frac{(s_{18}s_9 - x)}{s_{19}}, \quad s_{20} = \frac{(s_{10}s_{19} + y)}{s_9}. \quad (5.107)$$

From this, it is clear the locus  $s_9 = s_{19} = 0$  corresponding to hypermultiplets with charges  $(0, 1, 2)$  is excluded because of the denominators. Thus,  $(x, y)$  indeed parametrize the locus of the hypermultiplets of charges  $(0, 0, 2)$ .

We begin the computation of multiplicities with the simplest singularities in 5.3.1 located at the vanishing-loci of two coefficients  $s_i = s_j = 0$ . Their multiplicities are directly given by their homology classes, that are simply the product of the classes  $[s_i], [s_j]$ . We obtain

Loci	$q_Q$	$q_R$	$q_S$	Multiplicity
$s_8 = s_{18} = 0$	1	1	-1	$[s_8] \cdot [s_{18}]$
$s_9 = s_{19} = 0$	0	1	2	$[s_9] \cdot [s_{19}]$
$s_{10} = s_{20} = 0$	1	0	2	$[s_{10}] \cdot [s_{20}]$

(5.108)

Next we proceed to calculate the multiplicities of the loci given by the vanishing of three minors given in (5.93). The most direct way of obtaining these multiplicities is by using the Porteous formula to obtain the first Chern class of a determinantal variety. However, we will use here a simpler approach that yields the same results.

It was noted in section 5.3.1, that the locus described by the vanishing of the three minors can be equivalently represented as the vanishing of only two minors, after excluding the zero locus from the vanishing of the two coefficients  $s_i, s_j$  that appear in both two minors. Thus, the multiplicities can be calculated by multiplying the homology classes of

the two minors and subtracting the homology class  $[s_i] \cdot [s_j]$  of the locus  $s_i = s_j = 0$ .

For example the multiplicity of the locus  $|M_3^Q| = |M_2^Q| = |M_1^Q| = 0$  can be obtained from multiplying the classes of  $|M_3^Q| = |M_1^Q| = 0$  and subtracting the multiplicity of the locus  $s_8 = s_{18} = 0$  that satisfies these two equations, but not  $M_2^Q = -s_6 s_{19} + s_9 s_{16}$ :

$$\begin{aligned} x_{(-1,0,1)} &= [|M_3^Q|] \cdot [|M_1^Q|] - [s_8] \cdot [s_{18}] \\ &= ([p_2]^b)^2 + [p_2]^b \cdot (\hat{\mathcal{S}}_7 + \tilde{\mathcal{S}}_7 - 3\tilde{\mathcal{S}}_9) + [K_B^{-1}] \cdot \tilde{\mathcal{S}}_7 + \tilde{\mathcal{S}}_7^2 - \hat{\mathcal{S}}_7 \cdot \mathcal{S}_9 - 2\tilde{\mathcal{S}}_7 \cdot \mathcal{S}_9 + 2\mathcal{S}_9^2, \end{aligned} \quad (5.109)$$

Here we denote the multiplicity of hypermultiplets with charge  $(q_Q, q_R, q_S)$  by  $x_{(q_Q, q_R, q_S)}$ , indicate homology classes of sections of line bundles by  $[\cdot]$ , as before, and employ (5.47), (5.30) and the divisors defined in (5.49) to obtain the second line. Calculating the other multiplicities in a similarly we obtain

Charges	Loci	Multiplicity
$(-1, 0, 1)$	$ M_3^Q  =  M_2^Q  =  M_1^Q  = 0$	$x_{(-1,0,1)} = [ M_1^Q ] \cdot [ M_3^Q ] - [s_8] \cdot [s_{18}]$
$(0, -1, 1)$	$ M_3^R  =  M_2^R  =  M_1^R  = 0$	$x_{(0,-1,1)} = [ M_1^R ] \cdot [ M_3^R ] - [s_8] \cdot [s_{18}]$
$(-1, -1, -2)$	$ M_3^P  =  M_2^P  =  M_1^P  = 0$	$x_{(-1,-1,-2)} = [ M_2^P ] \cdot [ M_3^P ] - [s_{10}] \cdot [s_{20}]$
$(0, 0, 2)$	$ M_3^P  =  M_3^Q  =  M_3^R  = 0$	$x_{(0,0,2)} = [ M_3^Q ] \cdot [ M_3^P ] - [s_{19}] [s_9]$

(5.110)

It is straightforward but a bit lengthy to use (5.47) in combination with (5.30), (5.36) to obtain, as demonstrated in (5.109), the expressions for the multiplicities of all these matter fields explicitly. We have shown one possible way of calculating the multiplicities in (5.110), i.e. choosing one particular pair of minors. We emphasize that the same results for the multiplicities can be obtained by picking any other the possible pairs of minors.

Finally we calculate the hypermultiplets of the matter found in the WSF, as discussed in section 5.3.2. In each case, in order to calculate the multiplicity of the matter located at a generic point of the polynomials (5.104) we need to first identify all the loci, which

solve one particular constraint in (5.104), but support other charged hypermultiplets. Then, we have to find the respective orders of vanishing of the polynomial in (5.104) at these special loci using the resultant technique explained below (5.105). Finally, we compute the homology class of the complete intersection under consideration in (5.104) subtract the homology classes of the special loci with their appropriate orders.

We start with the matter with charges  $(1, 1, 1)$  in (5.104) which is located at a generic point of the locus  $h_1 = h_2 = 0$ . In this case, the degree of vanishing of the other loci are given by

Charge	$x_{(1,1,-1)}$	$x_{(0,1,2)}$	$x_{(1,0,2)}$	$x_{(-1,0,1)}$	$x_{(0,-1,1)}$	$x_{(-1,-1,-2)}$	$x_{(0,0,2)}$
$(1, 1, 1)$	0	1	1	0	0	4	0

(5.111)

Here we labeled the loci that are contained in  $h_1 = h_2 = 0$  by the multiplicity of matter which supported on them. We note that the other six matter fields in (5.104) do not appear in this table, because the matter with charges  $(1, 1, 1)$  is contained in their loci, as we demonstrate next. This implies that the multiplicity of the hypermultiplets with charge  $(1, 1, 1)$  is given by

$$\begin{aligned}
x_{(1,1,1)} &= [h_1] \cdot [h_2] - x_{(0,1,2)} - x_{(1,0,2)} - 4x_{(-1,-1,-2)}, \\
&= 4[K_B^{-1}]^2 - 3([p_2]^b)^2 - 2[K_B^{-1}] \cdot \hat{\mathcal{S}}_7 - 3([p_2]^b) \cdot \hat{\mathcal{S}}_7 - 2[K_B^{-1}] \cdot \tilde{\mathcal{S}}_7 - 3([p_2]^b) \cdot \tilde{\mathcal{S}}_7 \\
&\quad - 2\hat{\mathcal{S}}_7 \cdot \tilde{\mathcal{S}}_7 + 2[K_B^{-1}] \mathcal{S}_9 + 9([p_2]^b) \mathcal{S}_9 + 5\hat{\mathcal{S}}_7 \cdot \mathcal{S}_9 + 5\tilde{\mathcal{S}}_7 \cdot \mathcal{S}_9 - 8\mathcal{S}_9^2, \quad (5.112)
\end{aligned}$$

where the first term is the class of the complete intersection  $h_1 = h_2 = 0$  and the three following terms are the necessary subtractions that follow from (5.111). The homology classes of  $h_1, h_2$  can be obtained by determining the class of one term in (5.102), respectively, (5.103) using (5.47).

Proceeding in a similar way for the hypermultiplets with charges  $(1, 0, 1), (0, 1, 1)$

and  $(1, 1, 0)$  we get the following orders of vanishing of the loci supporting the remaining matter fields:

Charges	$x_{(1,1,-1)}$	$x_{(0,1,2)}$	$x_{(1,0,2)}$	$x_{(-1,0,1)}$	$x_{(0,-1,1)}$	$x_{(-1,-1,-2)}$	$x_{(0,0,2)}$	$x_{(1,1,1)}$
$(1, 0, 1)$	0	0	4	0	0	4	0	1
$(0, 1, 1)$	0	4	0	0	0	4	0	1
$(1, 1, 0)$	1	0	0	0	0	1	0	1

(5.113)

We finally obtain the multiplicities of these matter fields by computing the homology class of the corresponding complete intersection in (5.104) and subtracting the multiplicities the matter fields contained in these complete intersections with the degrees determined in (5.113). We obtain

$$\begin{aligned}
x_{(1,0,1)} &= 2[K_B^{-1}]^2 + 3([p_2]^b)^2 + 2[K_B^{-1}]\hat{\mathcal{S}}_7 + 3([p_2]^b)\hat{\mathcal{S}}_7 - 3[K_B^{-1}]\tilde{\mathcal{S}}_7 + 3([p_2]^b)\tilde{\mathcal{S}}_7 \\
&\quad + 2\hat{\mathcal{S}}_7\tilde{\mathcal{S}}_7 + \tilde{\mathcal{S}}_7^2 + 2[K_B^{-1}]\mathcal{S}_9 - 9([p_2]^b)\mathcal{S}_9 - 5\hat{\mathcal{S}}_7\mathcal{S}_9 - 4\tilde{\mathcal{S}}_7\mathcal{S}_9 + 6\mathcal{S}_9^2, \\
x_{(0,1,1)} &= 2[K_B^{-1}]^2 + 3([p_2]^b)^2 - 3[K_B^{-1}]\hat{\mathcal{S}}_7 + 3([p_2]^b)\hat{\mathcal{S}}_7 + \hat{\mathcal{S}}_7^2 + 2[K_B^{-1}]\tilde{\mathcal{S}}_7 \\
&\quad + 3([p_2]^b)\tilde{\mathcal{S}}_7 + 2\hat{\mathcal{S}}_7\tilde{\mathcal{S}}_7 + 2[K_B^{-1}]\mathcal{S}_9 - 9([p_2]^b)\mathcal{S}_9 - 4\hat{\mathcal{S}}_7\mathcal{S}_9 - 5\tilde{\mathcal{S}}_7\mathcal{S}_9 + 6\mathcal{S}_9^2, \\
x_{(1,1,0)} &= 2[K_B^{-1}]^2 + 3([p_2]^b)^2 + 2[K_B^{-1}]\hat{\mathcal{S}}_7 + 3([p_2]^b)\hat{\mathcal{S}}_7 + 2[K_B^{-1}]\tilde{\mathcal{S}}_7 + 3([p_2]^b)\tilde{\mathcal{S}}_7 \\
&\quad + \hat{\mathcal{S}}_7\tilde{\mathcal{S}}_7 - 3[K_B^{-1}]\mathcal{S}_9 - 9([p_2]^b)\mathcal{S}_9 - 4\hat{\mathcal{S}}_7\mathcal{S}_9 - 4\tilde{\mathcal{S}}_7\mathcal{S}_9 + 7\mathcal{S}_9^2. \tag{5.114}
\end{aligned}$$

Finally for the hypermultiplets of charges  $(1, 0, 0)$ ,  $(0, 1, 0)$  and  $(0, 0, 1)$  we obtain the following degrees of vanishing of the loci supporting the other matter fields:

Charges	$x_{(1,1,-1)}$	$x_{(0,1,2)}$	$x_{(1,0,2)}$	$x_{(-1,0,1)}$	$x_{(0,-1,1)}$	$x_{(-1,-1,-2)}$	$x_{(0,0,2)}$	$x_{(1,0,1)}$	$x_{(0,1,1)}$	$x_{(1,1,0)}$	$x_{(1,1,1)}$
$(1, 0, 0)$	1	0	1	1	0	1	0	1	0	1	1
$(0, 1, 0)$	1	1	0	0	1	1	0	0	1	1	1
$(0, 0, 1)$	1	16	16	1	1	16	16	1	1	0	1

(5.115)



Again we first computing the homology class of the complete intersection in (5.104) supporting the hypermultiplets with charges  $(1, 0, 0)$ ,  $(0, 1, 0)$ , respectively,  $(0, 0, 1)$  and subtracting the multiplicities the matter fields contained in these complete intersections with the degrees determined in (5.115). We obtain

$$\begin{aligned}
x_{(1,0,0)} &= 4[K_B^{-1}]^2 - 3([p_2]^b)^2 - 2[K_B^{-1}]\hat{\mathcal{S}}_7 - 3([p_2]^b)\hat{\mathcal{S}}_7 + 2[K_B^{-1}]\tilde{\mathcal{S}}_7 - 3([p_2]^b)\tilde{\mathcal{S}}_7 \\
&\quad - \hat{\mathcal{S}}_7\tilde{\mathcal{S}}_7 - 2\tilde{\mathcal{S}}_7^2 - 2[K_B^{-1}]\mathcal{S}_9 + 9([p_2]^b)\mathcal{S}_9 + 4\hat{\mathcal{S}}_7\mathcal{S}_9 + 5\tilde{\mathcal{S}}_7\mathcal{S}_9 - 6\mathcal{S}_9^2, \\
x_{(0,1,0)} &= 4[K_B^{-1}]^2 - 3([p_2]^b)^2 + 2[K_B^{-1}]\hat{\mathcal{S}}_7 - 3([p_2]^b)\hat{\mathcal{S}}_7 - 2\hat{\mathcal{S}}_7^2 - 2[K_B^{-1}]\tilde{\mathcal{S}}_7 \\
&\quad - 3([p_2]^b)\tilde{\mathcal{S}}_7 - \hat{\mathcal{S}}_7\tilde{\mathcal{S}}_7 - 2[K_B^{-1}]\mathcal{S}_9 + 9([p_2]^b)\mathcal{S}_9 + 5\hat{\mathcal{S}}_7\mathcal{S}_9 + 4\tilde{\mathcal{S}}_7\mathcal{S}_9 - 6\mathcal{S}_9^2, \\
x_{(0,0,1)} &= 4[K_B^{-1}]^2 - 4([p_2]^b)^2 + 2[K_B^{-1}]\hat{\mathcal{S}}_7 - 4([p_2]^b)\hat{\mathcal{S}}_7 - 2\hat{\mathcal{S}}_7^2 + 2[K_B^{-1}]\tilde{\mathcal{S}}_7 - 4([p_2]^b)\tilde{\mathcal{S}}_7 \\
&\quad - 2\hat{\mathcal{S}}_7\tilde{\mathcal{S}}_7 - 2\tilde{\mathcal{S}}_7^2 + 2[K_B^{-1}]\mathcal{S}_9 + 12([p_2]^b)\mathcal{S}_9 + 6\hat{\mathcal{S}}_7\mathcal{S}_9 + 6\tilde{\mathcal{S}}_7\mathcal{S}_9 - 10\mathcal{S}_9^2.
\end{aligned}$$

We conclude by showing that the spectrum of the theory we have calculated is anomaly-free, which serves also as a physically motivated consistency check for the completeness of analysis of codimension two singularities presented in sections 5.3.1 and 5.3.2. We refer to [45, 66] for a general account on anomaly cancellation and to [105, 97, 34] for the explicit form of the anomaly cancellation conditions adapted to the application to F-theory, c.f. for example Eq. (5.1) in [34]. Indeed, we readily check that the spectrum (5.108), (5.110), (5.112), (5.114) and (5.116) together with the height pairing matrix  $b_{mn}$  reading

$$b_{mn} = -\pi(\sigma(\hat{s}_m) \cdot \sigma(\hat{s}_n)) = \begin{pmatrix} -2[K_B] & -[K_B] & \mathcal{S}_9 - \tilde{\mathcal{S}}_7 - [K_B] \\ -[K_B] & -2[K_B] & \mathcal{S}_9 - \hat{\mathcal{S}}_7 - [K_B] \\ \mathcal{S}_9 - \hat{\mathcal{S}}_7 - [K_B] & \mathcal{S}_9 - \tilde{\mathcal{S}}_7 - [K_B] & 2(\mathcal{S}_9 - [K_B]) \end{pmatrix}_{mn} \quad (5.116)$$

with  $m, n = 1, 2, 3$  all mixed gravitational-Abelian and purely-Abelian anomalies in Eq. (5.1) of [34] are canceled.

# Compactifications on all Toric Hypersurface Fibrations

By now, we have learned that the ambient space of the elliptic fiber has direct implication on the low energy physics of the F-theory compactifications. We learned that the elliptic fibrations with fibers in  $dP_2$  give  $U(1)^2$  theories and fibers in  $B\mathbb{P}^3$  generate  $U(1)^3$  gauge groups. That points to the following line of study: take a list of fiber ambient spaces, build elliptic fibrations with them and study the low energy theory of the compactifications. The natural question is: what list should we use? Well, that is the hard part. However, toric geometry has been around with us, both  $dP_2$  and  $B\mathbb{P}^3$  are toric geometries. Also this set of varieties are finite and easy to construct.

Thus, in this chapter, we build elliptic fibrations using all 2D toric spaces as ambient spaces, the 16 of them, and study their low energy physics: gauge group, matter content and Yukawa couplings. We chose the 2D toric varieties only because the number of 3D toric geometries is too big, already in the order of thousands.

We take the content of this chapter from [80]. The author of this dissertation is a co-author of the mentioned article.

In the months previous to the appearance of this work, interest on genus one compactification surged in the F-theory community. The papers that rekindled the interest were [18], [3] and [99], with a few more following. What is interesting about these genus one curves is that they do not possess a zero point, thus the fibration does not have a section. To circumvent this problem, in [18] the authors use a closely related curve to the original one, a curve that actually possesses a zero point: the Jacobian of the original curve. And things get more interesting. There are different curves that have the same Jacobian, then, there are multiple genus fibrations with exactly the same jacobian fibration. Can we make sense of the low energy physics? Surprisingly, the answer is Yes. The key insights came from [3] and [99], where they show that the multiple geometries are tightly related to the appearances of discrete symmetries.

The machinery developed to study Jacobian fibrations is fundamental for this chapter and the study of all 2D toric fibrations. In fact there are three toric geometries that do not have sections, then we have to study them using their Jacobians. Not surprisingly, we find discrete symmetries in those cases.

Besides the discrete symmetries, and almost by accident, we find for the first time charge three matter under  $U(1)$ . Explicit geometries with this matter content, to the best of our knowledge, had never been constructed. We also find a web of relations between the different geometries that can be understood from field theory as the Higgs mechanism and from the geomtric point of view as conifold transitions.

The article [80] is 120 pages, single spaced. Copying the entire document here will make this dissertation unnecessarily long. Thus, we decided to cherry-pick only some sections of the article and invite the interested reader to the original source for more details.

## 6.1 Introduction & Summary of Results

We study all F-theory compactifications on Calabi-Yau manifolds  $X_{F_i}$  with genus-one fiber  $\mathcal{C}_{F_i}$  given as a hypersurface in the toric varieties associated to the 16 2D reflexive polyhedra, denoted by  $F_i$ ,  $i = 1, \dots, 16$ .<sup>1</sup> We refer to these Calabi-Yau manifolds as *toric hypersurface fibrations*. We determine the generic and intrinsic features of these  $X_{F_i}$  that are relevant to F-theory: the generic gauge group, the corresponding matter spectrum and the 4D Yukawa couplings corresponding to the codimension one, two and three singularities of  $X_{F_i}$ . These geometric results completely determine the 6D and non-chiral 4D SUGRA theories obtained by compactifying F-theory on Calabi-Yau threefolds and fourfolds without  $G_4$ -flux. We prove completeness of our analysis of codimension one and two singularities by checking cancellation of all 6D anomalies. All these results are base-independent in the sense that they follow directly from the geometry of the fiber  $\mathcal{C}_{F_i}$ . The only dependence on the base  $B$  enters through the choice of two divisors on  $B$  that label the possible Calabi-Yau fibrations of  $\mathcal{C}_{F_i}$  [34].

We highlight the following interesting geometrical findings of our analysis of F-theory on the Calabi-Yau manifolds  $X_{F_i}$ :

- Every  $X_{F_i}$  has an associated minimal gauge group  $G_{F_i}$  that is completely determined by the polyhedron  $F_i$ . In other words this gauge group is present without tuning the complex structure of  $X_{F_i}$  by means of Tate's algorithm [81, 112, 9] (see [75, 87] for recent refinements) or upon addition of tops. The gauge groups  $G_{F_i}$  and  $G_{F_i^*}$  associated to  $F_i$  and its dual polyhedron  $F_i^*$  obey the rank relation

$$\text{rk}(G_{F_i}) + \text{rk}(G_{F_i^*}) = 6. \quad (6.1)$$

---

<sup>1</sup>These genus-one curves have also been used in [67, 68] as mirror curves for the computation of refined stable pair invariants in the refined topological string.

- We consider three Calabi-Yau manifolds  $X_{F_i}$ ,  $i = 1, 2, 4$ , without section. Their fibers are the general cubic in  $\mathbb{P}^2$ , the general biquadric in  $\mathbb{P}^1 \times \mathbb{P}^1$  and the general quartic in  $\mathbb{P}^2(1, 1, 2)$ , respectively, where the latter is also studied in [18, 99, 3]. The fibrations  $X_{F_i}$ ,  $i = 1, 2, 4$ , only have a genus-one fibration with a three-, a two- and a two-section, respectively. As a direct consequence of this absence of sections, F-theory has discrete gauge group factors given by  $\mathbb{Z}_3$ ,  $\mathbb{Z}_2$  and  $\mathbb{Z}_4$ , respectively. We show that these Calabi-Yau manifolds, most notably the fibration of the cubic,  $X_{F_1}$ , have  $I_2$ -fibers at codimension two that support singlet matter with charge 1 under the respective discrete gauge groups. We explain how the charge of all matter fields under these discrete groups are computed from the intersections of the multi-sections with the relevant codimension two fibers.
- We show that both  $X_{F_2}$  and  $X_{F_3}$  give rise to one  $U(1)$ -factor, namely  $G_{F_2} = U(1) \times \mathbb{Z}_2$  and  $G_{F_3} = U(1)$ . To this end, we show that unlike  $X_{F_2}$ , the Weierstrass form of the Jacobian  $J(X_{F_2})$  has one rational section, whereas already  $X_{F_3}$  has two sections: a toric and a non-toric one. In both cases, we determine the coordinates of all sections explicitly.
- For the first time, we find F-theory compactifications with matter of  $U(1)$ -charge three. This matter is supported at a codimension two locus of  $X_{F_3}$  with an  $I_2$ -fiber where both the zero section and the non-toric rational section are ill-behaved and each “wrap” one irreducible fiber component.

We note that the 16 toric hypersurface fibrations  $X_{F_i}$  were considered in [19], were a thorough classification of their toric MW-groups was carried out. Further specializations of the  $X_{F_i}$  corresponding to toric tops [22, 15] (see [85] for a systematic approach based on Tate’s algorithm for elliptic fibers in  $\text{Bl}_1\mathbb{P}^2(1, 1, 2)$ ) permitted the engineering of toric F-theory models with certain gauge groups, in particular with an  $SU(5)$  GUT-group. Some

4D examples of chiral SU(5) GUTs were constructed in this manner [30, 14]. Since we determine here the intrinsic gauge groups and the non-toric MW-groups, as well as the full matter spectrum and the Yukawa couplings of  $X_{F_i}$ , our approach is complementary to these previous works.

We have to remark that none of the fibrations  $X_{F_i}$  yield an SU(5) gauge factor in their low-energy effective theories. Hence, strictly speaking, the intrinsic gauge symmetries associated to the toric hypersurface fibrations do not suffice to engineer SU(5) F-theory GUTs. There are, however, some arguments that challenge the simplest GUT picture in F-theory, and therefore, draw our attention towards alternative schemes which may be promising for particle physics models. In this spirit, we would like to briefly highlight some of the effective theories we obtain, which can potentially be used to construct promising particle physics models in F-theory. We find models with discrete symmetries and up to three U(1) factors. These additional symmetries can be used in order to forbid dangerous operators which would render the theory incompatible with observations, e.g. by mediating fast proton decay. In addition, we observe theories with interesting gauge groups and spectra. In fact,  $X_{F_{11}}$  precisely leads to an effective theory with the Standard Model gauge group and the usual representations<sup>2</sup>, and we further identify the trinification group for  $X_{F_{16}}$  as well as the Pati-Salam group for  $X_{F_{13}}$ . As we demonstrate explicitly, the matter spectra we obtain are very close to those one usually has in both of these theories.

In this paper we also work out the entire network of Higgsings relating the effective theories of F-theory on the toric hypersurface fibrations  $X_{F_i}$ . It is well-known that the toric varieties corresponding to the 16 2D reflexive polyhedra  $F_i$  are related by blow-downs. Consequently, the Calabi-Yau manifolds  $X_{F_i}$  are related by the extremal transitions induced by these birational maps and a subsequent toric complex structure deformation. These transitions can be understood as Higgsings in the effective SUGRA theories arising from

---

<sup>2</sup>See [88] for a different realization of a standard model like theory based on tops of  $X_{F_3}$ .

F-theory on the  $X_{F_i}$ : given two polyhedra  $F_i$  and  $F_{i'}$  related by a blow-down as  $F_i \rightarrow F_{i'}$ , we explicitly determine the Higgsing that relates the effective theory of F-theory on  $X_{F_i}$  to that on  $X_{F_{i'}}$ . The resulting diagram of all those Higgsings is given in Figure 6.1. Since this

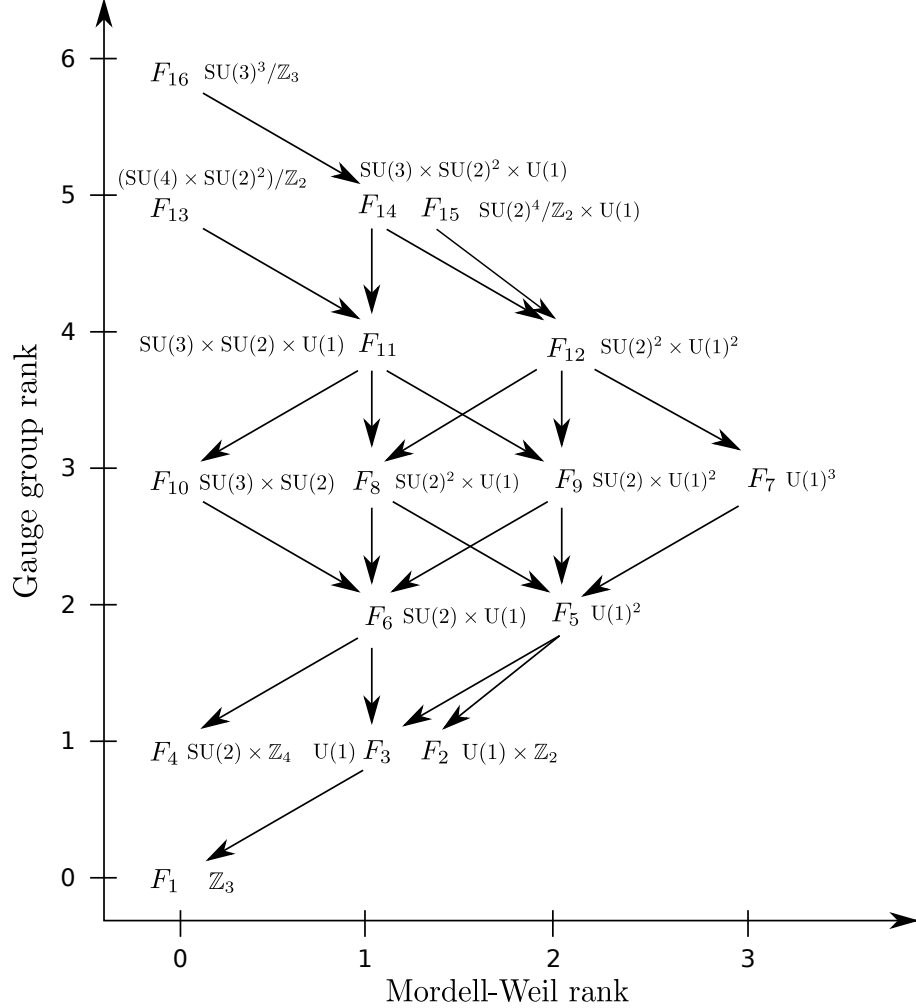


Figure 6.1: The network of Higgsings between all F-theory compactifications on toric hypersurface fibrations  $X_{F_i}$ . The axes show the rank of the MW-group and the total rank of the gauge group of  $X_{F_i}$ . Each Calabi-Yau  $X_{F_i}$  is abbreviated by  $F_i$  and its corresponding gauge group is shown. The arrows indicate the existence of a Higgsing between two Calabi-Yau manifolds.

chain of Higgsings is only a sub-branch of the full Higgs branch of the effective SUGRA theories of F-theory on  $X_{F_i}$ , we refer to it as the *toric Higgs branch*. We check that both the charged and the neutral spectrum of the SUGRA theories in 6D match. This involves the

computation of the number of neutral hyper multiplets, that in turn can be obtained from the Euler numbers of all  $X_{F_i}$ , which we also compute explicitly.

We point out some interesting observations about the Higgsing diagram in Figure 6.1:

- All effective theories can be obtained by appropriately Higgsing the theories with maximal gauge groups and matter spectra obtained from F-theory on  $X_{F_i}$ ,  $i = 13, 15, 16$ . We note that these are precisely the theories with non-trivial Mordell-Weil torsion.
- The network of Higgsings is symmetric around the horizontal line where the total rank of the gauge group is 3. Reflection along this line exchanges the polyhedron with its dual. This symmetry of Figure 6.1 reflects the rank condition (6.1). We emphasize that this symmetry maps theories with discrete gauge groups to theories with non-simply connected group, suggesting that multi-sections are somehow “dual” to MW-torsion.
- The three theories with discrete gauge groups arise by Higgsing theories with U(1)’s. It is also remarkable that all discrete symmetries found are surviving remnants of U(1) symmetries. It seems that discrete symmetries in F-theory are automatically in agreement with the early observation [82, 5, 72] that in a consistent theory of gravity, discrete global symmetries must be always embeddable into a local continuous symmetry.
- The toric Higgsings cannot change the rank of the F-theory gauge group by more than 1. This explains why there are no arrows with slope below 45 degrees.

This rest of this chapter is organized as follows. Section 6.2 contains a summary of the geometry of Calabi-Yau manifolds constructed as genus-one fibrations and the physics of F-theory compactified on them. We also present a basic account on toric geometry.



In Section 6.3 we discuss the construction and the different types of toric hypersurface fibrations  $X_{F_i}$ . Their codimension one, two and three singularities are analyzed, and the number of their complex structure moduli is computed. The F-theory gauge group, matter spectrum and Yukawa couplings are extracted from these results.

## 6.2 Geometry & Physics of F-theory Backgrounds

In this section, we summarize the key geometrical properties of Calabi-Yau manifolds  $X$  that are genus-one fibrations over a base  $B$  which are relevant for the study of F-theory compactifications, see Sections 6.2.1 and 6.2.2. The structure of the 6D effective SUGRA theories obtained by compactifying F-theory on these manifolds is discussed in Section 6.2.3. Since we study in this work Calabi-Yau manifolds  $X$  with their genus-one fibers realized as toric hypersurfaces, we introduce the necessary elements of toric geometry in Section 6.2.4.

Readers familiar with the tools and definitions presented here can safely skip this section and continue directly with Section 6.3.

### 6.2.1 Genus-one, Jacobian and elliptic fibrations with Mordell-Weil groups

We consider a smooth Calabi-Yau manifold  $\pi : X \rightarrow B$  with general fiber given by an algebraic curve  $\mathcal{C}$  of genus-one.  $\mathcal{C}$  is a non-singular curve defined over a field  $K$  that is not necessarily algebraically closed. In particular, we can think of the fibration  $X$  as an algebraic curve  $\mathcal{C}$  defined over the field  $K$  of meromorphic functions on the base  $B$ , which is clearly in general not algebraically closed. Thus, there are two qualitatively different situations to consider.

## Curves with points

First, if the curve  $\mathcal{C}$  has points with coordinates in  $K$ , then it is called an elliptic curve, which we denote by  $\mathcal{E}$ , and  $X$  is called an elliptic fibration. The points on  $\mathcal{E}$  form an Abelian group under addition: one point can be chosen as the zero point, denoted by  $P_0$ , and the additional points  $P_m$ ,  $m = 1, \dots, r$ , (more precisely the differences  $P_m - P_0$ ) are the generators of the Mordell-Weil group of rational points of  $\mathcal{E}$ . The Mordell-Weil theorem states that this group is finitely generated [111, 86]. Thus, it splits into a free part isomorphic to  $\mathbb{Z}^r$  and a torsion subgroup, where the latter has been fully classified for  $K = \mathbb{Q}$  by Mazur [95, 96], see [111] for a review.<sup>3</sup> Every point on  $\mathcal{E}$  gives rise to a section of the fibration  $X$ , i.e. rational maps from the base  $B$  into  $X$ . The section associated to  $P_0$  is the zero section, denoted by  $\hat{s}_0 : B \rightarrow X$ , and the  $r$  rational points  $P_m$  induce the rational sections  $\hat{s}_m : B \rightarrow X$ . The set  $\{\hat{s}_m\}$  can be seen to form a group, the MW-group of rational sections of  $X$ , by defining the addition of rational sections by addition of their corresponding points on  $\mathcal{E}$ . The free part of the MW-group gives rise to Abelian gauge symmetry in F-theory [101] and its torsion part yields non-simply connected gauge groups [4], see also [92] for a recent discussion of MW-torsion.

Every elliptic fibration  $X$  can be written in Weierstrass form (WSF) [103], i.e. as a hypersurface in the weighted projective bundle  $\mathbb{P}^{(1,2,3)}(\mathcal{O}_B \oplus \mathcal{L}^2 \oplus \mathcal{L}^3)$  over  $B$  of the form

$$y^2 = x^3 + fxz^4 + gz^6. \quad (6.2)$$

Here,  $\mathcal{O}_B$  is the trivial bundle on  $B$  and the line-bundle  $\mathcal{L}$  is fixed by the Calabi-Yau condition of  $X$  as  $\mathcal{L} = K_B^{-1}$ , with  $K_B$  denoting the canonical bundle of the base  $B$ . Then, the coefficients  $f$  and  $g$  have to be sections of  $K_B^{-4}$  and  $K_B^{-6}$ , respectively. The map from the canonical presentation of  $X$  inherited from the canonical presentation of the elliptic curve

---

<sup>3</sup>For the field of meromorphic functions on  $B$ , there are more torsion subgroups possible than for  $K = \mathbb{Q}$  [4].

$\mathcal{E}$  to the Weierstrass form (6.2) is birational. The zero section  $\hat{s}_0$  of  $X$  maps to the holomorphic zero section  $[z : x : y] = [0 : \lambda^2 : \lambda^3]$  in (6.2) and the rational sections  $\hat{s}_m$  map to rational sections in (6.2) with certain coordinates  $[z_{P_m} : x_{P_m} : y_{P_m}]$ , that are rational expressions in  $K$  (we can clear denominators to obtain holomorphic coordinates).

### Curves without points

Second, if the genus-one curve  $\mathcal{C}$  does not have a point, the fibration  $\pi : X \rightarrow B$  is without section. Such a fibration is referred to as a genus-one fibration [18]. Given a genus-one curve  $\mathcal{C}$ , one can construct an associated elliptic curve  $\mathcal{E} = J(\mathcal{C})$ , that is the Jacobian of the curve  $\mathcal{C}$ , i.e. the group of degree zero line bundles on  $\mathcal{C}$ . The zero point on  $J(\mathcal{C})$  is the trivial line bundle. Thus, there exists an elliptic fibration  $\pi : J(X) \rightarrow B$  associated to  $X$  with general fiber given by  $J(\mathcal{C})$ . This implies that  $J(X)$  can be represented as a Weierstrass model (6.2). Furthermore, it is a key property for F-theory that the  $\tau$ -function and the discriminant of  $X$  and  $J(X)$  are identical [18].

In this work, we consider concrete genus-one curves  $\mathcal{C}$  with  $K$ -rational divisors of degree  $n > 1$ , respectively.<sup>4</sup> The corresponding fibration  $X$  does not have a section, but an  $n$ -section, that we denote by  $\hat{s}^{(n)} : B \rightarrow X$ . Locally, at a point  $p$  on  $B$ , the function field  $K$  reduces to  $\mathbb{C}$  and the  $n$ -section  $\hat{s}^{(n)}$  maps  $p$  to  $n$  points in the fiber  $\mathcal{C}$ . Globally, however, upon moving around branch loci in  $B$  the individual points are exchanged by a monodromy action, so that only the collection of all  $n$  points together induce a well-defined divisor in  $X$ .

As we will see explicitly for concrete genus-one fibrations  $X$ , the map from  $X$  to the Weierstrass form (6.2) of  $J(X)$  can be obtained by an algebraic field extension  $L$  of  $K$ . This field extension is only necessary as an intermediate step, i.e. the final WSF (6.2) of  $J(X)$  is again defined over  $K$ . In Sections 6.4.1 and 6.4.2 we explicitly work out the maps from  $X$  to

---

<sup>4</sup>We expect that there always exists a degree  $n$  divisor on a given algebraic genus-one curve  $\mathcal{C}$ .

the WSF of their Jacobian fibrations  $J(X)$ , namely for the fibration of the cubic in  $\mathbb{P}^2$ , that has a three-section, and the two fibrations of the biquadric curve in  $\mathbb{P}^1 \times \mathbb{P}^1$  and the quartic curve in  $\mathbb{P}^2(1, 1, 2)$ , that both have a two-section.<sup>5</sup> We note that genus-one fibrations  $X$  by the quartic in  $\mathbb{P}^2(1, 1, 2)$  have been considered recently in an F-theory context in [18, 99, 3].

## 6.2.2 Divisors on genus-one fibrations and their intersections

In F-theory we are particularly interested in Calabi-Yau manifolds  $X$  that arise as a crepant resolution of singular genus-one or elliptic fibrations. These resolved manifolds exhibit three different classes of divisors, that we discuss in the following.

The first set of divisors on  $X$  is formed by the vertical divisors, i.e. divisors that arise as pullbacks of divisors on  $B$  under the projection map  $\pi : X \rightarrow B$ . Hence, there are  $h^{(1,1)}(B)$  such divisors on  $X$ . We denote the preimage under  $\pi$  of a vertical divisor  $D$  on  $X$  by  $D^b$  so that  $D = \pi^*(D^b)$ . Thus,  $D$  is a fibration of the curve  $\mathcal{C}$  (or its degenerations) over the base  $D^b$ .

The second class of divisors are the exceptional divisors of  $X$ . In more detail, if the discriminant  $\Delta = -16(4f^3 + 27g^2)$  of the WSF (6.2) of  $X$  or of its Jacobian  $J(X)$  vanishes to order higher than 1 at one of its irreducible components

$$\mathcal{S}_{G_I}^b := \{\Delta_I = 0\}, \quad I = 1, \dots, N, \quad (6.3)$$

in  $B$ , then the total space of the WSF is singular. These codimension one singularities are classified in [81, 112]. In the resolution  $X$  the fiber over each  $\mathcal{S}_{G_I}^b$  splits into a number of rational curves whose intersection pattern often agrees with the Dynkin diagram of a Lie group  $G_I$ .<sup>6</sup> The shrinkable irreducible components of the fiber at  $\mathcal{S}_{G_I}^b$  represent the simple roots of  $G_I$  and are denoted by  $c_{-\alpha_i}^{G_I}$  for  $i = 1, \dots, \text{rk}(G_I)$ . Thus,  $X$  has a set of exceptional

<sup>5</sup>These examples have been considered in the mathematics literature in [2].

<sup>6</sup>The fibers that do not have an associated group  $G_I$  are the unconventional fibers in Table 2 of [9].

divisors  $D_i^{G_I}$  given as the fibration of  $c_{-\alpha_i}^{G_I}$  over  $S_{G_I}^b$  for every  $I$ , to which we refer to as Cartan divisors of  $G_I$ . The  $D_i^{G_I}$  intersect the curves  $c_{-\alpha_i}^{G_I}$  as

$$D_i^{G_I} \cdot c_{-\alpha_j}^{G_J} = -C_{ij}^{G_I} \delta_{IJ}, \quad (6.4)$$

where  $C_{ij}^{G_I}$  denotes the Cartan matrix of  $G_I$ . The F-theory gauge group is then given by the product of all  $G_I$ , as discussed in Section 6.2.3.

Finally, the third class of divisors is induced by the independent sections and  $n$ -sections of the fibration of  $X$ . We denote the divisor classes of the zero section  $\hat{s}_0$  and the generators of the MW-group of rational sections  $\hat{s}_m$  by  $S_0$  and  $S_m$ , respectively. The class of a multi-section  $\hat{s}^{(n)}$  is denoted by  $S^{(n)}$ . Then, the intersections of these divisors with the fiber  $f \cong \mathcal{C}$ ,  $\mathcal{E}$  read

$$S_0 \cdot f = S_m \cdot f = \frac{1}{n} S^{(n)} \cdot f = 1. \quad (6.5)$$

The divisor classes that support Abelian gauge fields in F-theory [105, 97, 34], see also [58, 53, 57], are obtained from the Shioda map  $\sigma$  of the rational sections  $\hat{s}_m$ . To a given generator of the MW-group  $\hat{s}_m$  the Shioda map assigns the divisor

$$\sigma(\hat{s}_m) := S_m - S_0 + [K_B] - \pi(S_m \cdot S_0) + \sum_{I=1}^N (S_m \cdot c_{-\alpha_i}^{G_I}) (C_{G_I}^{-1})^{ij} D_j^{G_I}. \quad (6.6)$$

Here  $\pi(\cdot)$  denotes the projection of a codimension two variety in  $X$  to a divisor in the base  $B$  and  $[K_B]$  is the canonical bundle of  $B$ . The last term encodes contributions from non-Abelian gauge groups  $G_I$  in F-theory with  $(C_{G_I}^{-1})^{ij}$  denoting the inverse of the Cartan matrix  $C_{ij}^{G_I}$ .

The Shioda map (6.6) enables us to define the Néron-Tate height pairing of two rational

sections  $\hat{s}_m, \hat{s}_n$  as

$$\pi(\sigma(\hat{s}_m) \cdot \sigma(\hat{s}_n)) = \pi(S_m \cdot S_n) + [K_B] - \pi(S_m \cdot S_0) - \pi(S_n \cdot S_0) + \sum_I (\mathcal{C}_{G_I}^{-1})^{ij} (S_m \cdot c_{-\alpha_i}^{G_I}) (S_n \cdot c_{-\alpha_j}^{G_I}) S_{G_I}^b, \quad (6.7)$$

where  $\mathcal{C}_{ij}^{G_I}$  is the coroot matrix of  $G_I$ . We note that for evaluating this pairing in a concrete situation, the universal intersection relations

$$\pi(S_P^2 + [K_B^{-1}] \cdot S_P) = \pi(S_m^2 + [K_B^{-1}] \cdot S_m) = 0 \quad (6.8)$$

prove useful (cf. [97, 31, 34, 30] for details), whereas  $\pi(S_m \cdot S_n)$  and  $\pi(S_m \cdot S_0)$  are model-dependent.

We note that in F-theory both the vertical divisor (6.3) and the matrix (6.7) of vertical divisors enter the coefficients of the Green-Schwarz terms [105, 57, 31] and are thus essential for anomaly cancellation.

### 6.2.3 The spectrum of F-theory on genus-one fibrations

After the geometric preludes of sections 6.2.1 and 6.2.2, we are prepared to extract the spectrum of F-theory on a genus-one fibration  $X$ . The following discussion applies most directly to F-theory compactifications to 6D with effective theory given by an  $\mathcal{N} = (1, 0)$  SUGRA theory. However certain statements directly generalize to 4D F-theory vacua without  $G_4$ -flux.

For a more detailed derivation of some of the following results, that oftentimes require M-/F-theory duality, we refer [41, 53, 113] and references therein.

## Codimension one singularities

All vector fields and certain hyper multiplets in F-theory arise from the singularities of the WSF of  $X$  that are induced by codimension one singularities of its fibration. Over a given irreducible discriminant component  $\mathcal{S}_{G_I}^b$  defined in (6.3), the fiber of  $X$  is reducible. We assume that there is a Lie group  $G_I$  associated to this codimension one fiber of  $X$ . Then, the shrinkable holomorphic curves  $c_{-\alpha}^{G_I}$  in the fiber over  $\mathcal{S}_{G_I}^b$  represent all the positive roots of  $G_I$ . By quantization of the moduli space of an M2-brane wrapping such a curve  $c_{-\alpha}^{G_I}$  one finds BPS-states transforming in one charged vector multiplet and  $2g_I$  charged half-hyper multiplets with charge-vector  $-\alpha$  [117, 76]. Another vector multiplet and  $2g_I$  half-hyper multiplets with charges  $+\alpha$  are contributed by an M2-brane wrapping  $c_{-\alpha}^{G_I}$  with the opposite orientation. Here  $g_I$  is the genus of the curve  $\mathcal{S}_{G_I}^b$  in  $B$ , that is computed as

$$g_I = 1 + \frac{1}{2} \mathcal{S}_{G_I}^b \cdot (\mathcal{S}_{G_I}^b + [K_B]). \quad (6.9)$$

All these charged states become massless in the F-theory limit, when the volume of the class of the genus-one fiber of  $X$  is taken to zero. In this limit, these BPS-states fall into representations of the group  $G_I$  as follows.

First, we focus on the vector multiplets. All vector multiplets for every root  $\alpha$  of  $G_I$  are completed into one massless vector multiplet transforming in the adjoint representation  $\mathbf{adj}(G_I)$  of  $G_I$ . The additional vector multiplets are provided by the KK-reduction of the M-theory three-form  $C_3$  along the harmonic  $(1, 1)$ -forms in  $X$  that are dual to the Cartan divisor  $D_I^{G_I}$  of  $G_I$ . Thus, every irreducible component (6.3) of the discriminant with respective codimension one fiber classified by a Lie group  $G_I$ ,  $I = 1, \dots, N$ , gives rise to a  $G_I$  gauge symmetry in F-theory [101, 102, 9]. Furthermore, if  $X$  has a MW-group of rank  $r$ , there are additional  $(1, 1)$ -forms on  $X$ , which are the duals of the divisors (6.6), that give rise to vector multiplets of Abelian gauge groups [102]. Thus, the total gauge group  $G_X$  of

F-theory on  $X$  is

$$G_X = \mathrm{U}(1)^r \times \prod_{I=1}^N G_I. \quad (6.10)$$

This discussion and the results of Section 6.2.2 imply further that the rank of  $G_X$  can be directly computed in terms of the Hodge numbers  $h^{(1,1)}(X)$  and  $h^{(1,1)}(B)$  of  $X$  and  $B$ , respectively, as

$$\mathrm{rk}(G_X) = h^{(1,1)}(X) - h^{(1,1)}(B) - 1. \quad (6.11)$$

These results (6.10) and (6.11) hold in compactifications to eight<sup>7</sup>, six and four dimensions.

Second, we turn to the massless half-hyper multiplets over  $\mathcal{S}_{G_I}^b$ . In fact, also these fields are completed into the adjoint representation  $\mathbf{adj}(G_I)$  of  $G_I$ . In order to see this, we first note that there are neutral hyper multiplets induced by the complex structure moduli of  $X$ . Their total number, denoted by  $H_{\mathrm{neut}}$ , is computed by the Hodge number  $h^{(2,1)}(X)$  (or equivalently the Euler number  $\chi(X)$ ) of  $X$  as

$$H_{\mathrm{neut}} = h^{(2,1)}(X) + 1 = h^{(1,1)}(B) + 2 + \mathrm{rk}(G_X) - \frac{1}{2}\chi(X). \quad (6.12)$$

Then, for every group  $G_I$ , the  $2g_I$  half-hyper multiplets with charges  $-\alpha$  for all roots of  $G_I$  combine with  $g_I \cdot \mathrm{rk}(G_I)$  neutral hyper multiplets from (6.12) into  $g_I$  hyper multiplets in the adjoint  $\mathbf{adj}(G_I)$  of  $G_I$ . Thus, the number of hyper multiplets transforming in  $\mathbf{adj}(G_I)$  is given by (6.9) for every group  $G_I$ .

Let us emphasize that this discussion implies that  $h^{(2,1)}(X)$  contains information about the gauge groups  $G_I$  of  $X$ . Furthermore, also parts of the charged matter content from codimension two fibers are counted by  $h^{(2,1)}(X)$ , however of *another* theory related to the considered one by Higgsing.

---

<sup>7</sup>In 8D vacua, no non-split fibers are possible, i.e. all gauge groups are of *ADE*-type [9].



## Codimension two singularities

The rest of the charged spectrum of F-theory on  $X$  is encoded in the codimension two singularities of the WSF of  $X$ .

Non-Abelian charged matter is located at loci in  $\mathcal{S}_{G_I}^b$ , where the vanishing order of the discriminant  $\Delta$  of  $X$  enhances. These loci are typically complete intersections of  $\mathcal{S}_{G_I}^b$  with another divisor in  $B$ , that can be read off from  $\Delta$ . The fiber of  $X$  at these codimension two loci contains additional shrinkable rational curves  $c$  that are not present in codimension one. These curves correspond to the weights of a representation  $\mathbf{R}_{\underline{q}}$ , under the gauge group  $G_X$  in (6.10), where  $\underline{q} = (q_1, \dots, q_r)$  denotes the vector of U(1)-charges. The Dynkin labels  $\lambda_i^{G_I}$  of  $\mathbf{R}$  are computed according to

$$\lambda_i^{G_I} = D_i^{G_I} \cdot c, \quad (6.13)$$

and the  $m^{\text{th}}$  U(1)-charge  $q_m$  is computed using (6.6) as [105, 97], c.f. 3.15,

$$q_m = \sigma(\hat{s}_m) \cdot c = (S_m \cdot c) - (S_0 \cdot c) + \sum_I (S_m \cdot c_{-\alpha_i}) (C_{(I)}^{-1})^{ij} (D_{jI} \cdot c). \quad (6.14)$$

We emphasize that these charges are automatically quantized, but not necessarily integers due to the usually fractional contribution from the last term in (6.14).

We note that in the presence of U(1)'s, we automatically have additional matter that does not originate from intersections of codimension one discriminant components. In fact, the WSF of  $X$  automatically has codimension two singularities for every rational section  $\hat{s}_m$  with coordinates  $[z_{P_m} : x_{P_m} : y_{P_m}]$  at the following locus in  $B$ :

$$y_{P_m} = f z_{P_m}^4 + x_{P_m}^2 = 0, \quad m = 1, \dots, r. \quad (6.15)$$

This can be seen by inserting  $[z_{P_m} : x_{P_m} : y_{P_m}]$  into (6.2), which implies a relation between

$f$  and  $g$  which allows for a factorization of (6.2) that reveals the presence of conifold singularities in the WSF of  $X$  precisely at (6.15), see e.g. [97, 34] for details. In the crepant resolution  $X$ , there is a reducible  $I_2$ -fiber with one isolated rational curve at the codimension two loci (6.15). The matter at the loci (6.15) are charged singlets  $\mathbf{1}_q$  with their U(1)-charges computed according to (6.14). This is clear as generically (6.15) does not intersect any discriminant component, which are the loci where the Cartan divisors  $D_i^{G_I}$  are supported, so that (6.13) is trivial.

In concrete applications, the complete intersection (6.15) describes a reducible variety in  $B$  supporting multiple singlets with different charges. Matter at a generic point of (6.15) has U(1)-charge one, whereas matter at non-generic points, i.e. points along which other, oftentimes simpler constraints vanish, too, has different U(1)-charges. From a technical point of view, we are interested in all *prime ideals*, denoted throughout the paper by  $I_{(k)}$ , of the loci (6.15) for every  $m$ . These are obtained by a primary decomposition of the complete intersection (6.15), cf. [30] for details. The codimension two variety in  $B$  associated to  $I_{(k)}$  is denoted by  $V(I_{(k)})$ , which is the standard notation in algebraic geometry for an algebraic set, i.e. the set of points in  $B$  so that all constraints in  $I_{(k)}$  vanish. Then, we explicitly analyze the  $I_2$ -fibers of  $X$  over all these irreducible varieties  $V(I_{(k)})$  in order to compute the respective U(1)-charges via (6.14).

In general, the multiplicity of matter in the representation  $\mathbf{R}_q$  is given by the homology class of the corresponding codimension two locus in  $B$ . If the base  $B$  is two-dimensional, which is the case in compactifications to 6D, this is just a set of points and the multiplicity is the number of these points. In F-theory compactifications to 4D, the homology class of a codimension two locus is the class of the corresponding matter curve.

More specifically, the multiplicity of non-Abelian charged matter is computed easily as the homology class of the complete intersection with  $\mathcal{S}_{G_I}^b$ . However, the determination of the multiplicity of singlets  $\mathbf{1}_q$  is more involved since they are located on the varieties

$V(I_{(k)})$  associated to the usually very complex prime ideals  $I_{(k)}$  of the complete intersection (6.15). The respective matter multiplicities are then again given as the homology class of the variety  $V(I_{(k)})$ . It can be computed by the following procedure, see [34, 30, 33] for more details: we first compute the homology class of the reducible complete intersection (6.15). Given the list of its associated prime ideals  $I_{(k)}$ , we then subtract the multiplicities (homology classes) of those matter loci  $V(I_{(k')})$ ,  $\{k'\} \subset \{k\}$ , we already know. Here we have to take into account the order  $n_{k'}$  of the matter locus  $V(I_{(k')})$  inside the complete intersection (6.15). The order  $n_{k'}$  is computed using the *resultant technique* [34]. In all the cases considered below in Section 6.3, this strategy yields the homology classes of all singlets  $\mathbf{1}_q$ .

In summary, the 6D  $\mathcal{N} = (1, 0)$  SUGRA theory obtained by compactifying F-theory on a Calabi-Yau threefold  $X$  has

- a total number of vector multiplets  $V$  reading

$$V = \mathbf{adj}(G_X) = \sum_I \dim(\mathbf{adj}(G_I)) + r, \quad (6.16)$$

where  $\mathbf{adj}(G_X)$  and  $\mathbf{adj}(G_I)$  denote the adjoint representations of  $G_I$  and  $G_X$ , respectively, and  $r$  denotes the MW-rank of  $X$ ,

- a total number of hyper multiplets  $H$  given by

$$\begin{aligned} H &= H_{\text{codim}=2} + H_{\text{codim}=1} + H_{\text{mod}} \\ &= H_{\text{codim}=2} + \sum_{I=1}^n g_I (\dim(\mathbf{adj}(G_I)) - \text{rk}(G_I)) + h^{(2,1)}(X) + 1, \end{aligned} \quad (6.17)$$

where we split into contributions  $H_{\text{codim}=2}$ ,  $H_{\text{codim}=1}$  and  $H_{\text{mod}}$  from codimension two fibers, from codimension one fibers over higher genus Riemann surfaces in  $B$  and from complex structure moduli of  $X$  (plus 1), respectively,

- and a number of tensor multiplets  $T$  counted by

$$T = h^{(1,1)}(B) - 1 = 9 - [K_B^{-1}]^2. \quad (6.18)$$

For the second equality in (6.18) we have employed the identity

$$[K_B^{-1}] \cdot [K_B^{-1}] = \int_B c_1(B)^2 = 10 - h^{(1,1)}(B). \quad (6.19)$$

Here we used in the last equality the Euler number  $\chi(B) = (2 + h^{(1,1)}(B))$  of a simply-connected base  $B$  with  $h^{(2,0)} = 0$  and the index formula for the arithmetic genus  $\chi_0(B) = 1$ ,

$$1 = \chi_0(B) = \frac{1}{12} \int (c_2(B) + c_1(B)^2) = \frac{1}{12} (2 + h^{(1,1)}(B) + \int_B c_1(B)^2), \quad (6.20)$$

where  $c_i(B)$ ,  $i = 1, 2$ , denote the Chern classes of  $B$ .

### Codimension three singularities

For completeness we note that codimension three singularities of the WSF of a Calabi-Yau fourfold  $X$  support Yukawa points in F-theory compactifications to 4D. The codimension three singularities are at the points in the threefold base  $B$  of further enhancement of the vanishing order of the discriminant  $\Delta$ . All such enhancement points are given as intersections of three matter curves in  $B$ , including self-intersections. Technically, given three matter curves  $V(I_{(1)})$ ,  $V(I_{(2)})$  and  $V(I_{(3)})$  we have to check that the variety  $V(I_{(1)}) \cap V(I_{(2)}) \cap V(I_{(3)})$  contains a codimension three component in  $B$ . This is achieved by checking that the ideal  $I_{(1)} \cup I_{(2)} \cup I_{(3)}$  is codimension three in the ring of appropriate polynomials on  $B$ , where we used the well-known equality  $\bigcap_k V(I_{(k)}) = V(\bigcup_k I_{(k)})$  for a family of algebraic sets  $V(I_{(k)})$  [63].

As we see in Section 6.3, all gauge-invariant Yukawa couplings are realized for the case of toric hypersurface fibrations  $X_{F_i}$ .

## 6.2.4 Explicit examples: Calabi-Yau hypersurfaces in 2D toric varieties

All Calabi-Yau manifolds  $X$  considered in this work are constructed as fibrations of genus-one curves  $\mathcal{C}$  that have a natural presentation as hypersurfaces in 2D toric varieties. These fibrations are automatically smooth, if the toric ambient spaces of the fiber  $\mathcal{C}$  are fully resolved. In this section we present a very brief account on the construction of Calabi-Yau hypersurfaces in 2D toric varieties that are the basis for the rest of this work. For a more complete account, we refer to standard text books [46, 29].

A toric almost Fano surface is associated to each of the 16 two-dimensional reflexive polyhedra  $F_i$ ,  $i = 1, \dots, 16$ , in a lattice  $N = \mathbb{Z}^2$ .<sup>8</sup> These 16 reflexive polyhedra are given in a convenient presentation in Figure 6.2 [49]. As indicated there, the polyhedra  $F_i$  and  $F_{17-i}$  for  $i = 1, \dots, 6$  are dual to each other,  $F_i^* = F_{17-i}$ , and the  $F_i$  for  $i = 7, \dots, 10$  are self-dual,  $F_i = F_i^*$ , where the dual polyhedron  $F_i^*$  is defined in the dual lattice  $M = \mathbb{Z}^2$  of  $N$  as

$$F_i^* = \{q \in M \otimes \mathbb{R} \mid \langle y, q \rangle \geq -1, \forall y \in F_i\}, \quad (6.21)$$

where  $\langle \cdot, \cdot \rangle$  is the pairing between  $N$  and  $M$ .

For a given polyhedron  $F_i$ , we denote the associated toric variety by  $\mathbb{P}_{F_i}$ . Toric varieties are generalizations of weighted projective spaces [28]: to each integral point  $v_k$ ,  $k = 1, \dots, m+2$ , except the origin of  $F_i$ , we associate a coordinate  $x_k$  in  $\mathbb{C}$ . Next, we

---

<sup>8</sup>We refrain from the common notation  $\Delta$  for a polyhedron in order to avoid confusion with the discriminant.

introduce the lattice of relations between the  $v_k$  with generators  $\ell^{(a)}$  defined by

$$\sum_{k=1}^{m+2} \ell_k^{(a)} v_k = 0, \quad a = 1, \dots, m. \quad (6.22)$$

Then, a smooth toric variety  $\mathbb{P}_{F_i}$  is defined as the  $(\mathbb{C}^*)^m$ -quotient

$$\mathbb{P}_{F_i} = \frac{\mathbb{C}^{m+2} \setminus \mathbf{SR}}{(\mathbb{C}^*)^m} = \{x_k \sim \prod_{a=1}^m \lambda_a^{\ell_k^{(a)}} x_k \mid \underline{x} \notin \mathbf{SR}, \lambda_a \in \mathbb{C}^*\}, \quad (6.23)$$

where the points  $\underline{x} := (x_1, \dots, x_{m+2})$  are not allowed to lie in the Stanley-Reisner ideal  $\mathbf{SR}$ .

The construction (6.23) provides a dictionary between the combinatorics of the polyhedron  $F_i$  and the geometry of  $\mathbb{P}_{F_i}$ . For example, the toric divisor group on  $\mathbb{P}_{F_i}$  is generated by the divisors  $D_k = \{x_k = 0\}$  and the intersections of the  $D_k$  are encoded in the  $\mathbf{SR}$  ideal. A full basis of the divisor group on  $\mathbb{P}_{F_i}$  can be obtained using the linear equivalences between the  $D_k$ . Due to the relevance for the smoothness of a toric hypersurface fibration  $X$ , we stress here that points that are not vertices in  $F_i$  correspond to exceptional divisors resolving orbifold singularities in  $\mathbb{P}_{F_i}$ .

The polyhedra  $F_1, F_3, F_5, F_7$  describe the generic del Pezzo surfaces  $\mathbb{P}^2$  and  $dP_i$ ,  $i = 1, 2, 3$ , respectively,  $F_2$  yields  $\mathbb{P}^1 \times \mathbb{P}^1$ ,  $F_4$  describes  $\mathbb{P}^2(1, 1, 2)$  and  $F_{10}$  yields  $\mathbb{P}^2(1, 2, 3)$ . In fact all other toric varieties  $\mathbb{P}_{F_i}$  can be viewed as higher del Pezzo surfaces at a special point in their respective complex structure moduli spaces.

Every toric variety  $\mathbb{P}_{F_i}$  has an associated Calabi-Yau hypersurface, i.e. a genus-one curve  $\mathcal{C}_{F_i}$ . It is defined as the generic section of its anti-canonical bundle  $K_{\mathbb{P}_{F_i}}^{-1}$ . The Calabi-Yau hypersurface in  $\mathbb{P}_{F_i}$  is obtained by the Batyrev construction as the following polynomial [7]

$$p_{F_i} = \sum_{q \in F_i^* \cap M} a_q \prod_k x_k^{\langle v_k, q \rangle + 1}, \quad (6.24)$$

where  $q$  denotes all integral points in  $F_i^*$  and the  $a_q$  are coefficients in the field  $K$ .

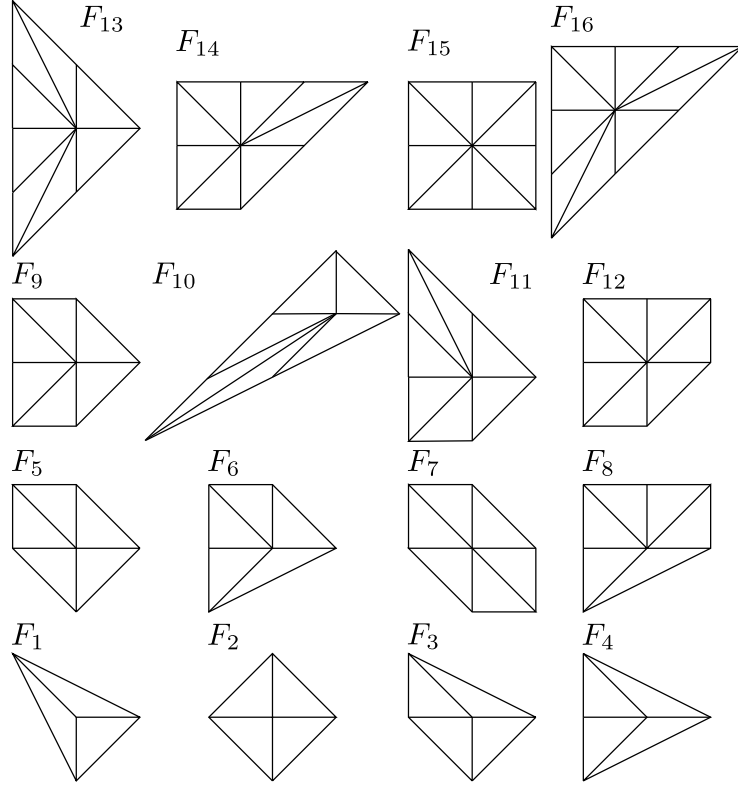


Figure 6.2: The 16 two dimensional reflexive polyhedra [49]. The polyhedron  $F_i$  and  $F_{17-i}$  are dual for  $i = 1 \dots 6$  and self-dual for  $i = 7 \dots 10$ .

We note that points  $v_i$  interior to edges in  $F_i$  are usually excluded in the product (6.24) because the corresponding divisors do not intersect the hypersurface  $\mathcal{C}_{F_i}$ . However, when considering Calabi-Yau fibrations  $X_{F_i}$  of  $\mathcal{C}_{F_i}$ , as in Section 6.3, these divisors intersect  $X_{F_i}$  and resolve singularities of  $X_{F_i}$  induced by singularities of its fibration, i.e. these divisors are related to Cartan divisors  $D_i^{G_I}$  discussed above in Section 6.2.2.

### 6.3 Analysis of F-theory on Toric Hypersurface Fibrations

In this section we analyze the geometry of the Calabi-Yau manifolds  $X_{F_i}$ , that are constructed as fibration of the genus-one curves  $\mathcal{C}_{F_i}$  over a generic base  $B$ . For each manifold

we calculate the effective theory resulting from compactifying F-theory on it. We calculate the gauge group, the charged and neutral matter spectrum and the Yukawa couplings.

We start with a quick summary of some interesting results of this study. There are three polyhedra leading to manifolds  $X_{F_i}$  without a section:  $F_1$ ,  $F_2$  and  $F_4$ , see sections 6.4.1 and 6.4.2. They yield the discrete gauge groups in F-theory. For three polyhedra we find associated gauge groups with Mordell-Weil torsion, giving rise to non-simply connected gauge groups:  $F_{13}$ ,  $F_{15}$  and  $F_{16}$ . The analysis of the hypersurface  $X_{F_3}$  and the corresponding effective theory of F-theory, whose spectrum contains a charged singlet with U(1)-charge three, can be found in section 6.4.3.

We obtain the following list of gauge groups  $G_{F_i}$  of F-theory on the  $X_{F_i}$ :

$G_{F_1}$	$\mathbb{Z}_3$	$G_{F_7}$	$U(1)^3$		
$G_{F_2}$	$U(1) \times \mathbb{Z}_2$	$G_{F_8}$	$SU(2)^2 \times U(1)$	$G_{F_{13}}$	$(SU(4) \times SU(2)^2) / \mathbb{Z}_2$
$G_{F_3}$	$U(1)$	$G_{F_9}$	$SU(2) \times U(1)^2$	$G_{F_{14}}$	$SU(3) \times SU(2)^2 \times U(1)$
$G_{F_4}$	$SU(2) \times \mathbb{Z}_4$	$G_{F_{10}}$	$SU(3) \times SU(2)$	$G_{F_{15}}$	$SU(2)^4 / \mathbb{Z}_2 \times U(1)$
$G_{F_5}$	$U(1)^2$	$G_{F_{11}}$	$SU(3) \times SU(2) \times U(1)$	$G_{F_{16}}$	$SU(3)^3 / \mathbb{Z}_3$
$G_{F_6}$	$SU(2) \times U(1)$	$G_{F_{12}}$	$SU(2)^2 \times U(1)^2$		

From this and as a simple consequence of (6.11), we see that there is the following rule of thumb for computing the rank of a gauge group  $G_{F_i}$ : given a polyhedron  $F_i$  with  $3 + n$  integral points without the origin, we have a gauge group with total rank  $n$ .

Let us outline the structure of this section. In the first subsection 6.3.1 we briefly discuss the three different representations of genus-one curves  $\mathcal{C}_{F_i}$  realized as toric hypersurfaces: the cubic, the biquadric and the quartic. There, we define the line bundles of the base  $B$  in which the coefficients in these constraints have to take values in order to obtain a genus-one fibered Calabi-Yau manifold. The functions  $f$  and  $g$  of the Weierstrass form (6.2) for the cubic, the biquadric and the quartic can be found in the appendix of Appendix [80]. By



appropriate specializations of the coefficients, one can obtain  $f$ ,  $g$  and  $\Delta = 4f^3 + 27g^2$  for all toric hypersurface fibration  $X_{F_i}$ .

In sections 6.4 we proceed to describe in detail each Calabi-Yau manifold  $X_{F_i}$ . In each case we first discuss the genus-one curve  $\mathcal{C}_{F_i}$  realized as a toric hypersurface in  $\mathbb{P}_{F_i}$ . We then construct the corresponding toric hypersurface fibration  $X_{F_i}$  and analyze its codimension one and two singularities from which we extract the non-Abelian gauge group and matter spectrum. If  $X_{F_i}$  has a non-trivial MW-group, we determine all its generators, their Shioda maps and the height pairing. For genus-one fibrations, we determine their discrete gauge groups. For completeness, we also determine the Yukawa couplings from codimension three singularities. In each case we show as a consistency check that the necessary 6D anomalies (pure Abelian, gravitational-Abelian, pure non-Abelian, non-Abelian gravitational, non-Abelian-Abelian and purely gravitational) are canceled implying consistency of the considered effective theories.

We organize the Calabi-Yau manifolds  $X_{F_i}$  into five categories: those with discrete gauge symmetries (Section 6.4), those with a gauge group of rank one and two but without discrete gauge groups, those with a gauge group of rank three, whose fiber polyhedra happen to be also self-dual, those with gauge groups of rank four and five without MW-torsion and those  $X_{F_i}$  with MW-torsion. This arrangement is almost in perfect agreement with the labeling of the polyhedra  $F_i$  in Figure 6.2 which facilitates the navigation through this section. We name the subsection containing the analysis of the specific manifold  $X_{F_i}$  by its corresponding fiber polyhedron  $F_i$ .

### 6.3.1 Three basic ingredients: the cubic, biquadric and quartic

#### Constructing toric hypersurface fibrations

In this section we explain the general construction of the Calabi-Yau manifolds  $X_{F_i}$  with toric hypersurface fiber  $\mathcal{C}_{F_i}$  and base  $B$ . The following discussion applies to Calabi-Yau  $n$ -folds  $X_{F_i}$  with a general  $(n-1)$ -dimensional base  $B$ . The cases of most relevance for F-theory and for this work are  $n=3,4$ . We refer to [34, 30] for more details on the following discussion.

The starting point of the construction of the genus-one fibered Calabi-Yau manifold  $X_{F_i}$  is the hypersurface equation (6.24) of the curve  $\mathcal{C}_{F_i}$ . In order to obtain the equation of  $X_{F_i}$ , the coefficients  $a_q$  and the variables  $x_i$  of (6.24) have to be promoted to sections of appropriate line bundles of the base  $B$ . We determine these line bundles, by first constructing a fibration of the 2D toric variety  $\mathbb{P}_{F_i}$ , which is the ambient space of  $\mathcal{C}_{F_i}$ , over the same base  $B$ ,

$$\begin{array}{ccc} \mathbb{P}_{F_i} & \longrightarrow & \mathbb{P}_{F_i}^B(D, \tilde{D}) . \\ & & \downarrow \\ & & B \end{array} \quad (6.25)$$

Here  $\mathbb{P}_{F_i}^B(D, \tilde{D})$  denotes the total space of this fibration. The structure of its fibration is parametrized by two divisors in  $B$ , denoted by  $D$  and  $\tilde{D}$ . This can be seen by noting that all  $m+2$  coordinates  $x_k$  on the fiber  $\mathbb{P}_{F_i}$  are in general non-trivial sections of line bundles on  $B$ . Then, we can use the  $(\mathbb{C}^*)^m$ -action of the toric variety  $\mathbb{P}_{F_i}$  to set  $m$  variables to transform in the trivial bundle of  $B$ . The divisors dual to the two remaining line bundles are precisely  $D, \tilde{D}$ .

Next we impose equation (6.24) in  $\mathbb{P}_{F_i}^B(D, \tilde{D})$ . Consistency fixes the line bundles in which the coefficients  $a_q$  have to take values in terms of the two divisors  $D$  and  $\tilde{D}$ . Then, we require (6.24) to be a section of the anti-canonical bundle  $K_{\mathbb{P}_{F_i}^B}^{-1}$ , which is the Calabi-Yau

condition. In addition, equation (6.24) imposed in  $\mathbb{P}_{F_i}^B(D, \tilde{D})$  clearly describes a genus-one fibration over  $B$ , since for every generic point on  $B$ , the hypersurface (6.24) describes exactly the curve  $\mathcal{C}_{F_i}$  in  $\mathbb{P}_{F_i}$ . The total Calabi-Yau space resulting from the fibration of the toric hypersurface  $\mathcal{C}_{F_i}$  is denoted by  $X_{F_i}$  in the following. It enjoys the fibration structure

$$\begin{array}{ccc} \mathcal{C}_{F_i} & \longrightarrow & X_{F_i} \\ & & \downarrow \\ & & B \end{array} . \quad (6.26)$$

In principle, this procedure has to be carried out for all Calabi-Yau manifolds  $X_{F_i}$  associated to the 16 2D toric polyhedra  $F_i$ . However, we observe that all the hypersurface constraints of the  $X_{F_i}$ , except for  $X_{F_2}$  and  $X_{F_4}$ , can be obtained from the hypersurface constraint for  $X_{F_1}$ , after setting appropriate coefficients to zero. This is possible because if  $F_1$  is a sub-polyhedron of  $F_i$ , then the corresponding toric variety  $\mathbb{P}_{F_i}$  is the blow-up of  $\mathbb{P}_{F_1} = \mathbb{P}^2$  at a given number of points, with the additional rays in  $F_i$  corresponding to the blow-up divisors. However, adding rays to the polyhedron  $F_1$  removes rays from its dual polyhedron  $F_1^* = F_{16}$ . By means of (6.24), this removes coefficients from hypersurface equation for  $X_{F_i}$ , i.e. the hypersurface for  $X_{F_i}$  is a certain specialization of the hypersurface of  $X_{F_1}$  with some  $a_q \equiv 0$ . We will be more explicit about this in the following subsection (Section 6.3.1).

Thus, we only have to explicitly carry out the construction of the toric hypersurfaces separately for the two Calabi-Yau manifolds  $X_{F_2}$  and  $X_{F_4}$ . The details of this are given in Sections 6.3.1 and in the [80].

### **Fibration by cubic curves: $X_{F_1}$ and its specializations**

We proceed to construct the Calabi-Yau manifold  $\mathcal{C}_{F_1} \rightarrow X_{F_1} \rightarrow B$  with fiber given by the curve  $\mathcal{C}_{F_1}$  in the toric variety  $\mathbb{P}_{F_1}$ . In addition, we argue how the Calabi-Yau manifolds  $X_{F_i}$ ,

whose fiber polyhedron  $F_i$  contains  $F_1$ , can be obtained from  $X_{F_1}$ .

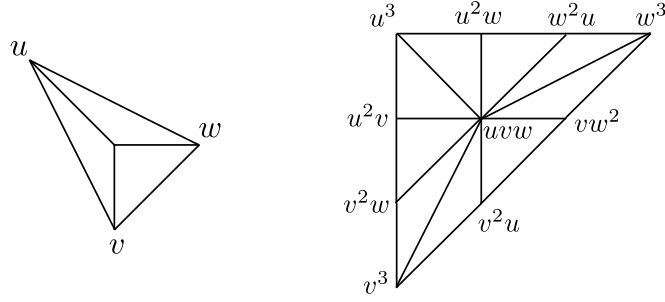


Figure 6.3: Polyhedron  $F_1$  with choice of projective coordinates and its dual with corresponding monomials.

The polyhedron  $F_1$  and its dual are shown in Figure 6.3. The toric variety  $\mathbb{P}_{F_1}$ , constructed using (6.23), is the well-known projective space  $\mathbb{P}^2$ . We introduce the projective coordinates  $[u : v : w]$  on  $\mathbb{P}^2$ . In terms of these coordinates, we can read off the SR-ideal from Figure 6.3 as

$$SR = \{uvw\}. \quad (6.27)$$

The divisor group of  $\mathbb{P}^2$  is generated by the hyperplane class  $H$ . The Calabi-Yau onefold in  $\mathbb{P}^2$  is the degree three  $\mathcal{C}_{F_1}$  in  $3H$ . Its defining equation, constructed using (6.24) and Figure 6.3, is the most general cubic

$$p_{F_1} = s_1u^3 + s_2u^2v + s_3uv^2 + s_4v^3 + s_5u^2w + s_6uvw + s_7v^2w + s_8uw^2 + s_9vw^2 + s_{10}w^3, \quad (6.28)$$

where the coefficients  $s_i$  take values in the field  $K$ .

Next, we follow the discussion of Section 6.3.1 to construct the toric hypersurface fibration  $X_{F_1}$ . We first construct the ambient space (6.25), which in the case at hand is a  $\mathbb{P}^2$ -fibration over the base  $B$ ,

$$\begin{array}{ccc} \mathbb{P}^2 & \longrightarrow & \mathbb{P}^2(\mathcal{S}_7, \mathcal{S}_9) . \\ & & \downarrow \\ & & B \end{array} \quad (6.29)$$

The two divisors parametrizing this fibration are  $\mathcal{S}_7$  and  $\mathcal{S}_9$ , cf. [34, 30]. Upon imposing the constraint (6.28) and requiring the Calabi-Yau condition for  $X_{F_1}$ , we see that these two divisors are precisely the classes of the coefficients  $s_7$  and  $s_9$ , respectively. Indeed, as mentioned above, we can use the  $\mathbb{C}^*$ -action on  $\mathbb{P}^2$  to turn e.g.  $w$  into a section of the trivial line bundle of the base. Then, we choose the variables  $u$  and  $v$  as sections of the bundles

$$u \in \mathcal{O}_B(\mathcal{S}_9 + [K_B]), \quad v \in \mathcal{O}_B(\mathcal{S}_9 - \mathcal{S}_7). \quad (3.111)$$

This allows us to compute the anti-canonical bundle of the  $\mathbb{P}^2$ -fibration (6.29) using adjunction as

$$K_{\mathbb{P}^2(\mathcal{S}_7, \mathcal{S}_9)}^{-1} = \mathcal{O}(3H + 2\mathcal{S}_9 - \mathcal{S}_7). \quad (6.30)$$

Finally, we impose the Calabi-Yau condition on the constraint (6.28) for  $X_{F_1}$  which fixes the divisor classes of the coefficients  $s_i$ . We summarize the divisor classes of the homogeneous coordinates  $[u : v : w]$  and the coefficients  $s_i$  in the following tables:

section	Divisor Class	section	Divisor Class
$u$	$H + \mathcal{S}_9 + [K_B]$	$s_1$	$3[K_B^{-1}] - \mathcal{S}_7 - \mathcal{S}_9$
$v$	$H + \mathcal{S}_9 - \mathcal{S}_7$	$s_2$	$2[K_B^{-1}] - \mathcal{S}_9$
$w$	$H$	$s_3$	$[K_B^{-1}] + \mathcal{S}_7 - \mathcal{S}_9$
		$s_4$	$2\mathcal{S}_7 - \mathcal{S}_9$
		$s_5$	$2[K_B^{-1}] - \mathcal{S}_7$
		$s_6$	$[K_B^{-1}]$
		$s_7$	$\mathcal{S}_7$
		$s_8$	$[K_B^{-1}] + \mathcal{S}_9 - \mathcal{S}_7$
		$s_9$	$\mathcal{S}_9$
		$s_{10}$	$2\mathcal{S}_9 - \mathcal{S}_7$

(6.31)

### $X_{F_i}$ as specialized cubics

As mentioned in the previous subsection, the equations of the Calabi-Yau manifolds  $X_{F_i}$  with  $i \neq 2, 4$  can be expressed as specialized versions of the cubic hypersurface equation (6.28) of  $X_{F_1}$ .

In order to find the hypersurface equation for an  $X_{F_i}$  we begin by calculating the anti-canonical class of the fibration  $\mathbb{P}_{F_i}^B(D, \tilde{D})$  defined in (6.25). To this end, we first note that toric ambient spaces  $\mathbb{P}_{F_i}$  are obtained from  $\mathbb{P}_{F_1}$  by a certain number of blow-ups at points  $P_j$ . Assuming the number of blow-ups is  $k$ , we have

$$\mathbb{P}_{F_i} = \text{Bl}_{P_1, \dots, P_k} \mathbb{P}_{F_1}. \quad (6.32)$$

Each blow-up adds a  $\mathbb{P}^1$  with an associated new variable  $e_j$  and divisor class  $E_j$ . From the combinatorial point of view, this means that there is an additional  $\mathbb{C}^*$ -action on  $\mathbb{P}_{F_i}$ .

Next we note that the fibration  $\mathbb{P}_{F_i}^B(D, \tilde{D})$  can be parametrized by the same base divisors  $\mathcal{S}_7$  and  $\mathcal{S}_9$  as the fibration (6.29), i.e. we identify  $D = \mathcal{S}_7$  and  $\tilde{D} = \mathcal{S}_9$ . Indeed, this is possible since we can use  $(\mathbb{C}^*)$ -actions, including the new  $(\mathbb{C}^*)$ -actions from the  $k$  blow-ups, to make the variables  $w$  and  $e_j$  transform in the trivial bundle on  $B$  while maintaining the assignments (3.111) for  $u$  and  $v$ . Employing these results we calculate the anti-canonical bundle of  $\mathbb{P}_{F_i}^B(\mathcal{S}_7, \mathcal{S}_9)$ , using the adjunction formula, yielding

$$K_{\mathbb{P}_{F_i}^B(\mathcal{S}_7, \mathcal{S}_9)}^{-1} = \mathcal{O}(3\tilde{H} - E_1 - E_2 - \dots - E_k + 2\mathcal{S}_9 - \mathcal{S}_7). \quad (6.33)$$

Here,  $\tilde{H}$  denotes the pull-back  $\tilde{H} = \tilde{\pi}^*(H)$  of the hyperplane class  $H$  on  $\mathbb{P}^2$  under the blow-down map  $\tilde{\pi} : \mathbb{P}_{F_i} \rightarrow \mathbb{P}^2$ . By abuse of notation, we will denote it throughout this work simply by  $H$ . It is to be observed that if the coefficient  $s_i$  is present in the constraint of  $X_{F_i}$ , i.e. if it is not removed by the  $k$  blow-ups, its corresponding class  $[s_i]$  remains unaltered

from the one given in Table (6.31).

This relation of the hypersurface constraints of the  $X_{F_i}$  for  $i \neq 2, 4$  and all the bundles entering it to the hypersurface equation (6.28) and bundles (6.31) of  $X_{F_1}$  will facilitate our following presentation. In particular, in the respective subsections on  $X_{F_i}$  for  $i \neq 2, 4$  only the classes for the variables  $u, v, w$  and  $e_j$  have to be given explicitly.

**Fibration by the biquadric:  $X_{F_2}$**

We construct the Calabi-Yau manifold  $\mathcal{C}_{F_2} \rightarrow X_{F_2} \rightarrow B$  as the fibration of the curve  $\mathcal{C}_{F_2}$  in the toric variety  $\mathbb{P}_{F_2}$  over  $B$ . As mentioned before, its hypersurface equation cannot be described as a cubic. Thus,  $X_{F_2}$  has to be analyzed separately.

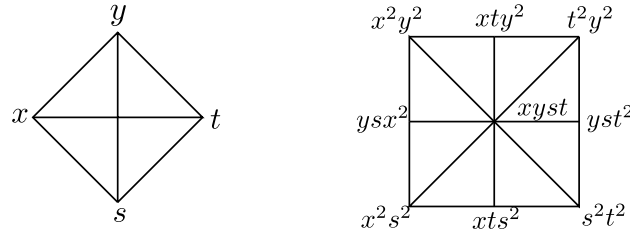


Figure 6.4: Polyhedron  $F_2$  with choice of projective coordinates and its dual with corresponding monomials.

The polyhedron  $F_2$  and its dual are presented in Figure 6.4. The toric variety associated to it is  $\mathbb{P}_{F_2} = \mathbb{P}^1 \times \mathbb{P}^1$  and we have introduced the projective coordinates  $[x : t]$  and  $[y : s]$  on the two  $\mathbb{P}^1$ 's, respectively. The Stanley-Reisner ideal of  $\mathbb{P}_{F_2}$  is given by

$$SR = \{xt, ys\}. \tag{6.34}$$

There are two divisor classes on  $\mathbb{P}_{F_2}$ , that we denote by  $H_1$  and  $H_2$  with respective representatives  $\{x = 0\}$  and  $\{y = 0\}$ . The Calabi-Yau onefold in  $\mathbb{P}_{F_2}$  is the curve  $\mathcal{C}_{F_2}$  in the class

$2H_1 + 2H_2$ . It is a biquadric of the form

$$p_{F_2} = (b_1y^2 + b_2sy + b_3s^2)x^2 + (b_5y^2 + b_6sy + b_7s^2)xt + (b_8y^2 + b_9sy + b_{10}s^2)t^2, \quad (6.35)$$

as can be shown using (6.24) and Figure 6.4. Here the  $b_i$  denote coefficients in the field  $K$ .

In order to find  $X_{F_2}$  we proceed to construct  $\mathbb{P}_{F_2}^B(D, \tilde{D})$ , the fibration of  $\mathbb{P}_{F_2}$  introduced in (6.25). It is possible to consistently parametrize this fibration in terms of the same divisor classes  $D = \mathcal{S}_7$  and  $\tilde{D} = \mathcal{S}_9$  as in (6.29). In the hypersurface constraint (6.35), they correspond to the classes of the coefficients  $b_7$  and  $b_9$  respectively.<sup>9</sup> This will facilitate the matching of the effective theories via Higgsings. Next, we use the  $(\mathbb{C}^*)^2$ -actions on  $\mathbb{P}_{F_2}$  to achieve that the variables  $x$  and  $y$  transform in the trivial line bundle on  $B$ . The other two variables  $s$  and  $t$  take values in the following line bundles on  $B$ :

$$t \in \mathcal{O}_B([K_B^{-1}] - \mathcal{S}_9), \quad s \in \mathcal{O}_B([K_B^{-1}] - \mathcal{S}_7). \quad (6.36)$$

With this assignment of line bundles to the coordinates on  $\mathbb{P}_{F_2}$ , the anti-canonical class of  $\mathbb{P}_{F_2}^B(\mathcal{S}_7, \mathcal{S}_9)$  is readily calculated as

$$K_{\mathbb{P}_{F_2}^B}^{-1} = \mathcal{O}(2H_1 + 2H_2 + 3[K_B^{-1}] - \mathcal{S}_7 - \mathcal{S}_9). \quad (6.37)$$

Finally, we require that the hypersurface (6.35) is Calabi-Yau, which fixes the divisor classes of the coefficients  $b_i$  in terms of  $\mathcal{S}_7$ ,  $\mathcal{S}_9$  and  $[K_B^{-1}]$ . In summary, we obtain that

---

<sup>9</sup>The consistency of this assignment can be seen by noting that  $\mathbb{P}_{F_2}$  is related to  $\mathbb{P}^2$  by the blow-up at  $x = y = 0$  setting  $b_{10} = 0$  and the subsequent blow-downs  $x = y = 1$ . Then, (6.35) precisely yields (6.28).



the coordinates on  $\mathbb{P}_{F_2}$  and the coefficients  $b_i$  have the following divisor classes:

section	Divisor Class	Section	Divisor Class
$x$	$H_1$	$b_1$	$3[K_B^{-1}] - \mathcal{S}_7 - \mathcal{S}_9$
$t$	$H_1 + [K_B^{-1}] - \mathcal{S}_9$	$b_2$	$2[K_B^{-1}] - \mathcal{S}_9$
$y$	$H_2$	$b_3$	$[K_B^{-1}] + \mathcal{S}_7 - \mathcal{S}_9$
$s$	$H_2 + [K_B^{-1}] - \mathcal{S}_7$	$b_5$	$2[K_B^{-1}] - \mathcal{S}_7$
		$b_6$	$[K_B^{-1}]$
		$b_7$	$\mathcal{S}_7$
		$b_8$	$[K_B^{-1}] + \mathcal{S}_9 - \mathcal{S}_7$
		$b_9$	$\mathcal{S}_9$
		$b_{10}$	$\mathcal{S}_9 + \mathcal{S}_7 - [K_B^{-1}]$

(6.38)

We emphasize that the classes of the coefficients  $b_i$ , except for  $b_{10}$ , agree with the classes of  $s_i$  of the cubic  $X_{F_1}$ , c.f. (6.31), as expected.

## 6.4 Fibration of the polyhedrons $F_1$ , $F_2$ and $F_3$

In this section we analyze the toric hypersurface fibrations based on the fiber polyhedra  $F_1$ ,  $F_2$  and  $F_3$ . Since the first two fibrations do not have a section, but only multi-sections, they are genus-one fibrations. We analyze the codimension one, two and three singularities of these models, employing also their respective associated Jacobian fibrations. We show that the effective theories of F-theory on these Calabi-Yau manifolds exhibit discrete gauge groups and include matter that is charged only under the respective discrete group.

### 6.4.1 Polyhedron $F_1$ : $G_{F_1} = \mathbb{Z}_3$

We consider the genus-one fibration  $X_{F_1}$  over an arbitrary base  $B$  with genus-one fiber  $\mathcal{C}_{F_1}$  realized as the Calabi-Yau hypersurface in  $\mathbb{P}_{F_1} = \mathbb{P}^2$ . The toric data of  $\mathbb{P}_{F_1} = \mathbb{P}^2$  and the construction of the Calabi-Yau manifolds  $X_{F_1}$  have been discussed in Section 6.3.1. The hypersurface equation for  $X_{F_1}$  is given by (6.28) with the relevant divisor classes of the coordinates  $[u : v : w]$  and the coefficients  $s_i$  summarized in (6.31).

The fibration  $\pi : X_{F_1} \rightarrow B$  does not have a section, but only a three-section. Thus,  $X_{F_1}$  is only a genus-one fibration, cf. the general discussion in Section 6.2.1. In order to obtain the WSF of  $X_{F_1}$ , given the absence of sections of its fibration, we have to calculate the associated Jacobian fibration  $J(X_{F_1})$ . The algorithm for computing  $J(X_{F_1})$  is well known in the mathematics literature, see for example [2], from where we calculate  $f$  and  $g$ , given explicitly in the appendix of [80], and subsequently the discriminant  $\Delta$ . The discriminant does not factorize, which shows the absence of codimension one singularities of  $X_{F_1}$  and therefore, the absence of non-Abelian gauge groups in the corresponding F-theory compactification.

The fibration  $X_{F_1}$  has a three-section that is given by

$$\hat{s}^{(3)} = X_{F_1} \cap \{u = 0\} : s_4 v^3 + s_7 v^2 w + s_9 v w^2 + s_{10} w^3 = 0, \quad (6.39)$$

as follows from the Calabi-Yau constraint (6.28). We denote its divisor class, that agrees with  $H + \mathcal{S}_9 + [K_B]$ , by  $S^{(3)}$ . Under the degree nine map from  $X_1$  to its Jacobian this three-section is mapped to the canonical zero section  $z = 0$  in the WSF of  $J(X_{F_1})$ . However, in  $X_{F_1}$ , the three-section  $\hat{s}^{(3)}$  locally maps a point on the base  $B$  to three points on the fiber  $\mathcal{C}_{F_1}$ . Globally, there exists a monodromy group that interchanges these three points, upon moving on the base  $B$ . This fact, together with the existence of  $I_2$ -fibers in  $X_{F_1}$  at codimension two on which the monodromy group acts non-trivially, as we present next, and the results from Higgsing the  $U(1)$  gauge group in the effective theory associated to  $X_{F_3}$

leads us to postulate the following *discrete* gauge group of  $X_{F_1}$ :

$$G_{F_1} = \mathbb{Z}_3. \quad (6.40)$$

In order to compute the charges of matter under this discrete group, we have to associate a divisor class to the three-section. As certain models with multi-section are related to models with multiple rational sections by conifold transitions, see [99, 3], a natural proposal for such a divisor class is an expression similar to the Shioda map (6.6). We recall the three defining properties of a Shioda map summarized on page 21 in [105]. Imposing these conditions on the divisor class associated to (6.39), we obtain the following divisor class,

$$\sigma_{\mathbb{Z}_3}(\hat{s}^{(3)}) = \mathcal{S}^{(3)} + [K_B] + \frac{4}{3}\mathcal{S}_9 - \frac{2}{3}\mathcal{S}_7. \quad (6.41)$$

We propose that matter charges under the discrete group  $\mathbb{Z}_3$  should be computed using this class. In fact, we demonstrate next, that the class (6.41) allows us to compute  $\mathbb{Z}_3$ -charges of matter-representations on  $X_{F_1}$ , that are consistent with 6D anomaly cancellation and the Higgsing from the model  $X_{F_3}$ , discussed in the next Section.

### **Charged and uncharged matter in $X_{F_1}$**

We proceed with determining the codimension two singularities of the WSF of  $J(X_{F_1})$ . This analysis is most easily carried out directly in the smooth fibration  $X_{F_1}$ . The same techniques presented here will also be used in a slightly modified form for the analysis of the fibration  $X_{F_2}$ ,  $X_{F_3}$  and  $X_{F_4}$ . We note that the same technique has been used recently in [18] and [3].

## Finding the loci of $I_2$ -fibers using elimination ideals

We are looking for loci of  $B$  that support  $I_2$ -fibers in  $X_{F_1}$ . At these loci, the genus-one fiber  $\mathcal{C}_{F_1}$  of  $X_{F_1}$  has to degenerate into two  $\mathbb{P}^1$ 's, i.e. the hypersurface equation (6.28) has to factor into two smooth polynomials. For a smooth cubic the only factorization with this property is the one into a conic and a line, i.e. a factorization of (6.28) of the form

$$p_{F_1} \stackrel{!}{=} s_1(u + \alpha_1 v + \alpha_2 w)(u^2 + \beta_1 v^2 + \beta_2 w^2 + \beta_3 uv + \beta_4 vw + \beta_5 uw), \quad (6.42)$$

where  $\alpha_j$  and  $\beta_k$  are seven unknown polynomials on  $B$ . We note that we can assume  $s_1 \neq 0$ , because otherwise we would obtain a locus of codimension three or higher. Making a comparison of coefficients on both sides of (6.42), we obtain a set of constraints that defines an ideal in the ring  $K[s_i, \alpha_j, \beta_k]$ , where  $s_i$  are the coefficients in (6.28). We denote this ideal by  $I_{(s_i, \alpha, \beta)}$ . We emphasize that there are two more constraints, namely nine, in  $I_{(s_i, \alpha, \beta)}$  than unknowns  $\alpha_j, \beta_k$ , i.e. the system is over-determined. Thus, there only exists a solution for  $\alpha_j, \beta_k$  satisfying (6.42), if two additional constraints on the  $s_i$  are obeyed. This implies that the ideal  $I_{(s_i, \alpha, \beta)}$  describes a codimension two locus of the  $s_i$ .

In order to obtain the constraints that the  $s_i$  have to obey for the factorization (6.42) to exist, we compute the elimination ideal  $I_{(s_i)} = I_{(s_i, \alpha, \beta)} \cap K[s_i]$ ,<sup>10</sup> where  $K[s_i]$  is the polynomial ring only in the variables  $s_i$ . We compute  $I_{(s_i)}$ , in the following abbreviated as  $I_{(1)} \equiv I_{(s_i)}$ , explicitly using Singular [40] and obtain an ideal with 50 generators. Furthermore, we calculate its codimension in the ring  $K[s_i]$  to be two. Thus, its vanishing locus  $V(I_{(1)})$  describes a codimension two variety in  $B$ . In summary, we have shown that the factorization (6.42) corresponding to an  $I_2$ -fiber in  $X_{F_1}$  happens at the codimension two locus  $V(I_{(1)})$  in  $B$ .

---

<sup>10</sup>Here we deviate from the notation in mathematics literature, where the subscripts of the elimination ideal indicate the eliminated variables.

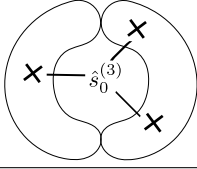
Representation	Multiplicity	Fiber	Locus
$\mathbf{1}_1$	$3(6[K_B^{-1}]^2 - \mathcal{S}_7^2 + \mathcal{S}_7\mathcal{S}_9 - \mathcal{S}_9^2 + [K_B^{-1}](\mathcal{S}_7 + \mathcal{S}_9))$		$V(I_{(1)})$

Table 6.1: Charged matter representation under  $\mathbb{Z}_3$  and corresponding codimension two fiber of  $X_{F_1}$ .

We note that (6.42) is the only type of factorization that can occur. Thus, we do not expect any further codimension two fibers and corresponding matter representation in  $X_{F_1}$ . The spectrum of  $X_{F_1}$  is summarized in Table 6.1. Next we argue how to compute the charge of the matter located at  $V(I_{(1)})$  under the discrete gauge group  $G_{F_1} = \mathbb{Z}_3$ . Due to the absence of a zero section on  $X_{F_1}$ , there is no preferred curve in the  $I_2$ -fiber in Table 6.1. As can be observed from (6.42), the two  $\mathbb{P}^1$ 's in this  $I_2$ -fiber have intersection numbers one and two with the three-section  $\hat{s}_0^{(3)}$ . By naively applying (6.14) using the divisor class (6.41), we compute the charges  $q = 1$  and  $q = 2$  for the two rational curves, respectively. Thus, it seems that there is no meaningful way to assign a discrete charge to the matter located at  $V(I_{(1)})$ . However, this seeming contradiction is resolved by noting that a 6D hyper multiplet of charge  $q = 1$  is the same as one with charge  $q = -1$ . In addition, employing the discrete  $\mathbb{Z}_3$  symmetry, we have  $-1 = 2 \pmod{3}$ , showing that a 6D hyper multiplet of charge  $q = 1$  under a  $\mathbb{Z}_3$  symmetry is physically equivalent to one with charge  $q = 2$ . Thus, the matter at  $V(I_{(1)})$  has charge  $q = 1$  which is the same as  $q = 2$  under the discrete gauge group  $G_{F_1} = \mathbb{Z}_3$ .

We proceed to calculate the multiplicity of  $V(I_{(1)})$ . Unfortunately given the size and number of polynomials in the ideal  $I_{(1)}$ , we are unable to obtain its multiplicity geometrically with the available computing power. Instead, we invoke the results for its multiplicity using the Higgs transition  $X_{F_3} \rightarrow X_{F_1}$ . It is shown in Table 6.1 for completeness.

We complete the discussion of the matter spectrum of  $X_{F_1}$  by calculating the number of neutral hyper multiplets. We use (6.12) and the explicit expression for the Euler number  $\chi(X_{F_1})$  of  $X_{F_1}$  to obtain

$$H_{\text{neut}} = 12 + 11[K_B^{-1}]^2 - 3[K_B^{-1}]\mathcal{S}_7 + 3\mathcal{S}_7^2 - 3[K_B^{-1}]\mathcal{S}_9 - 3\mathcal{S}_7\mathcal{S}_9 + 3\mathcal{S}_9^2. \quad (6.43)$$

Employing this together with the number of vector multiplets  $V = 0$  and the charged spectrum in Table 6.1 we check cancellation of the 6D gravitational anomaly in (3.100).

### Yukawa couplings in $X_{F_1}$

We conclude this section by noting that there is only one gauge-invariant Yukawa coupling possible:

Yukawa	Locus
$\mathbf{1}_1 \cdot \mathbf{1}_1 \cdot \mathbf{1}_1$	$V(I_1) \cap V(I_1) \cap V(I_1)$

(6.44)

Again, we cannot check for its presence explicitly due to the complexity of the ideal  $I_{(1)}$ .<sup>11</sup>

### 6.4.2 Polyhedron $F_2$ : $G_{F_2} = \mathbf{U}(1) \times \mathbb{Z}_2$

Here, we analyze the genus-one fibration  $X_{F_2}$  constructed as a fibration of the Calabi-Yau onefold  $\mathcal{C}_{F_2}$  in  $\mathbb{P}_{F_2} = \mathbb{P}^1 \times \mathbb{P}^1$ . The toric data of  $\mathbb{P}^1 \times \mathbb{P}^1$  and the construction of the toric hypersurface fibration  $X_{F_2}$  have been presented in Section 6.3.1. The hypersurface constraint for  $X_{F_2}$  is given in (6.35) and the relevant divisor classes are summarized in (6.38).

First, we note that the fibration  $\pi : X_{F_2} \rightarrow B$  does not have a section, i.e. it is a genus-one fibration. We obtain its WSF by computing its associated Jacobian fibration  $J(X_{F_2})$ , employing again the straightforward algorithms from the mathematics literature [2]. The

---

<sup>11</sup>The presence of this coupling can be deduced considering the Higgsing from  $X_{F_3}$  to  $X_{F_1}$ . Decomposing the states in  $X_{F_3}$  in terms of states in  $X_{F_1}$ , we observe that after Higgsing, the Yukawa coupling  $\mathbf{1}_1 \cdot \mathbf{1}_1 \overline{\mathbf{1}}_2$  in  $X_{F_3}$  (see Table 6.5) gives rise to  $\mathbf{1}_1 \cdot \mathbf{1}_1 \cdot \mathbf{1}_1$  in  $X_{F_3}$ .

results for the functions  $f$  and  $g$  can be found in the appendix of [80], from which the discriminant can be readily computed. The discriminant does not factorize, which again shows the absence of codimension one singularities. Thus, there is no non-Abelian gauge symmetry for this F-theory compactification.

The fibration of  $X_{F_2}$  has two independent two-sections, that are given by

$$\begin{aligned}\hat{s}_0^{(2)} &= X_{F_2} \cap \{x = 0\} : \quad b_8 y^2 + b_9 s y + b_{10} s^2 = 0, \\ \hat{s}_1^{(2)} &= X_{F_2} \cap \{y = 0\} : \quad b_3 x^2 + b_7 x t + b_{10} t^2 = 0,\end{aligned}\tag{6.45}$$

where we used the hypersurface constraint (6.35) and the SR-ideal (6.34). We denote the two corresponding divisor classes, that agree with  $H_1$  and  $H_2$ , by  $S_0^{(2)}$  and  $S_1^{(2)}$ , respectively. Analogous to the previous Section 6.4.1, we expect a discrete  $\mathbb{Z}_2$  gauge group associated to the two-section  $S_0^{(2)}$ , cf. the similar discussion in [99]. We will provide independent evidence for this by the analysis of the Higgsing of the effective theory of F-theory on  $X_{F_3}$ , that has a  $U(1)^2$  gauge group, to the one arising from  $X_{F_2}$ .

The role of the other two-section  $\hat{s}_1^{(2)}$ , however, is less clear in the biquadric representation. Its meaning for F-theory is unraveled by transforming the biquadric (6.35) defining  $X_{F_2}$  into a cubic hypersurface and then by computing its Weierstrass form, which is precisely the WSF of the Jacobian fibration of  $X_{F_2}$ , as we show. This detour via the cubic yields a direct map to the Jacobian fibration  $J(X_{F_2})$ , which allows us to follow the two-section  $\hat{s}_1^{(2)}$  in (6.45).

### **Map to the cubic in $\mathbb{P}_{F_3}$ & the MW-group of $J(X_{F_2})$**

The curve  $\mathcal{C}_{F_2}$  given as the biquadric (6.35) in  $\mathbb{P}_{F_2}$  can be treated as the cubic in  $\mathbb{P}_{F_3}$  after an appropriate change of variables. Indeed, by applying the transformation  $x \rightarrow x + \alpha t$  or  $y \rightarrow y + \beta s$ , we can set the coefficient of the monomial  $s^2 t^2$  (6.35) to zero for an appropriate

$\alpha$  or  $\beta$ . We note that both  $\alpha$  and  $\beta$  have to involve square roots of the coefficients  $b_i$  in (6.35), i.e. the two variable transformations are only defined in a field extension. As we will see, this field extension will only be an intermediate step, since all square roots will drop out in the final result of our computation. After the change of variables, we obtain a polynomial of the following form:

$$\tilde{p} = (\tilde{s}_1 y^2 + \tilde{s}_2 s y + \tilde{s}_3 s^2) x^2 + (\tilde{s}_5 y^2 + \tilde{s}_6 s y + \tilde{s}_7 s^2) x t + (\tilde{s}_8 y^2 + \tilde{s}_9 s y) t^2, \quad (6.46)$$

where the redefined coefficients  $\tilde{s}_i$  depend on the variables  $b_i$ . We note that  $\tilde{p}$  is precisely of the form of the cubic in  $\mathbb{P}_{F_5}$  after identifying

$$t \rightarrow w, \quad s \rightarrow v, \quad x \rightarrow e_2, \quad y \rightarrow e_1, \quad u = 1. \quad (6.47)$$

Since the curve  $\tilde{p} = 0$  is an elliptic curve, we can compute its WSF, in particular the functions  $f$  and  $g$ . Inserting the explicit expressions of the transformation for the sections  $\tilde{s}_i$  in (6.46) in terms of the  $b_i$  in (6.35) into the expressions for  $f$  and  $g$ , we precisely recover  $f$  and  $g$  obtained from the WSF of the Jacobian fibration  $J(X_{F_2})$ . Most notably, all square roots in the coefficients  $\tilde{s}_i$  have dropped out, as claimed.

Next, we note that the two-section  $\hat{s}_1^{(2)}$  in (6.45) formally maps to the section

$$s = 1, \quad t = -\frac{\tilde{s}_3}{\tilde{s}_7} \quad y = 0, \quad x = 1, \quad (6.48)$$

in (6.46). Under the identification of coordinates (6.47), this is precisely the section  $\hat{s}_1$  of



$X_{F_5}$ . Inserting the explicit expressions for the  $\tilde{s}_i$  into the WS-coordinates of  $\hat{s}_1$ , we obtain

$$\begin{aligned} z_1 &= 1, \\ x_1 &= \frac{1}{12}(8b_1b_{10} + b_6^2 - 4b_5b_7 + 8b_3b_8 - 4b_2b_9), \\ y_1 &= \frac{1}{2}(b_{10}b_2b_5 - b_1b_{10}b_6 + b_3b_6b_8 - b_2b_7b_8 - b_3b_5b_9 + b_1b_7b_9). \end{aligned} \quad (6.49)$$

We emphasize that all square roots in the coefficients  $b_i$  in the transformation have dropped out and we obtain completely rational WS-coordinates for the two-section  $\hat{s}_1^{(2)}$ . We double-check that (6.49) solves the WSF of the Jacobian  $J(X_{F_2})$ .

In summary, we have shown for the first time that the associated Jacobian fibration  $J(X_{F_2})$  exhibits a *rank one* MW-group of rational sections generated by the section in (6.49), which is precisely the image of the two-section  $\hat{s}_1^{(2)}$  in  $X_{F_2}$  under the map  $X_{F_2} \rightarrow J(X_{F_2})$ . This means that there is an associated Abelian gauge field in the F-theory compactified on  $X_{F_2}$ . We note that application of the same logic to the two-section  $\hat{s}_0^{(2)}$ , which formally maps to the section  $\hat{s}_2$  defined in  $X_{F_5}$ , does not lead to a rational section of the Jacobian  $J(X_{F_2})$  since its WS-coordinates still contain square roots. Hence,  $\hat{s}_0^{(2)}$  does not yield an additional U(1)-factor, but corresponds to a discrete group  $\mathbb{Z}_2$ , as claimed.

Having proven the presence of a MW-group on  $J(X_{F_2})$ , we compute the Shioda map of its generator. We note that the usual expression (6.6) has to be modified since  $\hat{s}_1^{(2)}$  is a two-section. It can be shown that the following expression obeys all conditions listed in [105] that have to be obeyed by a Shioda map:

$$\sigma(\hat{s}_1^{(2)}) = S_1^{(2)} - S_0^{(2)} + \frac{1}{2}([K_B] - \mathcal{S}_7 + \mathcal{S}_9) \quad (6.50)$$

Then we obtain the corresponding height pairing, using (6.7), as

$$b_{11} = -\pi(\sigma(\hat{s}_1^{(2)}) \cdot \sigma(\hat{s}_1^{(2)})) = 2[K_B^{-1}]. \quad (6.51)$$

Here, we used the following intersections

$$\pi((S_0^{(2)})^2) = -2([K_B^{-1}] - \mathcal{S}_9), \quad \pi((S_1^{(2)})^2) = -2([K_B^{-1}] - \mathcal{S}_7), \quad \pi(S_0^{(2)} \cdot S_1^{(2)}) = \mathcal{S}_7 + \mathcal{S}_9 - [K_B^{-1}]. \quad (6.52)$$

The first two equalities are just a translation of the SR-ideal (6.34) into intersection relations of divisor classes on  $X_{F_2}$ , employing (6.38) and (6.5) for  $n = 2$ . The third relation follows by noting that according to (6.45) the two two-sections  $\hat{s}_0^{(2)}$  and  $\hat{s}_1^{(2)}$  intersect precisely at  $b_{10} = 0$ , whose class is  $[b_{10}] = \mathcal{S}_7 + \mathcal{S}_9 - [K_B^{-1}]$ , cf. (6.38).

We conclude by summarizing the full gauge group of the theory:

$$G_{F_2} = \text{U}(1) \times \mathbb{Z}_2. \quad (6.53)$$

We highlight again that the  $\text{U}(1)$  corresponds to a rational section in the Jacobian fibration  $J(X_{F_2})$ , that is the image of the two-section  $\hat{s}_1^{(2)}$  under the degree four map  $X_{F_2} \rightarrow J(X_{F_2})$ .

As mentioned before, the discrete gauge  $\mathbb{Z}_2$  symmetry is induced by the two-section  $\hat{s}_0^{(2)}$ . For the computation of charges of matter w.r.t. the  $\mathbb{Z}_2$ , we have to associate a divisor class to it. Imposing conditions on this divisor class similar to the one that have lead to the Shioda map (6.6) [105], we obtain

$$\sigma_{\mathbb{Z}_2}(\hat{s}_0^{(2)}) = S_0^{(2)} + [K_B^{-1}] - \mathcal{S}_9. \quad (6.54)$$

We use this divisor class to successfully compute the  $\mathbb{Z}_2$ -charges of matter in the following.

### **Charged and uncharged matter in $X_{F_2}$**

Now that we know the gauge group of the theory, we proceed to derive first the matter representation and then the corresponding 6D matter multiplicities. As in Section 6.4.1, we use the elimination ideal technique to show directly the presence of three matter representations

in  $X_{F_2}$ , namely  $\mathbf{1}_{(1,+)}$ ,  $\mathbf{1}_{(1,-)}$  and  $\mathbf{1}_{(0,-)}$ , where  $\pm$  denote the two possible  $\mathbb{Z}_2$ -eigenvalues. Then, we compute their multiplicities, where we also invoke the equivalent presentation of  $X_{F_2}$  as a quartic.

In order to find the three  $I_2$ -fibers at codimension two in  $X_{F_2}$ , we first note that there are three different possible ways to factorize the biquadric (6.35), that correspond to the three inequivalent ways to split its degree  $(2, 2)$  w.r.t. the classes  $H_1$  and  $H_2$  in  $\mathbb{P}^1 \times \mathbb{P}^1$ , namely as  $(2, 2) = (1, 1) + (1, 1)$ ,  $(2, 2) = (1, 0) + (1, 2)$  and  $(2, 2) = (0, 1) + (2, 1)$  respectively.

The first type of factorization of (6.35) corresponding to  $(2, 2) = (1, 1) + (1, 1)$  is given by

$$p_{F_2} \stackrel{!}{=} b_1 [(y + \alpha_1 s)x + (\alpha_2 y + \alpha_3 s)t] [(y + \beta_1 s)x + (\beta_2 y + \beta_3 s)t]. \quad (6.55)$$

Clearly, both factors are bilinear in  $[x : t]$  and  $[y : s]$ , respectively, as required. As before, we can factor out  $b_1$  because it must not vanish at a codimension two locus. We note that there are six unknown polynomials  $\alpha_j$  and  $\beta_k$  and eight non-trivial constraints, as can be seen by a comparison of coefficients on both sides. Thus, the ideal of constraints is over-determined and imposes a codimension two condition on the coefficients  $b_i$  for a solution to (6.55) to exist. The elimination ideal, that we call  $I_{(1)}$ , obtained by eliminating the unknowns  $\alpha_j$  and  $\beta_k$  from the ideal of constraints is generated by 50 polynomials. It is checked to be codimension two in the ring, as expected, proving the existence of the factorization (6.55) at codimension two. We denote the zero set of  $I_{(1)}$  by  $V(I_{(1)})$ , which is the geometric codimension two locus in  $B$ .

Next, we note that each curve of the  $I_2$ -fiber described by (6.55) has intersection one with both two-sections  $\hat{s}_0^{(2)}$  and  $\hat{s}_1^{(2)}$ . The U(1)-charge computed using (6.14) and (6.50) is zero. We also note that the representation has charge  $(-)$  under the discrete symmetry because the two intersection points of  $\hat{s}_0^{(2)}$  with the fiber are interchanged under a monodromy action. Formally, the charge under  $\mathbb{Z}_2$  is computed using (6.14) together with the

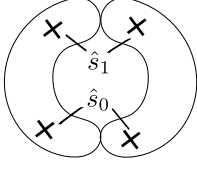
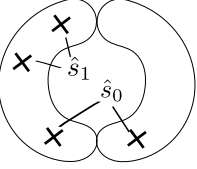
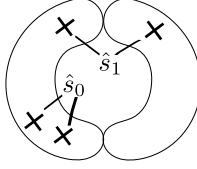
Representation	Multiplicity	Fiber	Locus
$\mathbf{1}_{(0,-)}$	$6[K_B^{-1}]^2 + 4[K_B^{-1}](\mathcal{S}_7 + \mathcal{S}_9) - 2\mathcal{S}_7^2 - 2\mathcal{S}_9^2$		$V(I_{(1)})$
$\mathbf{1}_{(1,-)}$	$6[K_B^{-1}]^2 + 4[K_B^{-1}](\mathcal{S}_9 - \mathcal{S}_7) + 2\mathcal{S}_7^2 - 2\mathcal{S}_9^2$		$V(I_{(2)})$
$\mathbf{1}_{(1,+)}$	$6[K_B^{-1}]^2 + 4[K_B^{-1}](\mathcal{S}_7 - \mathcal{S}_9) - 2\mathcal{S}_7^2 + 2\mathcal{S}_9^2$		$V(I_{(3)})$

Table 6.2: Charged matter representations under  $U(1) \times \mathbb{Z}_2$  and corresponding codimension two fibers of  $X_{F_2}$ .

divisor class (6.54), showing that both curves in the  $I_2$ -fiber have  $\mathbb{Z}_2$ -charge  $(-)$ . Thus, the representation at the locus  $V(I_{(1)})$  is  $\mathbf{1}_{(0,-)}$  as shown in Table 6.2.

The second type of factorization of (6.35) into two polynomials of degrees  $(1, 0)$  and  $(1, 2)$ , respectively, takes the following explicit form

$$p_{F_2} \stackrel{!}{=} b_1 [y + \alpha_1 s] [(y + \beta_1 s)x^2 + (\beta_2 y + \beta_3 s)xt + (\beta_4 y + \beta_5 s)t^2], \quad (6.56)$$

where  $\alpha_1$  and the  $\beta_k$  are six unknown polynomials. We compute again the elimination ideal, denote  $I_{(2)}$ , that is generated by eight polynomials in the  $b_i$  and check that it is codimension two in the ring. The corresponding codimension two locus in  $B$  supporting this type of  $I_2$ -fiber is denoted by  $V(I_{(2)})$ . The intersection pattern of the two-sections with the  $I_2$ -fiber is shown in the second entry of Table 6.2. The  $U(1)$ - and  $\mathbb{Z}_2$ -charges readily follow as discussed before and we find the representation at this locus to be  $\mathbf{1}_{(1,-)}$ .

Finally, the last type of factorization corresponds to a split of (6.35) into two polynomials of degrees  $(0, 1)$  and  $(2, 1)$ . It can be written down explicitly and takes a similar form as (6.56). The codimension two elimination ideal corresponding to this factorization, denoted by  $I_{(3)}$ , is generated by eight polynomials and its vanishing set is denoted by  $V(I_{(3)})$ . The intersection pattern of the two-sections with this type of  $I_2$ -fiber is shown in the last entry of Table 6.2. Using the charge formula (6.14) and the Shioda map (6.50), as well as (6.54) we show that the representation at  $V(I_{(3)})$  is  $\mathbf{1}_{(1,+)}$ .

As a confirmation of the completeness of our analysis of codimension two singularities of  $X_{F_2}$  supporting  $U(1)$ -charged matter, we recall that the codimension two locus supporting all  $I_2$ -singularities associated to a  $U(1)$  is given by (6.15). In the case at hand we have to evaluate this constraint for the rational sections of  $J(X_2)$  with coordinates  $[x_1 : y_1 : z_1]$  given in (6.49). We calculate all associated prime ideals of the obtained complete intersection using Singular [40] and indeed find precisely the two prime ideals  $I_{(2)}$  and  $I_{(3)}$  corresponding to the two representations  $\mathbf{1}_{(1,-)}$  and  $\mathbf{1}_{(1,+)}$  found previously using the elimination ideal technique.

As a next step, we calculate the homology classes in  $B$  for the three codimension two loci supporting the  $I_2$ -fibers, which determine, according to Section 6.2.3, the multiplicities of 6D charged hyper multiplets in the corresponding representations. We begin with the variety  $V(I_{(3)})$ , whose multiplicity we denote by  $x_{\mathbf{1}_{(1+)}}$ , supporting the representation  $\mathbf{1}_{(1,+)}$ . Its homology class is computed by taking two constraints of the ideal  $I_{(3)}$  and computing the homology class of the complete intersection described by them. Then, we subtract (with their corresponding orders) those components that are inside this complete intersection but do not satisfy the other generators of the ideal  $I_{(3)}$ . We obtain:

$$\begin{aligned} x_{\mathbf{1}_{(1+)}} &= [b_2^2 b_{10}^2] \cdot [b_{10} b_2 b_5] - 2([b_2 b_{10}] \cdot [b_2 b_7] - [b_2] \cdot [b_3]), \\ &= 6[K_B^{-1}]^2 + 4[K_B^{-1}](\mathcal{S}_7 - \mathcal{S}_9) - 2\mathcal{S}_7^2 + 2\mathcal{S}_9^2. \end{aligned} \tag{6.57}$$

The multiplicity of  $V(I_{(2)})$ , denoted by  $x_{\mathbf{1}_{(1,-)}}$ , can be calculated in a similar way. It is given in the third row of Table 6.2. As a consistency check, we calculate the sum of both multiplicities and it agrees with  $[y_1] \cdot [fz_1^4]$  as it should, because the  $I_{(2)}$  and  $I_{(3)}$  are the two associated prime ideals of (6.15) for the section (6.49).

For the computation of the multiplicity of the variety  $V(I_{(1)})$ , denoted by  $x_{\mathbf{1}_{(0,-)}}$ , we cannot carry out the previously mentioned algorithm, due to the size and complexity of the ideal  $I_{(1)}$ . Instead,  $x_{\mathbf{1}_{(0,-)}}$  is obtained by first calculating the multiplicity of all hyper multiplets charged under the discrete symmetry, namely the  $\mathbf{1}_{(0,-)}$  and  $\mathbf{1}_{(1,-)}$ , and then subtracting the number of hyper multiplets in the representation  $\mathbf{1}_{(1,-)}$ , that we already know.

We begin by noting that the total number of charge  $(-)$  hyper multiplets under the  $\mathbb{Z}_2$  symmetry was calculated geometrically in [99, 3] for a genus-one fibration given by the quartic curve in  $\mathbb{P}^2(1, 1, 2)$ . Indeed, we can directly use their results since we can transform the biquadric (6.35) to a quartic presentation. This quartic is to be obtained by taking the discriminant of the biquadric (6.35) with respect to  $y$ . To this end, we rewrite the biquadric in the suggestive form

$$p = A(x, t)y^2 + B(x, t)ys + C(x, t)s^2 \quad (6.58)$$

and then take the discriminant of this quadric in  $y$  (we also set  $s = 1$ ). We construct a genus-one curve as the double cover over this discriminant, which is then a quartic in  $[x : t]$  and a new variable  $w$  of weight two of the form

$$w^2 = B(x, t)^2 - 4A(x, t)C(x, t) \equiv e_0x^4 + e_1x^3t + e_2x^2t^2 + e_3xt^3 + e_4t^4. \quad (6.59)$$

Here we used the conventions of [99] in the last equality. The coefficients  $e_i$  can be expressed in terms of the  $b_i$  in (6.35) by a comparison of coefficients.

In this form the reason for choosing the quadric w.r.t. to  $y$  in order to construct the

quartic (6.59) is evident, because the two-section  $\hat{s}_0^{(2)} = X_{F_2} \cap \{x = 0\}$  is mapped to the two-section  $x = 0, w^2 = e_4 t^4$  in (6.59). Using the results in [99, 3], we calculate the multiplicities of all charge  $(-)$  hyper multiplets, both  $\mathbf{1}_{(0,-)}$ ,  $\mathbf{1}_{(1,-)}$ , using the one-to-one correspondence between the loci of  $I_2$ -fibers in (6.59) with the following complete intersection, c.f. equation (2.22) in [99],

$$\{e_1^4 - 8e_0e_1^2e_2 + 16e_0^2e_2^2 - 64e_0^3e_4 = 0\} \cap \{e_3 = 0\}. \quad (6.60)$$

Its homology class is readily given as  $[4e_1] \cdot [e_3]$ , which has to agree as mentioned before with the sum  $x_{\mathbf{1}_{(1,-)}} + x_{\mathbf{1}_{(0,-)}}$ . Thus, the multiplicity  $x_{\mathbf{1}_{(0,-)}}$  follows by subtracting the multiplicity  $x_{\mathbf{1}_{(1,-)}}$  calculated previously from  $[4e_1] \cdot [e_3]$ . The result is given in the second row of Table 6.2.

To complete the matter spectrum we calculate the number of neutral hyper multiplets. Using (6.12) and the explicit formula for the Euler number of  $X_{F_2}$ , we obtain

$$H_{\text{neut}} = 13 + 11[K_B^{-1}]^2 - 4[K_B^{-1}]\mathcal{S}_7 + 2\mathcal{S}_7^2 - 4[K_B^{-1}]\mathcal{S}_9 + 2\mathcal{S}_9^2. \quad (6.61)$$

Using this together with the charged matter spectrum in Table 6.2, the number of vector multiplets  $V = 1$  and the height pairing (6.51) we confirm that all anomalies, including the purely gravitational one, are canceled.

### **Yukawa couplings in $X_{F_2}$**

We conclude this section by stating the geometrically realized Yukawa couplings. We find the single Yukawa coupling in Table 6.3, by checking explicitly that the corresponding varieties intersect at codimension three, i.e. that the ideal  $I_{(1)} \cup I_{(2)} \cup I_{(3)}$  is codimension three in the ring generated by the coefficients  $b_i$ .

### 6.4.3 Polyhedron $F_3$ : $G_{F_3} = \mathbf{U}(1)$

We construct a Calabi-Yau manifold, denoted  $X_{F_3}$ , as a fibration of the toric hypersurface in  $\mathbb{P}_{F_3} = dP_1$  over a base  $B$ . The polyhedron of  $F_3$  along with a choice of projective coordinates as well as its dual polyhedron are depicted in Figure 6.5. The coordinate  $e_1$  vanishes on

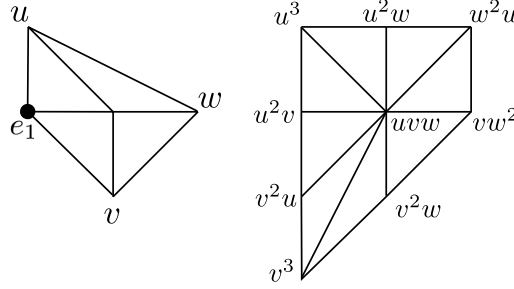


Figure 6.5: Polyhedron  $F_3$  with a choice of projective coordinates and its dual  $F_{14}$  with the corresponding monomials. We have set  $e_1 = 1$  for brevity of our notation. The zero section is indicated by the dot.

the exceptional divisor  $E_1$  of  $dP_1$  and  $[u : v : w]$  are the pullback under the blow-down map  $dP_1 \rightarrow \mathbb{P}^2$  of the  $\mathbb{P}^2$ -coordinates. The SR-ideal of  $dP_1$  reads

$$SR_{F_3} = \{uv, we_1\}. \quad (6.62)$$

Using (6.24) we construct the Calabi-Yau manifold  $X_{F_3}$  as the hypersurface

$$p_{F_3} = s_1 u^3 e_1^2 + s_2 u^2 v e_1^2 + s_3 u v^2 e_1^2 + s_4 v^3 e_1^2 + s_5 u^2 w e_1 + s_6 u v w e_1 + s_7 v^2 w e_1 + s_8 u w^2 + s_9 v w^2, \quad (6.63)$$

in the ambient space (6.25), that in the case at hand is a  $dP_1$ -fibration over  $B$ . The coordinates  $[u : v : w : e_1]$  and the coefficients  $s_i$  take values in the line bundles in (6.31).

The Calabi-Yau manifold  $X_{F_3}$  is an elliptic fibration. This is clear because for a generic point on  $B$  there is one marked point  $P_0$  on its fiber, which is the intersection of  $e_1 = 0$  with (6.63). This point gives rise to a section of  $X_{F_3}$ , which we choose as the zero section. Its



generic coordinates read

$$\hat{s}_0 = X_{F_3} \cap \{e_1 = 0\} : [s_9 : -s_8 : 1 : 0]. \quad (6.64)$$

There always exists a second section of  $X_{F_3}$ , which generates a rank one MW-group.<sup>12</sup> We emphasize that this second section is not toric, i.e. not given as the intersection of a toric divisor in the fiber  $\mathbb{P}_{F_3}$  with the hypersurface (6.63), in contrast to the zero section (6.64).

This can be seen as follows. Without loss of generality, set  $e_1 = 1$  in (6.63) and consider it as an elliptic curve  $\mathcal{E}$  over a field  $K$ . Then construct the tangent  $t_P$  to the point  $P_0$  which now is at  $[u : v : w] = [0 : 0 : 1]$ . It is determined by requiring that along  $t_P$  both  $p_{F_3}$  and its first derivative vanish at  $P_0$ , i.e. that  $P_0$  is a point of intersection two of  $\mathcal{E}$  and  $t_P$ . It is described by

$$t_P = s_8 u + s_9 v. \quad (6.65)$$

Since (6.63) is a curve of degree three, every line has to intersect it at three points. Thus,  $t_P = 0$  intersects  $\mathcal{E}$  at a third point, denoted by  $P_1$ , which is automatically rational. It gives rise to a *rational section* of  $X_{F_3}$ , with generic coordinates

$$\hat{s}_1 = X_{F_3} \cap \{t_P = 0\} : [-s_9 : s_8 : s_1 s_9^3 - s_4 s_8^3 + s_3 s_9 s_8^2 - s_2 s_9^2 s_8 : s_7 s_8^2 - s_6 s_9 s_8 + s_5 s_9^2]. \quad (6.66)$$

Thus, the elliptic fibration  $X_{F_3}$  indeed has a rank one MW-group with a non-toric generator, as claimed. The Shioda map (6.6) of the section  $\hat{s}_1$  reads

$$\sigma(\hat{s}_1) = S_1 - S_0 + 3[K_B] + S_7 - 2S_9, \quad (6.67)$$

where  $S_1, S_0$  are the divisor classes of the rational sections  $\hat{s}_1$  and  $\hat{s}_0$ .

---

<sup>12</sup>We note that this is not in contradiction with the results of [19]. There the toric Mordell-Weil group is computed, which is indeed trivial.

This result allows us to compute the height pairing of the section  $\hat{s}_1$ . We obtain

$$b_{11} = -2(3[K_B] + \mathcal{S}_7 - 2\mathcal{S}_9), \quad (6.68)$$

where we employed (6.7) along with the self-intersection (6.8) for the section  $\hat{s}_1$  as well as

$$\pi(\mathcal{S}_1 \cdot \mathcal{S}_0) = [z_1] = 2[K_B^{-1}] + 2\mathcal{S}_9 - \mathcal{S}_7. \quad (6.69)$$

This follows by noting that  $\pi(\mathcal{S}_0 \cdot \mathcal{S}_1)$  is the locus in  $B$  where the coordinates (6.64) and (6.66) of the two sections agree, which happens at  $z_1 := s_7 s_8^2 - s_6 s_8 s_9 + s_5 s_9^2 = 0$ , that is precisely the  $z$ -coordinate of  $\hat{s}_1$  in the WSF, cf. (6.70). The divisor class of  $z_1$  is read off from (6.31).

### Weierstrass form and gauge group

We can apply Nagell's algorithm to the cubic (6.63) with respect to the point  $P_0$  to obtain a birational map to its WSF. We plug the coordinates of the rational section (6.66) into this map to obtain its coordinates in WSF,

$$z_1 = s_7 s_8^2 - s_6 s_8 s_9 + s_5 s_9^2, \quad x_1 = s_4^2 s_8^6 + \dots = p_8(\underline{s}), \quad y_1 = -s_4^3 s_8^9 + \dots = p_{12}(\underline{s}). \quad (6.70)$$

Here  $p_8(\underline{s})$  and  $p_{12}(\underline{s})$  are two homogeneous polynomials in the coefficients  $s_i$  of degree eight and twelve, respectively. We have written out only one monomial in  $x_{Q_1}$  and  $y_{Q_1}$ , respectively, in order to be able to determine their divisor classes. We refer the reader to the Appendix in [80] for the explicit and lengthy expressions for  $p_8(\underline{s})$  and  $p_{12}(\underline{s})$ .

Furthermore, we determine the functions  $f$ ,  $g$  and the discriminant  $\Delta$  of the WSF for  $X_{F_3}$ . They are given by specializing the cubic as  $s_{10} = 0$ . We observe that there is no factorization of  $\Delta$  indicating the absence of codimension one singularities and a non-Abelian

gauge group. Thus, the full gauge group on  $X_{F_3}$  is given by the single  $U(1)$  associated to its rank one MW-group,

$$G_{F_3} = U(1). \quad (6.71)$$

We emphasize again that the generator (6.66) of the MW-group of  $X_{F_3}$  is not toric.

### **Charged and uncharged matter**

Since the Calabi-Yau manifold  $X_{F_3}$  has a non-trivial MW-group, it automatically has  $I_2$ -fibers at codimension two in  $B$ , that support  $U(1)$ -charged matter.

We first summarize the charged matter spectrum of  $X_{F_3}$  before we discuss its derivation in detail. The full charged matter spectrum is shown in Table 6.4, which includes the  $U(1)$ -charges and the multiplicities of 6D charged hyper multiplets, as well as a schematic presentation of the corresponding reducible fibers and the full expressions for the codimension two loci.

The starting point for the derivation of the matter spectrum of  $X_{F_3}$  is, as discussed in Section 6.2.3, the complete intersection (6.15) in  $B$  with the WS-coordinates (6.66) of the section  $\hat{s}_1$  inserted:

$$y_1 = fz_1^4 + 3x_1^2 = 0. \quad (6.72)$$

We show that (6.72) is a reducible variety with three irreducible components supporting matter with charges one, two and three. The corresponding codimension two loci are denoted  $V(I_{(1)})$ ,  $V(I_{(2)})$  and  $V(I_{(3)})$ , respectively, with  $I_{(1)}$ ,  $I_{(2)}$  and  $I_{(3)}$  denoting the corresponding prime ideals, cf. Table 6.4. In order to strictly prove that these three varieties are all irreducible components of the complete intersection (6.72), we have to compute all its associated prime ideals. Unfortunately, this is unfeasible with the available computing power and computer algebra programs, due to the high degree of the two polynomials in (6.72). However, we explain that  $X_{F_3}$  has three possible types of  $I_2$ -fibers corresponding to

the three possible factorizations of (6.63) and that these factorization happen precisely at the codimension two loci  $V(I_{(1)})$ ,  $V(I_{(2)})$  and  $V(I_{(3)})$ . Thus, we claim that the corresponding ideals  $I_{(1)}$ ,  $I_{(2)}$  and  $I_{(3)}$  are the only associated prime ideals of (6.72). We will further substantiate this claim by checking 6D anomaly cancellation at the end of this section as well as by reproducing the spectrum of  $X_{F_3}$  by Higgsing the effective theories of  $X_{F_5}$  and  $X_{F_6}$ .

We begin by analyzing the fiber at the first two codimension two loci in Table 6.4. These are precisely the loci where the coordinates (6.66) of the section  $\hat{s}_1$  are ill-defined, since they are forbidden by the SR-ideal (6.62). This indicates, that the section  $\hat{s}_1$  does not mark a point on the elliptic fiber of  $X_{F_3}$ , but does wrap an entire  $\mathbb{P}^1$ . Since the rational section is non-toric, determining the wrapped  $\mathbb{P}^1$  is slightly more involved than usual, as we demonstrate next.

First, we consider the locus  $V(I_{(3)}) = \{s_8 = s_9 = 0\}$ , which we readily check to obey (6.72). At this locus the constraint (6.63) factorizes as

$$p_{F_3}|_{s_8=s_9=0} = e_1(s_1u^3e_1 + s_2u^2ve_1 + s_3uv^2e_1 + s_4v^3e_1 + s_5u^2w + s_6uvw + s_7v^2w). \quad (6.73)$$

Clearly,  $V(I_{(3)})$  is the only codimension two locus where this factorization can occur. We immediately observe that the zero section  $\hat{s}_0$  defined by (6.64) has wrapped the entire rational curve  $e_1 = 0$  in (6.73). The rational section  $\hat{s}_1$  can be identified at this locus by recalling the definition of the point (6.66) as the second intersection point of the tangent to  $P_0$  with  $\mathcal{E}$ . However, at  $s_8 = s_9 = 0$  the curve (6.73) is singular (after setting  $e_1 = 1$ ) precisely at  $P_0$ . Thus, *every* line through  $P_0$  is automatically tangential at  $P_0$ . This simply means that  $P_1$  has become the *entire* singular fiber at  $s_8 = s_9 = 0$ , since given any point on (6.73) (for  $e_1 = 1$ ) we can construct a tangent at  $P_0$  that passes through that point. Thus, at  $s_8 = s_9 = 0$  the section  $\hat{s}_1$  wraps the rational curve described by the parenthesis in (6.73). The resulting

fiber at  $V(I_{(3)})$  is shown in the second column of Table 6.4. We readily compute using the charge formula (6.14) that the U(1) charge of the matter is indeed  $q = 3$  and its multiplicity is given by  $[s_8] \cdot [s_9]$ , which after using (6.31), yields the result shown in Table 6.4. We emphasize that this is the first occurrence of matter with charge  $q > 2$  in models with Abelian gauge symmetry in F-theory.

Second, we consider the locus  $V(I_{(2)})$ . The complete intersection in  $V(I_{(2)})$  shown in Table 6.4 has two irreducible components, one of which given by  $V(I_{(3)})$ , that we forbid by requiring  $(s_8, s_9) \neq (0, 0)$ , and a second one described by a prime ideal  $I_{(2)}$  with ten generators.<sup>13</sup> The variety  $V(I_{(2)})$  supports matter of charge two. We can check this locally by solving the complete intersection inside  $V(I_{(2)})$  e.g. for  $s_3$  and  $s_6$  and by plugging this solution into (6.63). Indeed, the fiber splits into a line and a non-singular quadric  $q_2(e_1u, e_1v, w)$ ,

$$p_{F_3} \rightarrow (s_8u + s_9v)q_2(e_1u, e_1v, w). \quad (6.74)$$

Furthermore, we prove that  $V(I_{(2)})$  is the only locus that can yield an  $I_2$ -fiber of this type by computing the elimination ideal of the ideal of constraints necessary for the factorization (6.74). We see that the zero section (6.64) is well-defined at  $V(I_{(2)})$  and passes through the line. However, the rational section (6.66) is ill-defined. This is clear because the line in (6.74) is precisely the tangent  $t_P$  at  $P_0$  defined in (6.65) and since the section  $\hat{s}_1$  is defined as the intersection of  $t_P$  with  $\mathcal{E}$ . Thus, the section  $\hat{s}_1$  at  $V(I_{(2)})$  wraps the entire rational curve given by the line in (6.74). Again we use (6.14) to show that the U(1)-charge is  $q = 2$ , as claimed in Table 6.4. The multiplicity of a 6D hyper multiplet in the representation  $\mathbf{1}_2$  is given by the homology class of  $V(I_{(2)})$ . It is computed by first computing the homology class of the complete intersection in  $V(I_{(2)})$  in Table 6.4 using (6.31) and by subtracting the class of the unwanted component  $V(I_{(3)})$  with the appropriate order. We determine it to be six using the resultant technique of [34], which precisely yields the multiplicity in the third

---

<sup>13</sup>As all prime ideals in this work, it is computed by the primary decomposition function in Singular [40].

row of Table 6.4.

Finally, we turn to the codimension two locus  $V(I_{(1)})$  supporting matter of charge one. In order for the charge formula (6.14) to produce charge one for an  $I_2$ -fiber, both  $\hat{s}_0$  and  $\hat{s}_1$  have to be regular and pass through different rational curves in the  $I_2$ -fiber. This can only happen for a factorization of (6.63) of the form (we can set  $e_1 = 1$ )

$$p_{F_3} \rightarrow (d_1u + d_2v + d_3w)q_2(u, v, w), \quad (6.75)$$

with  $q_2(u, v, w)$  denoting a quadric without the monomial  $w^2$ . We note that all coefficients  $d_i$ ,  $i = 1, 2, 3$ , have to be non-vanishing since  $d_1 = 0$ ,  $d_2 = 0$  or  $d_3 = 0$  lead to a factorization in (6.75) that cannot happen at codimension two. We see that  $\hat{s}_0$  intersects the quadric  $q_2 = 0$  and  $\hat{s}_1$  intersects the line, as required for matter with charge one. Furthermore, we compute the elimination ideal, denoted by  $I_{(1)}$ , of the ideal of constraints necessary for the factorization (6.75). It is prime and of codimension two in the ring, that means that the factorization (6.75), indeed, occurs in codimension two in  $B$ . In addition, we check that the complete intersection (6.15) is inside the ideal  $I_{(1)}$  and that  $I_{(1)}$  is in turn not contained in  $I_{(3)}$  or  $I_{(2)}$ , as required. Thus, we identify  $I_{(1)}$  as the third and last associated prime ideal of (6.72).

Under the well-motivated assumption that  $I_{(3)}$ ,  $I_{(2)}$  and  $I_{(1)}$  are the only associated prime ideals of (6.72), we determine the multiplicity of the  $\mathbf{1}_1$ -matter as follows. First, we determine the orders of the loci  $V(I_{(3)})$  and  $V(I_{(2)})$  in the complete intersection (6.14). Using the resultant technique of [34] and random integers for some of the  $s_i$  we find the orders 81 and 16 for these loci, respectively. Then, we subtract their multiplicities with these orders from the class of the complete intersection (6.72) and obtain, using (6.31), the multiplicity in the last row of Table 6.4.

The matter spectrum of  $X_{F_3}$  is completed by the number of neutral hyper multiplets

$H_{\text{neut}}$ . Employing (6.12) and the Euler number  $\chi(X_{F_3})$  of  $X_{F_3}$ , we obtain

$$H_{\text{neutral}} = 13 + 11[K_B^{-1}]^2 - 3[K_B^{-1}]\mathcal{S}_7 + 3\mathcal{S}_7^2 - 4[K_B^{-1}]\mathcal{S}_9 - 2\mathcal{S}_7\mathcal{S}_9 + 2\mathcal{S}_9^2. \quad (6.76)$$

Finally, we check anomaly-freedom of the full 6D SUGRA theory. To this end we use (6.68), the charged spectrum in Table 6.4 and (6.76), together with  $V = 1$ , to show that all relevant anomalies of the 6D SUGRA theory in (3.100) are canceled.

There is another quantum consistency condition the spectrum in Table 6.4 has to pass. In order to have an effective theory that makes sense also in a quantum gravity model, it has been argued in [6] that all charges allowed by Dirac quantization have to be present in the spectrum. Indeed, it is clear from the multiplicity formulas in Table 6.4 (e.g. by evaluation for a concrete base  $B$ , that if matter with a maximal charge  $q$  is present in the spectrum, also matter with all lower charges  $q' < q$  is automatically there, as required.

For completeness, we include a discussion of the Yukawa couplings. Forming the union of the ideals and computing their codimension to be three in the polynomial ring  $K[s_i]$ , we find the two Yukawa couplings given in Table 6.5.

### **An alternative perspective: $X_{F_3}$ from $X_{F_5}$ by an extremal transition**

There is a second perspective on  $X_{F_3}$  that provides an alternative explanation for the presence of the rational point (6.66) and that will be useful for the understanding of the Higgs transition. The following can be skipped on a first reading, as it is not important for the main thread of this work.

We begin by noting that (6.63) becomes singular if we tune the complex structure so that  $s_4 \equiv 0$ . The induced  $I_2$ -singularities occur at codimension two and can be resolved by the blow-up in the fiber at  $u = w = 0$ . The Calabi-Yau manifold after this extremal

transition is precisely  $X_{F_5}$ . It has been shown that  $X_{F_5}$  has a rank two Mordell-Weil group [74, 34].

In the singular fibration with all exceptional divisors blown down, the three rational points on the fiber  $\mathcal{C}_{F_5}$  are the three intersection points with the line  $u = 0$ . One point agrees with the origin (6.64) of  $X_{F_3}$ . We denote the other two points by  $Q_1, Q_2$ . This implies that the point  $Q_1 + Q_2$  is precisely given by (6.66), in the limit  $s_4 \equiv 0$ . Indeed, the group law on a cubic curve is defined so that the point  $Q_1 + Q_2$  is found by first constructing the third intersection point of the line through  $Q_1$  and  $Q_2$  and then by forming the line through that point and the origin  $P_0$ . This line again has a third intersection point with the curve, which is defined to be  $Q_1 + Q_2$ . In our situation, the line through  $Q_1$  and  $Q_2$  is  $u = 0$ . Thus, the third intersection point of  $u = 0$  with  $\mathcal{E}$  is the origin  $P_0$ . Consequently, the point  $Q_1 + Q_2$  is the second intersection point of the *tangent* through  $P_0$  with the elliptic curve. In fact, it can be checked by performing this addition on the fiber of  $X_{F_5}$  explicitly that the coordinates of the point  $Q_1 + Q_2$  on the fiber of  $X_{F_5}$  agree with the coordinates (6.66) after setting  $s_4 \equiv 0$ . Furthermore, we compute the Weierstrass coordinates of  $Q_1 + Q_2$  that also agree with (6.70) after setting  $s_4 \equiv 0$ .<sup>14</sup>

This is not surprising since we recall that the  $P_1$  in  $X_{F_3}$  has been constructed as the second intersection of the tangent (6.65) to  $P_0$ . Thus, we see that the section  $\hat{s}_1$  can be understood as the sum of the sections  $\hat{s}_1 + \hat{s}_2$  on  $X_{F_5}$ , which *survives* the extremal transition  $X_{F_5} \leftrightarrow X_{F_3}$ , i.e. the complex structure deformation associated to switching on  $s_4$ . In contrast, the individual sections  $\hat{s}_1$  and  $\hat{s}_2$  on  $X_{F_5}$  do not map to rational sections on  $X_{F_3}$ . As consequence, the U(1)-charges of matter in  $X_{F_3}$  are given by the sum of the U(1)-charges  $q_1 + q_2$  on  $X_{F_5}$ .

---

<sup>14</sup>The coordinates of  $Q_1 + Q_2$  in WSF are obtained by inserting its coordinates into the birational map from  $X_{F_5}$  to its WSF. We note that the result agrees with the WS-coordinates of  $Q_1 + (-Q_2)$ , *not*  $Q_1 + Q_2$ , where ‘+’ denotes here the addition in the WSF of  $X_{F_5}$ .



We can make these statements even more explicit by mapping  $X_{F_3}$  to  $X_{F_5}$ . The shift

$$w \mapsto w - \frac{s_7 + \sqrt{s_7^2 - 4s_4s_9}}{2s_9} e_1 v \quad (6.77)$$

precisely cancels the monomial proportional to  $s_4$  in (6.63). Clearly, this requires an extension of the field of meromorphic functions on  $B$  by the square root  $\sqrt{s_7^2 - 4s_4s_9}$ . Thus, this map is certainly not birational. After this shift, we precisely obtain the hypersurface of  $X_{F_5}$ , for  $e_2 = 1$ . Due to the shift (6.77), the coefficients  $s_i$  in  $X_{F_5}$  have to be replaced by

$$\begin{aligned} s_2 &\mapsto s_2 - s_5 \frac{s_7 + \sqrt{s_7^2 - 4s_4s_9}}{2s_9}, & s_3 &\mapsto s_3 - \frac{s_4s_8}{s_9} + \frac{(s_7s_8 - s_6s_9)(s_7 + \sqrt{s_7^2 - 4s_4s_9})}{s_9^2}, \\ s_6 &\mapsto s_6 - s_8 \frac{s_7 + \sqrt{s_7^2 - 4s_4s_9}}{s_9}, & s_7 &\mapsto -\sqrt{s_7^2 - 4s_4s_9}, \end{aligned} \quad (6.78)$$

with  $s_1, s_5, s_8$  and  $s_9$  unchanged. If we insert this variable transformation into the expressions for  $\hat{s}_1$  or  $\hat{s}_2$  in the  $F_5$  section of [80], we introduce square roots, i.e. these sections do not map to rational sections on  $X_{F_3}$ . However, if we insert (6.78) into the coordinates for  $\hat{s}_1 + \hat{s}_2$  on  $X_{F_5}$ , we precisely reproduce (6.66), i.e. all square roots cancel.

Furthermore, we can re-derive the Weierstrass coordinates (6.70) of  $\hat{s}_1$  on  $X_{F_3}$  by first computing the Weierstrass coordinates of  $Q_1 + Q_2$  and then inserting (6.78). In addition,  $f$  and  $g$  of the WSF of  $X_{F_3}$  can be obtained from the WSF for  $X_{F_5}$  by insertion of (6.78).

Yukawa	Locus
$\mathbf{1}_{(1,-)} \cdot \overline{\mathbf{1}}_{(1,+)} \cdot \mathbf{1}_{(0,-)}$	$V(I_{(1)}) \cap V(I_{(2)}) \cap V(I_{(3)})$

Table 6.3: Codimension three locus and corresponding Yukawa coupling for  $X_{F_2}$ .

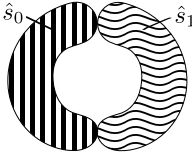
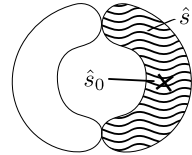
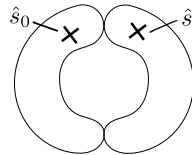
Representation	Multiplicity	Fiber	Locus
$\mathbf{1}_3$	$\mathcal{S}_9([K_B^{-1}] + \mathcal{S}_9 - \mathcal{S}_7)$		$V(I_{(3)}) := \{s_8 = s_9 = 0\}$
$\mathbf{1}_2$	$6[K_B^{-1}]^2 + [K_B^{-1}](4\mathcal{S}_9 - 5\mathcal{S}_7) + \mathcal{S}_7^2 + 2\mathcal{S}_7\mathcal{S}_9 - 2\mathcal{S}_9^2$		$V(I_{(2)}) := \{s_4s_8^3 - s_3s_8^2s_9 + s_2s_8s_9^2 - s_1s_9^3 = s_7s_8^2 + s_5s_9^2 - s_6s_8s_9 = 0 \text{ with } (s_8, s_9) \neq (0, 0)\}$
$\mathbf{1}_1$	$12[K_B^{-1}]^2 + [K_B^{-1}](8\mathcal{S}_7 - \mathcal{S}_9) - 4\mathcal{S}_7^2 + \mathcal{S}_7\mathcal{S}_9 - \mathcal{S}_9^2$		$V(I_{(1)}) := \{(6.72)\} \setminus (V(I_{(2)}) \cup V(I_{(3)}))$

Table 6.4: Charged matter representation under U(1) and codimension two fibers of  $X_{F_3}$ .

Yukawa	Locus
$\mathbf{1}_1 \cdot \mathbf{1}_1 \cdot \overline{\mathbf{1}}_2$	$V(I_{(1)}) \cap V(I_{(2)})$
$\mathbf{1}_1 \cdot \mathbf{1}_2 \cdot \overline{\mathbf{1}}_3$	$V(I_{(1)}) \cap V(I_{(2)}) \cap V(I_{(3)})$

Table 6.5: Codimension three loci and corresponding Yukawa couplings for  $X_{F_3}$ .

## Vacua with $\mathbb{Z}_3$ Gauge Symmetry

In the previous chapter we discovered compactifications that support the discrete  $\mathbb{Z}_3$  gauge group. They are the elliptic fibrations where the ambient space of the fiber is  $\mathbb{P}^2$  or  $X_{F_1}$ . Although we did a thorough study of the physics of the compactification, there were some loose ends. Specifically, the underlying Tate-Shafarevich group was not computed. Even worse, three different geometries are supposed to be the three different elements of this Tate-Shafarevich group. However, only two of them were known, the cubic curve and the jacobian fibrations.

In this chapter, that follows [36] closely, we solve the mystery of the third geometry. We make use of the 6D/5D F- M-theory duality and the Higgs mechanism.

### 7.1 Introduction

Discrete symmetries play a key rôle for constructing extensions of the standard model of particle physics. In particular, discrete symmetries are used to forbid terms in the MSSM superpotential that would allow for fast proton decay or other processes which are highly suppressed in the standard model. Well known examples are provided by R-parity ( $\mathbb{Z}_2$ ), baryon triality ( $\mathbb{Z}_3$ ) and proton hexality ( $\mathbb{Z}_6$ ) [70, 71, 44]. Conceptually, these discrete

symmetries must be realized as discrete gauge symmetries arising, for example, as remnants of a broken  $U(1)$  symmetries because global discrete symmetries cannot exist in a theory of quantum gravity [6].

The understanding of the geometrical origin of discrete gauge symmetries in F-theory compactifications is therefore of crucial interest both for conceptual as well as for phenomenological reasons. Here, discrete gauge symmetries arise from Calabi-Yau geometries which are only genus-one fibrations without section, in contrast to elliptic fibrations with sections. Recently, there has been progress in understanding the physics of such compactifications, starting with [18] and followed by [99, 3, 48, 21, 93, 94, 80]. A natural object which is attached to this kind of compactifications is given by the Tate-Shafarevich (TS) group of the genus-one fibration which is a discrete group that organizes inequivalent genus-one geometries which share the same associated Jacobian fibration. An F-theory compactification on a genus-one fibration does only depend on the Weierstrass equation, that is the Jacobian fibrations, and is, thus, insensitive to the chosen element of the TS-group. The TS-group determines the resulting discrete gauge symmetries of the F-theory compactification. In contrast, M-theory compactifications on different elements in the TS-group of the genus-one fibration are physically distinct. This is consistent with M-/F-theory duality due to the additional degree of freedom of the Wilson line of the discrete group in the circle compactification from F-theory to M-theory [39].

Genus-one fibrations do not possess a section, but only multi-sections. A multi-section defining an  $n$ -fold branched cover over the base of the genus-one fibration is referred to as a  $n$ -section. The moduli space of F-theory compactifications on genus-one fibrations with an  $n$ -section is connected by an extremal transition to that of compactifications on elliptic fibrations with  $n$  sections. Explicit models with up to three  $U(1)$  factors have been systematically constructed and analyzed for F-theory in [74, 34, 33, 35]. This allows an analysis of the physics using the two dual pictures before and after the transition. This

transition has been identified in the analyzed situations and for Calabi-Yau threefolds as a conifold transition [3, 48]. The vanishing cycles in this transition are rational curves that appear as components of  $I_2$ -fibers which occur at certain codimension two loci in the base of the elliptic fibration. The resulting singular geometry is deformed by a three-sphere  $S^3$  which glues several sections into a multi-section [99]. From the effective field theory point of view, in the blow-down appear a number of massless fields from M2-branes wrapping the vanishing cycle, that acquire a vacuum expectation value (VEV) corresponding to the deformation. In particular, the Higgsing of a  $U(1)^n$  symmetry to  $\mathbb{Z}_n$  symmetry requires for the final step in the chain of Higgsings with a single remaining  $U(1)$  a massless scalar field of charge  $n$ . When compactifying on a circle to M-theory, there is a choice of Wilson line for this  $U(1)$ . There are  $n$  different choices to turn on a Wilson line along the compactification circle yielding  $n$  different vacua of M-theory. Indeed, as this Wilson line also affects the mass formula for the Kaluza-Klein modes one can see that there will be  $n$  inequivalent Kaluza Klein towers that can arise in five dimensions. Notably for each choice of Wilson line, there is one Kaluza-Klein mode within each tower that becomes massless and serves as five-dimensional Higgs field which - once they acquire a vacuum expectation value - lead to  $n$  different five-dimensional vacua. These are to be compared with the  $n$  different M-theory compactifications on the respective elements of the TS group. Geometrically, one thus has to identify  $n$  different vanishing curves that correspond to these  $n$  Kaluza Klein modes of the Higgs field.

Most of the recent works have focused on the case of the gauge group  $\mathbb{Z}_2$  which is the simplest case to consider as the TS-group consists in this case only of the genus one fibration (realized as a hypersurface in  $\mathbb{P}[1, 1, 2]$ ) and its Jacobian. Accordingly, it is possible to identify the two corresponding Higgs fields as arising from the two rational components of the same  $I_2$ -fiber [93, 94].

In this note we extend the above analysis beyond  $\mathbb{Z}_2$  concentrating mainly on the case of

$\mathbb{Z}_3$  which arises from the most general cubic admitting a trisection only, although we expect our findings will also have to play a key role for the understanding of TS-groups of higher order. In the case of  $\mathbb{Z}_3$ , there are three different M-theory vacua. We pursue the strategy to geometrically identify three different curves that give rise to the three different 5D Higgs fields in M-theory that lead to these inequivalent vacua. The main obstacle in identifying these curves is the fact all three curves should be located in the reducible  $I_2$ -fiber at the same codimension two locus in the two-dimensional base. However, an  $I_2$ -fiber naively has only two rational curves, so that the presence of the wanted third curve is elusive. The key result of this note is to identify the third rational curve inside the  $I_2$ -fiber.

We will use two different methods to demonstrate its existence. As a first evidence, we compute a non-zero Gromov-Witten invariant for the elliptic fibration in the class of the purported third curve, that, as expected, agrees with the number of the relevant  $I_2$ -loci. As a stronger check, we consider two different phases of the resolution of the elliptic fibration before the Higgsing. The corresponding geometry is the  $dP_1$ -elliptic fibration considered in [80]. In other words, we extend the above conifold picture by also taking flop transitions<sup>1</sup> into account<sup>2</sup>. In one resolution phase, we are able to manifestly see two curves of the  $I_2$ -fiber leading to two inequivalent vacua after the transition, while the third curve remains invisible. In the second resolution phase, we see again two curves in the  $I_2$ -fiber, however, one of which was not present in the first phase and leading to the *third* vacuum, while one of the original two curves in the first resolution has become invisible. In addition, we argue that there are also in the case of TS-group  $\mathbb{Z}_3$  just two different geometries, namely the most general cubic and its Jacobian. However, the former can be equipped with two different actions of the Jacobian which make them differ as elements of the Tate Shafarevich group,

---

<sup>1</sup>It is worth mentioning that we have to consider a non-toric flop.

<sup>2</sup>A similar phenomenon has already been observed in [117] in the context of tensionless strings in six and five dimensions. In that case too, M-theory is able to see the different phases of the theory arising from flop transitions, while these coincide in the six-dimensional F-theory compactification.

thereby yielding the claimed three different M-theory vacua.

This note consists of two sections. In Section 7.2 we review some aspects of the TS-group and its appearance in M- and F-theory. In particular, we review how the different M-theory vacua can be obtained from a circle compactification with discrete choices for the Wilson line from the unique F-theory compactification, both before and after Higgsing. Then, in Section 7.3, we focus on the explicit construction of the three different curves supporting the Higgses which lead to the three different M-theory vacua. For this analysis we discuss two different resolution phases of the  $dP_1$  geometry.

## 7.2 The Tate-Shafarevich group in M- and F-theory

In this section we discuss some background material that is necessary for our geometrical analysis in section 7.3. We start by elaborating on some mathematical facts about the Tate-Shafarevich group. Then, we continue with a review and slight clarification of the field theory formalisms in 6D and 5D developed in [94, 93, 3, 48].

As already discussed in the introduction, discrete groups naturally arise in F-theory compactifications on genus-one fibered Calabi-Yau manifolds  $X$  that admit instead of a globally well-defined section just an  $n$ -section. To every such genus-one fibration one can associate its corresponding Jacobian fibration  $J(X)$ , whose fibers are the Jacobian  $J(C)$  of the genus one curve  $C$ . The Jacobian  $J(C)$  is given by the degree zero part of the Picard group  $\text{Pic}(C)$  which has a distinguished point given by the trivial line bundle. Thus,  $J(C)$  is an elliptic curve and  $J(X)$  an elliptic fibration. In addition, the Jacobian  $J(C)$  equips  $C$  with the structure of a homogeneous space over  $J(C)$ . This additional structure is crucial for the notion of the TS-group  $\text{III}(J(X))$  associated to the Jacobian fibration which comprises all genus one fibrations that share the same Jacobian. While the latter statement describes the TS-group only as a set, the group structure is related to the Jacobian action on the different

genus one fibrations  $\text{III}(J(X))$  and is discussed in further detail in the appendix of . Since the discriminant locus and  $\tau$  function of every element  $X$  in  $\text{III}(J(X))$  are identical to those of  $J(X)$ , their corresponding F-theory compactifications are identical. The TS-group  $\text{III}(J(X))$  is manifest in the corresponding F-theory compactification as its discrete gauge group. In particular, we expect  $\mathbb{Z}_n \subset \text{III}(J(X))$  for a genus-one fibration  $X$  with only an  $n$ -section and the discrete gauge group of F-theory to contain a  $\mathbb{Z}_n$ -factor.

A different point of view on a genus-one fibration admitting an  $n$ -section is to start with an elliptic fibration with  $n$  rational sections. Then, one performs a chain of complex structure deformations that merge the  $n$  sections into a single  $n$ -section. Technically, if we define the  $n$  sections as the  $n$  rational roots of a polynomial, we can understand this deformation as introducing additional terms to the polynomial so that its roots are no longer rational, but involve taking roots. In other words, the sections can only be defined over a certain field extension<sup>3</sup>. Upon considering a family of these polynomials parametrized by the base of the elliptic fibration, the  $n$  individual roots are not well-defined anymore due to branch cuts around which they are exchanged by monodromies. Only monodromy-invariant combinations are globally well-defined in the fibration, giving rise to the  $n$ -section which is an appropriate union of the original roots.

In contrast to the F-theory picture, one obtains different vacua by compactifying the dual M-theory on the corresponding elements of the Tate-Shafarevich group. These are related to the F-theory vacuum by an additional  $S^1$ -compactification in which we in addition specify a certain flux choice along the compactification circle. This flux choice introduces the sought for additional degree of freedom, that is needed to reproduce the different lower-dimensional M-theory vacua starting from a unique F-theory compactification before circle compactification, as we explain next.

---

<sup>3</sup>In general, given a field  $K$  with closure  $\bar{K}$ , a divisor  $D$  is defined over  $K$ , if  $\sigma(D) = D$  for all elements  $\sigma$  in the absolute Galois group  $G_{\bar{K}/K}$ . Also note that, as we are dealing with a function field associated to the two-dimensional base, the notion of roots refers to taking suitable covers of the base.



The following, purely field theoretical analysis of the emergence of the different M-theory vacua has been proposed in [94, 93, 3, 48]. Here, we review the aspects essential to our discussion and elucidate some additional important insights. Although the following similarly applies to four-dimensional F-theory compactification, we focus here on F-theory in 6D with an M-theory dual in 5D for clarity of our discussion. The crucial point in the following is the fundamental difference between the Higgs effect in 6D and in 5D due to the presence of another U(1) gauge field in 5D, that is the Kaluza-Klein U(1).

The starting point is a six-dimensional  $U(1)_{6d}$  gauge theory that we want to break by a Higgs field  $\Phi$  of charge  $q$  to  $\mathbb{Z}_q$ . As a next step, we compactify this theory on a circle  $S^1$ . The Higgs field enjoys accordingly an expansion of the form

$$\Phi(x, y) = \sum_{n \in \mathbb{Z}} \phi_n(x) e^{2\pi i n y}. \quad (7.1)$$

In addition, one can turn on a flux (Wilson line)  $\xi = \int_{S^1} A_{6d}$  along the  $S^1$ . The full mass formula for the  $n$ th KK-mode then reads

$$m_n^q = |q\xi + n|, \quad (7.2)$$

where  $q$  and  $n$  refer to the charges under  $U(1)_{6d}$  and  $U(1)_{KK}$ , the Kaluza-Klein (KK) U(1) gauge field, respectively.

It is crucial to note that these gauge groups and their corresponding charges are only well-defined up to unimodular transformations that act on the charge vector  $(q, n)$  and the

two U(1) fields as

$$\begin{aligned} \begin{pmatrix} q & n \end{pmatrix} &\mapsto \begin{pmatrix} q & n \end{pmatrix} \begin{pmatrix} d & -b \\ -c & a \end{pmatrix}, \\ \begin{pmatrix} \text{U}(1)_{6d} \\ \text{U}(1)_{KK} \end{pmatrix} &\mapsto \begin{pmatrix} a & b \\ c & d \end{pmatrix} \begin{pmatrix} \text{U}(1)_{6d} \\ \text{U}(1)_{KK} \end{pmatrix}, \quad \begin{pmatrix} a & b \\ c & d \end{pmatrix} \in \text{SL}(2, \mathbb{Z}). \end{aligned}$$

These transformations allow us to identify different 5D KK-towers that arise from different choices for the flux  $\xi$ . Indeed, if one re-defines the five-dimensional U(1) fields according to

$$\begin{pmatrix} \text{U}(1)_{6d} \\ \text{U}(1)_{KK} \end{pmatrix} \mapsto \begin{pmatrix} 1 & -r \\ 0 & 1 \end{pmatrix} \begin{pmatrix} \text{U}(1)_{6d} \\ \text{U}(1)_{KK} \end{pmatrix} \quad (7.3)$$

while shifting  $\xi \mapsto \xi + r$  at the same time, the mass formula (7.2) is invariant. Thus, one obtains again the same KK-tower.

Varying the circle-flux  $\xi$ , we see that we have phase transitions at  $\xi = \frac{k}{q}$  for  $k \in \mathbb{Z}$  since the KK-tower gets shifted, according to (7.2). For a given flux  $\xi$ , the mode  $\phi_n$  triggering the Higgsing in 5D, which has to be chosen so that its mass in (7.2) vanishes, is changed. Each different choice for the 5D Higgs yields a *different* theory after Higgsing. Thus, we see that there are  $q$  inequivalent Higgses (for each different value of  $\xi$ ) and corresponding five-dimensional vacua after Higgsing. These  $q$  different vacua precisely correspond to the different M-theory compactifications obtained from the different elements of the TS-group.

As a concrete example, let us focus on the case of interest, which is 6D F-theory compactification with one  $\text{U}(1)_{6d}$  with a Higgs  $\Phi$  of charge  $q = 3$ . This is realized by F-theory compactified on  $dP_1$ -elliptic fibrations [80] and the Higgsed theory has a  $\mathbb{Z}_3$  discrete group. In 5D, one obtains the following gauge groups depending on the KK-charge of the 5D

Higgs:

$$\begin{cases} U(1) \times \mathbb{Z}_3, & \text{if } n = 0 \pmod{3} \\ U(1), & \text{if } n \neq 0 \pmod{3} \end{cases} . \quad (7.4)$$

By the above discussion, we expect  $q = 3$  M-theory vacua with massless Higgses fixed by (7.2) for  $\xi = 0, \frac{1}{3}, \frac{2}{3}$ , respectively. By (7.4) we see that only one of which has discrete gauge group  $\mathbb{Z}_3$  and two of which have no discrete gauge group. Geometrically, this is expected as the TS-group of the cubic, which is the geometry obtained by deforming the  $dP_1$ -elliptic fibration in the Higgsing [80], contains  $\mathbb{Z}_3$ , see Appendix in . The geometric identification of these three Higgs field in terms of holomorphic curves wrapped by M2-branes is the subject of Section 7.3.

Before turning to this discussion, we would like to briefly mention a dual reformulations of the above picture in terms of a Stückelberg mechanism [3, 48]. We identify an axion as the phase of the six-dimensional Higgs field  $\Phi = he^{ic}$ . In the circle compactification from 6D to 5D, the axion  $c$  can acquire a vacuum expectation value

$$n = \int_{S^1} \langle dc \rangle \quad (7.5)$$

along the circle. Clearly, the VEV (7.5) signals a non-trivial profile of  $c$  along the  $S^1$ , so that the flux (7.5) agrees with the KK mode number  $n$  of  $c$ . In this flux background, the surviving massless U(1) is a linear combination of the two 5D U(1) fields  $U(1)_{6d}$  and  $U(1)_{KK}$ . Geometrically, a non-trivial vacuum expectation value of the axion is exactly expected to arise in compactifications involving multi-sections and takes into account the generalized T-duality transformation rules that govern the physics in the presence of off-diagonal terms in the metric [3].

This picture is dual to the above discussion with a corresponding Wilson line  $\xi$  that has to be chosen so that the massless Higgs by (7.2) yields precisely the same linear combina-

tion of  $U(1)_{6d}$  and  $U(1)_{KK}$  of the remaining massless  $U(1)$  determined by the Stückelberg mechanism of the 5D axion  $c$ .

### 7.3 Identifying 5D Higgs Fields for the $\mathbb{Z}_3$ Tate-Shafarevich group

In this section we construct explicitly the different Higgs fields that lead to the three inequivalent five-dimensional M-theory vacua corresponding to the three different elements of the Tate-Shafarevich group of the most general cubic. These Higgs fields are obtained from M2-branes wrapping three different holomorphic curves in  $I_2$ -fibers of the elliptic fibration with fiber in  $dP_1$ , that we identify explicitly. F-theory compactifications both on Calabi-Yau fibrations with the most general cubic and the elliptic curve in  $dP_1$  have been studied recently in [80] to which we refer for further details.

A genus-one fibration by the most general cubic in  $\mathbb{P}^2$  is defined by the hypersurface

$$p_{\text{cub}} = s_1 u^3 + s_2 u^2 v + s_3 u v^2 + s_4 v^3 + s_5 u^2 w + s_6 u v w + s_7 v^2 w + s_8 u w^2 + s_9 v w^2 + s_{10} w^3 = 0. \quad (7.6)$$

Here the  $s_i$  are polynomials of appropriate degree of the coordinates on  $B$  or, more generally, sections of appropriate line bundles on  $B$ . By making specific choices for these line bundles and taking general sections, we obtain a genus one fibered Calabi-Yau threefold  $X_{p_{\text{cub}}}$ . Clearly, for generic  $s_i$  this genus one-fibration admits only a tri-section only.

Our strategy is to start in a six-dimensional F-theory compactification with a  $U(1)$  gauge group that we want to break down to  $\mathbb{Z}_3$  by a Higgsing. Such a geometry is provided by the  $dP_1$ -elliptic fibration which has been considered in great detail in [80]. It is related to

the geometry of the cubic by the tuning and resolution of the form

$$\text{cubic} \xrightarrow{s_{10} \rightarrow 0} \text{singular } dP_1 \xrightarrow{\text{blowing up } e_1} \text{resolved } dP_1, \quad (7.7)$$

which is geometrically a conifold transition. Thus, the singular  $dP_1$  model is given (7.6) for  $s_{10} = 0$ ,

$$p_{dP_1}^s = s_1 u^3 + s_2 u^2 v + s_3 u v^2 + s_4 v^3 + s_5 u^2 w + s_6 u v w + s_7 v^2 w + s_8 u w^2 + s_9 v w^2 = 0. \quad (7.8)$$

One observes that it has conifold singularities at co-dimension two in the base at  $s_8 = s_9 = 0 = u = v$ . In the following two subsections, we argue that this singularity admits two different resolutions related by a flop. These resolutions lead to the same F-theory vacuum, but the corresponding M-theory vacua are different as we demonstrate by analysing the charges of the corresponding  $I_2$ -fibers in the respective resolutions.

The crucial point is that in the first resolution two holomorphic curves are manifest that correspond to two of the three wanted 5D Higgs fields, whereas the curve supporting the third Higgs is obscured. In contrast, in the second resolution, again two curves are manifest that, however, correspond to the *third* wanted 5D Higgs field, while one of the curves manifest in the first resolution is obscured now. Thus, we see that by using different phases of the resolution of the singularity at  $s_8 = s_9 = 0$  in the  $dP_1$ -elliptic fibration, we can indeed manifestly see three different holomorphic curves to be used as the 5D Higgses yielding the three different M-theory vacua from compactification on the three elements of the TS-group of the cubic (7.6).

### 7.3.1 Resolving by the toric blow-up

The obvious resolution of the singularities in elliptic fibration (7.8) is obtained by performing the toric blow-up in the ambient space of the elliptic fiber defined by

$$u \longrightarrow e_1 u, \quad v \longrightarrow e_1 v, \quad (7.9)$$

where the coordinate  $e_1$  vanishes at the exceptional divisor. This is precisely toric  $dP_1$ , which yields a resolution of the singular fibration with the cubic (7.8). The corresponding smooth elliptic fibration has been extensively studied in [80] and we just summarize the most important results here. First of all the toric data of  $dP_1$  is given by

$$\left( \begin{array}{cc|cc|c|c} 1 & 0 & 1 & 0 & w & U \\ -1 & 1 & 0 & 1 & u & U - S \\ -1 & 0 & 1 & -1 & e_1 & S \\ 0 & -1 & 0 & 1 & v & U - S \end{array} \right). \quad (7.10)$$

Here the first two columns display the points of the toric diagram, written as row vectors, followed by the generators of the Mori cone in the third and fourth column, while the last two columns refer to the coordinates and the corresponding divisor classes being assigned to the rays of the diagram, respectively. The fan of the toric variety  $dP_1$  is obtained by a fine star-triangulation of the polytope defined by (7.10), from which one immediately obtains the Stanley Reisner ideal as well as the intersection numbers

$$SR = \{uv, e_1 w\}, \quad U^2 = 1, \quad S^2 = -1, \quad U \cdot S = 0. \quad (7.11)$$

The resolved curve takes the form

$$p_{dP_1}^r = s_1 u^3 e_1^2 + s_2 u^2 v e_1^2 + s_3 u v^2 e_1^2 + s_4 v^3 e_1^2 + s_5 u^2 w e_1 + s_6 u v w e_1 + s_7 v^2 w e_1 + s_8 u w^2 + s_9 v w^2 = 0. \quad (7.12)$$

Over the locus defined by  $s_8 = s_9 = 0$ , the fiber degenerates as

$$\underbrace{e_1}_{c_1} \underbrace{(s_1 u^3 e_1 + s_2 u^2 v e_1 + s_3 u v^2 e_1 + s_4 v^3 e_1 + s_5 u^2 w + s_6 u v w + s_7 v^2 w)}_{c_2} = 0, \quad (7.13)$$

which is a smooth  $I_2$ -fiber. Here  $c_1$  and  $c_2$  denote the two  $\mathbb{P}^1$  components of the resulting  $I_2$ -fiber which have classes  $S$  and  $3U - 2S$ .

Next, we investigate the sections, starting from the singular model before the blow-up (7.9). It has two sections which take the form

$$S_0 = [0 : 0 : 1], \quad S_1 = \left[ -s_9 : s_8 : \frac{s_4 s_8^3 - s_3 s_8^2 s_9 + s_2 s_8 s_9^2 - s_1 s_9^3}{-s_7 s_8^2 + s_6 s_8 s_9 - s_5 s_9^2} \right] \quad (7.14)$$

in terms of the projective coordinates  $[u : v : w]$  on  $\mathbb{P}^2$ . While the first section is toric and taken to define the zero-point  $O$  on the elliptic curve, the second section is found by constructing the tangent line

$$t_O : s_8 u + s_9 v = 0 \quad (7.15)$$

to the origin  $O$  which has to intersect the cubic in precisely one third point, provided  $s_8 \neq 0$  or  $s_9 \neq 0$ . This third intersection point is rational and defines the section  $S_1$ . In contrast, at the singular locus  $s_8 = s_9 = 0$ , the curve becomes singular precisely at  $O$  which implies that any line through  $O$  is tangent and therefore  $S_1$  degenerates to the whole singular curve. The two curves  $c_1$  and  $c_2$  support the Higgs field in question.

Passing to the resolved geometry, the two sections (7.14) lift to

$$\tilde{S}_0 = [s_9 : -s_8 : 1 : 0], \quad \tilde{S}_1 = [-s_9 : s_8 : s_4 s_8^3 - s_3 s_8^2 s_9 + s_2 s_8 s_9^2 - s_1 s_9^3 : -s_7 s_8^2 + s_6 s_8 s_9 - s_5 s_9^2]. \quad (7.16)$$

Note that these expressions are only valid away from the locus  $s_8 = s_9 = 0$ . In fact,  $\tilde{S}_0$  as well as  $\tilde{S}_1$  are rational sections that wrap the components  $c_1$  and  $c_2$  completely, respectively.

We note that the classes of the divisors associated to the sections are given by

$$[\tilde{S}_0] \cong S, \quad [\tilde{S}_1] \cong U - 2S, \quad (7.17)$$

where, by abuse of notation, we denoted the divisors  $S$  and  $U$ , defined in (7.10), on the ambient space by the same symbols as their intersections with the Calabi-Yau hypersurface (7.12). While the class of the zero section is obvious, the class of the second section is obtained by noting that the tangent line defines a tri-section. Subtracting from its class two times the class of the zero section<sup>4</sup>, one is left with  $U - 2S$ .

Knowing the classes of the sections as well as those of the fiber components  $c_1, c_2$ , one can evaluate the corresponding charges w.r.t. the  $U(1)_{6d}$  and the KK  $U(1)$ -field  $U(1)_{KK}$ . Recalling that the charge under  $U(1)_{6d}$  is computed from the intersection of the Shioda map for  $\tilde{S}_0$ , that is  $\tilde{S}_1 - \tilde{S}_0$ , with the respective curve  $c_i$  while the KK-charge is given by the intersection number with the zero section  $\tilde{S}_0$ , we obtain the charges summarized in Table 7.1. One observes that the shrinking of  $c_1$  and  $c_2$  gives massless states with charges  $(-3, -1)$  and  $(3, 2)$ , respectively. According to (7.2), these states are massless for the associated (inverse) choices of flux  $\xi_1 = -\frac{1}{3} \bmod 1$  and  $\xi_2 = -\frac{2}{3} \bmod 1$ . By (7.4) the remaining gauge group in 5D after Higgsing is  $U(1)$ .

Geometrically, we have to shrink the respective curves  $c_1$  and  $c_2$  and deform the arising

---

<sup>4</sup>Recall that the tangent line was defined in the singular geometry, where the class of  $u$  reads  $U$  instead of  $U - S$ .



	$c_1$	$c_2$
$\tilde{S}_0$	-1	2
$\tilde{S}_1$	2	-1
$\tilde{S}_1 - \tilde{S}_0$	3	-3

Table 7.1: Intersection numbers of the sections  $\tilde{S}_0, \tilde{S}_1$  with the curves in the  $I_2$ -fiber at  $s_8 = s_9 = 0$  and corresponding  $U(1)_{6d}$  charges in the toric resolution of the  $dP_1$ -model.

singularity, cf. the inverse process of (7.7). While the shrinking of the first component  $c_1$  is performed by taking the blow-down  $e_1 \rightarrow 1$ , the shrinking of the second component  $c_2$  is more elaborate. Instead of describing this directly, we choose the following short-cut. Observe that the charges in Table 7.1 are symmetric in the curves  $c_1$  and  $c_2$  as well as in  $\tilde{S}_0$  and  $\tilde{S}_1$ . Therefore, we can also change the roles of  $\tilde{S}_0$  and  $\tilde{S}_1$ , i.e. we take  $\tilde{S}_1$  to be the zero section<sup>5</sup>. Then, we obtain the second vacuum again by blowing down  $e_1 \rightarrow 1$ . Geometrically, this gives the same cubic after Higgsing which corresponds to switching on a non-zero value for  $s_{10}$ . However, this is precisely what we expect. The two non-trivial elements of the Tate Shafarevich group are given by the same cubic that only differs through inverse actions of the Jacobians, cf. Appendix of .

It remains to show how to obtain the massless mode of the Higgs that yields the third vacuum which must correspond to the Jacobian. The relevant Higgs field has to have charge  $(3, 0)$  with  $\xi = 0$ , so that the gauge group is  $\mathbb{Z}_3$ , according to (7.4). However, the associated curve is not manifest in the Calabi-Yau manifold (7.12). Nevertheless, one can argue for its existence by studying the enumerative geometry of the  $dP_1$ -fibration, which can be accomplished evaluating the non-perturbative part of the prepotential of the topological string,

$$F_{\text{non-pert}}^0 = \sum_{\beta} N_{\beta}^0 Q^{\beta}, \quad (7.18)$$

---

<sup>5</sup>As shown in [55], such a change of the choice of zero section is always possible in an anomaly-free theory, which is the case for the theory at hand, cf. [80].

analogously to the analysis performed in [78]. Here,  $N_\beta^0$  denote the (genus zero) Gromov-Witten invariants of the classes  $\beta$ .

To this end, we construct explicitly all Calabi-Yau manifolds (7.12) with base  $B = \mathbb{P}^2$  following the algorithm in Appendix G of [30] and compute all Gromov-Witten invariants up to a suitable degree. We find that in all these cases the invariant  $N_{[c_1+T^2]} = [s_8] \cdot [s_9]$ , i.e. agrees precisely with the number of  $I_2$ -fibers at  $s_8 = s_9 = 0$ . This is a strong indication that there exists a third holomorphic curve of genus zero inside the  $I_2$ -fiber (7.13) at  $s_8 = s_9 = 0$ , that is harder to manifestly see in geometry. In fact, using the classes (7.17) we check that this curve has precisely the right charges,  $(q, n) = (3, 0)$ , that are required for obtaining the third geometry according to (7.4).

Next we consider a different resolution which makes the curves in the classe  $[c_1 + T^2]$  directly manifest in the geometry.

### 7.3.2 Resolving by a complete intersection resolution

Let us begin by noting that in the toric blow-up (7.9), the zero section is ill-behaved, i.e. wraps a fiber component, precisely at the  $I_2$ -locus of interest at  $s_8 = s_9 = 0$ . Therefore, the two manifest curves  $c_1$  and  $c_2$  in (7.13) have to have a non-trivial KK-charge by construction. One way to manifestly see the third curve at  $s_8 = s_9 = 0$  with KK-charge zero is to consider a different phase of the resolution of the  $dP_1$ -elliptic fibration (7.8) where the zero section remains *holomorphic*. In the following, we construct this resolution explicitly and show the existence of the desired curve with KK-charge zero. We note that such a resolution has been considered in a different context in [16, 14].

To get started, we rewrite the singular  $dP_1$  geometry (7.8) in the form of a determinantal variety,

$$p_{dP_1}^s = uP_1 - vP_2. \tag{7.19}$$

Here we have defined the two summands as

$$P_1 = s_1 u^2 + s_2 uv + s_3 v^2 + s_5 uw + s_6 vw + s_8 w^2, \quad P_2 = -(s_4 v^2 + s_7 vw + s_9 w^2). \quad (7.20)$$

For a variety of the form (7.19), we can perform a small resolution. This means we introduce the coordinates  $\lambda_1, \lambda_2$  parameterizing a  $\mathbb{P}^1$  and impose

$$u\lambda_1 = \lambda_2 P_2. \quad (7.21)$$

The proper transform of the  $dP_1$  geometry (7.8) is accordingly given by

$$v\lambda_1 = \lambda_2 P_1. \quad (7.22)$$

In contrast to the toric blow-up in (7.9) that does not change the dimension of the ambient space, the two equations (7.21) and (7.22) define the resolved fiber as a complete intersection in a three-dimensional ambient space that can be torically characterized as

$$\left( \begin{array}{ccc|cc|c|c} -1 & -1 & -1 & 0 & 1 & u & L \\ -1 & 0 & 0 & 1 & -1 & \lambda_2 & H \\ 0 & 0 & 1 & 0 & 1 & v & L \\ 0 & 1 & 0 & 0 & 1 & w & L \\ 1 & 0 & 0 & 1 & 0 & \lambda_1 & H+L \end{array} \right). \quad (7.23)$$

Again, the first three columns specify the points of the toric diagram, written as row vectors, followed by the two generators of the Mori cone. The last two columns display the coordinates and the divisor classes which are associated to the rays, respectively. From the toric data one obtains immediately the Stanley Reisner ideal as well as the triple intersection

numbers as

$$SR = \{\lambda_1 \lambda_2, uvw\}, \quad L^3 = 0, \quad L^2 \cdot H = 1, \quad L \cdot H^2 = -1, \quad H^3 = 1. \quad (7.24)$$

The evaluation of the irreducible components of the  $I_2$ -fiber is slightly more involved in this case and is best performed using a primary decomposition. At the locus  $s_8 = s_9 = 0$  we find that the two rational components of the  $I_2$  fiber are given by

$$\begin{aligned} c_+ &= V(u, v), \\ c_- &= V(s_4 v^2 \lambda_2 + s_7 v w \lambda_2 + u \lambda_1, s_1 u^2 \lambda_2 + s_2 u v \lambda_2 + s_3 v^2 \lambda_2 + s_5 u w \lambda_2 + s_6 v w \lambda_2 - v \lambda_1, \\ &\quad s_1 u^3 + s_2 u^2 v + s_3 u v^2 + s_4 v^3 + s_5 u^2 w + s_6 u v w + s_7 v^2 w, s_1 s_4 u v \lambda_2^2 + s_1 s_7 u w \lambda_2^2 \\ &\quad + s_4 s_5 v w \lambda_2^2 + s_5 s_7 w^2 \lambda_2^2 - s_2 u \lambda_1 \lambda_2 - s_3 v \lambda_1 \lambda_2 - s_6 w \lambda_1 \lambda_2 + \lambda_1^2). \end{aligned} \quad (7.25)$$

Here,  $V(I)$  denotes the zero set of the ideal  $I$  and  $(p_1, \dots, p_k)$  denotes the ideal generated by the polynomials  $p_1, \dots, p_k$ . Applying again prime ideal techniques, one determines their respective homology classes of the curves  $c_+$  and  $c_-$  as

$$[c_+] = L^2, \quad [c_-] = (2L + H)(2L + H) - L^2. \quad (7.26)$$

Next, we turn to the analysis of the sections (7.14). Outside  $s_8 = s_9 = 0$  the simultaneous vanishing of  $u$  and  $v$  implies that  $\lambda_2 = 0$  as well. Thus, we identify the coordinates  $[u : v : w : \lambda_1 : \lambda_2]$  of the zero section and its homology class as

$$S'_0 = [0 : 0 : 1 : 1 : 0], \quad [S'_0] = H. \quad (7.27)$$

In contrast to the toric blow-up,  $S'_0$  is also well-defined at the singular locus and defines, therefore, a holomorphic zero section. In order to find the second section, we note that

away from the singular locus there is a unique solution for  $\lambda_1$  and  $\lambda_2$  if one plugs the coordinates of the section  $S_1$  given in (7.14) into (7.21) and (7.22). Its coordinates are given by

$$\begin{aligned}
S'_1 = [s_9 : -s_8 : & \frac{-s_4 s_8^3 + s_9 (s_3 s_8^2 + s_9 (-s_2 s_8 + s_1 s_9))}{s_7 s_8^2 + s_9 (-s_6 s_8 + s_5 s_9)} : ( -s_4 s_6 s_7 s_8^5 + s_3 s_7^2 s_8^5 + s_4^2 s_8^6 + s_4 s_6^2 s_8^4 s_9 \\
& + s_4 s_5 s_7 s_8^4 s_9 - s_3 s_6 s_7 s_8^4 s_9 - s_2 s_7^2 s_8^4 s_9 - 2s_3 s_4 s_8^5 s_9 - 2s_4 s_5 s_6 s_8^3 s_9^2 + s_3 s_5 s_7 s_8^3 s_9^2 + s_2 s_6 s_7 s_8^3 s_9^2 \\
& + s_1 s_7^2 s_8^3 s_9^2 + s_3^2 s_8^4 s_9^2 + 2s_2 s_4 s_8^4 s_9^2 + s_4 s_5^2 s_8^2 s_9^3 - s_2 s_5 s_7 s_8^2 s_9^3 - s_1 s_6 s_7 s_8^2 s_9^3 - 2s_2 s_3 s_8^3 s_9^3 + s_1^2 s_9^6 \\
& - 2s_1 s_4 s_8^3 s_9^3 + s_1 s_5 s_7 s_8 s_9^4 + s_2^2 s_8^2 s_9^4 + 2s_1 s_3 s_8^2 s_9^4 - 2s_1 s_2 s_8 s_9^5) : (s_7 s_8^2 + s_9 (s_5 s_9 - s_6 s_8))^2]. \quad (7.28)
\end{aligned}$$

A slightly alternative way to obtain this section is to compute the intersection of the hyperplane given by

$$s_8 u + s_9 v = 0 \quad (7.29)$$

with the complete intersection manifold specified by (7.21) and (7.22). Analogous to the case of the toric blow-up, its class is computed as

$$[S'_1] = [u] - 2[\tilde{S}_0] = L - 2H. \quad (7.30)$$

Finally, we compute the one finds the charges to the two rational curves  $c_+$ ,  $c_-$  in the  $I_2$ -fiber at  $s_8 = s_9 = 0$  in this resolution. Here, we use their homology classes in (7.26) and the homology classes of the zero and rational sections in (7.27) and (7.30) to obtain the charges summarized in Table 7.2. In particular, we observe that one obtains a mode with KK-charge zero by shrinking the component  $c_-$ . It supports precisely the third Higgs necessary to obtain the third 5D M-theory vacuum with  $U(1) \times \mathbb{Z}_3$  gauge group in (7.4). We emphasize that the curve  $c_-$  has precisely the same charges as the curve in the class  $[c_1 + T^2]$  for whose existence we argued in the last subsection by computing the corresponding Gromov-Witten invariants. In analogy to the analysis performed in [93, 94], it is expected that the

	$c_+$	$c_-$
$S'_0$	1	0
$S'_1$	-2	3
$S'_1 - S'_0$	-3	3

Table 7.2: Intersection numbers of the sections  $S'_0$ ,  $S'_1$  with the curves in the  $I_2$ -fiber at  $s_8 = s_9 = 0$  and corresponding  $U(1)_{6d}$  charges in the complete intersection resolution of the  $dP_1$ -model.

corresponding geometry after the deformation is given by the Jacobian of the most general cubic (7.6).

## Concluding Remarks

In this dissertation we have expanded our understanding of F-theory compactifications in diverse directions. Our main line of research was inspired in abelian and discrete symmetries, however, the contributions go well beyond those topics. Let us summarize the main results of this dissertation:

- We have expanded the understanding of the abelian sector in F-theory in three directions: rank, dimensions and representations. We explicitly constructed geometries that supported abelian groups of ranks bigger than one. In chapters 3 and 4 we engineered rank 2 abelian groups and in chapter 5 geometries supporting  $U(1)^3$ . We studied in detail the low energy spectrum and the Yuwawa couplings of the theories. We also studied compactifications of different dimensions: see 3 and 4 for six and four compactifications respectively. Finally, in terms of the abelian sector, in this dissertation we studied examples with higher representations under  $U(1)$ . In chapter see 6, we explicitly constructed geometries that supported novel charge three matter.
- We explicitly constructed geometries that supported discrete symmetries. See chapter 6 for the gauge groups  $\mathbb{Z}_3$  and  $U(1) \times \mathbb{Z}_2$ . We study in detail the mathematical

structure, the Tate–Shafarevich group, that give rise to the  $\mathbb{Z}_3$  gauge symmetry in F-theory, see chapter 7.

- We found, studied and emphasized the importance of non-holomorphic rational sections in F-theory compactifications, see chapters 3, 4, 5, 6 and 7. We find its connection to the realization of higher charges. We also studied the effect of non-holomorphic sections in the F- M- theory duality and its consequences in the 3D Chern Simons terms of the low energy theory, see chapter 4.
- We unveiled connections between different geometries using the Higgs mechanism, see 6. The connection between geometric transitions and the Higgs mechanism was also studied in chapters 6 and 7.
- Finally, we reminded some mathematical results, particularly from algebraic geometry, to the F-theory community. Among them, the resultant technique are, the use of ideals and their decomposition and the power of toric geometry.

As further directions of research, we believe that more exciting connections between geometry and physics are still unveiled and waiting to be discovered, and, F-theory will play a central role in it. In fact, we think that there are some topics where we are already seeing the tip of the iceberg: higher representations and higher abelian ranks. From the phenomenology perspective, we also believe that F-theory provides the most complete framework to build and study particle phenomenology models. Thus, we encourage new and current scientists to continue pursuing research in the fascinating topic of F-theory compactifications.



# Bibliography

- [1] Ofer Aharony, Amihay Hanany, Kenneth A. Intriligator, N. Seiberg, and M.J. Strassler. Aspects of N=2 supersymmetric gauge theories in three-dimensions. *Nucl.Phys.*, B499:67–99, 1997.
- [2] Sang Yook An, Seog Young Kim, David C Marshall, Susan H Marshall, William G McCallum, and Alexander R Perlis. Jacobians of genus one curves. *Journal of Number Theory*, 90(2):304–315, 2001.
- [3] Lara B. Anderson, Iñaki García-Etxebarria, Thomas W. Grimm, and Jan Keitel. Physics of F-theory compactifications without section. *JHEP*, 1412:156, 2014.
- [4] Paul S. Aspinwall and David R. Morrison. Nonsimply connected gauge groups and rational points on elliptic curves. *JHEP*, 9807:012, 1998.
- [5] Tom Banks. Effective Lagrangian Description of Discrete Gauge Symmetries. *Nucl.Phys.*, B323:90, 1989.
- [6] Tom Banks and Nathan Seiberg. Symmetries and Strings in Field Theory and Gravity. *Phys.Rev.*, D83:084019, 2011.

- [7] Victor V. Batyrev. Dual polyhedra and mirror symmetry for Calabi-Yau hypersurfaces in toric varieties. *J.Alg.Geom.*, 3:493–545, 1994.
- [8] Chris Beasley, Jonathan J. Heckman, and Cumrun Vafa. GUTs and Exceptional Branes in F-theory - I. *JHEP*, 01:058, 2009.
- [9] M. Bershadsky, Kenneth A. Intriligator, S. Kachru, David R. Morrison, V. Sadov, et al. Geometric singularities and enhanced gauge symmetries. *Nucl.Phys.*, B481: 215–252, 1996.
- [10] Adel Bilal and Steffen Metzger. Anomaly cancellation in M theory: A Critical review. *Nucl.Phys.*, B675:416–446, 2003.
- [11] Ralph Blumenhagen, Thomas W. Grimm, Benjamin Jurke, and Timo Weigand. Global F-theory GUTs. *Nucl.Phys.*, B829:325–369, 2010.
- [12] Federico Bonetti and Thomas W. Grimm. Six-dimensional (1,0) effective action of F-theory via M-theory on Calabi-Yau threefolds. *JHEP*, 1205:019, 2012.
- [13] Federico Bonetti, Thomas W. Grimm, and Stefan Hohenegger. A Kaluza-Klein inspired action for chiral p-forms and their anomalies. *Phys.Lett.*, B720:424–427, 2013.
- [14] Jan Borchmann, Christoph Mayrhofer, Eran Palti, and Timo Weigand. SU(5) Tops with Multiple U(1)s in F-theory. 2013.
- [15] Vincent Bouchard and Harald Skarke. Affine Kac-Moody algebras, CHL strings and the classification of tops. *Adv.Theor.Math.Phys.*, 7:205–232, 2003.
- [16] Andreas P. Braun, Andres Collinucci, and Roberto Valandro. G-flux in F-theory and algebraic cycles. *Nucl.Phys.*, B856:129–179, 2012.

- [17] Volker Braun. Toric Elliptic Fibrations and F-Theory Compactifications. *JHEP*, 1301:016, 2013.
- [18] Volker Braun and David R. Morrison. F-theory on Genus-One Fibrations. 2014.
- [19] Volker Braun, Thomas W. Grimm, and Jan Keitel. Geometric Engineering in Toric F-Theory and GUTs with U(1) Gauge Factors. 2013.
- [20] Volker Braun, Thomas W. Grimm, and Jan Keitel. New Global F-theory GUTs with U(1) symmetries. 2013.
- [21] Volker Braun, Thomas W. Grimm, and Jan Keitel. Complete Intersection Fibers in F-Theory. *JHEP*, 03:125, 2015.
- [22] Philip Candelas and Anamaria Font. Duality between the webs of heterotic and type II vacua. *Nucl.Phys.*, B511:295–325, 1998.
- [23] John William Scott Cassels. *LMSST: 24 Lectures on Elliptic Curves*, volume 24. Cambridge University Press, 1991.
- [24] Ching-Ming Chen, Johanna Knapp, Maximilian Kreuzer, and Christoph Mayrhofer. Global SO(10) F-theory GUTs. *JHEP*, 1010:057, 2010.
- [25] Cyril Closset, Thomas T. Dumitrescu, Guido Festuccia, Zohar Komargodski, and Nathan Seiberg. Contact Terms, Unitarity, and F-Maximization in Three-Dimensional Superconformal Theories. *JHEP*, 1210:053, 2012.
- [26] Cyril Closset, Thomas T. Dumitrescu, Guido Festuccia, Zohar Komargodski, and Nathan Seiberg. Comments on Chern-Simons Contact Terms in Three Dimensions. *JHEP*, 1209:091, 2012.
- [27] Ian Connell. Elliptic curve handbook. *Preprint*, 1996.

- [28] David A. Cox. The Homogeneous coordinate ring of a toric variety, revised version. 1993.
- [29] David A. Cox, John B. Little, and Henry K. Schenck. *Toric varieties*. American Mathematical Soc., 2011.
- [30] Mirjam Cvetič, Antonella Grassi, Denis Klevvers, and Hernan Piragua. Chiral Four-Dimensional F-Theory Compactifications With SU(5) and Multiple U(1)-Factors. 2013.
- [31] Mirjam Cvetič, Thomas W. Grimm, and Denis Klevvers. Anomaly Cancellation And Abelian Gauge Symmetries In F-theory. *JHEP*, 1302:101, 2013.
- [32] Mirjam Cvetič, James Halverson, and Hernan Piragua. Stringy Hidden Valleys. *JHEP*, 02:005, 2013.
- [33] Mirjam Cvetič, Denis Klevvers, and Hernan Piragua. F-Theory Compactifications with Multiple U(1)-Factors: Addendum. *JHEP*, 1312:056, 2013.
- [34] Mirjam Cvetič, Denis Klevvers, and Hernan Piragua. F-Theory Compactifications with Multiple U(1)-Factors: Constructing Elliptic Fibrations with Rational Sections. 2013.
- [35] Mirjam Cvetič, Denis Klevvers, Hernan Piragua, and Peng Song. Elliptic fibrations with rank three Mordell-Weil group: F-theory with U(1) x U(1) x U(1) gauge symmetry. *JHEP*, 1403:021, 2014.
- [36] Mirjam Cvetič, Ron Donagi, Denis Klevvers, Hernan Piragua, and Maximilian Poretschkin. F-Theory Vacua with  $Z_3$  Gauge Symmetry. 2015.

- [37] Mirjam Cvetič, Denis Klevers, Hernan Piragua, and Washington Taylor. General  $U(1) \times U(1)$  F-theory Compactifications and Beyond: Geometry of unHiggsings and novel Matter Structure. 2015.
- [38] Keshav Dasgupta, Govindan Rajesh, and Savdeep Sethi. M theory, orientifolds and G - flux. *JHEP*, 08:023, 1999.
- [39] Jan de Boer, Robbert Dijkgraaf, Kentaro Hori, Arjan Keurentjes, John Morgan, David R. Morrison, and Savdeep Sethi. Triples, fluxes, and strings. *Adv. Theor. Math. Phys.*, 4:995–1186, 2002.
- [40] Wolfram Decker, Gert-Martin Greuel, Gerhard Pfister, and Hans Schönemann. SINGULAR 3-1-6 — A computer algebra system for polynomial computations. <http://www.singular.uni-kl.de>, 2012.
- [41] Frederik Denef. Les Houches Lectures on Constructing String Vacua. pages 483–610, 2008.
- [42] Ron Donagi and Martijn Wijnholt. Model Building with F-Theory. 2008.
- [43] Ron Donagi and Martijn Wijnholt. Breaking GUT Groups in F-Theory. *Adv.Theor.Math.Phys.*, 15:1523–1604, 2011.
- [44] Herbi K. Dreiner, Christoph Luhn, and Marc Thormeier. What is the discrete gauge symmetry of the MSSM? *Phys.Rev.*, D73:075007, 2006.
- [45] Jens Erler. Anomaly cancellation in six-dimensions. *J.Math.Phys.*, 35:1819–1833, 1994.
- [46] William Fulton. *Introduction to toric varieties*. Number 131. Princeton University Press, 1993.

- [47] William Fulton. *Intersection theory*, volume 2. Springer Science & Business Media, 2012.
- [48] Iñaki García-Etxebarria, Thomas W. Grimm, and Jan Keitel. Yukawas and discrete symmetries in F-theory compactifications without section. *JHEP*, 11:125, 2014.
- [49] Antonella Grassi and Vittorio Perduca. Weierstrass models of elliptic toric K3 hypersurfaces and symplectic cuts. 2012.
- [50] Michael B. Green and John H. Schwarz. Anomaly Cancellation in Supersymmetric D=10 Gauge Theory and Superstring Theory. *Phys.Lett.*, B149:117–122, 1984.
- [51] Brian R. Greene, David R. Morrison, and M. Ronen Plesser. Mirror manifolds in higher dimension. *Commun.Math.Phys.*, 173:559–598, 1995.
- [52] Phillip Griffiths and Joseph Harris. *Principles of algebraic geometry*. John Wiley & Sons, 2014.
- [53] Thomas W. Grimm. The N=1 effective action of F-theory compactifications. *Nucl.Phys.*, B845:48–92, 2011.
- [54] Thomas W. Grimm and Hirotaka Hayashi. F-theory fluxes, Chirality and Chern-Simons theories. *JHEP*, 1203:027, 2012.
- [55] Thomas W. Grimm and Andreas Kapfer. Anomaly Cancellation in Field Theory and F-theory on a Circle. 2015.
- [56] Thomas W. Grimm and Raffaele Savelli. Gravitational Instantons and Fluxes from M/F-theory on Calabi-Yau fourfolds. *Phys.Rev.*, D85:026003, 2012.
- [57] Thomas W. Grimm and Washington Taylor. Structure in 6D and 4D N=1 supergravity theories from F-theory. *JHEP*, 1210:105, 2012.

- [58] Thomas W. Grimm and Timo Weigand. On Abelian Gauge Symmetries and Proton Decay in Global F-theory GUTs. *Phys.Rev.*, D82:086009, 2010.
- [59] Thomas W. Grimm, Tae-Won Ha, Albrecht Klemm, and Denis Klevers. Computing Brane and Flux Superpotentials in F-theory Compactifications. *JHEP*, 1004:015, 2010.
- [60] Thomas W. Grimm, Andreas Kapfer, and Jan Keitel. Effective action of 6D F-Theory with U(1) factors: Rational sections make Chern-Simons terms jump. 2013.
- [61] Thomas W. Grimm, Denis Klevers, and Maximilian Poretschkin. Fluxes and Warping for Gauge Couplings in F-theory. *JHEP*, 1301:023, 2013.
- [62] Sergei Gukov, Cumrun Vafa, and Edward Witten. CFT's from Calabi-Yau four folds. *Nucl.Phys.*, B584:69–108, 2000.
- [63] Robin Hartshorne. *Algebraic geometry*. Number 52. Springer, 1977.
- [64] Hirotaka Hayashi, Radu Tatar, Yukinobu Toda, Taizan Watari, and Masahito Yamazaki. New Aspects of Heterotic–F Theory Duality. *Nucl.Phys.*, B806:224–299, 2009.
- [65] Hirotaka Hayashi, Craig Lawrie, and Sakura Schafer-Nameki. Phases, Flops and F-theory: SU(5) Gauge Theories. *JHEP*, 1310:046, 2013.
- [66] Gabriele Honecker. Massive U(1)s and heterotic five-branes on K3. *Nucl.Phys.*, B748:126–148, 2006.
- [67] Min-xin Huang, Albrecht Klemm, and Maximilian Poretschkin. Refined stable pair invariants for E-, M- and [p,q]-strings. 2013.

- [68] Min-xin Huang, Albrecht Klemm, Jonas Reuter, and Marc Schiereck. Quantum geometry of del Pezzo surfaces in the Nekrasov-Shatashvili limit. 2014.
- [69] Luis E. Ibanez. THE SEARCH FOR A STANDARD MODEL  $SU(3) \times SU(2) \times U(1)$  SUPERSTRING: AN INTRODUCTION TO ORBIFOLD CONSTRUCTIONS. In *Latin American School of Physics (ELAF 87): Contacts among Particle Physics, Nuclear Physics, Statistical Mechanics and Condensed Matter La Plata, Argentina, July 6-24, 1987*, 1987. URL <http://alice.cern.ch/format/showfull?sysnb=0091664>.
- [70] Luis E. Ibanez and Graham G. Ross. Discrete gauge symmetry anomalies. *Phys. Lett.*, B260:291–295, 1991.
- [71] Luis E. Ibanez and Graham G. Ross. Discrete gauge symmetries and the origin of baryon and lepton number conservation in supersymmetric versions of the standard model. *Nucl.Phys.*, B368:3–37, 1992.
- [72] Luis E. Ibanez and Graham G. Ross. Should discrete symmetries be anomaly free? 1991.
- [73] Kenneth Intriligator, Hans Jockers, Peter Mayr, David R. Morrison, and M. Ronen Plesser. Conifold Transitions in M-theory on Calabi-Yau Fourfolds with Background Fluxes. *Adv.Theor.Math.Phys.*, 17:601–699, 2013.
- [74] E. Palti J. Borchmann, C. Mayrhofer and T. Weigand. Elliptic fibrations for  $SU(5) \times U(1) \times U(1)$  F-theory vacua. 2013.
- [75] Sheldon Katz, David R. Morrison, Sakura Schafer-Nameki, and James Sully. Tate’s algorithm and F-theory. *JHEP*, 1108:094, 2011.



- [76] Sheldon H. Katz, David R. Morrison, and M. Ronen Plesser. Enhanced gauge symmetry in type II string theory. *Nucl.Phys.*, B477:105–140, 1996.
- [77] A. Klemm, B. Lian, S.S. Roan, and Shing-Tung Yau. Calabi-Yau fourfolds for M theory and F theory compactifications. *Nucl.Phys.*, B518:515–574, 1998.
- [78] Albrecht Klemm, Peter Mayr, and Cumrun Vafa. BPS states of exceptional noncritical strings. 1996.
- [79] D. Klevers. Holomorphic Couplings In Non-Perturbative String Compactifications. *Fortsch.Phys.*, 60:3–213, 2012.
- [80] Denis Klevers, Damian Kaloni Mayorga Pena, Paul-Konstantin Oehlmann, Hernan Piragua, and Jonas Reuter. F-Theory on all Toric Hypersurface Fibrations and its Higgs Branches. *JHEP*, 1501:142, 2015.
- [81] Kunihiko Kodaira. On compact analytic surfaces: Ii. *The Annals of Mathematics*, 77(3):563–626, 1963.
- [82] Lawrence M. Krauss and Frank Wilczek. Discrete Gauge Symmetry in Continuum Theories. *Phys.Rev.Lett.*, 62:1221, 1989.
- [83] Vijay Kumar, David R. Morrison, and Washington Taylor. Mapping 6D  $N = 1$  supergravities to F-theory. *JHEP*, 02:099, 2010.
- [84] Vijay Kumar, Daniel S. Park, and Washington Taylor. 6D supergravity without tensor multiplets. *JHEP*, 1104:080, 2011.
- [85] Moritz Kuntzler and Sakura Schafer-Nameki. Tate Trees for Elliptic Fibrations with Rank one Mordell-Weil group. 2014.

- [86] Serge Lang and André Neron. Rational points of abelian varieties over function fields. *American Journal of Mathematics*, pages 95–118, 1959.
- [87] Craig Lawrie and Sakura Schafer-Nameki. The Tate Form on Steroids: Resolution and Higher Codimension Fibers. 2012.
- [88] Ling Lin and Timo Weigand. Towards the Standard Model in F-theory. *Fortsch. Phys.*, 63(2):55–104, 2015.
- [89] Joseph Marsano and Sakura Schafer-Nameki. Yukawas, G-flux, and Spectral Covers from Resolved Calabi-Yau's. *JHEP*, 1111:098, 2011.
- [90] Joseph Marsano, Natalia Saulina, and Sakura Schafer-Nameki. Monodromies, Fluxes, and Compact Three-Generation F-theory GUTs. *JHEP*, 0908:046, 2009.
- [91] Christoph Mayrhofer, Eran Palti, and Timo Weigand. U(1) symmetries in F-theory GUTs with multiple sections. 2012.
- [92] Christoph Mayrhofer, David R. Morrison, Oskar Till, and Timo Weigand. Mordell-Weil Torsion and the Global Structure of Gauge Groups in F-theory. 2014.
- [93] Christoph Mayrhofer, Eran Palti, Oskar Till, and Timo Weigand. Discrete Gauge Symmetries by Higgsing in four-dimensional F-Theory Compactifications. *JHEP*, 12:068, 2014.
- [94] Christoph Mayrhofer, Eran Palti, Oskar Till, and Timo Weigand. On Discrete Symmetries and Torsion Homology in F-Theory. *JHEP*, 06:029, 2015.
- [95] Barry Mazur. Modular curves and the eisenstein ideal. *Publications Mathématiques de l'Institut des Hautes Études Scientifiques*, 47(1):33–186, 1977.

- [96] Barry Mazur and D Goldfeld. Rational isogenies of prime degree. *Inventiones mathematicae*, 44(2):129–162, 1978.
- [97] David R. Morrison and Daniel S. Park. F-Theory and the Mordell-Weil Group of Elliptically-Fibered Calabi-Yau Threefolds. *JHEP*, 1210:128, 2012.
- [98] David R. Morrison and Washington Taylor. Classifying bases for 6D F-theory models. *Central Eur.J.Phys.*, 10:1072–1088, 2012.
- [99] David R. Morrison and Washington Taylor. Sections, multisections, and U(1) fields in F-theory. 2014.
- [100] David R. Morrison and Washington Taylor. Non-Higgsable clusters for 4D F-theory models. *JHEP*, 1505:080, 2015.
- [101] David R. Morrison and Cumrun Vafa. Compactifications of F theory on Calabi-Yau threefolds. 1. *Nucl. Phys.*, B473:74–92, 1996.
- [102] David R. Morrison and Cumrun Vafa. Compactifications of F theory on Calabi-Yau threefolds. 2. *Nucl.Phys.*, B476:437–469, 1996.
- [103] Noboru Nakayama. On weierstrass models. *Algebraic geometry and commutative algebra*, Vol. II:pp. 405–431. Kinokuniya, 1988.
- [104] A.J. Niemi and G.W. Semenoff. Axial Anomaly Induced Fermion Fractionization and Effective Gauge Theory Actions in Odd Dimensional Space-Times. *Phys.Rev.Lett.*, 51:2077, 1983.
- [105] Daniel S. Park. Anomaly Equations and Intersection Theory. *JHEP*, 1201:093, 2012.

- [106] A.N. Redlich. Parity Violation and Gauge Noninvariance of the Effective Gauge Field Action in Three-Dimensions. *Phys.Rev.*, D29:2366–2374, 1984.
- [107] V. Sadov. Generalized Green-Schwarz mechanism in F theory. *Phys.Lett.*, B388: 45–50, 1996.
- [108] Augusto Sagnotti. A Note on the Green-Schwarz mechanism in open string theories. *Phys.Lett.*, B294:196–203, 1992.
- [109] S. Sethi, C. Vafa, and Edward Witten. Constraints on low dimensional string compactifications. *Nucl.Phys.*, B480:213–224, 1996.
- [110] Tetsuji Shioda. On the Mordell-Weil lattices. *Comment. Math. Univ. St. Paul*, 39(2): 211–240, 1990.
- [111] Joseph H Silverman. *The arithmetic of elliptic curves*, volume 106. Springer, 2009.
- [112] John Tate. Algorithm for determining the type of a singular fiber in an elliptic pencil. *Modular functions of one variable IV*, pages 33–52, 1975.
- [113] Washington Taylor. TASI Lectures on Supergravity and String Vacua in Various Dimensions. 2011.
- [114] Cumrun Vafa. Evidence for F theory. *Nucl.Phys.*, B469:403–418, 1996.
- [115] Rania Wazir. Arithmetic on Elliptic Threefolds. 2001.
- [116] Edward Witten. On flux quantization in M theory and the effective action. *J.Geom.Phys.*, 22:1–13, 1997.
- [117] Edward Witten. Phase transitions in M theory and F theory. *Nucl.Phys.*, B471: 195–216, 1996.